sustainability

Sustainable Lighting & Lighting for Sustainability

Selected articles published by MDPI

MDPI

Sustainable Lighting & Lighting for Sustainability

Sustainable Lighting & Lighting for Sustainability

Selected Articles Published by MDPI

MDPI • Basel • Beijing • Wuhan • Barcelona • Belgrade • Manchester • Tokyo • Cluj • Tianjin

This is a reprint of articles published online by the open access publisher MDPI (available at: http://www.mdpi.com). The responsibility for the book's title and preface lies with Antonio Peña-García, who compiled this selection.

For citation purposes, cite each article independently as indicated on the article page online and as indicated below:

LastName, A.A.; LastName, B.B.; LastName, C.C. Article Title. *Journal Name* **Year**, *Article Number*, Page Range.

ISBN 978-3-03928-344-6 (Pbk)
ISBN 978-3-03928-345-3 (PDF)

Contents

About Special Issue Coordinator

Antonio Peña-García (Dr.) (Granada, Spain, 1977) holds a Ph.D. and a Master in Physics from the University of Granada, where he is an Associate Professor of Lighting Technology for the Department of Civil Engineering, and the director of the research group Lighting Technology for Safety and Sustainability, which he founded in 2012. Before joining the university, he was responsible for the regulation and homologation of the Lighting System Branch of the Valeo Group in Spain. He has published more than 100 articles in high ranked journals and for international congresses, advised several doctoral theses, and been IP of more than 10 projects with public administrations and private companies, always in the field of sustainable lighting. He was a Visiting Professor at the "Sapienza" University of Rome (Italy) for three months, and an ERASMUS+ professor at the Universities of Porto and Vila Real (Portugal). Prof. Dr. Peña-García regularly evaluates project proposals in different countries and institutions, as well as acting as reviewer for several journals indexed in the Journal Citation Report. His main research topics are the decrease of energy consumption and environmental impact in tunnel lighting, and the influence of lighting on human safety and well-being.

Preface to "Sustainable Lighting & Lighting for Sustainability"

This book is the result of two years of hard work. After the success of the Special Issues "Sustainable Lighting and Energy Saving" (2018), and "Lighting at the Frontiers of Sustainable Development" (2019), MDPI kindly asked me to make a selection for the present book, which aims to summarize the conclusions of both Special Issues.

Given the quality and originality of the 28 published papers, the choice has been rather complex. I, in no way, pretend to have selected the best papers because, honestly, they were impossible to rank. My task here was to demonstrate that a new perspective of lighting, what I call total lighting, may have arisen from these two Special Issues. Thus, I had to make coherent choices so that the selected papers and their order in the book sent a message to the reader.

With this target in mind, I selected twelve articles, six of which deal with what we classically call "sustainable lighting" (light pollution and the optimization of indoor and outdoor lighting). Meanwhile, the six other papers belong to what could be best described as "lighting for sustainability", the way in which accurate and smart lighting can ensure the availability of resources for the future generations. In this category I selected articles dealing with the use of lighting to improve agrarian production, the attachment of people to traditional ways of life, and the preservation of cultural heritage. These fields are closely and indisputably related to migration, cultural identity, well-being and equality, hot topics for the achievement of the 17 Sustainable Development Goals. As demonstrated in the two aforementioned Special Issues, particularly that of "Lighting at the Frontiers of Sustainable Development" (2019), lighting can provide a new perspective in all these new areas.

I hope this book linking sustainable lighting with lighting for sustainability will contribute to an understanding of their key roles in the path to truly sustainable development.

Antonio Peña-García

sustainability

MDPI

Article

Roadway Lighting Retrofit: Environmental and Economic Impact of Greenhouse Gases Footprint Reduction

Adam Sędziwy [1,*], Artur Basiura [1,2] and Igor Wojnicki [1]

[1] Department of Applied Computer Science, AGH University of Science and Technology, al. Mickiewicza 30, 30-059 Kraków, Poland; artur.basiura@gradis.pl (A.B.); wojnicki@agh.edu.pl (I.W.)
[2] GRADIS Sp. z o.o., ul.Jasnogórska 9 kl. B, 31-358 Kraków, Poland
* Correspondence: sedziwy@agh.edu.pl; Tel.: +48-12-617-5204

Received: 14 August 2018; Accepted: 26 October 2018; Published: 29 October 2018

Abstract: Roadway lighting retrofit is a process continuously developed in urban environments due to both installation aging and technical upgrades. The spectacular example is replacing the high intensity discharge (HID) lamps, usually high pressure sodium (HPS) ones, with the sources based on light-emitting diodes (LED). The main focus in the related research was put on energy efficiency of installations and corresponding financial benefits. In this work, we extend those considerations analyzing how lighting optimization impacts greenhouse gas (GHG) emission reduction and what are the resultant financial benefits expressed in terms of emission allowances prices. Our goal is twofold: (i) obtaining a quantitative assessment of how a GHG footprint depends on a technological scope of modernization of a city HPS-based lighting system; and (ii) showing that the costs of such a modernization can be decreased by up to 10% thanks to a lowered CO_2 emission volume. Moreover, we identify retrofit patterns yielding the most substantial environmental impact.

Keywords: street lighting; energy efficiency; greenhouse gases; CO_2 emission; LED lighting; lighting control

1. Introduction

Retrofitting a roadway lighting is a process continuously developed in urban environments due to installations aging and technical upgrades. The common example is replacing high pressure sodium fixtures with LED, plasma or induction ones (the last two also belong to gas discharge sources) [1] and involving various hardware modules (e.g., occupancy sensors) enabling lighting control [2]. The main problems being analyzed in the related research were reducing energy consumption, improving illumination quality [3], optimizing investment and maintenance costs [4].

It is worth noting that financial optimization of roadway lighting solutions applies also to such non-trivial cases as road tunnel illumination [5,6].

To support retrofit related optimization, a range of computing approaches are proposed including graph-based modeling of lighting systems [7] or evolutionary algorithms [8].

While the computational, technological and financial aspects of lighting design/retrofit are commonly discussed in the literature, a detailed analysis of an environmental impact of lighting system modernization is rather rarely present in the domain research [7,9,10].

To go beyond the obvious fact that a reduced power usage leads to a decreased GHG footprint, we made both qualitative and quantitative analysis of how using advanced lighting solutions influences a greenhouse gases emission. Moreover, we analyzed economic benefits resulting from a lowered CO_2 emission, showing that the retrofit investment costs can be effectively reduced by up to 10%.

Similarly, as for the roadway lighting optimization improving energy efficiency, we distinguished three possible retrofit scopes.

1. HID to LED replacement: The only action is installing LED sources in places of HID ones. An upgraded installation is not additionally adjusted (e.g., by fixture dimming).
2. Optimization of an installation: The scope of this process may vary depending on a particular case, from appropriate lamp dimming and changing the fixture mounting angles or arm lengths to displacement of selected poles. Note that, due to the certain limitations of HID sources, an HID-based installation should be migrated to LEDs prior to luminous flux adjustments.
3. Introducing control systems: This most advanced approach to upgrading a lighting installation performance can be made at several levels. In the simplest case, it relies on scheduling, where luminous fluxes change according to the predefined rules at fixed hours [11,12] and do not depend on actual environment conditions such as traffic flow intensity, ambient light level or weather conditions. In the advanced scenarios, a lighting installation performance is adjusted dynamically on the basis of environment state's changes reported by a telemetry layer (induction loops, weather and occupancy sensors, etc.).

As CO_2 and other GHG emissions are linearly dependent on the energy usage, we made a parallel analysis of both. This analysis was based on the real-life retrofit, the details of which are presented in Section 3.

In this work, we propose the way of linking a quantitative analysis of financial aspects of a lighting installation retrofit with considerations on an environmental influence (in terms of CO_2 emission) of such a modernization. Thus, an environmental influence can be included quantitatively in a retrofit strategy planning. The goal of this work was threefold: (i) finding an impact of the above three retrofit approaches on the resultant CO_2 emissions, in terms of their volumes; (ii) finding which lighting classes [13] contribute the most, in the context of emission reduction, to the final financial gains; and (iii) how the reduced CO_2 emissions change the annual costs of a lighting installation performance.

This article is structured as follows. In Section 2, we overview the approaches listed above and present estimations of expected energy savings for each of them. Section 3 contains the case study of the retrofit carried out in Cracow, Poland. Beginning with the presentation of its background, we show how particular strategies (i.e., relamping, adjusting lighting installations, and introducing control capabilities) decrease power usage and thus the GHG emission volumes. The extrapolation of results to the scale of a lighting system of the entire city is also presented. Further, we convert CO_2 emission volumes to the costs related to the corresponding emission allowances. We show that those costs can reach 10% of savings achieved thanks to decreased power usage. In Section 4, we discuss obtained results. The final conclusions are contained in Section 5.

2. Retrofit Strategies–State of the Art

In this section, the detailed overview of retrofit approaches enumerated in the previous section are presented. The relevant GHG emission reductions are expressed in terms of power reduction ratios as the GHG emissions can be simply obtained on this basis.

2.1. Light Sources Replacement

Replacing HID-based luminaires (in particular, the HPS sources) with LEDs is a common retrofit pattern. What is interesting, due to the significant financial benefits, the municipalities decide to install LEDs, even if the end of an HPS fixtures' life cycle is not reached.

Typically, during an HID to LED migration, conversion charts provided by lamp vendors are used (see Table 1). Such a chart allows finding, for a given HID lamp's power, a rough estimation of an equivalent (in terms of a desired luminosity) LED's wattage to be installed.

Table 1. HID to LED conversion chart [14].

HID System	HID Wattage [W]	LED Wattage [W]	Savings
70 W Pulse MH	88	53	40%
100 W Pulse MH	129	53	59%
150 W Pulse MH	190	80	58%
250 W Pulse MH	291	156	46%
320 W Pulse MH	368	232	37%
400 W Pulse MH	452	309	32%
70 W HPS	85	53	38%
100 W HPS	115	53	54%
150 W HPS	170	103	39%
250 W HPS	300	183	39%
400 W HPS	465	309	34%

Although the unit savings shown in Table 1 are, as mentioned, only the rough estimations supplied by a specific manufacturer, they express the order of magnitude of available power reduction ratios. For the considered example, those ratios vary between 32% and 59%. It is obvious that total power savings for any real-life case will depend on both the lighting system structure, i.e., the ratios of particular fixture types being retrofitted, and the installation's size.

2.2. Lighting Design Tunning

Power savings can be obtained thanks to a well suited lighting design. It is achieved by adjusting lamp parameters such as the fixture's photometric solid, dimming, pole height, arm length, fixture's mounting angles, etc. The above installation tuning may be done according to the either standard or customized design approach. In the first case, one assumes regularity and uniformity of a lighting situation, namely, a constant road width and evenly spaced luminaires (Figure 1a). In the second approach, an actual roadway layout is assumed (Figure 1b).

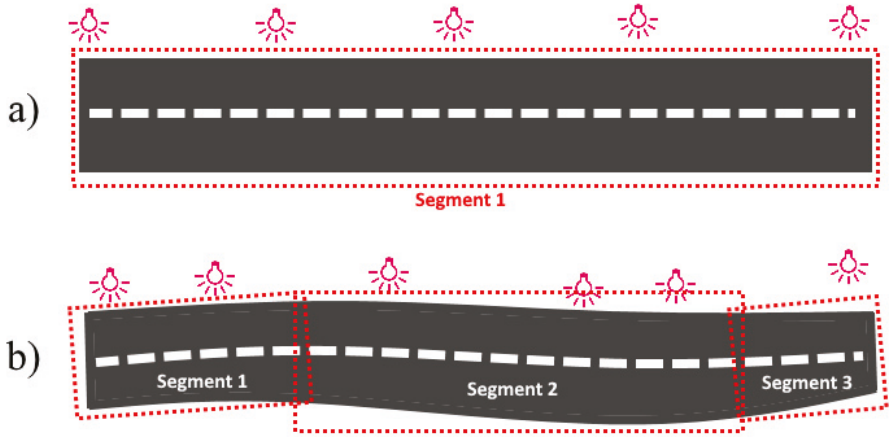

Figure 1. The typical (**a**) and customized (**b**) approaches to photometric computations. In the former case, a roadway layout is uniform (averaged). In the latter, an actual roadway layout used in the computations is decomposed into multiple segments which are processed consecutively.

The former method makes an installation meet performance requirements imposed by a lighting standard and minimize power usage. This approach, as a multivariate optimization, requires advanced software tools capable of solving the problem in an acceptable time. It has to be noted that imposing

uniformity of a lighting situation leads to over-lighting due to the conservative assumptions on the road width and lamp spacing.

The latter design scheme, relying on the different design paradigm, was introduced in the work [15]. In this approach, the lighting situation is regarded strictly as is, i.e., with its actual geometry recovered on the basis of GIS coordinates (Figure 1b). In addition, the coordinates of luminaires are taken from a GIS data repository. In such an approach, the lighting situation is no longer uniform, which means that neither road width is constant nor luminaires are distributed evenly along a road. Although this method implies a significant computational overhead (one has to analyze multiple road segments rather than a single roadway, as shown in Figure 1), the resultant installation's configuration is designed in such a way that over-lighting is minimized. As shown in [15,16], the customized design method reduces a power usage by 15% compared to the standard approach described above.

2.3. Control

While assessing lighting class selection for a given street segment there are certain measurable coefficients that influence this process. One of them is traffic intensity, or volume. Depending on the number of vehicles passing, there could be up to three different lighting classes assigned. Varying lighting classes lead to different dimming settings of the luminaires, which results in energy savings. While assigning a lighting class, the maximum traffic volume should be considered. For such a class, power levels of the luminaires should be selected accordingly by means of photometric calculations. If information about a current traffic volume is available, then changing the classes for a given street segment can be performed efficiently [17,18], which leads to energy savings [19] and CO_2 emission reduction.

Table 2 presents the 24-h lighting class assignment structure and the comparison of obtained savings for various control approaches. The table is made for the arterial road with a dominant lighting class ME2.

Table 2. Different lighting control strategies and corresponding energy saving (lighting classes according CEN/TR 13201-1:2004). Any lighting class change is triggered by a varying traffic volume.

Control Strategy	ME2 [%]	ME3b [%]	ME4a [%]	Energy Saving [%]
Calendar	100	0	0	0
Statistics	46.5	15	38.5	24
Dynamic	27	14	59	34

Remark 1. *It should be noted that the new release of the standard CEN 13201 was issued in 2014 but its Polish localization was published two years later, in 2016. For that reason, the calculations presented below was initially made in accordance with CEN 13201:2004.*

The analysis was based on 100 luminaires and one year worth of traffic data. The *calendar* control strategy assumes that ME2 is assigned regardless of an actual traffic intensity and lighting is turned on at sunset and turned off at sunrise, totaling 4292 on-hours. The *dynamic* assumes reading traffic intensity every 15 min. The lighting classes are adjusted accordingly which leads to the 34% energy saving comparing to the *calendar* approach. ME2 is used 27% of the time, while the lower class, ME3b, is assigned 14%, and ME4a 59%.

In some situations, a statistic approach is also used. In this case, the control is not based on actual traffic volume but on statistical analysis of its historical data records—separately for working days, holidays, Saturdays, and Sundays. Even though it is commonly used, it very often leads to lighting class violations because of a high traffic variability. An actual traffic volume can surpass the statistics based on historical or incomplete data. An example for the aforementioned arterial road is also presented for comparison. For more diverse road and street infrastructure, actual savings obtained by application of dynamic control are expected to be at the level of 27% [20].

The above findings regard CEN/TR 13201-1:2004. The current release of the standard (since 2014) alters number of regulations, lighting class names and their assignment methods, among others. It also introduces a notion of an adaptive control. This gives greater flexibility for dynamic control applicability. A comparison of energy savings achieved thanks to application of a dynamic control, made for a slightly larger and more representative area with variable, high volume traffic, is given in Table 3. There are 210 luminaires installed, with the total power of 26,933 W. The total annual operation time is 4292 h. In this table, we compare the performance structure for both 2004 and 2014 releases of CEN/TR 13201-1. As can be seen, following the 2014 revision leads to significant savings, from 35% to 46%, which gives the motivation to upgrading a lighting infrastructure performance to the new release of the standard. It is mainly due to introduction of maximum traffic capacity indicator on which assignment of lighting classes is based now. The M2 class is assigned 8% of the time only.

Table 3. Dynamic lighting control energy saving for ME2 and M2 base lighting classes; comparison between CEN/TR 13201-1 releases 2004 and 2014.

Standard	ME2/M2 [%]	ME3b/M3 [%]	ME4a/M4 [%]	Energy Saving [%]
CEN/TR 13201-1:2004	50	15	35	33
CEN/TR 13201-1:2014	8	32	59	46

The energy saving is also influenced by the traffic intensity parameters, in particular how often the data are read from sensors and how wide is the averaging time window [20].

3. Case Study

In this section, we analyze in depth the case of retrofit carried out in the city of Cracow, Poland. After making an overview of the lighting system being modernized and the structure of lighting classes of relevant roads (Section 3.1), we analyze how the power usage can be decreased by selecting a given retrofit approach (Section 3.2). Next, those savings are converted into the emission reductions (Section 3.3) and extrapolated to a scale of the entire city area (Section 3.4). In the last subsection (Section 3.5), we assess how a lower CO_2 emission influences an ultimate financial balance.

Remark 2. *It should be stressed here that the emission values presented in this section depend strongly on emission factors which vary for different countries (for details, see [21]). For the purposes of this analysis, we assumed Polish emission factors [22], which are shown in Table 4.*

Table 4. Emission factors for Poland.

Gas	Factor Value [kg/MWh]
CO_2	806
SO_2	0.844
NO_x	0.850
CO	0.260
Particulate matter	0.054

3.1. The Installation's Setup

The modernization of a lighting system covered 3768 out of 80,000 luminaires installed in Cracow. Those sodium fixtures were replaced by LED sources (see Section 2.1). Additionally, newly installed LEDs were dimmed to adjust luminous fluxes to actual needs, defined by relevant lighting classes (see Section 2.2). The charts illustrating the considered system's structure are shown in Figure 2 (the structure of lighting classes (Figure 2a) and powers of HID sources being replaced (Figure 2b)). The circuits were connected to 81 control cabinets.

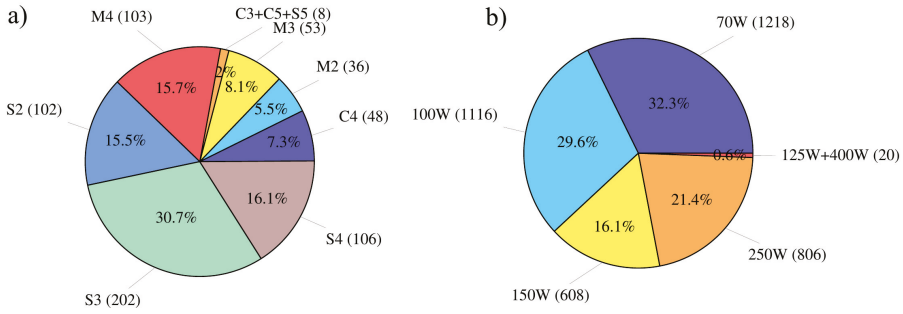

Figure 2. (**a**) Numbers of lighting situations (in parentheses) in the retrofitted area, grouped by lighting classes. (**b**) Numbers of HID fixtures (in parentheses) being replaced in the retrofitted area, grouped by nominal power.

3.2. Power Usage Optimization

The total power of the initial, sodium-based installation was P_{Na} = 311.9 kW. Replacing HID fixtures by non-dimmed LEDs reduced it to P_{LED} = 183.2 kW, and dimming them brought finally P_{LED}^{dim} = 157.8 kW. Average dimming per cabinet varied between 0.63 and 0.97 (where 0 denotes full dimming, i.e., a fixture being switched off, and 1 corresponds to a non-dimmed state). Frequencies of particular dimming ranges are shown in Figure 3.

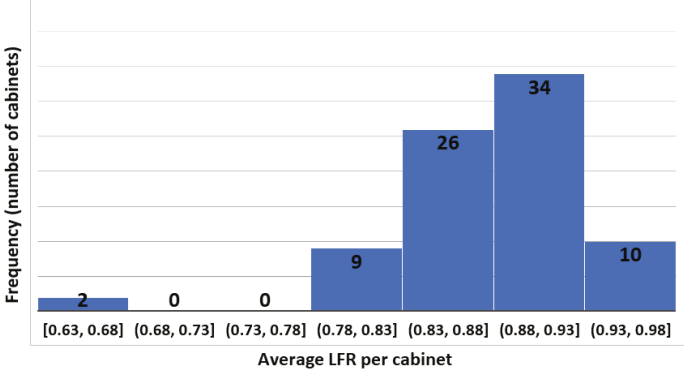

Figure 3. The histogram representing frequencies (bar heights) of average luminaire luminous flux ratios per cabinet.

Taking into account the total annual operation time of the lighting system T = 4292 h [18], the above powers give annual energy usages E_{Na} = 1338.7 MWh, E_{LED} = 786.3 MWh and E_{LED}^{dim} = 677.3 MWh, respectively. Additionally, adding control capabilities to a lighting system reduces E_{LED}^{dim} by 27% (see Section 2.3): $E_{LED}^{dim,ctrl}$ = 494.4 MWh.

3.3. Greenhouse Gas Emission Reductions

Table 5 groups all data obtained in the previous subsection and presents the savings in terms of a GHG emissions reduction, as calculated according to the emission factors for Poland [22] (see Table 4). As shown, replacing HPS fixtures with LEDs gives the 41% reduction while adjusting LED dimmings brings additional 8%, thus reducing the GHG emission corresponding to sodium lamps by 49%. Introducing lighting control increases this ratio to 63%. Thus, finally, we obtain that 1 MT (metric ton) of

CO_2 (the same applies to other greenhouse gases) emitted when producing energy required by sodium vapor lamps is reduced to 0.37 MT of CO_2 for an adjusted, controlled, LED-based lighting installation.

Table 5. The energy usage and GHG emissions corresponding to 3768 lighting points, for four setups: Na (sodium based–before retrofit), LED (relamping only), dimmed LEDs (after additional luminous flux tunning) and dimmed LEDs with control.

	Na	LED	LED Dimmed	LED Dimmed + Control
Power usage [kW]	311.9	183.2	157.8	115.2
Annual Energy consumption [MWh]	1338	786	677	494.4
CO_2 emission [MT]	1079	634	546	398
SO_2 emission [MT]	1.13	0.66	0.57	0.42
NO_x emission [MT]	1.14	0.67	0.58	0.42
CO emission [MT]	0.35	0.20	0.18	0.13
particulate matter [kg]	72	42	37	27

3.4. City-Scale Power and Emission Reductions

Having the reductions achieved for a representative set of lighting situations (in terms of lighting classes and fixture powers) (Table 5), we can estimate the total GHG emission reduction for the entire city with 80,000 luminaires. The results are shown in Table 6.

Table 6. The estimated energy usage and GHG emissions corresponding to 80,000 lighting points, for four setups: Na (sodium based–before retrofit), LED (relamping only), dimmed LEDs (after additional luminous flux tunning) and dimmed LEDs with control.

	Na	LED	LED Dimmed	LED Dimmed + Control
Power usage [MW]	6.6	3.9	3.4	2.4
Annual Energy consumption [GWh]	28.4	16.7	14.4	10.5
CO_2 emission [MT]	22,908	13,455	11,590	8461
SO_2 emission [MT]	23.99	14.09	12.14	8.86
NO_x emission [MT]	24.16	14.19	12.22	8.92
CO emission [MT]	7.39	4.34	3.74	2.73
particulate matter [kg]	1535	901	776	567

Figure 4 gives a more intuitive view of the contributions brought by particular retrofit methods.

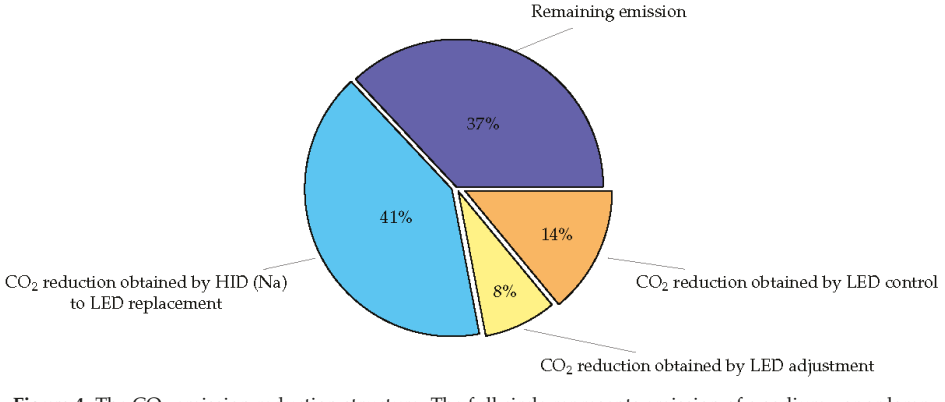

Figure 4. The CO_2 emission reduction structure. The full circle represents emission of a sodium vapor lamp.

An interesting problem related to lighting system retrofit, in the context of GHG emission reduction, is finding the relation between a lighting class of a given area and a potential emission

reduction. This relation can be obtained on the basis of statistical analysis of data gathered for a considered case. Finding this relation allows answering the question of which lighting installations should be upgraded first (e.g., in a situation of limited financial resources) to achieve the maximum environmental impact. Figure 5 presents an annual reduction of CO_2 emission corresponding to the retrofit considered in this case study, broken down into contributions brought by particular lighting classes. As can be seen, the most GHG reduction was contributed by retrofitting roadways/areas of M2 and S2 classes.

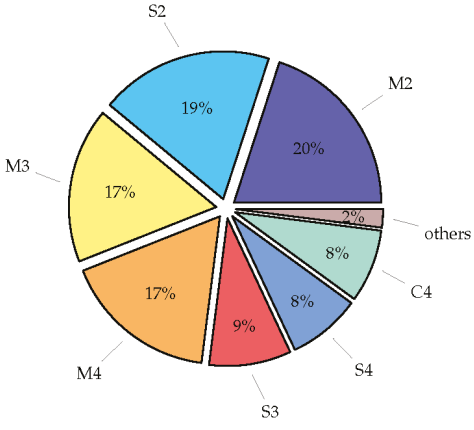

Figure 5. The annual CO_2 emission reduction (full circle) broken down into ratios contributed by particular lighting classes [13].

Figure 6 shows the above results in more tangible form, i.e., in terms of an annual CO_2 emission reduction volume expressed in metric tons per 1000 luminaires.

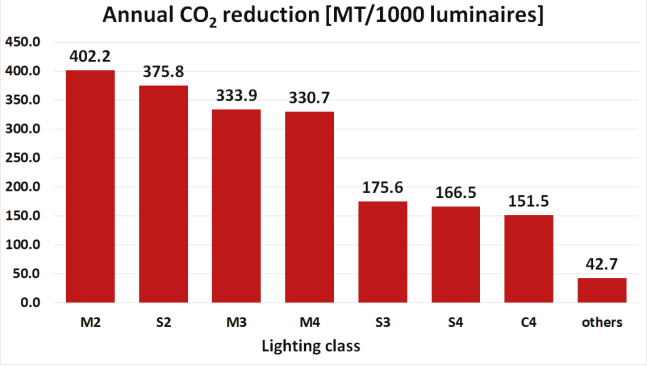

Figure 6. The annual CO_2 emission reduction broken down into volumes (metric tons per 1000 luminaires) contributed by particular lighting classes [13].

3.5. Decreased CO_2 Emission and Financial Savings

Let us compare now the direct financial benefits achieved thanks to the retrofit-based energy savings (i.e., reduced power consumption) and the savings derived from a reduced CO_2 emission, computed on the basis of prices of European Union emission allowances (EEX EUA, or simply "EUA") traded on secondary market. The former component is calculated for the average electricity price for non-household consumers for EU-28 (second half of 2017) which equals €0.14 per kWh [23]. In turn, the EUA price is assumed to be €17.00/MT [24].

The values presented in Table 7 show that, besides the environmental impact, the CO_2 reduction increases by 10% annual profits brought by a retrofit.

Table 7. Annual energy savings and CO_2 reduction in terms of financial benefits. The average electricity price €0.14/kWh for non-household consumers for EU-28 (second half of 2017) and the EUA price €17.00/MT were assumed. Results correspond to data in Table 6.

		LED	LED Dimmed	LED Dimmed + Control
Energy savings	[GWh]	11.7	14.0	17.9
	[€]	€1,641,895	€1,965,936	€2,509,484
CO_2 reduction	[MT]	9453	11318	14,447
	[€]	€160,695	€192,409	€245,607

Remark 3. *The following simple reasoning shows that annual financial savings (S) increased by* $\Delta = 10\%$ *(CO_2-related component) can reduce an investment payback period (T) by 9%. Indeed, if C stands for the retrofit investment costs, then* $T = C/S$. *After increasing an S value by 10%, we obtain:*

$$T' = \frac{C}{S + \Delta \cdot S} = \frac{C}{1.1 \cdot S} = 91\%T.$$

It should be remarked that, since an actual EUA price is subject to stock fluctuations this ratio can change (see Table 8).

Table 8. Retrofit payback growth related to CO_2 reduction vs. EUA price.

EUA Price [€/MT]	10.00	15.00	17.00	20.00
Retrofit payback growth	6%	9%	10%	12%

4. Discussion

Several comments related to the above analysis have to be made.

Volumes of GHG emissions presented in the previous section may be slightly different for other countries due to different structure of energy sources (see [25]) and different emission factors. For example, countries with an overwhelming share of nuclear plants in the total electricity production can have a lower CO_2 emission factor than countries where most electric energy is produced in the coal plants.

As mentioned previously, although lighting class and luminaire power structures of the considered case (see Figure 2) are sufficiently representative for the presented analysis, one has to keep in mind that such an extrapolation estimates results rather than gives the precise values. Regardless, those numbers give a reasonable measure of an overall reduction of a GHG related pollution in the scale of the entire city.

The results shown in Figure 5 correspond to the roadway structure of the city of Cracow and may be subject to changes for a city having a different road network structure. Additionally, municipalities can apply other lighting class assignment policies resulting in dominance of high or low energy demanding classes.

A highly important issue for authorities planning lighting retrofit works are investment costs. One has to be aware that a final decision on retrofit strategy is usually a trade-off between financial constraints and other, non-fiscal (from the investor's perspective) factors such as environment protection. The presented results shed light on how the latter can be taken into account when assessing an investment's financial profitability.

In the presented considerations, we did not discuss maintenance costs of a lighting installation. They are another factor which leads to choosing LEDs [26]. It is worth mentioning that the total maintenance cost savings achieved thanks to upgrading 300 fluorescent tubes with 100 ballasts to

LEDs is over $ 16,500 over an LED lifetime. For the case of HIDs, upgrading 100 bulbs to LEDs yields over $45,000 of the total maintenance cost savings, over an LED lifetime [27].

5. Conclusions

In this work, we considered how modernization of HPS-based lighting installations influences CO_2 emission volumes related to urban roadway lighting. CO_2 and other greenhouse gases emissions are linearly dependent on the energy usage so a parallel analysis of both was made. Our study relied on the real-life case of the retrofit made in the city of Cracow.

In our research, we show that:

1. The highest contribution (41%) to the emission reduction was generated by relamping, i.e. replacing HPS fixtures by LEDs. The next factor (14%) was introducing an adaptive lighting control system. An important condition which was imposed on the control was that the resultant luminaire performances had to comply with the EN 13201-2 lighting standard [13]. In third place (8%) was preparing well suited lighting designs of installation being retrofitted.
2. The most demanding lighting classes (i.e., having the least indices x for Mx, Cx, and Sx) contribute the most to an overall emission reduction. It should be noted, however, that this result cannot be replicable if, for a given city, a number of lighting points illuminating low classes, say M5 or C5, is predominant.
3. The value of emission allowances (with the EUA price at the level of €17.00/MT) corresponding to the reduced CO_2 emission volume, reached 10% of relevant energy savings. This rate yields the 9% reduction of a retrofit payback period.

The presented work links well defined, quantitative analysis of financial aspects of a public lighting retrofit investment with considerations on environmental influence of such a modernization. This link is obtained thanks to assessing the money savings corresponding to a reduced CO_2 emission. Thus the environmental impact can be included quantitatively in the retrofit strategy planning. Moreover, for investments financed in the ESCO (Energy Service Company) model [28,29], we show that a payback period can be shortened by 9% (or even more, taking into account the current trend of the EUA price) thanks to incomes achieved due to the reduced CO_2 emission.

Author Contributions: Conceptualization, A.S.; Data curation, A.B.; Funding acquisition, A.B.; Validation, A.B.; Writing—original draft, I.W.; Writing—review & editing, A.S.

Funding: This research was funded by The National Centre for Research and Development grant number POIR.01.01.01-00-0037/17-00.

Conflicts of Interest: The author declare no conflict of interest.

References

1. Jiang, Y.; Li, S.; Guan, B.; Zhao, G.; Boruff, D.; Garg, L.; Patel, P. Field evaluation of selected light sources for roadway lighting. *J. Traffic Transp. Eng.* **2018**, *5*, 372–385. [CrossRef]
2. Cacciatore, G.; Fiandrino, C.; Kliazovich, D.; Granelli, F.; Bouvry, P. Cost analysis of smart lighting solutions for smart cities. In Proceedings of the 2017 IEEE International Conference on Communications (ICC), Paris, France, 21–25 May 2017 .
3. Hyari, K.H.; Khelifi, A.; Katkhuda, H. Multiobjective Optimization of Roadway Lighting Projects. *J. Transp. Eng.* **2016**, *142*, 04016024. [CrossRef]
4. Jiang, Y.; Li, S.; Guan, B.; Zhao, G. Cost effectiveness of new roadway lighting systems. *J. Traffic Transp. Eng.* **2015**, *2*, 158–166. [CrossRef]
5. Salata, F.; Golasi, I.; Bovenzi, S.; Vollaro, E.d.L.; Pagliaro, F.; Cellucci, L.; Coppi, M.; Gugliermetti, F.; Vollaro, A.d.L. Energy Optimization of Road Tunnel Lighting Systems. *Sustainability* **2015**, *7*, 9664–9680. [CrossRef]
6. Peña-García, A.; Gil-Martín, L.; Hernández-Montes, E. Use of sunlight in road tunnels: An approach to the improvement of light-pipes' efficacy through heliostats. *Tunn. Undergr. Space Technol.* **2016**, *60*, 135–140. [CrossRef]

7. Sędziwy, A. Sustainable Street Lighting Design Supported by Hypergraph-Based Computational Model. *Sustainability* **2016**, *8*, 13. [CrossRef]
8. Gómez-Lorente, D.; Rabaza, O.; Estrella, A.E.; Peña-García, A. A new methodology for calculating roadway lighting design based on a multi-objective evolutionary algorithm. *Expert Syst. Appl.* **2013**, *40*, 2156–2164. [CrossRef]
9. Clinton Climate Initiative. Street Lighting Retrofit Projects: Improving Performance, while Reducing Costs and Greenhouse Gas Emissions. Available online: https://goo.gl/iV32FL (accessed on 21 January 2018).
10. Molina-Moreno, V.; Leyva-Díaz, J.C.; Sánchez-Molina, J.; Peña-García, A. Proposal to Foster Sustainability through Circular Economy-Based Engineering: A Profitable Chain from Waste Management to Tunnel Lighting. *Sustainability* **2017**, *9*, 2229. [CrossRef]
11. Schréder. Owlet. Available online: http://bit.ly/2Oz2uqk (accessed on 11 August 2018).
12. Philips. CityTouch. Available online: http://www.lighting.philips.com/main/systems/lighting-systems/citytouch (accessed on 11 August 2018).
13. *Road Lighting. Performance Requirements, en 13201-2:2015*; European Committee for Standarization: Brussels, Belgium, 2015.
14. EAOTN. Area/Roadway–HID to LED Equivalency. Available online: http://bit.ly/2OxbOLA (accessed on 29 June 2018).
15. Sędziwy, A. A New Approach to Street Lighting Design. *LEUKOS* **2015**, *12*, 151–162. [CrossRef]
16. Sędziwy, A.; Basiura, A. Energy Reduction in Roadway Lighting Achieved with Novel Design Approach and LEDs. *LEUKOS* **2018**, *14*, 45–51. [CrossRef]
17. Wojnicki, I.; Ernst, S.; Kotulski, L.; Sędziwy, A. Advanced street lighting control. *Expert Syst. Appl.* **2013**, *41*, 999–1005. [CrossRef]
18. Wojnicki, I.; Kotulski, L. Improving Control Efficiency of Dynamic Street Lighting by Utilizing the Dual Graph Grammar Concept. *Energies* **2018**, *11*, 402. [CrossRef]
19. Wojnicki, I.; Ernst, S.; Kotulski, L. Economic Impact of Intelligent Dynamic Control in Urban Outdoor Lighting. *Energies* **2016**, *9*, 314. [CrossRef]
20. Wojnicki, I.; Kotulski, L. Empirical Study of How Traffic Intensity Detector Parameters Influence Dynamic Street Lighting Energy Consumption: A Case Study in Krakow, Poland. *Sustainability* **2018**, *10*, 1221. [CrossRef]
21. United Nations Framework Convention on Climate Change. National Inventory Submissions 2018. Available online: https://bit.ly/2zcY3v5 (accessed on 9 August 2018).
22. The National Centre for Emissions Management. Emission Factors for CO_2, SO_2, NO_x, CO and Particulate Matter (In Polish). Available online: https://bit.ly/2npZjCq (accessed on 9 August 2018).
23. Eurostat. Electricity Price Statistics. Available online: http://bit.ly/2Ou6Mzu (accessed on 13 August 2018).
24. European Energy Exchange Group. European Emission Allowances (EUA). Available online: http://bit.ly/2Oue8CZ (accessed on 13 August 2018).
25. United States Environmental Protection Agency. Greenhouse Gas Equivalencies Calculator. Available online: http://bit.ly/2Oug2DD (accessed on 6 August 2018).
26. Nick Heeringa. Benefits of LED Retrofits—Lower Maintenance Cost. Available online: http://bit.ly/2JgFVlk (accessed on 24 October 2018).
27. Patrick Clouden. Save Big On Maintenance Costs By Retrofitting Your Business Lighting to LED. Available online: http://bit.ly/2Jeopy5 (accessed on 24 October 2018).
28. The European Parliament and The Council. Directive 2006/32/EC on Energy End-Use Efficiency and Energy Services and Repealing Council Directive 93/76/EEC. Available online: http://bit.ly/2Ox5dRa (accessed on 24 October 2018).
29. Asian Development Bank. Led Street Lighting Best Practices. Available online: http://bit.ly/2Ox4Wh6 (accessed on 21 January 2018).

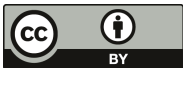

sustainability

MDPI

Article

Evaluation and Improvement of Lighting Efficiency in Working Spaces

Ana Castillo-Martinez [1,*], Jose-Amelio Medina-Merodio [1], Jose-Maria Gutierrez-Martinez [1], Juan Aguado-Delgado [1], Carmen de-Pablos-Heredero [2] and Salvador Otón [1]

[1] Department of Computer Sciences, Polytechnic School, University of Alcala, 28871 Alcalá de Henares, Spain; josea.medina@uah.es (J.-A.M.-M.); josem.gutierrez@uah.es (J.-M.G.-M.); j.aguado@edu.uah.es (J.A.-D.); salvador.oton@uah.es (S.O.)

[2] Faculty of Law and Social Sciences, University Rey Juan Carlos, Paseo de los Artilleros, s/n, 28032 Madrid, Spain; carmen.depablos@urjc.es

* Correspondence: ana.castillo@uah.es; Tel.: +34-918-856-650

Received: 9 March 2018; Accepted: 4 April 2018; Published: 8 April 2018

Abstract: Lighting is an essential element for modern life, promoting a sense of wellbeing for users. However, bad illumination may produce health problems such as headaches and fatigue, among other vision problems. For that reason, this paper proposes the development of a smartphone-based application to help in lighting evaluation to guarantee the compliance of illumination regulations and to help increase illuminance efficiency, reducing its energy consumption. To perform this evaluation, the smartphone can be used as a lighting measurement tool, evaluating those measurements through an intelligent agent based in rules capable of guiding the decision-making process. As a result, this tool allows the evaluation of the real working environment to guarantee lighting requirements, helping in the prevention of health problems derived from bad illumination and improving the lighting efficiency at the same time.

Keywords: mobile device; lighting management; lighting optimization; luxmeter; intelligent agent based in rules

1. Introduction

Lighting is an essential element in modern life with a high impact on three basic human needs: visual comfort to provide a sense of wellbeing, visual performance to allow the carrying out of visual tasks, even in difficult circumstances and for long periods, and security, reducing the risk of suffering an accident. Despite the many regulations which aim to ensure a correct lighting level, in many cases it can be poor or inadequate for users. This problem happens because the regulations don't take into account all the lighting parameters which influence visual comfort, it being necessary to take the measurements in situ [1]. Furthermore, it must be considered that aspects such as sensitivity or character could influence user lighting preferences [2] as well as cultural differences [3]. If we focus on the concept of lighting in workplaces, it is possible to see how proper lighting is essential, allowing users to see without difficulties the tasks being carried out, increasing productivity [4], and reducing accident risk and fatigue. In the same way, bad lighting can cause eye strain, which may involve problems in the eyes (dryness, itching, or burning), headaches, tiredness, irritability, moodiness, etc. Consequently, correct lighting should allow the distinguishing of shapes, colors, and objects in movement and the appreciation of the relief, and furthermore, allow everything to be done easily and without fatigue, i.e., to ensure visual comfort permanently [5].

The evolution of the technology in lighting aims to accomplish three objectives: better photometrical performance, which allows the improvement of the quality of the light regarding

the user's needs, better energy efficiency, offering a higher illuminance with less energy consumption, and improving the performance of users while ensuring the visual comfort in task developing [6].

Moreover, lighting is one of the largest sources of energy consumption in buildings and accounts for 5–15% of the total electric energy consumption [7,8]. For this reason, when we adjust the lighting we have also the opportunity of improving its energy efficiency.

To achieve proper lighting in workplaces, two standards were analyzed: EN 12464-1 [9], which is relative to lighting of indoor workplaces, making special emphasis on the fulfillment of visual comfort and the performance of colors and standard requirements, and EN 12464-2 [10], relative to the lighting of outdoor work places. In both regulations, the lighting requirements are established regarding the activity.

On the other hand, the current mobile phones, or smartphones, are rapidly becoming the primary computing platform for many users [11]. Smartphones have turned out as the key between human interaction and digital devices [12,13].

Keeping in mind the fact of the importance of smartphones, joint with the problems found in lighting management, this research aims to analyze how the development of a mobile application-based intelligent agent based in rules may help to enhance the lighting levels (illuminance) in workplaces, allowing users to manage and assess consumption and providing information about occupational risks prevention.

Mobile applications may create a huge amount of information. To take advantage of this information, a new concept is gaining attention worldwide: open data. This new concept is related to the disclosure and reuse of data for anyone to use to help invigorate society and the economy [14]. The application will be developed with the aim of generating an open data set with anonymous information about lighting measurements performed.

The paper has been divided as follows: Section 2 contains the analysis of prior research made on areas such the existing lighting regulations, lighting evaluation software, or the health problems derived from bad illumination. Section 3 shows the methodology followed to develop the system. Section 4 includes the architecture of the proposed system. Section 5 shows the main results obtained through the mobile application developed and the paper finishes with the discussion and conclusions obtained throughout the research.

2. Prior Research

Prior research has been focused on three different areas. The first point shows European regulations that allow the control of the level of illuminance in different areas. The second point shows the existing software solutions for the lighting evaluation, while the last point carries out a brief study about the health problems derived from bad illumination to highlight the advantages of the proposed tool in the health field.

2.1. Regulations for Lighting Evaluation

Artificial lighting has become in an essential service for modern life. There is no doubt about its benefits, because it allows users to increment the activity in spaces without enough quality of light and also creates a welcoming feeling, making it possible to increment the night activity while reducing crime at the same time [15]. Due to its importance in our lives, it is necessary to control it.

One of the aspects where artificial lighting has a high impact is in energy consumption. Only taking into account the street lighting installations, the amount of energy rises up to 2.3% of the global electricity consumption [16]. To control this amount of energy, different countries have set regulations to help to improve the energy efficiency of its installation. It is the case of the Royal Decree 1890/2008 [17] which established, by the Spanish Government, the standard called EN 13201-5 [18] set by the European Union or the British Standard BS 5489 [19], among others.

Despite energy being an important aspect to take into consideration, mostly in outdoor spaces, there are other regulations to control the amount of light in working spaces in both outdoor and indoor spaces. Here is the case of the EN 12464-1 [9] and EN 12464-2 [10] regulations.

The regulation EN 12464-1 [9] specifies the lighting's requirements for most indoor working places and their associated areas in terms of quantity and quality of lighting. In addition, this regulation gives recommendations for a good practice of lighting through qualitative and quantitative satisfaction.

Another important regulation related to lighting requirements is EN 12464-2 [10]. This regulation allows the guarantee that the visual tasks performed in outdoor spaces can be carried out in an efficient way, especially during night time.

2.2. Light Evaluation Software

There are different programs that must be used to evaluate lighting requirements in different kinds of spaces. Most of those programs allow the performance of a quantitative analysis of scenarios, thanks to their capability of creating a 3D virtual world where lighting effects are recreated and analyzed in both artificial lighting and daylighting scenes [20].

One evaluation software that is used in this field is called RELUX. This software allows users to generate quantitative and qualitative analysis of buildings' lighting thanks to simulation models created with specific materials, colors, reflection factors, and natural and artificial lighting elements to get a closer possible view of reality [21].

Another renowned and well-known tool to evaluate energy efficiency is the SEAD street lighting evaluation toolkit. It can help make better choices regarding street lighting fixtures, which can lead to a maximum of 50% in energy savings [22], by providing an easy way of performing evaluations of light quality, energy consumption, and life cycle costs of efficient street lighting alternatives. This tool is supported by Mexico's National Commission for Energy Efficiency, India's Bureau of Energy Efficiency, Natural Resources Canada, the Swedish Energy Agency, and the U.S. Department of Energy.

Another of the programs used in lighting analysis is called BTwin [23]. It was designed to plan the street lighting installation based on the standard EN 12464-2 [24], as the program can import the manufacturer's luminance information to give more accuracy to the calculations. In addition, an evaluation of the installation's energy efficiency to obtain the energy label before carrying out its implementation can be performed by using the extended feature called AEwin. Vertical obstacles can be considered as well, as they can affect the lighting, and by doing so it is possible to increase the precision of the program.

However, the most important software in this field is called DIALux. The main strength of this software is its complete database about lighting products of the main manufacturers, giving more accuracy to the analysis. It also provides information about power consumption of elements to guarantee compliance with the regulations [25].

2.3. Health Problems Derived from Bad Illumination

Lighting has become one of the most important aspects in efficient building design due to its impact on energy consumption. However, it must be taken into consideration that a good lighting approach should have benefits not only for economic or environmental aspects but also for comfort and health due to its influence on people's quality of life and wellbeing [6,26].

Most office tasks are linked to document processing, whether through paper or digital documents. Therefore, these activities have high visual requirements, making lighting an important factor to prevent discomfort and vision problems.

One of the main lighting problems is derived from over-illumination which occurs due to multiple artificial lights in the ceiling and/or daylight penetrating the room. For example, in a shared space office, the light illuminates not only the cubicle of one worker but also the rest of the cubicles. In addition, the contribution of a light to the light level of the other cubicles is the cross-illumination

effect of the particular light. When these effects arise, lighting control requires a regulation between the lights in order to obtain a desired light level across the room [27].

This situation of over-illumination is linked to several negative health effects. Different studies attribute migraine headaches, fatigue, medically defined stress, anxiety, or decreases in sexual function among others to overly intense light [28–31].

Despite most of these symptoms possibly being caused by light that is simply too intense, the color spectrum of fluorescent lighting is another factor that might cause problems, since this sort of lighting is significantly different from sunlight [28,32]. Fatigue is another common complaint from individuals exposed to over-illumination, especially with fluorescent media. For that reason, natural light is preferred over purely artificial light by office workers from both eastern and western cultures [33].

3. Methodology

Along the study and development of the tool, different hypotheses have been proposed to help analyze the process of data acquisition and subsequent presentation of results. The proposed hypotheses are the following:

Hypothese 1 (H1): *The use of mobile applications could help in the prevention of occupational risks.*

Hypothese 2 (H2): *The use of mobile applications may help on energy saving.*

Hypothese 3 (H3): *Mobile devices can be used by any smartphone user as a fairly accurate light meter tool.*

Hypothese 4 (H4): *The use of mobile applications could facilitate the regulations' fulfillment regarding the illuminance in work spaces.*

Hypothese 5 (H5): *The use of an intelligent agent based in rules could help in decision-making about recommended light intensity.*

Finally, we have developed the system and applied it to a real case in order to obtain the level of the user's degree with the proposed implementation. For this task, we have developed an easy-to-use interface which reduces the transitions between screens.

4. System Architecture

The aim of the application developed is to allow users to ease the evaluation of the lighting requirements needed to perform their work without risk to their health. To help in this issue, a mobile application has been developed for Android platforms, called appLux, which is an intelligent agent based in rules that allows the measurement and evaluation of the illuminance level of each space.

To perform this task, the application measures the illuminance to evaluate a wide range of spaces, making it possible to assess both indoor and outdoor spaces. Along with the measurements, the system provides additional information, giving users a new perspective to help them in the decision-making about increasing or decreasing the illuminance levels. The aim is to keep the spaces with an adequate illuminance level for the workers to ensure their eyes' comfort. This is achieved by the integration of a rule engine in the intelligent agent developed.

To accomplish this objective, an intelligent agent based in rules has been developed where the lighting reference level information, which is stored in the device's database, is compared with the real level, obtained through the illuminance measurement. To perform this comparison, an analysis based on a rule engine has been developed, whose objective is to inform the user about the possible actions to adapt the light to the requirements of the specific scenario. To ensure the level of reference, the stored values for the comparison have been obtained from the European Union regulations (EN 12464-1 [9] and EN 12464-2 [10]), where the minimum illuminance is set.

Thus, the proposed system has been divided into five parts, as can be seen in Figure 1: mobile application, database, light sensor, rule engine, and Web server.

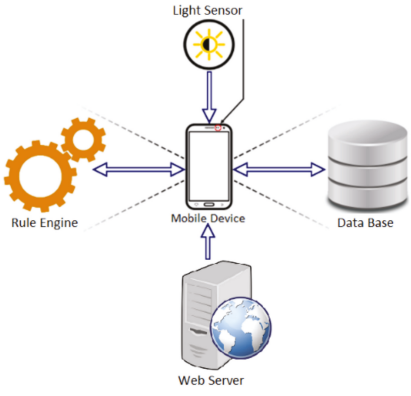

Figure 1. System structure.

4.1. Mobile Device

The application was developed using the Android SDK provided by Google and using Java as the programming language. As the development environment, Android Studio was used since the provided tools integrate seamlessly with IDE using the ADT plugin, which allows debugging code in connected devices and in the emulators included.

At all times, we have followed the design patterns specified by Google for our system, using light colors and maintaining consistency with the rest of the interface devices. The guidance is horizontal because of its greater flexibility of space, and display menus are shown in an intuitive way and leading to a partitioning of space in which several graphs simultaneously are appreciated.

During the development of the application, we have the MVC pattern (Model View Controller), which is very useful to separate the operation of the visual layers. All the logic part was programmed in Java and the visual part was defined with an XML layer, later modified and improved by Java.

4.2. Database

The system is provided with a database used to store information about users' profiles, predefined locations with their light requirements, and information about registered locations and light measurements performed until the date.

The first time the application is running, the database will only have information about the different locations and their characteristics. This information will be the base for the light analysis done by the application.

To ease the use of this tool by different users, it provides a local user register, making it possible to personalize the information about the measurements performed by each user in the same device.

The developed system has two databases. On one hand, a database for the mobile application has been developed using SQLite, since Android has integrated a complete API that allows the management of this kind of database. The main advantages of SQLite, along with the fact that it is open source, are the use of small size records, it meets the SQL-92 standard, and it does not need a server to run [34]. On the other hand, a Web server database was developed to store all the information and share it with other users. At this point, the database was developed using MySQL. In this case, to avoid all the personal information related to the user, it will only store the number of users in the application, making it necessary to check this value each time that a user is registered in the mobile application. In this way, all the information has an anonymous origin, thus fulfilling the Constitutional Law for Data Protection (LOPD) [35].

4.3. Light Sensor

In recent years, smartphones have prevailed as sophisticated, multifunction mobile phones. One of their main advantages is the incorporation of sensors that lets us monitor environmental properties as illuminance or ambient temperature, among others. These sensors are hardware-based and are not available in all of the products; its presence depends on the manufacturer's decision.

An ambient light sensor is a simple sensor included in most of the recent smartphones and is used commonly to control the screen brightness based on the surroundings, therefore saving battery from energy consumption from the screen and at the same time optimizing the visibility [24]. This sensor has been used in different research in different ways to study the color scheme adoption of smartphone displays [36], or to analyze the oscillation movement of coupled springs [37].

Despite the advances performed on this hardware, its accuracy cannot be compared with the accuracy of dedicated hardware devices [34]. However, the results obtained show that it can be useful in practical cases as in the undergraduate physics laboratory [36] where a high level of accuracy is not needed.

Some operating systems, like Android OS, allow the user to obtain the values from the light sensor through APIs which collect data in the runtime of the application. These APIs will return a single value for each data event [24], whereas most motion and static sensors return a multidimensional array of values.

4.4. Rule Engine

The rule engine has a specific function and it may be labeled as the most important piece of the system regarding the application objectives, due to its capability to analyze information and ease decision-making. A rule engine may be viewed as a sophisticated "if/then" statement interpreter. In addition, the rules engine can handle a large number of rules with minimum impact on the normal execution flow of the process [38].

The main task of the rules engine is to ensure that the light values measured by the application are within the proper range. To perform this evaluation, the rules engine has several inputs, such as the measured illuminance, maintained illuminance, or the location characteristics, as well as the XML with the rules to perform the evaluation. Once the inputs have been analyzed, the results will show the recommended actions to guarantee the proper illuminance (Figure 2). Among the actions recommended by the application are: reducing or increasing the power of the lamp to adapt the lighting to the requirements of the regulation, reducing or increasing the distance from the light source, moving closer to or farther from the windows, or using light dimmers.

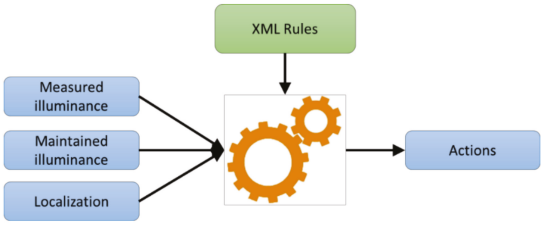

Figure 2. Rules engine working chart.

The selected rule engine was JRuleEngine, due to its open license, availability of source code, and practicality in the development of rules which may be described through an XML file. The Algorithm 1 shows an example of a rule extracted from the XML file. In this case, the rule checks if the level of measured light is correct. To perform this evaluation, the value measured is compared with maximum and average levels of illuminance required by the space regarding its specifications.

As a result, if the measured level is between those two levels, the rule will call to a method that will inform the user that the level is correct.

Algorithm 1. Rule example

```
<rule name="RuleGoodIlluminance" description="Good illuminance control, well done.">
<if leftTerm="illuminati.getE" op="&lt;=" rightTerm="illuminati.getEmax"/>
<if leftTerm="illuminati.getE" op="&gt;=" rightTerm="illuminati.getEm"/>
<then arg1="-1" method="illuminati.addAdvice"/>
</rule>
```

4.5. Web Server

Despite the main aim of the developed application being to help in the evaluation of the lighting requirements of different working spaces, there are others interests behind the development of the application. One of those aims is to evaluate the level of compliance of the directives that regulate the lighting levels through the measurements performed by users. To make this possible, the user must accept sharing voluntarily the information captured by the application for their use in future research projects. To protect users' anonymity, all the data is sent to the server in an anonymous way, according to Spanish Organic Law 15/1999 on the Protection of Personal Data (LOPD) [35].

With the information collected through application usage, it is possible to perform different studies about lighting as well as the effect of climatological conditions on the lighting of the working spaces, or to study the level of regulations compliance in different areas.

To collect the data, a Web server, which was developed as a PHP Webpage where all the information is stored on a MySQL database, was created in [39].

The obtained results can set the basis for future research, as it happened in some studies performed where it was shown that the improvement of the light quality in health centers have a positive impact on the reduction of the hospital stays and increase in the outsourcing of treatment for many patients. For that reason, the server was created with an option to download the information related to the measurements performed with the application. To ease the reuse of the information, the Webpage offers several formats such as .txt, json, xml, xlsx, or csv as is shown in Figure 3.

Figure 3. AppLux Server download option.

5. AppLux Mobile Application

There is no doubt that lighting has an essential role in our lives. For this reason, the application developed aims to control the minimum lighting levels in order to guarantee eye comfort at the same time that it helps reduce energy consumption derived from over-illumination. To carry out this task, the application measures the illuminance level of a space and compares it with the minimum level required by regulations according to the locations profiles.

To ease the use of the application, it has been developed with a user register. Thus, the application adapts to the user requirements, showing only the relevant information about the evaluations performed previously, making it possible for the application to be used by more than one user. Due to the high investigation interest, when a new user is registered in the system, he agrees to give the measurement information for research purposes.

From the application, any user can manage their own information through the following options:

- *Create a new location*. Whenever a user wants to perform the analysis of a location that is not in the list, it is possible to register a new one. To create a new location, the following information is required:
    - *Name*. Helps the management of different areas stored on the device.
    - *Space type*. Defines where the activities are carried out, indoors or outdoors.
    - *Area of establishment*. Defines the general purpose of the area.
    - *Zone type*. Regarding the previous value, helps to clarify the task performed in the area.
    - *Dimensions of the space*. To know the amount of measurement points to calculate the average illuminance of the space.
- *Manage location list*. All the locations registered by the user will be shown in a list (Figure 4a). To act on a given location, its name should be pressed. After that, a list of the following actions is shown (Figure 4b):
    - *Edit location information*. It is possible to see and edit the characteristics of the selected location. In addition, the information about the different measurements done in this location can be displayed but never edited.
    - *View location information*. It is possible to access the location information through this option, including the historic values of the light measurements performed on it (Figure 4c).
    - *Measure and evaluate light quality*. To evaluate the illuminance level, a process of measurement is needed (Figure 4d). To start it, the first task is to choose the method to read the illumination from a selector, where there are two options:
        - Manual input.
        - Mobile's ambient light sensor.

      Once the lighting sensor is selected, it is possible to perform the evaluation, comparing two values which are displayed by the application:
        - *Maintained illuminance*: The minimum illuminance required by the regulations for a location.
        - *Current illuminance*: The value registered by the selected sensor.

      To carry out the evaluation, with the values displayed on the screen, it is required that the previous result of the measurement is stored. Once we pulse the button to start the evaluation, the result will be shown in an alert dialog.
    - *Delete locations*. When this option is pressed, all the information related to this location (description and measurements) will be deleted.

One of the most important points of the application is the method to perform the measurement of the illuminance to be able to carry out the evaluation. The importance of performing a good measurement is an important point to be able to compare with those specified in the regulations. To calculate the illuminance of an area, it is necessary to perform different measurements distributed on a grid to guarantee the compliance of the regulation in all the areas. To know where to perform those measurements, the application will give the number of points and their distribution in the area. Thereby, the program will calculate the value as average maintenance illuminance to compare with those defined by the regulations. In addition, the need to enter multiple measured points allows the

uniformity of the area to be calculated. This point is important to guarantee eye comfort and it is another parameter determined by the regulations.

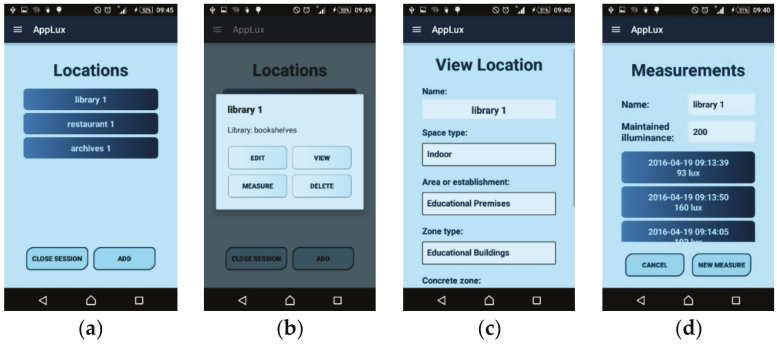

(**a**) (**b**) (**c**) (**d**)

Figure 4. AppLux application's screens. (**a**) Location list; (**b**) Location options; (**c**) View Location; (**d**) New Measurement.

6. Evaluation of the System

As a feedback step, and in order to check the application, it was essential to make a validation to verify its effectiveness. To perform this task, the following reviews were carried out:

- *Lighting measurement evaluation*: Despite allowing the value of the average illuminance to be inserted in the application manually, the application allows users to perform the measurement directly with the smartphone. The method used to measure the illuminance with the device has been tested to check its accuracy.
- *Lighting requirements evaluation*: Studies if the application evaluates properly the lighting requirements, evaluating also the compliance of regulations, in different scenarios.
- *Users' evaluation*: The application is tested by real users to know if it is easy and interesting enough to be used as a lighting evaluation tool.

6.1. Evaluation of the Lighting Measurement

There is no doubt that the data acquisition has an important role in the developed application. For that reason, an evaluation of the accuracy of the application's measurements has been performed. The measurement methodology evaluated is based on the ambient light sensor.

To ensure that the obtained information is as accurate as possible, all the measurements were performed in the same scenario, in a dark room with a light bulb and a dimmer. The light source was a 220 W dimmable incandescent light bulb and it was connected to a dimmer, which controlled the light intensity level as desired. As a reference value for the measurements, the authors used a standard lux meter modeled PCE-174 () [40], which has an accuracy of 5% of reading, which had been previously calibrated.

When the measured data obtained with the smartphone was compared with the data acquired from a reference lux meter, an absolute error of 39.08% was obtained, which was not good enough. Despite this huge difference, when analyzing the data, it is possible to appreciate that the tendency of this measure is similar to the data obtained from the lux meter. This indicates that it is necessary to make the sensor go through a process of calibration to adjust the model developed to the characteristics of the devices. To ensure the accuracy of this calibration, all the measured points were used in order to have a good sample of data, where different lux levels were measured to find the calibration factor of the device. The calibration defines which digital output value relates to which luminance input signal. This relationship between scene luminance and digital output levels of a digital image capture

system is called optoelectronic conversion function (OECF) [21]. Once the calibrated factor is obtained to acquire the real measured data, it is necessary to multiply the measured value by this factor as Equation (1) shows.

$$Lux_{real} = Lux_{measured} \times C_{calibration} \quad (1)$$

After calibrating the measures performed with the calibration factor, the absolute error of the measurements was reduced to 13.74%. However, if we analyze again the accuracy of the data, it is possible to sort out different groups. In the case of the mobile phone used, it was possible to divide the measurements into three groups and recalculate the calibration factor of each one separately, and the accuracy of the sensor can be increased showing an absolute error of 8.41%. The number of groups and the range of the values may vary depending on the device used. Figure 5 shows the data analysis of this measurement methodology.

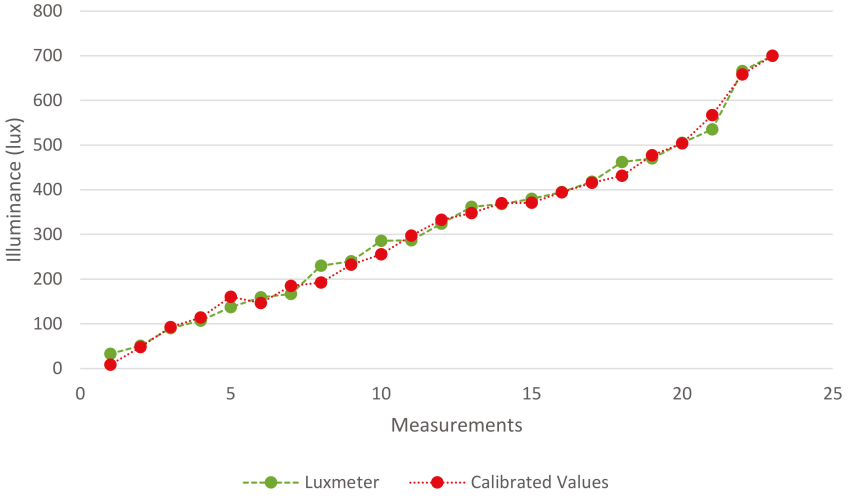

Figure 5. Mobile ambient light sensor vs. Luxmeter.

Due to the importance of good calibration, an option has been integrated into the application to calibrate the ambient light sensor, reducing the error of the measurements.

6.2. Evaluation of the Lighting Analysis

To answer the second question, a practical evaluation of the developed tool was performed. This time the validation was focused on testing if the application was able to analyze the lighting requirements of a working space. Therefore, two different kinds of scenarios were selected:

- *Offices*. In this area, are carried out the tasks of writing/reading documents, mainly with a computer.
- *Common areas*. These sorts of areas are opened to all users of the building. In the case of the evaluation, the sort of common areas used were different halls in the same building.

Despite having shown that it is possible to use the mobile phone as measurement tool, for this evaluation the measurements were taken with a calibrated luxmeter and incorporated into the mobile tool to perform the analysis. As a result, a total of 30 evaluations were divided as shown in Table 1.

Table 1. Lighting evaluations performed.

Sort of Space	Number of Evaluations
Offices	20
Common Areas	10

In order to make a complete evaluation of the analysis performed by the developed tool, and to also evaluate the user satisfaction with the results, the study was divided in two, one for each sort of scenario evaluated.

6.2.1. Offices

To select the scenarios, and in order to evaluate real cases, a survey was performed where users were asked about their interest in checking the lighting conditions of their workplace and if they thought that their level of light could be improved to achieve a better lighting quality. From the survey's respondents a total of 20 random cases were selected from the users who were interested in checking their lighting conditions and who thought that these conditions could be improved.

Once the scenarios were checked with the application, the results were divided into three different groups: places with a correct level of light, places with excess light, and places with a lack of light. Table 2 shows the number of cases selected for each.

Table 2. Lighting evaluation on offices.

Correct Light	Excess of Light	Lack of Light
7	6	7

The first point that must be highlighted is that 35% of the evaluated cases has a level of light in compliance with the standards, even when the users think that the lighting conditions could be improved. On the other hand, the rest of the evaluated cases shows a problem with lighting, where 35% have a lack of light and the other 30% have an excess of light.

As it was said, when the application detects that the lighting requirements do not comply with the lighting regulations, different tips are shown in order to solve the problem. On one hand, in cases of a lack of light, those tips go from the substitution of the lamp for others with higher illuminance, showing as a recommendation LED lamps which have high energy efficiency, to the removing of the protector of the fluorescent lamps. On the other hand, the recommendation in cases of excess illumination are the substitution of the lamp for another with lower illuminance, decreasing at the same time the energy consumption. In the case of the study performed, the replacement of the lamp protections in cases of a lack of light and the substitution of the lamps in cases of excess light were enough to ensure the regulations' compliance. At the end, the solutions carried out not only improve and correct lighting conditions, but also help to reduce the energy consumption.

A few days after correcting the lighting problems, a new survey was conducted to analyze the user satisfaction with the lighting changes. In this new survey, when asked if they could detect the changes in lighting conditions, 69.23% of the respondents detected the differences in the lighting level of their workspaces. After, they were asked about the feeling of improvement of the lighting quality, and 53.84% of the respondents said that the new conditions were better, helping them feel less stress on the eyes. If we make a distinction between cases of excess and lack of light, it is possible to see how the users with a lack of light detect easily the differences in the light, detecting also an improvement in the quality of lighting conditions.

6.2.2. Common Areas

The second kind of scenario selected was common areas. In this case we focused the evaluation on different corridors of the same building with a large influx of users because they connect areas such as coffee shops and classrooms.

To select the specific scenarios to evaluate, a new survey for the users of the building was also performed. This survey asked them about the lighting conditions of different halls of the building and if they thought that their level of light could be improved to achieve a better lighting quality. From the answers of the survey, 10 cases in which users thought that the lighting conditions could be improved were selected.

After checking the scenarios with the developed application, the results were divided once again into three different groups: places with a correct level of light, places with excess light, and places with a lack of light. Table 3 shows the number of cases selected for each.

Table 3. Lighting evaluation on common areas.

Correct Light	Excess of Light	Lack of Light
4	2	4

In this case, 40% of the evaluated cases had a level of lighting that was in compliance with the standards, even when the users thought that the lighting conditions could be improved. On the other hand, the rest of the evaluated cases showed a problem with lighting, where 40% had a lack of light and the other 20% had an excess of light. In cases where the application detected that the lighting requirements did not comply with the lighting regulations, the same corrections as for the office's study were adopted.

After a few days to correct the lighting problems, a new survey between the installation users was conducted to analyze the user satisfaction with the lighting changes. When they were asked if they could detect the changes in lighting conditions, 50% of the respondents claimed that they could detect the difference in the lighting level of their workspaces. Therefore, they were asked about the feeling of improvement of the lighting quality, and only 25% of the respondents said that the feeling was that the lighting conditions had been improved. The most interesting point is that, in areas with an excess of lighting, there was no feeling of improvement of the lighting. This could have happened due to, in most cases, the perception of a lower level of light in common areas being associated with a feeling of insecurity.

6.3. Users' Evaluation

Once the application was developed and had passed through a practical validation, the next step was to perform a validation from the point of view of the user. To perform this evaluation, an experiment where 20 subjects tested the tool was conducted. To be sure about the developed application being easily understood, the selected users had different levels of knowledge about lighting analysis.

During the first step of this evaluation, the application was given to users in order to check the lighting quality of their workspaces. Once the users finished the evaluation, they had to fill out a Likert scale questionnaire (1 to 5) [41] of 9 questions with several questions to evaluate and give their opinion about the application.

Analyzing the results of the questionnaire, it is important to highlight how users qualified the complexity of use of the developed tool as medium, even when users had little knowledge about lighting analysis. Regarding the interoperability with the interface, users marked the application with a 4.37, highlighting the easy use of the application. When they were asked about the reason for their answer, 60% of the respondents highlighted how the interface and the messages shown in the application helped them to use it correctly, rating with a 4.47 the accessibility of the information.

Regarding the question about whether the proposed mobile application reached the aim of easing the measurement of work space illuminance, it was punctuated as 4.72. On the other hand, when asked if the developed application was handy to have as a reference about the level of compliance of the European Standards EN 12464-1 [9] and EN 12464-02 [10], the respondents answered affirmatively with a mark of 4.62. To conclude the questionnaire, the respondents were asked if the recommendations given by the application improved the working lighting environment, which users marked as 4.47.

7. Discussion and Hypotheses Validation

At a methodological level, this work contributes with the presentation and the implementation of an engine of rules that facilitates decision-making in an efficient way, telling users if the lighting complies with the European standard and, in the case of deviation, indicating the value of this.

Regarding the hypotheses proposed previously, they can be answered thanks to the research performed in the study. As for the first hypothesis (H1), which stated that the usage of mobile applications could help in disease prevention, it has been observed along the study that this tool eases occupational health and safety prevention related to lighting. This is possible due to the developed application allowing users to evaluate their lighting levels regarding the task that they perform in the evaluated area, allowing them to obtain a better working environment, and preventing at the same time the possible damage derived from bad illumination. Analyzing the studies performed on real scenarios, it is possible to observe that, in most cases when the lighting has been improved, the users noticed the changes in the lighting and also recognized the improvement of the lighting. This feeling is higher in the case of offices, where 53.84% of users saw the improvements, also recognizing having less eye problems once the lighting requirements were improved.

Regarding the second hypothesis (H2), we can assert that the use of mobile applications may help on energy saving as was probed along the practical evaluation of the tool. It must be taken into consideration the power of this sort of application not only in the evaluation of the measurements, but also in giving tips to improve them. In the case of the application developed, the tips shown in cases of noncompliance of the regulations assisted in the improvement of the lighting quality as well as in the reduction of energy consumption. If we analyze the corrections performed in the cases of study, the results highlight a reduction of energy consumption thanks to the tips offered by the application.

In relation to the third hypothesis (H3), which stated that mobile devices can be used as a fairly accurate light meter tool, we can assert that it is not possible. Despite the study highlighting the use of mobiles devices as measurement tools, the process of calibration could be difficult to be performed by any user, as well as necessitate the use of a calibrated luxmeter as a reference, a device that not all users have at their disposal. Besides, the differences of the hardware of each smartphone model makes setting a process of calibration harder. For these reasons, mobile phones should be used as light measurement tools with medium accuracy and should not be used for situations where high reliability is required unless calibrated.

Concerning the fourth hypothesis (H4), which stated that the mobile applications could facilitate the compliance of lighting regulations in working spaces, along the validation of the study's results, it was observed that the use of this sort of application helps in light measuring tasks and gives more information in order to improve the lighting by providing an orientative value by using the ambient light sensor and a measure of quality by using external sensors.

The last hypothesis studied (H5) stated how the use of an intelligent agent based in rules helps in decision-making, providing information to the user. Along the validation, it was observed that the use of rule engines in the mobile applications allows the user to detect the illuminance variation in working spaces regarding the regulations, making it possible to recommend different alternatives to improve the quality of the light.

On the other hand, the use of a rule engine has allowed the development of an intelligent agent based in rules that compares the values acquired by the sensors with the values of the UNE regulations, helping users to adopt the better option to improve the lighting level.

8. Conclusions

In this research we have designed, developed, and evaluated a new tool based on the usage of lighting sensors, which allows users to evaluate the level of illuminance in both working spaces, outside and inside. So, it allows users to know the degree of compliance of UNE standards, allowing its use in the prevention of occupational risks.

The results suggest that the usage of this tool allows users to obtain, with enough accuracy, the value of the illuminance in a working place. In addition, the rules engine implemented offers useful information through recommendations for improvement, helping with decision-making tasks, allowing the decrease in the number of sick leaves caused by bad lighting in the workplace.

The developed system was evaluated by professionals from two points of view: practical and technical. The results offered some feedback and suggestions about the system. The feedback from caregivers showed that the proposed system can streamline and improve the process of risk prevention due to illumination of jobs and workplaces.

The use of a Web server where all the measurements are performed with the application allows us to collect information about the level of compliance with the standard, and to use this information in other future studies about the compliance of regulations among others.

Acknowledgments: The authors want to thank the effort and the support that University of Alcalá and University Rey Juan Carlos have offered to the Department of Computer Science of UAH and Business Economics Department of URJC in the "CEI 2017 Intelligent Energy" project. V638.

Author Contributions: Ana Castillo-Martinez and Jose-Amelio Medina-Merodio have developed the mobile application used along the experiments and performed the analysis of the results obtained on the different experiments; Jose-Maria Gutierrez-Martinez and Juan Aguado-Delgado have been in charge of the experiments performed, and Carmen de Pablos-Heredero and Salvador Otón have coordinate the work and validated the results.

Conflicts of Interest: The authors declare no conflict of interest.

References

1. Leccese, F.; Salvadori, G.; Casini, M.; Bertozzi, M. Lighting of indoor work places: Risk assessment procedure. *WIT Trans. Inf. Commun. Technol.* **2012**, *44*, 89–101.
2. Chraibi, S.; Lashina, T.; Shrubsole, P.; Aries, M.; van Loenen, E.; Rosemann, A. Satisfying light conditions: A field study on perception of consensus light in Dutch open office environments. *Build. Environ.* **2016**, *105*, 116–127. [CrossRef]
3. Kim, D.H.; Mansfield, K.P. A cross-cultural study on perceived lighting quality and occupants' well-being between UK and South Korea. *Energy Build.* **2016**, *119*, 211–217. [CrossRef]
4. Leblebici, D. Impact of workplace quality on employee's productivity: Case study of a bank in Turkey. *J. Bus. Econ. Financ.* **2012**, *1*, 38–49.
5. Chavarría, R. Iluminación de los Centros de Trabajo; Madrid: Instituto Nacional de los Centros de Trabajo; Notas Técnicas de Prevención NTP 211. 1998. Available online: http://www.insht.es/InshtWeb/Contenidos/Documentacion/FichasTecnicas/NTP/Ficheros/201a300/ntp_211.pdf (accessed on 5 April 2018).
6. Montoya, F.G.; Peña-García, A.; Juaidi, A.; Manzano-Agugliaro, F. Indoor lighting techniques: An overview of evolution and new trends for energy saving. *Energy Build.* **2017**, *140*, 50–60. [CrossRef]
7. Nicol, F.W.M.; Chiancarella, C. Using field measurements of desktop illuminance in European offices to investigate its dependence on outdoor conditions and its effect on occupant satisfaction, and the use of lights and blinds. *Energy Build.* **2006**, *38*, 802–813. [CrossRef]
8. Ryckaert, W.R.; Lootens, C.; Geldof, J.; Hanselaer, P. Criteria for energy efficient lighting in buildings. *Energy Build.* **2010**, *42*, 341–347. [CrossRef]
9. CEN, European Comittee for Standardization. *Light and lighting—Lighting of Work Places—Part 1: Indoor Work Places*; EN 12464–1:2011 CEN; European Committee for Standardization: Brussels, Belgium, 2011.
10. CEN, European Comittee for Standardization. *Light and Lighting—Lighting of Work Places—Part 2: Outdoor Work Places*; EN 12464–2:2007; CEN, European Committee for Standardization: Brussels, Belgium, 2007.

11. Bajad, R.; Srivastava, M.; Sinsha, A. Survey on mobile cloud computing. *Eng. Sci. Emerg. Technol.* **2012**, *1*, 8–19.
12. Park, B.S.; Choi, H.H. Design and implementation of interactive-typed bluetooth device interact with android platform-based contents character. *J. Korea Soc. Comput. Inf.* **2014**, *19*, 127–135. [CrossRef]
13. Hong, S.P.; Kang, S.; Kim, J. Design and implementation of reliable content transaction system in smartphone environment. *Int. J. Smart Home* **2013**, *7*, 333–342. [CrossRef]
14. Thomas, R. *IBM Big Data Success Stories*; IBM: Armonk, NY, USA, 2011.
15. Lorenc, T.; Petticrew, M.; Whitehead, M.; Neary, D.; Clayton, S.; Wright, K.; Thomson, H.; Cummins, S.; Sowden, A.; Renton, A. Environmental interventions to reduce fear of crime: Systematic review of effectiveness. *J. Syst. Rev.* **2013**, *2*. [CrossRef] [PubMed]
16. Reusel, K.V. A look ahead at energy-efficient electricity applications in a modern world. In Proceedings of the European Conference on Thermoelectrics, Bergen, Norway, 16–20 June 2008.
17. FosterREG. Royal Decree 1890/2008, by Approving Energetic Efficiency. Regulation in Outdoor Lighting Installations and Their Complementary Instructions EA-01 and EA-07. In *Energy efficiency in Urban Regeneration Framework Report*; FosterREG: Zagreb, Croatia, 2008.
18. CEN, European Comittee for Standardization. *Road Lighting—Part 5: Energy Performance Indicators*; EN 13201–5:2015; CEN, European Comittee for Standardization: Brussels, Belgium, 2015.
19. British Standard Institution (BSI). *Code of Practice for Design of Road Lighting—Part 1: Lighting of Roads and Public Amenity Areas*; BS 5489–1:2003; BSI: London, UK, 2003.
20. Zatari, A.; Dodds, G.; Rafferty, K.; Robinson, R. Glare, luminance and illuminance measurements of road lighting using vehicle mounted CCD cameras. *J. Illum. Eng. Soc. North Am.* **2004**, *1*, 85–106. [CrossRef]
21. Wüller, D.; Gabele, H. The usage of digital cameras as luminance meters. *Proc. SPIE 6502* **2007**. [CrossRef]
22. Ismail, A.H.; Muhamad Azmi, M.S.; Hashim, M.A.; Ayob, M.N.; Hashim, M.S.M.; Hassrizal, H.B. Development of a webcam based lux meter. In Proceedings of the IEEE Symposium on Computers & Informatics, Langkawi, Malaysia, 7–9 April 2013.
23. Sumriddetchkajorn, S.; Somboonkaew, A. Low-cost cell phone-based digital lux meter. *Proc. SPIE* **2010**, *7853*. [CrossRef]
24. Dhondge, K.; Choi, B.Y.; Song, S.; Park, H. Optical wireless authentication for smart devices using an onboard ambient light sensor. In Proceedings of the 23rd International Conference in Computer Communication and Networks, Shanghai, China, 4–7 August 2014.
25. Manzano, E.R.; Cabello, AJ. Visibility measurements with CCD in road lighting. *J. Ing. Iliminatilui.* **2000**, 59–63. Available online: https://upcommons.upc.edu/bitstream/handle/2117/93852/19anexo6.pdf (accessed on 8 April 2018).
26. U.S. Environmental Protection Agency. Available online: http://www.epa.gov/greenbuilding (accessed on 13 February 2018).
27. Koroglu, M.T.; Passino, K.M. Illumination balancing algorithm for smart lights. *IEEE Trans. Control Syst. Technol.* **2014**, *22*, 557–567. [CrossRef]
28. Baum, A.; West, R.; Weinman, J.; Newman, S.; McManus, C. *Cambridge Handbook of Psychology, Health and Medicine*; Cambridge University Press: Cambridge, UK, 1997.
29. Burks, S.L. *Managing Your Migraine: A Migraine Sufferer's Practical Guide*; Humana Press: Totowa, NJ, USA, 1994.
30. Knez, I. Effects of colour of light on nonvisual psychological processes. *J. Environ. Psychol.* **2001**, *21*, 201–208. [CrossRef]
31. Pijnenburg, L.; Camps, M.; Jongmans-Liedekerken, G. *Looking Closer at Assimilation Lighting*; Venlo, G.G.D., Ed.; Noord-Limburg: Maastricht, The Netherlands, 1991.
32. Boyce, P.R. *Human Factors in Lighting*; CRC Press: Boca Raton, FL, USA, 2014.
33. Edit, N.; Yasunaga, S.; Kose, S. Japanese office employees' psychological reactions to their underground and above-ground offices. *J. Environ. Psychol.* **1995**, *15*, 123–134.
34. Báez, M.; Borrego, Á; Cordero, J.; Cruz, L.; González, M.; Hernández, F.; Palomero, D.; Rodríguez de Llera, J.; Sanz, D.; Saucedo, M.; et al. *Introducción a Android*; E.M.E. Editorial: Madri, Spain, 1997.
35. Estado, J.D. Ley Orgánica 15/1999, de 13 de Diciembre, de Protección de Datos de Carácter Personal. *BOE* **1999**, *298*, 43088–43099.

36. Yu, J.; Chen, Y.; Li, J. Color scheme adaptation to enhance user experience on smartphone displays leveraging ambient light. *IEEE Trans. Mobile Comput.* **2016**, *16*, 688–701. [CrossRef]
37. Sans, J.A.; Manjón, F.J.; Pereira, A.L.J.; Gómez-Tejedor, J.A.; Monsoriu, J.A. Oscillations studied with the smartphone ambient light sensor. *Eur. J. Phys.* **2013**, *34*. [CrossRef]
38. Magaña, C.V.; Organero, M.M. Artemisa: Using and android device as an eco-driving assistant. *JMTC* **2011**, 1–8. Available online: https://e-archivo.uc3m.es/bitstream/handle/10016/13091/android_JMTC_2011.pdf;jsessionid=42076F8E308B9D804693FF56578741D0?sequence=1 (accessed on 8 April 2018).
39. Applux Web Page. Available online: http://applux.pmi-uah.info/ (accessed on 30 March 2018).
40. Luxómetro PCE-174. PCE Instruments, Tobarra, Spain. Available online: https://www.pce-instruments.com/espanol/instrumento-medida/medidor/luxometro-pce-instruments-lux_metro-pce-174-det_91663.htm (accessed on 8 April 2018).
41. Likert, R. *A Technique for the Measurement of Attitudes*; Series: Archives of Psychology, No. 140; The Science Press: New York, NY, USA, 1932.

sustainability

MDPI

Article

Experimental Study of the Levels of Street Lighting Using Aerial Imagery and Energy Efficiency Calculation

Ovidio Rabaza * , Evaristo Molero-Mesa, Fernando Aznar-Dols and Daniel Gómez-Lorente

Department of Civil Engineering, University of Granada, 18071 Granada, Spain; emolerom@ugr.es (E.M.-M.); faznar@ugr.es (F.A.-D.); dglorente@ugr.es (D.G.-L.)

* Correspondence: ovidio@ugr.es; Tel.: +34-958-249-517

Received: 17 September 2018; Accepted: 21 November 2018; Published: 23 November 2018

Abstract: This article describes an innovative method for measuring lighting levels and other lighting parameters through the use of aerial imagery of towns and cities. Combined with electricity consumption data from smart electricity meters, it was possible to measure the energy efficiency of public lighting installations. The results of this study also confirmed that lighting measurements, installation material, luminaire position, and electricity consumption data can be easily integrated into geographic information systems (GIS). The main advantage of this new methodology is that it provides information about lighting installations in large areas in less time than more conventional procedures. It is thus a more effective way of obtaining the data required to calculate the energy efficiency of lighting levels and electricity consumption. There is even the possibility of generating street lighting maps that provide local administrations with up-to-date information regarding the status of public lighting installations in their city. In this way, modifications or improvements can be made to achieve greater energy savings and, if necessary, to correct the distribution or configuration of public lighting systems to make them more efficient and sustainable. This research studied levels of street lighting and calculated the energy efficiency in various streets of Deifontes (Granada), through the use of aerial imagery.

Keywords: street lighting; energy efficiency; aerial imagery; GIS

1. Introduction

The European Union has set itself the ambitious goal of increasing energy efficiency by 20% by the year 2020. Lighting represents approximately 50% of the electricity consumption of cities. Therefore, European cities can play a very important role in reducing their carbon footprint by implementing innovative solutions that respect the environment in public lighting installations. Examples of such solutions are lighting installations powered by renewable sources [1] or the replacement of lamps by others with better chromatic reproduction [2]. More specifically, it was found that for lighting classes with lower luminance levels, metal halides (MH) lamps were economically comparable or even more favorable than high pressure sodium (HPS) lamps.

Now more than ever, after the recent economic crisis, local governments are obliged to reduce their expenses in order to meet their financial commitments. In this regard, one of the largest expenses in towns and cities is energy consumption, especially by public lighting [3]. Another important consideration is the need to comply with local, national and international regulations [4–6] regarding the optimization of lighting levels in order to reduce or eliminate light pollution [7]. Precisely for this reason, administrations must have access to up-to-date information regarding public lighting and light values in order to remedy any actual or potential non-compliance.

This paper presents an innovative method for compiling information on lighting levels, uniformity and energy consumption in geographic information systems (GIS) [8,9]. Such data are extremely useful when performing energy audits of public lighting. All the information is stored as layers, which form maps of public lighting. This method provides valuable data to town and city administrators, who need to know the current state of their street lighting installations. It also generates street lighting maps of their cities with real luminance or illuminance values as well as electricity consumption levels. This information can thus be used to make decisions and carry out corrective actions.

Currently, public lighting maps are based on countless measurements of luminance or illuminance values at street level (obtained with luminance meters or luxmeters). These values are then transferred to a map. Since each measurement must be associated with a value that identifies its geographic coordinates, measurements must also be georeferenced. The number of measurements required for these maps complicates data collection considerably.

Nowadays, the illumination of roads or streets is evaluated with different methods. For example luminance can be determined with spot luminance meters (or photometers), which measure the luminance of a small area [10]. This method involves making many measurements to evaluate the illumination of a road. Other authors [11] measured illuminance levels using a luxmeter placed on top of a moving vehicle and combined measurements with the location data of a distance measurement instrument or GPS. To quickly measure luminance at various points, another alternative is the use of digital cameras [12,13], where a single image evaluates the illumination of a larger road area.

Our study used digital cameras integrated in low-weight drones to take nocturnal orthoimages [14] of streets or roads and thus evaluate their lighting levels. Unlike other options, this method permitted a more rapid evaluation because a single image provided simultaneous information of several streets. The methodology described in this paper allowed us to obtain a large quantity of luminous data. For this purpose, extensive areas were covered in a short time in order to determine the average real values of luminance or illuminance, electricity consumption, and the energy efficiency of public lighting installations. Our research objectives were the following:

- To obtain reliable information that allows local administrations to make decisions about their public lighting, based on knowledge of which areas have correct lighting levels, according to the classification of roads [15].
- To ascertain the energy efficiency levels of public lighting installations in each street and the entire urban area.
- To obtain a decision-making tool for the application of appropriate actions that influence energy consumption and economic savings, and therefore improve the energy efficiency of public lighting installations [16,17].
- To create a tool based on geographic information systems [8,9] with all information pertaining to public lighting installations.

The rest of the paper is organized as follows: Section 2 explains the materials and methods used in the procedure and the background of energy efficiency in street lighting and energy classification. Sections 3 and 4 present the results and discuss them in the context of various examples; and finally, Section 5 lists the most important conclusions that can be derived from this research.

2. Materials and Methods

The general procedure for obtaining lighting levels with airborne digital cameras and estimating energy efficiency levels was composed of the following stages:

- Calibration of the digital camera using light patterns of known luminance. This calibration must be carried out in the final working conditions.
- Capture of nocturnal images (orthoimages) of illuminated streets/roads. The previously calibrated airborne digital camera measures the light reflected by the pavement (luminance of the pavement).

- Calculation of the average values of the lighting parameters in the streets/roads with image processing tools.
- Calculation of the electrical power consumed by the lighting installations on each street, using the smart meters located in the public lighting control boxes. To carry out this calculation, it was necessary to have previously audited the elements of the installation (lamps, auxiliary equipment, etc.). Generally speaking, this work is carried out by the public administration that manages the installation.
- Implementation of the lighting levels, luminaire locations, electrical characteristics of the lighting systems, and power consumed on each street into GIS. With all this information, GIS can automatically calculate the energy efficiency of each street. In the GIS software, equations are used to obtain the energy efficiency levels that must be implemented.

Aerial images (orthoimages) were captured with an airborne digital camera with a 4056 × 3040 pixels CMOS (Complementary Metal-Oxide-Semiconductor) sensor, ISO (ISO is a photographic film's sensitivity to light and acronym of International Organization for Standardization) range of 100–1600/3200 (auto/manual mode) and shutter speed ranging from 8 to 1/8000 s. Regarding optics, the camera has a lens with 85^0 Field of View (FOV) and f/2.8.

Even though this camera is not an instrument that measures luminance magnitude, it is possible to transform it into a photometer [12,18]. The information obtained in each pixel of its sensor can thus be related to the real luminance value of luminance captured in an image. To detect the luminance through any image (object image), we used a standard image of a luminous source of known luminance. Both images (object and standard images) had to be taken under the same conditions (exposure time, ISO value, aperture, camera-object distance, etc.). The luminous source consisted of a system of 15 halogen lamps arranged inside a box and covered by a diffusing screen. As shown in Figure 1, the lamps are connected in parallel to a variable power supply, which provided different luminance values. To ascertain the luminance emitted by the luminous source as a function of electrical power, we used a photometer that measures luminance (see Figure 2) and a wattmeter that measures electrical power.

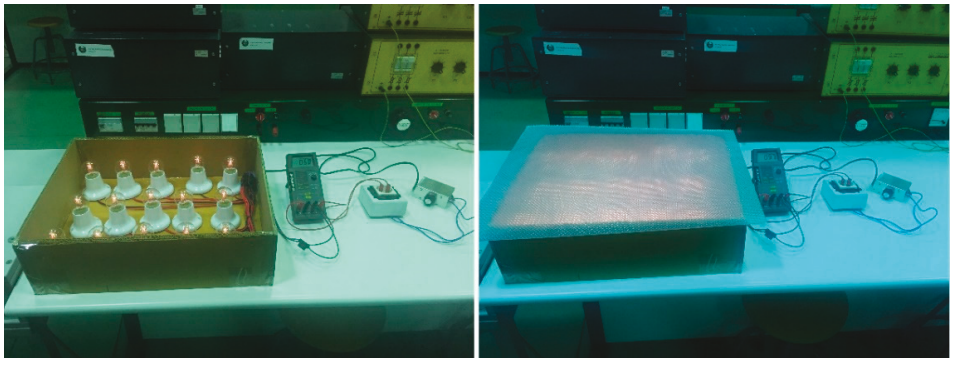

Figure 1. Source used as a luminance pattern. The left image shows the lamp distribution inside the box connected to the wattmeter and a variable power supply. The right image shows the screen diffuser over the box.

Figure 2. Hagner universal photometer S3 used to measure luminance.

2.1. Camera Calibration Procedure

The average luminance values in street lighting range from 0.2 to 5 cd/m^2, depending on the lighting class of the road. This is thus the luminance range of the pattern. To obtain this range of luminance, the lighting source is connected to a variable voltage source. Accordingly, for each voltage or power consumed (measured with a wattmeter), the system emits a certain luminance value. Figure 3 shows the relationship between the luminance emitted and the electrical power consumed. All measurements were carried out in the laboratory, after which a polynomial was formulated to fit them.

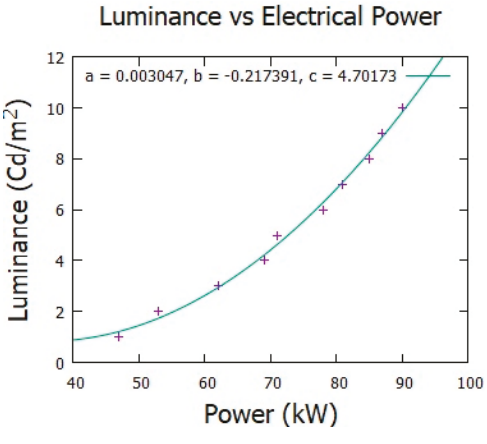

Figure 3. Relationship between the luminance emitted by the standard luminous source as a function of the electrical power consumed and the coefficients of a second-order polynomial ($ax^2 + bx + c$) fit to the measured values.

The exposure time of the camera can be adapted to the luminance level of the road, so as not to saturate the detector. For this same reason, it is also necessary to adapt the luminance of the light source (lighting pattern) to the illumination level of the road. To do this, the voltage of the source is modified where the pattern is connected. The luminance is obtained by reading the wattmeter and applying the polynomial adjustment in Figure 3.

The luminance value in cd/m^2 from *RGB* (*RGB* refers to additive primary colors Red, Green and Blue, a color model used in digital cameras) images is calculated with the following expression [12,15]:

$$L = \frac{Y \cdot f_s^2}{K \cdot t \cdot S_{ISO}} \quad (1)$$

where f_s is the aperture of the camera; t is the exposure time in seconds; S_{ISO} is the ISO value; K is the calibration constant; and Y is the photopic luminance value [19] calculated from the *RGB* color space [20] as follows:

$$Y = 0.2126 \cdot R + 0.7152 \cdot G + 0.0722 \cdot B \quad (2)$$

Accordingly, the calibration procedure involves obtaining the constant K. For this purpose, we employed an image in RAW (RAW format refers to digital natives) format of the luminous pattern. The values R, G and B of each pixel were used to obtain the Y value, and the camera parameters and the known luminance of the pattern were used to deduce the calibration constant. The image processing tool for the treatment of the digital images was IRIS, a software for astrophotography [21]. This software is free for non-commercial usage and is able to process images of different formats, including photographic ones.

2.2. Method for Measuring Road Lighting

According to European standard EN 13201-3 [22,23], the average luminance of a surface must be calculated as shown in Figures 4 and 5. A photometer is used to measure luminance at several points located in an area delimited by two consecutive street lights. The photometer must be at a distance of 60 m from the calculation area and at a height above the ground of 1.5 m. In our case, instead of a photometer we used the airborne camera, calibrated as described in the previous section. However, the procedure followed was the one indicated in the European standard.

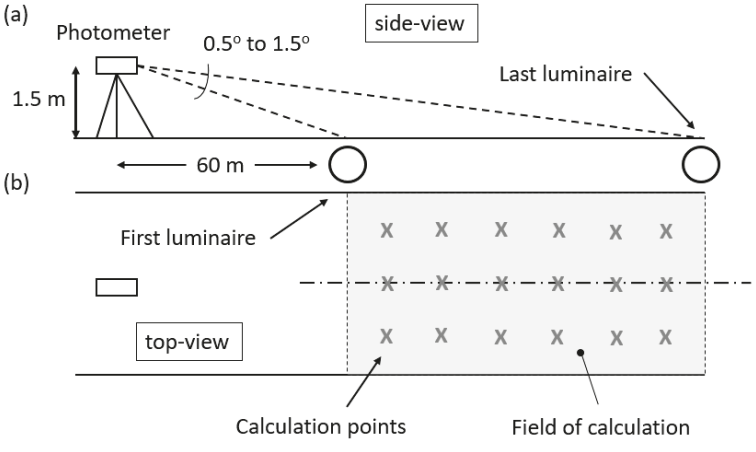

Figure 4. Field of calculation for carriage luminance, where (**a**) is the side-view and (**b**) the top-view.

Figure 5. Digital image in which the calculation area of average luminance is indicated by a red frame. According to the standard procedure the camera is located at a distance of 60 m from the calculation area and at a height of 1.5 m.

2.3. Energy Efficiency of Street Lighting Installation

The energy efficiency of the lighting installation can be defined as follows:

$$\varepsilon_X = \frac{A_T X_{av}}{P_T} \tag{3}$$

where A_T is the total illuminated surface in m^2 of the street; P_T is the total electrical power in watts installed, including the light sources or lamps and electrical auxiliary devices; and X_{av} is the average value (luminance, in cd/m^2, or illuminance, in lx) on the ground. Depending on the road type, the lighting class must be based on the luminance or illuminance magnitude.

A common approach to the energy classification of public lighting installations is the use of the *SLEEC* (street lighting energy efficiency criterion) [5,22] as a whole system indicator, based on the efficiency of the lamp, ballast (when used) and luminaire. The formula for the *SLEEC* indicator (or power density indicator) depends on the photometric measurement (illuminance or luminance) used to calculate street lighting for specific road classes and is the following:

$$SX = \frac{1}{\varepsilon_X} \tag{4}$$

where ε_X is the energy efficiency of the street lighting installation; and X refers to the type of luminous parameter, based on illuminance (E) or luminance (L).

Although the definition of this indicator is still a topic of debate [24], various compatible approaches are currently available (see Table 1), in which *SLEEC* values are combined with the energy labelling system based on the European standard EN 13201-5. As can be observed in Table 1, the lower the consumption is, the better the energy class of the lighting installation. Therefore, the inverse of energy efficiency is a reasonable indicator that can be used to allocate an energy class to the installation.

Lighting engineering software applications base their calculations on data specifications of the street to be illuminated (i.e., dimensions, desired average illuminance, luminaire height in relation to building height, etc.). Another aspect considered is the configuration or arrangement of the installation (one-sided, two-side staggered, two-sided coupled, etc.). The main parameters obtained are the spacing between luminaires and overall uniformity.

Table 1. Energy efficiency classification of street lighting installations according to the street lighting energy efficiency criterion (*SLEEC)* indicator [25].

Energy Class	SE (W/lx·m^2)	SL (W/cd)
A	0.000–0.014	0.00–0.21
B	0.015–0.024	0.22–0.36
C	0.025–0.034	0.37–0.51
D	0.035–0.044	0.52–0.66
E	0.045–0.054	0.67–0.81
F	0.055–0.064	0.82–0.96
G	0.065–0.074	0.97–1.11

Notwithstanding, energy efficiency has become an increasingly important topic. Indeed, in many countries (e.g., the 28 European Union countries), the classification of lighting installations is based on this parameter [5,6]. It is also used in others, such as Australia and New Zealand [26].

2.4. Geographic Information System

The geographic information system used in our research was QGIS [27], a free and open source software. We used QGIS to show different layers with several georeferenced attributes related to the public lighting installation. For each street or road, each layer showed the average luminance or illuminance value, uniformity (ratio of the minimum and average magnitude), position of luminaries, electrical energy consumed by luminaries and along the street, energy efficiency for each street or road, and the corresponding energy class (A, B, C, etc.). Figure 6 shows an example of one of the aerial images georeferenced with the QGIS software.

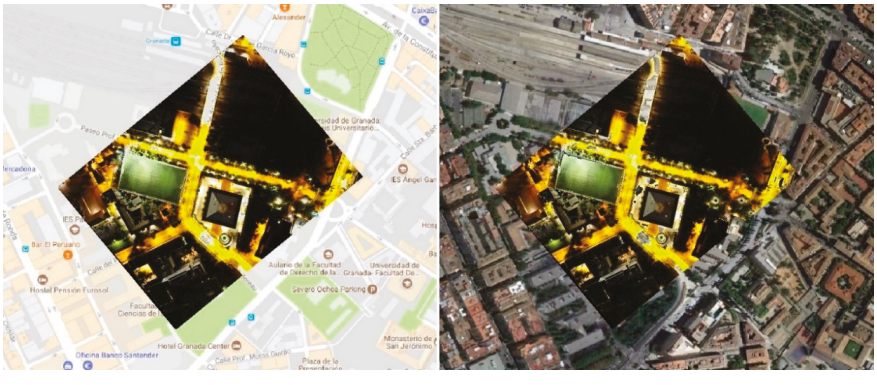

Figure 6. Aerial image taken with an airborne camera. The image was georeferenced with QGIS.

3. Results

3.1. Calibration Constant K

All images had to be captured without saturating the pixels of the camera detector. With this in mind and after several tests, we found that a good compromise was to take images with a maximum exposure time t = 1 s and ISO 1600. The luminance of the light source had to have the same order of magnitude as the lighting levels of the road. The luminance of the source when the tests were performed with the photometer (see Figure 2) was $L = 1.22$ cd/m^2 (the light source consumed an electric power of 47 W). When Equation (1) was applied, the calibration constant of the airborne camera was $K = 0.964$.

As a demonstration of the consistency of the camera calibration, in Figure 7 we can see the luminance value of the light source. Figure 7 shows the relative coordinates of the position in pixels of the light source in the image and the magnitude of its luminance in mCd/m^2.

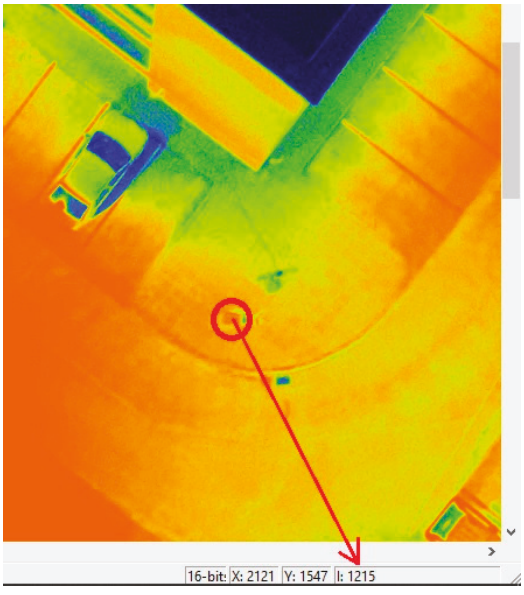

Figure 7. The image processing tool IRIS gives the luminance values at mCd/m^2 emitted by the ground surface. The red circle depicts the position of the light source and the arrow shows the relative coordinates in pixels (X = 2121, Y = 1547) and the luminance value L = 1215 mCd/m^2.

3.2. Luminance Measures from Orthoimages

As mentioned in Section 2.2, the standard procedure for measuring the luminance of the road is not to place the photometer in a vertical position perpendicular to the road surface, but rather to place it horizontally 60 m from the area to be measured, and at a height of 1.5 m. Both methods do not give exactly the same result. Since the surface of the asphalt is not perfectly Lambertian [28], the reflection of the light is a combination of specular and diffuse reflection. This signifies that the light is reflected on the asphalt differently, depending on the direction.

Based on this argument, we calculated the relationship between the measurement from above using an orthoimage (Figure 8) and the measurement obtained with the standard procedure (photometer in an almost horizontal position). For this purpose and as shown in Figure 9, we calculated the average luminance of all the pixels enclosed in the red box. In each image (ortho and horizontal), the statistical analysis of the calculation surface showed that that there was an approximate ratio of 1.06 between the average luminance obtained with the horizontal image and the average luminance obtained with the ortho image. This means that the luminance of ortho images had to be multiplied by a factor of 1.06 to obtain the luminance value, according to the standard road measurement procedure.

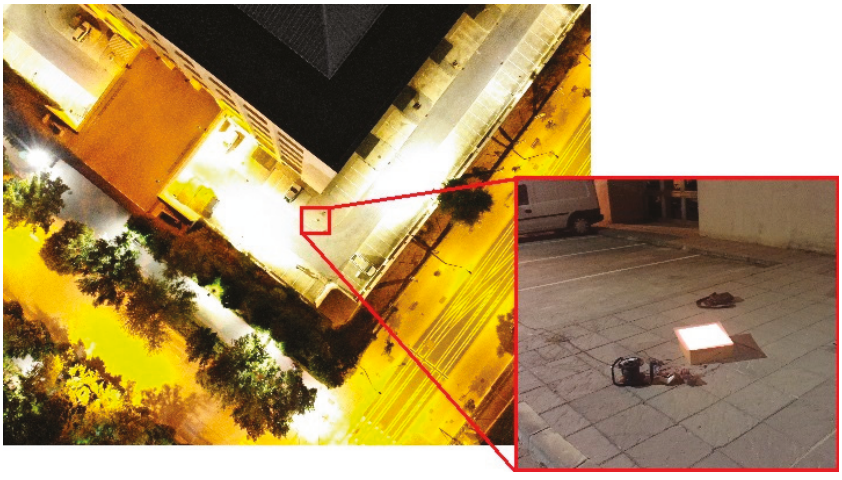

Figure 8. Aerial photo image of the area where the light source and the wattmeter were placed. Depending on the electrical power demanded by the source, we were able to deduce the luminance emitted.

Figure 9. Average luminance and other statistical values (at mCd/m^2) of the calculation area from the aerial image or orthoimage (**a**) and the image where the standard procedure was applied (**b**).

3.3. Examples of Application

The application examples were the study of lighting and energy efficiency of various streets in Deifontes, a town in southern Spain. Specifically, we studied the level of lighting, uniformity, energy consumption, energy efficiency, and energy class (A, B, C, etc.). The results indicated which improvements should be addressed to make the installation more sustainable while maintaining its functional requirements.

As a first step, the image processing software IRIS was used to transform an image in RAW format (Figure 10) into another that showed the reflected light (luminance) of the pavement, due to the information stored in each pixel. The transformation process involved obtaining the value Y for each pixel. Accordingly, Equation (2) was applied, followed by Equation (1) to obtain the vertical luminance value for each pixel. The next step involved multiplication by the correction factor 1.06 to obtain the real luminance value, according to the measurement process in the standard (Figure 11).

Figure 10. Orthoimage of a street obtained by the airborne camera. The image is in RAW format and had not yet been treated with the image processing software.

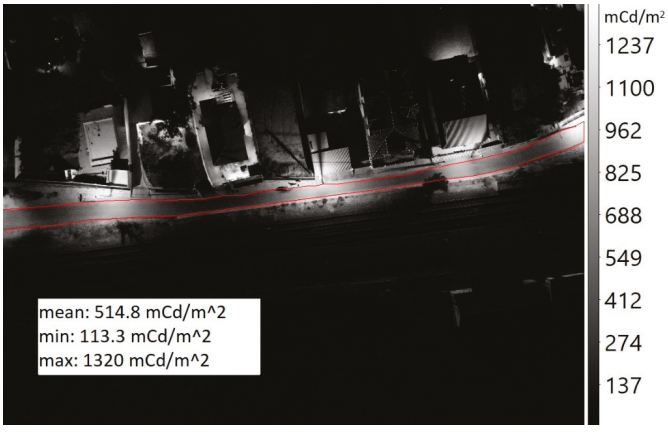

Figure 11. Orthoimage treated with IRIS software and visualized with DS9. The figure shows the luminance values for each pixel and a statistical analysis of the corresponding lighting values of the road (only for the calculation area in the red polygon).

Any astronomical image viewer, such as IRIS or DS9 [29], can give the value of the magnitude in each pixel of the image, as well as a statistical result for all pixels in a large area. These statistical values provide average luminance or illuminance values as well as others that help to calculate lighting quality parameters, such as uniformity in a street or highway.

An example of this is depicted in Figure 11, where the minimum luminance (L_{min} = 0.11 cd/m^2) and the average luminance (L_{ave} = 0.52 cd/m^2) are obtained. These data made it possible to deduce that the luminance uniformity (L_{min}/L_{ave}) in the street sector was 0.22. Obviously these results are not significant because the magnitude values must be calculated for the whole street and not only for one section, but in this case it is an example of the procedure described above.

There are other kinds of lighting whose magnitude of illumination is illuminance. Although luminance and illuminance are two different concepts (light emitted in one direction and light received from all directions), it is possible to relate them by taking certain margins of error into account because, in most cases, pavement characteristics are not known. However, such errors are acceptable in the field of lighting. The relationship between luminance and illuminance is shown in the following equation [15]:

$$L_{ave} = q_0 E_{ave} \tag{5}$$

where L_{ave} and E_{ave} are the average magnitudes in cd/m^2; and lx respectively, and q_0 is the average luminance coefficient. If nothing is known about the reflection properties of the pavement, a coefficient q_0 = 0.07 cd/m^2/lx can be applied [15].

In the following example, the procedure was simultaneously performed on several streets, captured in a single image (Figure 12). Using the previously described procedure, we calculated the luminance values in each pixel and averaged them to obtain the lighting levels of each street.

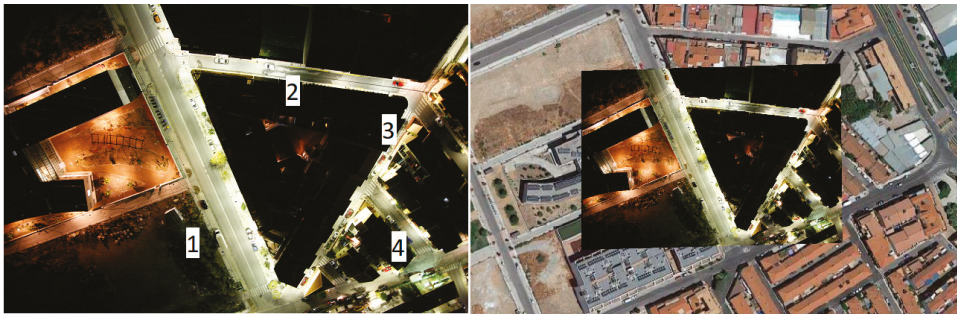

Figure 12. Aerial image in RAW (**left**) and georeferenced (**right**) format

With the luminance values in each pixel, it was easy to calculate the average luminance reflected by the pavement of each street. Equation (5) was applied to obtain the average illuminance value (see Figure 13).

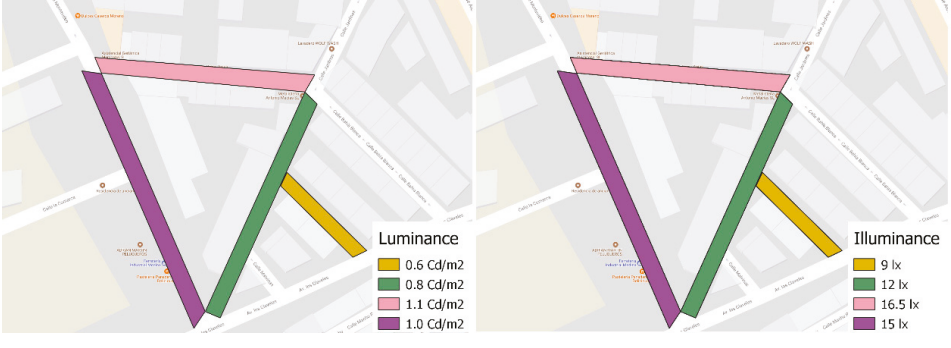

Figure 13. Average luminance (**left**) and illuminance (**right**) levels of some streets.

Another parameter obtained, which is directly related to the quality of street lighting, was the uniformity of the illuminance. This was possible because we knew the minimum illuminance in each street. Figure 14 shows this parameter represented in QGIS together with the position and electrical power of the luminaires.

Figure 14. Illuminance uniformity (**left**) and luminaires position (**right**).

With respect to the energy parameters, Table 2 shows the electricity consumption, the surface to be illuminated, and the average illuminance levels. Equations (3) and (4) were used to calculate the energy efficiency of the installation in each street. The electricity consumption data were obtained from the smart electric meters located in the streetlight control boxes.

Table 2. Lighting and electrical parameters of each street used to calculate the energy efficiency of the installation.

Street	Pavement Area (m^2)	Electrical Power (W)	Illuminance (lx)	SE (W/lx/m^2)	Energy Class
1	890	267.0	15	0.020	B
2	290	191.4	16.5	0.040	D
3	460	182.2	12	0.033	C
4	250	63.0	9	0.028	C

Since we knew the electric power installed in a particular street, it was then possible to calculate its real electricity consumption (from data provided by the smart electric meter). This was done by applying the following equation:

$$P_{M_T} \frac{P_j}{P_T} = P_{M_j} \quad (6)$$

where P_{MT} is the measure of the total electrical power (provided by the smart electric meter); P_j is the known installed power in the "j" street; P_T is the known installed power in all the streets connected to the smart electric meter; and P_{Mj} is the real electrical power calculated in the "j" street. This real electrical power includes the losses of the distribution lines and the actual electricity consumption of lamps and auxiliary equipment of all street lights.

4. Discussion

The standard procedure to obtain illumination levels of a street or road consists of measuring luminance or illuminance with photometers at street level at a few discrete points on the pavement. The standard procedure would be more precise if the number of measurement points was greater. However, this would obviously be a great deal more work. The methodology proposed (see Figure 15) allowed us to obtain the same parameters but with a greater number of measurement points (all pixels of an image or large surfaces such as roads, streets, etc.). This was accomplished by covering a larger

area with a single image captured with an airborne camera. In addition, decision-making capability was improved because geographical information systems were used to implement the levels of lighting and uniformity in addition to the electrical consumption of the installation. This allowed us to calculate the energy efficiency of the installation and its energy class.

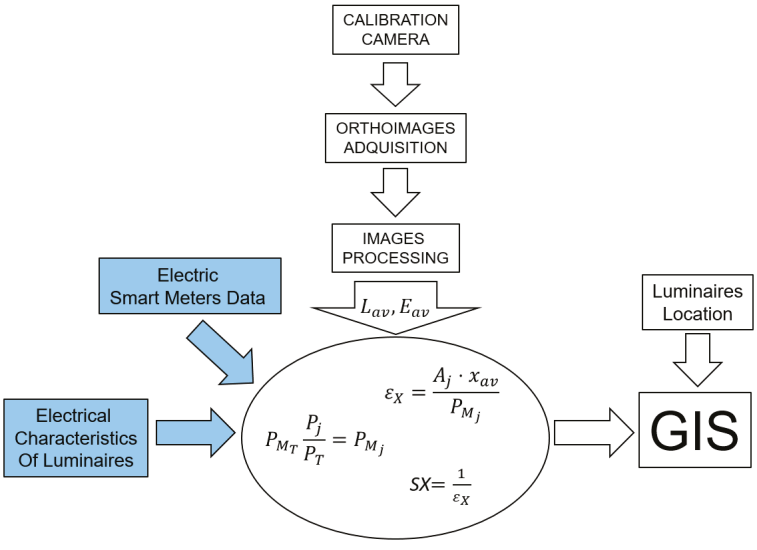

Figure 15. Diagram of the stages of the methodology. The blue boxes indicate the information provided by the local city council.

In the first example, the proposed method was applied to a small section of a street after calibrating the camera. The only information obtained was the luminance (through each pixel of the image) of the pavement. With these data we were able to calculate illuminance and uniformity. In addition, knowledge of the electrical consumption of the luminaires, the electrical energy lost by the distribution lines (electrical energy lost by the distribution lines is calculated by Boucherot's theorem, where $P_{Lines} = P_{Total} - P_{Lamps}$. The P_{Lamps} is obtained through the manufacturer's data sheet and P_{Total} through the smart electric meters located in the street light control box) and the area of the surface to be illuminated made it possible to calculate the energy efficiency of the installation. All of this information was used to ascertain whether lighting levels were optimal or whether there was an excessive consumption of electrical energy.

The second example in Figure 12 focused on pedestrian streets and streets with slow traffic in a residential area. Based on these characteristics, we deduced that the lighting class according to the CIE (CIE refers to Commission Internationale de l´Eclairage, in english International Commission of Illumination.) was P [15] (formerly known as S class). More specifically, it was P2, where the recommended illuminance level is 10–15 lx and the recommended uniformity greater than 0.3.

The information provided by the GIS showed that two of the four streets were correctly lit, whereas one of them (street number 2) was overlit. This clearly indicated the need to reduce either the lighting points or the electrical power of the luminaries. Of these two options, the most successful would be to reduce the electrical power of the luminaires, because removing points of light would lessen uniformity. As shown in Figure 14, the uniformity is at the limit of what is recommended by the standard. Still another reason to reduce the electrical power is the energy efficiency of the installation in that street. Figure 16 shows that its efficiency corresponds to energy class D, which means that there is room for improvement.

Figure 16. Power consumed in each street (**left**) and energy class (**right**).

In contrast, street number 4 was under illuminated. Figures 13 and 14 show that even though the uniformity is correct, it is very close to the minimum because there is only one luminary on the street. The energy efficiency is low but still acceptable. In this case it would be necessary to redesign the street lighting by adding one more luminaire with slightly lower electrical power. This action would improve the level of lighting and uniformity, while maintaining the same energy classification.

5. Conclusions

This research has demonstrated the viability of a method for calculating the energy efficiency of public lighting installations. It also provides a very useful tool that can be used to show their electrical and lighting properties in geographic information systems.

The electricity consumption data were obtained from smart electric meters in the streetlight control box. These meters provide information regarding the entire installation in real time. These consumption data take into account the energy consumed by lamps, auxiliary equipment, and energy losses due to the Joule effect of the distribution lines.

The geometrical distribution of the luminaires, as well as the streetlight control box, were easily georeferenced through the aerial images provided by the camera. Finally, the luminous properties were obtained by calculating the luminance emitted by the surface of the road. For this purpose, it was necessary to calibrate the airborne camera by using the image of a light source of known luminance. The calculation of the energy efficiency is almost immediate based on the electricity consumption, luminance of the road surface, and road surface dimensions.

Another important aspect is the scalability of the method. This procedure can be easily extrapolated to entire neighborhoods or cities because the only difference is the number of images needed to cover the entire metropolitan area. However, the methodology is always the same because each image is analyzed individually.

Author Contributions: Conceptualization, Methodology and Writing-Original Draft Preparation, O.R.; Investigation and Resources, E.M.-M.; Validation and Formal Analysis, D.G.-L. and F.A.-D.

Funding: This research received no external funding.

Acknowledgments: We wish to thank the city council of Deifontes (Granada) and its mayor, Francisco Abril Tenorio, for facilitating the tests carried out in the municipality. We also would like to thank Norberto Laborías Olmedo for the technical support in the Electrical Engineering Laboratory of the University of Granada.

Conflicts of Interest: The authors declare no conflict of interest.

References

1. Sperber, A.N.; Elmore, A.C.; Crow, M.L.; Cawlfield, J.D. Performance evaluation of energy efficient lighting associated with renewable energy applications. *Renew. Energy* **2012**, *44*, 423–430. [CrossRef]
2. Kostic, M.; Djokic, L.; Pojatar, D.; Strbac-Hadzibegovic, N. Technical and economic analysis of road lighting solutions based on mesopic vision. *Build. Environ.* **2009**, *44*, 66–75. [CrossRef]

3. Kostic, M.; Djokic, L. Recommendations for energy efficient and visually acceptable street lighting. *Energy* **2009**, *34*, 1565–1572. [CrossRef]
4. European Commission, DG Environment-C1. Green Public Procurement—Street Lighting and Traffics Lights. Available online: http://ec.europa.eu/environment/gpp/pdf/tbr/street_lighting_tbr.pdf (accessed on 8 August 2018).
5. European Committee for Standardization (CEN). *Road Lighting. Part 5: Energy Efficiency Requirements*; CEN EN 13201:5; CEN: Brussels, Belgium, 2015.
6. Ministry of Industry, Tourism and Trade of Spain. *R.D. 1890/2008 (Regulation of Energy Efficiency in Outdoor Lighting Installations and Their Complementary Technical Instructions EA-01 to EA-07)*; BOE núm. 279; 19 November 2008.
7. Riegel, K.W. Light Pollution: Outdoor lighting is a growing threat to astronomy. *Science* **1973**, *30*, 1285–1291. [CrossRef] [PubMed]
8. Fichera, A.; Inturri, G.; LaGreca, P.; Palermo, V. A model for mapping the energy consumption of buildings, transport and outdoor lighting of neighbourhoods. *Cities* **2016**, *55*, 49–60. [CrossRef]
9. Sedziwy, A.; Kotulski, L. Multi-agent system supporting automated GIS-based photometric computations. *Procedia Comput. Sci.* **2016**, *80*, 824–833. [CrossRef]
10. Ekrias, A.; Eloholma, M.; Halonen, L.; Song, X.J.; Zhang, X.; Wen, Y. Road lighting and headlights: Luminance measurements and automobile lighting simulations. *Build. Environ.* **2008**, *43*, 530–536. [CrossRef]
11. Zhou, H.; Pirinccioglu, F.; Hsu, P. A new roadway lighting measurement system. *Transp. Res. Part C Emerg. Technol.* **2009**, *17*, 274–284. [CrossRef]
12. Vaaja, M.T.; Kurkela, M.; Virtanen, J.P.; Maksimainen, M.; Hyyppä, H.; Hyyppä, J.; Tetri, E. Luminance-corrected 3D point clouds for road and street environments. *Remote Sens.* **2015**, *7*, 11389–11402. [CrossRef]
13. Wüller, D.; Gabele, H. The usage of digital cameras as luminance meters. *Proc. SPIE* **2007**, *6502*, 65020U.
14. Xu, Y.; Knudby, A.; Côté-Lussier, C. Mapping ambient light at night using field observations and high-resolution remote sensing imagery for studies of urban environments. *Build. Environ.* **2018**, *145*, 104–114. [CrossRef]
15. International Commission on Illumination (CIE). *Lighting of Roads for Motor and Pedestrian Traffic*; CIE Public 115; CIE: Vienna, Austria, 2010.
16. Beccali, M.; Bonomolo, M.; Ciulla, G.; Galatioto, A.; Lo Brano, V. Improvement of energy efficiency and quality of street lighting in South Italy as an action of Sustainable Energy Action Plans. The case study of Comiso (RG). *Energy* **2015**, *92*, 394–408. [CrossRef]
17. Carli, R.; Dotoli, M.; Pellegrino, R. A decision-making tool for energy efficiency optimization of street lighting. *Comput. Oper. Res.* **2018**, *96*, 223–235. [CrossRef]
18. Hiscocks, P.D.; Eng, P. Measuring Luminance with a Digital Camera: Case History. Available online: http://www.ee.ryerson.ca:8080/~{}phiscock/astronomy/light-pollution/luminance-case-history.pdf (accessed on 18 August 2018).
19. CIE. *Commission Internationale de l'Eclairage Proceedings, 1924*; Cambridge University Press: Cambridge, UK, 1926.
20. Süsstrunk, S.; Buckley, R.; Swen, S. Standard RGB Color Spaces. In Proceedings of the IS&T/SID's 7th Color Imaging Conference, Scottsdale, AZ, USA, 16–19 November 1999; pp. 127–134.
21. Spectroscopy, CCD and Astronomy. Available online: http://www.astrosurf.com/buil/iris-software.html (accessed on 28 August 2018).
22. European Committee for Standardization (CEN). *Road Lighting. Part 3: Calculation of Performance*; CEN EN 13201:3; CEN: Brussels, Belgium, 2003.
23. International Commission on Illumination (CIE). *Road Lighting Calculations*; CIE Public 140; CIE: Vienna, Austria, 2000.
24. Domke, K.; Brebbia, C.A. *Light in Engineering, Architecture and Environment*; WIT Press: Southampton, UK, 2011; pp. 135–137. ISBN 978-1-84564-550-2.
25. Rabaza, O.; Gómez-Lorente, D.; Pérez-Ocón, F.; Peña-García, A. A simple and accurate model for the design of public lighting with energy efficiency functions based on regression analysis. *Energy* **2016**, *107*, 831–842. [CrossRef]

26. King, B.; Bridger, G. Review of Road Lighting Design Classification System. 2015. Available online: http://www.energyrating.gov.au/document/report-review-road-lightingdesign-classification-system (accessed on 16 August 2018).
27. QGIS. Available online: https://www.qgis.org/en/site/ (accessed on 10 September 2018).
28. Alamdarlo, M.N.; Hesami, S. Optimization of the photometric stereo method for measuring pavement texture properties. *Measurement* **2018**, *127*, 406–413. [CrossRef]
29. SAOImage DS9. Available online: http://ds9.si.edu/site/Home.html (accessed on 10 September 2018).

sustainability

MDPI

Review

A Comparative Study on Current Outdoor Lighting Policies in China and Korea: A Step toward a Sustainable Nighttime Environment

Wu Guanglei, Jack Ngarambe and Gon Kim *

Department of Architectural Engineering, Kyung Hee University, Yongin 17104, Korea
* Correspondence: gonkim@khu.ac.kr

Received: 22 March 2019; Accepted: 16 July 2019; Published: 23 July 2019

Abstract: Light pollution is a serious environmental issue with many adverse effects on human health and the ecosystem as a whole. Accordingly, many countries have issued laws and regulations to limit the effects of artificial lighting at night (ALAN). The Republic of Korea and China are among the few countries that have drafted laws to curb light pollution. In the present study, we gathered data related to light pollution regulations and ordinances in both China and Korea. We then carried out a comparative analysis of the light pollution laws of both countries. We found that, although the two countries share a similar socio-economic background, they have different approaches to the issue of light pollution. The information provided in this study serves as a guideline to countries that wish to develop their own light pollution policies. In addition, the conclusions provided in our study offer potential improvements to local and national light pollution policies in both the Republic of Korea and China.

Keywords: light pollution; ULOR; lighting intensity; outdoor lighting measurements; local laws; landscape lighting; decorative lighting

1. Introduction

Light pollution is one of the most rapidly increasing forms of environmental degradation. There is increasing evidence that draws potential linkages between artificial light at night (ALAN) and certain human health conditions. For example, a study by Rybnikova et al. [1], based on World Bank databases, reported a statistically significant association between ALAN and prostate cancer incidence. A potential correlation between outdoor LAN and breast cancer incidence was also reported by Peter et al. [2]. In addition, ALAN has been linked to diabetes [3], fatigue, and depression [4]. In addition to the effects of ALAN on the well-being of humans, sky glow resulting from ALAN is a major interference to astronomical activities [5,6]. Furthermore, excessive and unnecessary ALAN is a key contributing factor to energy waste [7].

As such, these rapidly increasing adverse effects of ALAN on humans and the general interactions between ecosystems have led to subsequent legal actions against improper usage of light, especially at night. The involvement of governmental institutions, in the form of ordinances or laws against ALAN, has increased over the years [8]. Light pollution laws, ordinances, and prescriptive measures are becoming common in many parts of Europe [9], Asia [10,11], and America [12].

Although the effects of ALAN are primarily the same in all areas, different countries have adopted diverse legal approaches to reduce light pollution. For example, as discussed by Martin-Taylor [13], the United Kingdom has extended the previously existing law on air pollution to include light pollution. Many Italian regions have employed individual ordinances to prevent or reduce specific light-related issues prevalent in given regions [14]. There is a variety of factors that influence the type of light pollution laws employed by a country or region. For instance, bolt-on laws are likely to be less

expensive than stand-alone laws adopted for the specific issue of light pollution [12]. In addition, ordinances are likely to provide better solutions in countries with cities or regions that experience diverse forms of light pollution [14]. China and Korea are among the countries that recently established light pollution preventive measures through city ordinances. Given the social similarities between China and Korea, which may give rise to similar artificial lighting trends, the current study provides a comparative analysis of the Seoul light pollution ordinance and the regional light pollution laws and preventive measures in China. The contents of this study provide an extensive technical guideline to countries or regions that wish to draft their own regional or city-based light pollution laws.

2. Methods

A literature review plays a key role in the field of scientific development [15]. In order to better understand the background of the light pollution policy in China and South Korea, this study searched for relevant information on the website of the Chinese People's Congress, the site of the Shanghai People's Government, the site of the Guangzhou People's Government, Beijing People's Government site, Tianjin People's Government website, and other related websites using the search term "light pollution policy, light pollution law, and light pollution ordinance". We also searched for the legal administration services website in Seoul, South Korea. Furthermore, we used a lot of relevant literature from Google Scholar, MDPI, Elsevier, and other related literature search engines to provide constructive opinions.

3. Seoul Light Pollution Ordinance

The Seoul metropolitan government enacted an ordinance on the prevention and management of light pollution, herein referred to as the ordinance, on 15 July 2010. The purpose of the ordinance is to improve the quality of life for citizens, protect ecosystems, and save energy by preventing unnecessary lighting practices. It is applied under three categories of lighting practices: Space lighting, advertisement lighting, and decorative lighting. In addition, the ordinance classifies all areas in Seoul into four classes based on land usage as dictated by the Korean Ministry of Transport [16]. These classes are known as "light environment management zones". The idea behind light management zones is to allow different levels of lighting in areas that serve different purposes; for instance, lighting levels in a commercial area should be relatively higher than those in a residential area. Permissible lighting levels are, therefore, provided for lighting in each of the four land use categories. Table 1 shows the classification of areas in the city of Seoul based on land usage.

Table 1. Classification of areas for lighting management.

Light Environment Management Zone	Description
Class 1	Green areas for conservation
Class 2	Natural green areas and productive green areas
Class 3	Residential areas
Class 4	Semi-industrial and commercial areas

3.1. Space Lighting

Space lighting includes any type of lighting installed for the purpose of facilitating safe and pleasant nighttime activities and consists of security and road lighting. The Seoul light pollution prevention ordinance specifies the maximum vertical illuminance value for space lighting in each of the four light management zones (illuminance is a measure of photometric flux per unit area or visible flux density. Illuminance is measured in either lux (lm/m^2) or foot candles (lm/ft^2) [17]). This facet of the ordinance mainly addresses light pollution, in the form of light trespass, intruding into enclosed areas at night. Table 2 shows permissible luminance values dictated by the Seoul light pollution ordinance.

Table 2. Permissible luminance values for space lighting.

Light Environment Management Zone	Class 1	Class 2	Class 3	Class 4	
				Semi-Industrial Area	Commercial Area
Maximum vertical illuminance / [lux]	<10	<10	<10	<25	<25

3.2. Advertisement Lighting

The ordinance defines advertisement lighting as lighting devices installed outdoors for advertising purposes [16]. The ordinance provides lighting maximum luminance values that are legally accepted in each light management zone. Table 3 shows the allowable luminance values for advertisement lighting (luminance (Lv) is the density of visible radiation (photopic or scotopic) in a given direction, measured in $lm/m^2/sr$) [17].

Table 3. Permissible luminance values for advertisement lighting.

Light Environment Management Zone	Class 1	Class 2	Class 3	Class 4	
				Semi-Industrial Area	Commercial Area
Maximum luminance / [cd/m^2]	<50	<400	<800	<900	<1000

3.3. Decorative Lighting

Decorative lighting refers to outdoor lighting installed for decorative or recreational purposes [16]. The ordinance provides lighting limits for decorative lighting in the form of mean and maximum permissible luminance values. Table 4 shows the allowable lighting levels for decorative lighting.

Table 4. Permissible luminance values for decorative lighting.

Light Environment Management Zone	Class 1	Class 2	Class 3	Class 4	
				Semi-Industrial Area	Commercial Area
Maximum luminance/ [cd/m^2]	<20	<60	<180	<240	<300
Mean luminance / [cd/m^2]	<5	<5	<15	<20	<30

4. The laws of China

Attention to light pollution is a recent activity in China, and theoretical research results are relatively limited. Light pollution prevention legislation is also scarce. So far, China has not issued special light pollution preventions or control legislation. The current law has failed to effectively solve China's current light pollution problems. Therefore, it is necessary to evaluate the status quo of China's light pollution prevention legislation.

4.1. Relevant Provisions of the Constitution of the People's Republic of China

According to Article 26 [18], "The state protects and improves the environment in which people live and the ecological environment. It prevents and controls pollution and other public hazards". This provision can be regarded as the basis and premise for all laws and regulations on environmental pollution prevention, but it is only a principled provision of the general outline. It does not specify which types of pollution should be controlled. The expression of "other public hazards" is also vague. It cannot be used as a direct legal basis for relief.

4.2. Relevant Provisions of the General Principles of the Civil Law of the People's Republic of China

According to Article 83 [19], "In the spirit of helping production, making things convenient for people's lives, enhancing unity and mutual assistance, and being fair and reasonable, neighboring users of real estate shall maintain proper neighborly relations over such matters as water supply, drainage, passageway, ventilation, and lighting. Anyone who causes obstruction or damage to his neighbor, shall stop the infringement, eliminate the obstruction, and compensate for the damage". Article 83 is a provision on the principles of neighbor relations. The law states that it is necessary to correctly deal with the problem of "lighting" in neighbor relations. The so-called "lighting" means that the light is sufficient without interference from external adverse factors and harmful light. In the current case of light pollution, the court's judgment is mostly based on neighbor relations. Therefore, it is not difficult to see that the limitations of the law in application of the case must first satisfy the condition of occurrence between adjacent real estate. This makes the neighboring right seem to be a little powerless in the relief of light pollution.

4.3. Relevant Provisions of the Property Law of the People's Republic of China

According to Article 90 [20] , "An oblige of immovable shall not, in violation of State regulations, discard solid waste or discharge hazardous substances, such as air and water pollutants, noises, and optical and electromagnetic radiation". In the legislation, the Property Law is the first to incorporate light pollution into the scope of legal regulation. It strictly prohibits destruction of the light environment and sets mandatory restrictions for emitted light. However, the provisions on light pollution in this article are too simple and have obvious limitations. This article stipulates that "obligations" are mainly restricted to real estate owners, and light pollution regulations in China require further improvement.

4.4. Relevant Provisions of the Environmental Protection Law of the People's Republic of China

According to Article 24 [21], "Units that cause environmental pollution and other public hazards shall incorporate the work of environmental protection into their plans and establish a responsibility system for environmental protection, and must adopt effective measures to prevent and control the pollution and harm caused to the environment by waste gas, wastewater, waste residues, dust, malodorous gases, radioactive substances, noise, vibration, and electromagnetic radiation generated in the course of production, construction, or other activities."

4.5. China's Local Laws and Regulations

Although China lacks national laws and regulations on light pollution prevention, the government has introduced many measures to prevent and control light pollution. Table 5 summarizes the lighting specifications issued by four different cities and the regulations and targets related to light pollution. Table 6 summarizes relevant preventive measures and related standards from relevant specifications. These standards illustrate which cities provide more comprehensive and effective measures.

Table 5. Some of the existing regional ordinances against light pollution.

Country	City/Province	Year of Enforcement	Title	Purpose	Departments
China	Shanghai	2011	Measures for the management of glass curtain walls of buildings in Shanghai	To reduce the environmental impact of light reflection and ensure social and public security	Shanghai Municipal People's Government
		2012	Specifications on Urban Environment (Decoration) Lighting	To provide safety, environmental protection, and energy saving	Shanghai Municipal Bureau of Quality and Technical Supervision
		2013	Limits and measurement methods of maximum visible brightness for public places' light emitting diode (LED) panels	To reduce light pollution and interference caused by LED displays and to save energy	Shanghai Municipal Bureau of Quality and Technical Supervision
	Tianjin	2013	Tianjin City Lighting Management Regulations	To improve lighting environments and save energy, while ensuring economic prosperity	Tianjin Municipal People's Government
	Guangzhou	2014	Guangzhou light radiation environment management specifications (draft for comment)	To strengthen the management of light spillage, protect public health, and improve the ecological environment	Guangzhou Environmental Protection Bureau
		2014	Guangzhou outdoor advertising and signboard management methods	To manage outdoor advertisement signboards and to beautify the environment	Guangzhou Municipal People's Government
		2017	Guangzhou building glass curtain wall management measures	To reduce the environmental impacts of light pollution and to ensure public safety	Guangzhou Municipal People's Government
	Beijing	2006	Technical specification of urban nightscape lighting	To provide safety, environmental protection, and energy savings	Beijing Municipal Administration of Quality and Technology Supervision

Table 6. Light pollution prevention measures in various cities.

Strategy	City/Province			
	Shanghai	**Tianjin**	**Guangzhou**	**Beijing**
Urban environmental brightness area division	Yes·	N/A	Yes	Yes
Prevention and control of light pollution in urban environmental lighting	Yes	Yes	Yes	Yes
The maximum value of the upward light output ratio (ULOR) on the luminaire	Yes	N/A	N/A	N/A
Residential lighting	Yes	N/A	Yes	Yes
Public area lighting	Yes	N/A	Yes	N/A
Commercial center lighting	Yes	N/A	Yes	N/A
Administrative office lighting	Yes	N/A	N/A	N/A
Building exterior lighting	Yes	N/A	Yes	Yes
Greenbelt and square landscape lighting	Yes	N/A	Yes	N/A
Illumination of rivers, bridges, ponds, fountains, and other water bodies	Yes	N/A	N/A	N/A
Advertising, signage, display, and logo lighting	Yes	N/A	Yes	N/A
Limits and measurement methods of maximum visible brightness for public places light emitting diode (LED) panels	Yes	N/A	Yes	N/A
Contravention fines	N/A	N/A	Yes	N/A

4.5.1. Urban Environmental Brightness Area Division

According to CIE (Commission Internationale de L'Eclairage) [22], there are four types of environmental regions; namely, a naturally dark environmental region, a low-brightness environmental region, a medium-brightness environmental region, and a high-brightness environmental region, as detailed in the "Guide on the Limitation of the Effects of Obtrusive Light from Outdoor Lighting Installations". Shanghai, Guangzhou, and Beijing also use the division of environmental areas to understand night lighting design and light radiation environmental management [23–25]. Only Tianjin does not categorize brightness areas. Table 7; Table 8 show the division of urban environmental brightness.

Table 7. Division of urban environmental brightness in Shanghai.

Environment Zones	Natural Dark Environment	Low Light Environment	Moderate Light Environment	High Light Environment
Code	**E1**	**E2**	**E3**	**E4**
Description	National parks, nature reserves, and observatories	Suburbs and residential areas	Areas outside the sub-center of the city and corresponding residential areas	City center and business district of the sub-center

Table 8. Division of urban environmental brightness in Beijing.

Environment Zones	Low Light Environment	Moderate Light Environment	High Light Environment
Description	Residential area, leisure area	Common area	Urban center, commercial center

4.5.2. Prevention and Control of Light Pollution in Urban Environmental Lighting

In the prevention and control of light pollution in urban environmental lighting, the laws of Shanghai are clearly against direct light falling into residential buildings. All lighting facilities opposite residential buildings must take corresponding measures to prevent stray light from entering a home. To achieve this goal, building decoration materials should not use floodlighting materials [23]. According to paragraph 2 of article 14 of the Tianjin City Lighting Management Regulations, the establishment of urban lighting facilities shall conform to the control standards of light pollution and shall be coordinated with the surrounding environment [26]. Guangzhou Municipality stipulates that outdoor advertising, sign lighting, etc., should strictly abide by national and local lighting design standards, technical specifications, and light environment control zoning, and a rational selection of lighting sources, lamps, and lighting methods is necessary to reduce the effects of artificial lighting on the environment [24]. Beijing has also imposed restrictions on artificial lighting at night. The specification proposes that light trespass and light interference be considered in the design of lighting systems [25].

4.5.3. The Maximum Value of the Upward Light Output Ratio (ULOR) on a Luminaire

To better view the night sky, the brightness of the earth atmosphere must be reduced, so the upward light output ratio (ULOR) of outdoor lamps is important. Shanghai has a standard for the ULOR of different areas. Only Shanghai has this standard among many cities [23]. Table 9 shows the maximum ULOR of luminaires in Shanghai (the upward light output ratio, sometimes called "upward efficiency of the luminaire", is the fraction of the luminous flux emitted by the lamp going outside the luminaire in the upward direction. It is expressed in per cent [26]).

Table 9. The maximum upward light output ratio (ULOR) of luminaires in Shanghai.

Environment Zones	E1	E2	E3	E4
The maximum upward light output ratio (ULOR) of a luminaire	1	5	10	25

4.5.4. Residential Lighting

Regarding residential lighting, Shanghai, Guangzhou, and Beijing have corresponding regulations, but Tianjin does not. A residential area is a low-light area with low illumination. Shanghai limits the maximum vertical illumination on the surface of a residential building's windows and the maximum light intensity for luminaires that point to the windows of the residential building. This effectively controls the impact of public road lighting [23]. Guangzhou has drafted light radiation environmental management specifications (draft for comment). Lighting-related restrictions in residential areas

have not been separately proposed. However, prohibition of housing, hospital outpatient emergency buildings and ward buildings, teaching buildings, and kindergartens is mentioned in the prohibition range of the glass curtain wall [24]. In the interference light limitation, Beijing has proposed strict control of interference light from night lighting facilities on houses, apartments, hospital wards, etc. The maximum vertical illumination on the windows of residences and hospital wards is given, and the maximum light intensity of the illuminant is directly seen from the inside [25]. Table 10 shows the maximum vertical illumination on windows in Shanghai. Table 11 shows the maximum light intensity limit on windows in Shanghai. Table 12 shows the vertical illumination limit on windows and light intensity of the illuminator on windows in Beijing (light intensity is the amount of visible power per unit solid angle, measured in candelas (cd, or lm/sr) [17]).

Table 10. The maximum vertical illuminance on the surface of a residential building window in Shanghai.

Time	Environment Zones			
	E1	**E2**	**E3**	**E4**
Evening	2 lx	5 lx	10 lx	25 lx
After 23 o'clock	0.5 lx	1 lx	5 lx	10 lx
The latest time to deactivate decorative landscape lighting according to the Shanghai municipal lighting management department is 23 o'clock.				

Table 11. The maximum light intensity limit for a luminaire in a residential building window in Shanghai.

Time	Environment Zones			
	E1	**E2**	**E3**	**E4**
Evening	2500 cd	7500 cd	10,000 cd	25,000 cd
After 23 o'clock	10 cd	500 cd	1000 cd	2500 cd

Table 12. Interference light control in residential rooms and hospital ward windows in Beijing.

	Residential Areas not Adjacent to Streets		Residential Areas Adjacent to Streets	
	Before 23 o'clock	**After 23 o'clock**	**Before 23 o'clock**	**After 23 o'clock**
Vertical illumination on windows	<10 lx	<2 lx	<25 lx	<5 lx
Direct view of the light intensity of the illuminator	<2500 cd	<1000 cd	<7500 cd	<2500 cd

4.5.5. Public Area Lighting

In the lighting restrictions of public activity areas, Shanghai provides lighting requirements for public activity areas and sets illumination standards for grasslands, gardens, platforms, and children's playgrounds, where minimum illumination levels, illumination uniformity, and minimum vertical illumination are proposed [23]. Guangzhou has imposed time limits on nighttime lighting in public areas. It is prohibited to have lighting in public areas from 22:00 to 6:00 in the evening and when it affects the normal rest of the surrounding residents. The luminaires and upward light output ratio (ULOR) of the night illumination of the square should conform to the urban nighttime lighting design specifications and must not cause glare or light environmental effects on pedestrians or motor vehicle drivers [24]. Tianjin and Beijing have not imposed lighting restrictions on public areas. Table 13 shows the minimum illumination limit, illuminance uniformity, and minimum vertical illumination for public areas in shanghai.

Table 13. Lighting requirements for public areas in Shanghai.

Zones	Minimum Illumination Level (lx)	Illuminance Uniformity (E min/E max)	Minimum Vertical Illumination (lx)
Lawn	2	1:6	2
Garden	5	1:6	3
Playground	10	1:6	4

Note: E min refers to the vertical illumination in the direction of observation.

4.5.6. Commercial Center Lighting

Commercial areas are high-brightness areas. The average illuminance level of an entire shopping center (including pedestrian streets) and a square floor in Shanghai is no less than 20lx, and the uniformity (Emin/Eav) is 0.1–0.3. The vertical illumination at 1.5 m above the ground facing the viewing direction should be greater than 16 lx of uniformity (Emin/Eav) ≥ 0.2 [23]. Article 34 of the draft for comments in Guangzhou refers to the timing of signage lighting in stylistic and commercial places. The residential community and surrounding cultural and commercial establishments shall be provided with advertisements and signs that do not have outdoor lighting functions. If the surrounding interference light exceeds the technical requirements and causes complaints from residents, the city management comprehensive law enforcement department shall enforce the relevant regulations. Businesses should deactivate ads, logos, and signboard lighting at night before 23:30. This article only regulates the lighting time of style and commercial venues, which fully reduces residents' complaints and the problem of urban light pollution [24]. No such relevant regulations and restrictions exist in Beijing and Tianjin.

4.5.7. Administrative Office Lighting

Administrative office areas belong to medium-brightness areas. The ambient lighting in the prescribed area of Shanghai should maintain the outdoor lighting level until the turn on/off light period and then reduce the minimum requirements to ensure pedestrians' safety and security. After public illumination is reduced, the average vertical illumination on a floor of an office building or industrial plant floor should be less than 4lx, and the average illumination on the surrounding road should be no more than 2lx. However, this regulation only addresses safety-related issues and does not address lighting restrictions or light pollution restrictions [23]. Other Chinese cities have no laws addressing lighting related to administrative offices.

4.5.8. Building Exterior Lighting

In the architectural exterior lighting restrictions, Shanghai aims to determine the scale and intensity of floodlighting, the scale relationship between objects of floodlighting and the surrounding environment, and the viewing range. The direction of light projection of the building's exterior lighting and the luminaires used should prevent glare and minimize light trespass. If the building facade is illuminated by floodlights, the direct luminous flux outside the illuminated surface should not exceed 25% of the total luminous flux of the fixture. Hospitals and residential buildings should not use floodlighting in outdoor spaces. Shanghai laws also provide maximum limit values for building surface brightness [23]. In addition, Guangzhou City has proposed nighttime lighting requirements for buildings, glass curtain wall buildings, and night illumination of the main part of buildings, hospitals, residential buildings, etc., with a surface material reflectance less than 0.2; floodlighting shall not be used. Floodlight luminaires shall not project the beam into the interior of the illuminated building. The spilled light beyond the illuminated area shall not exceed the design specifications of the urban nightscape lighting. The main part of buildings including hotels should be encouraged to adopt the illuminating night illumination method of façade floodlighting and to use internal light-transmissive lighting. The use of internal light-transmitting illumination should limit internal light transmission

and ambient light brightness and color to prevent the light from being affected by the internal light [24]. Beijing offers a brightness limit for building facades [25]. No regulations have been enacted in Tianjin. Tables 14 and 15 show the maximum surface brightness of buildings in Shanghai and Beijing.

Table 14. Maximum surface brightness of buildings in Shanghai.

Environment Zones	E1	E2	E3	E4
Maximum brightness on the surface of a building	0 cd/m^2	10 cd/m^2	60 cd/m^2	150 cd/m^2

Table 15. Maximum surface brightness of buildings in Beijing.

Environment Zones	Low Light Environment	Moderate Light Environment	High Light Environment
Maximum brightness on the surface of a building	<10 cd/m^2	<20 cd/m^2	<45 cd/m^2

4.5.9. Greenbelt and Square Landscape Lighting

In green space and square landscape lighting, Shanghai proposed that a tree be irradiated from 3m to 5m, and a floodlight should be installed on the ground and not produce glare. Flowers should be illuminated from top to bottom, light sources containing wavelengths harmful to trees should be strictly limited around trees, and lighting time and intensity should be controlled for general trees. Lighting facilities should not be entangled or installed on trees for long periods of time and should not affect the growth of plants [23]. Guangzhou City proposed that glass curtain walls are forbidden to be installed in natural dark areas, such as nature reserves and forest parks [24]. Other regulations have not been raised. Similarly, Beijing and Tianjin did not propose relevant regulations.

4.5.10. Lighting of Rivers, Ponds, Fountains, and Other Water Bodies

Since rivers, bridges, ponds, fountains, and other bodies of water are commonly illuminated, Shanghai has proposed regulations for lighting rivers with seasonal or periodic water level changes. Lighting equipment on river banks and bridges must consider the effects of changes in the water level. Bridge floodlighting illuminates the upper and lower sides of the bridge deck. When the surface of the static water is arranged, the glare of the light source of the lightbox should be avoided [23]. Other cities have not yet established any such regulations.

4.5.11. Advertising, Signboards, Display Signage, and Logo Lighting

In advertising, signboards, display screens, and logo lighting, Shanghai limits self-illuminating billboards and surface brightness of signboards and displays and also gives a maximum for functional lighting of urban commercial areas, public event areas, stadiums, and other places. The maximum vertical illuminance value of nighttime lights (including self-illuminating advertisements, signboards, displays, signs, etc.) relative to the obstacle light is generated at the observer's eyes [23]. Guangzhou City proposed that, to set up a large electronic display of neon light-illuminating materials and video outdoor advertising facilities, its location, brightness, and operating time should meet the technical specifications and light environment control requirements of the area [24]. There are no relevant regulations in Beijing and Tianjin. Tables 16 and 17 show the self-illuminating billboard, signboards, display screen, and logo surface brightness maximum limit and maximum vertical illumination of the interference light produced in Shanghai.

Table 16. Self-illuminating billboard, signboards, display screen, and logo surface brightness maximum limit value in Shanghai.

Environment Zones	E2	E3	E4
Self-illuminating billboard, signboards, display screen, and logo surface brightness maximum limit value	200 cd/m^2	500 cd/m^2	1,000 cd/m^2
According to the regulations on the forbidden zone proposed in the layout plan of the outdoor advertising facilities in Shanghai, national parks, nature reserves, and observatories are prohibited areas.			

Table 17. The maximum vertical illumination of the interference light produced by self-illuminating billboards, signboards, display screens, and logos at the height of the human eye in Shanghai.

Environment Zones	E1	E2	E3	E4
Additional vertical illumination at eye level of 1.5m	1 lx	3 lx	8 lx	15 lx
Note: Refers to values other than those generated by the environment.				

4.5.12. Limits and Measurement Methods of Maximum Visible Brightness for Light Emitting Diode (LED) Displays in Public Places

Shanghai has a limit for the maximum visible brightness of outdoor LED displays when the outdoor natural environment illumination is not more than 200lx (when the outdoor natural environment illumination is greater than 200lx, there is no limit to the maximum visible brightness of LED displays).

The maximum visible brightness of the indoor LED display is limited when the screen environment illumination is not more than 400lx (when the ambient illumination of the screen is greater than 400lx, there is no limit to the maximum visible brightness of the LED display).

The selection of test points was proposed in Shanghai using the measurement method. The test should be performed at multiple points suitable for viewing the display screen or possibly affecting the crowd. The measurement results can be listed or considered as the maximum value.

The measurement of natural environment illuminance was applied to the outdoor screen smoothly, and the position with only natural light outside the room was selected. The horizontal illuminance at 1.5 m from the ground was the natural ambient illuminance of the test site.

The illumination of the ambient environment of the screen was determined by selecting at least four points as close as possible to the periphery of the display screen, measuring the incident illuminance in the normal direction of the screen at each point, and calculating the arithmetic mean to illuminate the ambient environment around the display screen.

In the measurement step, there are four steps: 1. Determine that the running status of the LED display and the displayed image signal are the same as when the display is actually running. 2. Measure the relevant ambient illuminance with an illuminometer and record the ambient illuminance conditions. 3. In the visible range of the LED display audience, select the test point where you may observe the peak brightness of the screen, the position of the test point is extremely high, and the LED screen is tested at this position. 4. In a certain period of time, use the luminance meter to capture the peak brightness on the LED display and record it as L (i). In the measurement of brightness, the optical probe should not collect less than 16 adjacent pixels. You can select N test points and repeat the steps noted above. The luminance peak value L (i) of one test point is obtained (i: 1 ~ N). Then, the maximum visible brightness of the LED display is the maximum value Lmax among the brightness peaks of the N test points [27].

Guangzhou utilizes several outdoor advertising and signboard management methods. In the fourth paragraph of Article 12, lighting of advertisements and signs in the form of LED outdoor electronic displays is prohibited from 22:30 to 7:30 the next day. Similarly, Guangzhou light radiation environment management specifications (draft for comment) Article 33 proposes that outdoor advertising and signs set up in the form of LED outdoor electronic displays are prohibited from 22:30 to 7:30 at night, except airport and train display screens that announce information on stations, bus stops, etc. Guangzhou City only controls the timing of lighting, and there is no objective limit to lighting [28]. Tianjin and

Beijing have not put any regulations on LEDs. Tables 18 and 19 show the maximum visible brightness of outdoor and indoor LED displays in Shanghai.

Table 18. Limit of the maximum visible brightness of outdoor LED displays in Shanghai.

NO	Area S (m^2)	Limit of the Maximum Visible Brightness		
		Commercial Center Area	Public Area	Residential Area
1	S ≦ 10	800 cd/m^2	600 cd/m^2	300 cd/m^2
2	S < 10	600 cd/m^2	400 cd/m^2	300 cd/m^2

Table 19. Limit of the maximum visible brightness of indoor light emitting diode (LED) displays in Shanghai.

NO	Area S (m^2)	Limit of the Maximum Visible Brightness		
		Commercial Center Area	Public Area	Residential Area
1	S ≦ 10	1,200 cd/m^2	800 cd/m^2	400 cd/m^2
2	S < 10	960 cd/m^2	640 cd/m^2	320 cd/m^2

4.5.13. Contravention Fines

In the Guangzhou light radiation environmental management specifications (draft for comment), if a glass curtain wall is installed in a prohibited place, a fine of no more than 50,000 yuan (7450 USD) will be imposed. If a glass curtain wall material that does not meet the requirements is used, a fine of no more than 30,000 yuan (4470 USD) shall be imposed. If light source, lighting, and lighting methods that do not meet the requirements are used, a fine of no more than 30,000 yuan (4470 USD) shall be imposed. If municipal road tunnel lighting adopts a light source that does not meet the requirements for lighting mode, the dimming design does not meet the requirements of the specifications, or if the luminaire is not turned off at night, a fine of no more than 30,000 yuan (4470 USD) shall be imposed. If city night lighting facilities are not closed in accordance with the prescribed time, a fine of no more than 50,000 yuan (7450 USD) shall be imposed. The above noted penalties are imposed by the construction administrative department. Article 37 proposes that, if the existing glass curtain wall is ordered to be rebuilt within a time limit and the builder refuses or does not complete the task by the time limit, a fine of no more than 50,000 yuan (7450 USD) will be imposed. This article details the punishments to be imposed by the administrative department of land and resources. Article 39: The penalties imposed by the administrative departments of forestry and principles shall be as follows. First, those who install glass curtain walls in buildings in natural dark areas, such as nature reserves and forest parks, shall be fined no more than 50,000 yuan (7450 USD). Second, those who use night scene lighting, lighting, and lighting of outdoor advertising in dark environment areas shall be fined less than 50,000 yuan (7450 USD) [24]. Only Guangzhou has put forward relevant contravention fines.

5. Comparative Analysis of the Seoul and Chinese Light Pollution Ordinances

As indicated in Table 7; Table 8, the lighting divisions are listed separately according to the CIE standard for Shanghai and Beijing. Since there is no dark–light area in the Beijing area, it does not appear on the standard. Guangzhou City has proposed to organize the development of light environment control areas with relevant departments. However, the provision does not give a specific division, which cannot constitute legal benefits. By comparison, Shanghai is the most comprehensive in the lighting division, although Seoul City and Shanghai are almost the same. Therefore, China has followed international standards in the lighting division.

In the lighting division, Shanghai has mentioned the maximum value of the upward light output ratio. In road lighting design, people often underestimate the increase in light pollution caused by the

direct upward discharge of lamps [29]. The upward light output ratio is often used to compare these emissions. Cinzano and Diaz Castro [30] suggested that the direction of light emission is important for determining the amount of light scattered in the atmosphere and the size of the contaminated area. The spread of light pollution is also related to the direction of the launch. Therefore, decreasing the light output ratio is necessary to curb light pollution.

Furthermore, in residential lighting, Shanghai not only gives the maximum vertical illumination of windows, but also gives the standard of lighting intensity for residential areas. Falchi et al. [31] reported that human exposure to light at night (LAN) reduces the production and secretion of pineal melatonin (MLT). Restraining the production of MLT requires two optical variables: Light intensity and wavelength. Therefore, an increase in light intensity may inhibit the production of MLT and have serious negative impacts on health. Light intensity has a negative impact not only on humans, but also on animals. Anika et al. [32] experimented with perch, using aquariums to simulate four different light intensities for 14 days of observation. Through analysis, it was found that nighttime melatonin was inhibited as light intensity increased.

Meanwhile, Shanghai has only proposed minimum horizontal illuminance and vertical illuminance, but has not given a maximum limit for public area lighting. It has been documented that the main factor of the human sensation of glare is high light source brightness [33–35], and the overall brightness in human vision is closely related to the feeling of glare [36]. Therefore, Shanghai has not paid much attention to the possibility of glare in public areas. The specification only mentions that the lighting in public activity areas should create a bright, clear, and friendly atmosphere. Therefore, its regulations do not constitute a standard for light pollution. In contrast, Guangzhou has clearly defined a design standard for public areas and proposed night lighting that effectively control the glare and light environment affecting pedestrians and motor vehicles.

However, although the specification mentions that lighting facilities need to meet design standards, the standards are subtly explained. In practical applications, there is a tendency for formalism and lack of maneuverability, and prevention and control of light pollution are not achieved. In addition, since commercial center lighting areas and administrative office lighting areas are in high-brightness areas, neither Shanghai nor Tianjin have given relevant restrictions on light pollution, and no specific solutions have been given. However, Guangzhou has pointed out that specific departments should solve the relevant complaints. As mentioned above in how to resolve related disputes, if there are no clear relevant standards, it is difficult for government departments to convince other departments, which brings difficulties to management. In addition, in green space and plaza landscape lighting, to avoid unnatural plant growth and generation of glare, Shanghai limits the distance, location, and time of illumination. Intense light pollution at night may disturb the growth of plants [37]. More and more artificial lighting is used to grow plants in greenhouses, causing light pollution [38]. Most creatures tend to be active at night, but, unfortunately, night lighting is also the most important for humans. Excessive artificial lighting not only interferes with the growth of plants, but also causes serious damage to the health of birds, fish, insects, and even humans [39–42]. Therefore, a consideration of the effects on the human ecological environment is crucial. Although Shanghai has relatively curbed the production of light pollution, it has not proposed relevant standards. Similarly, Guangzhou has only limited the use of glass curtain walls, and Tianjin has only mentioned the prevention of glare.

In contrast, the emergence of floodlights has increased artistic beauty due to the emergence of modern buildings. Most floodlighting starts at the bottom of the object [43]. This means that most of the luminous flux is directed to the sky, causing it to miss objects, especially in projects where inappropriate design or poor-quality fixtures are often used. This will lead to a huge loss of energy and light pollution [44]. Krzysztof [45] said that the ratio of luminous flux of floodlighting needs to be determined on the surface of the object and named this measure the floodlighting utilization factor, which is part of the luminous flux of an object. Therefore, the portion of light not directed at the object is the loss of luminous flux. He used formulas and computer simulations to calculate the floodlighting utilization factor and loss of luminous flux at different angles of illumination. Thus, the angle, the loss

of luminous flux, and the floodlighting utilization factor can be used to determine the production of light pollution and the loss of energy. In Shanghai, clear regulations and standards are given for the floodlighting utilization factor and loss of luminous flux, which states that the luminous flux outside the building surface must not exceed 25% of the total luminous flux, and it gives the maximum limit of the brightness of a building surface. All in all, this measure can relatively reduce the occurrence of light pollution.

In advertising lighting, both the Illuminating Engineering Society of North America (IESNA) [46] and the International Commission on Illumination (CIE) [22] recommend limiting outdoor lighting. Although both give attention to this issue, the limits given by the two are different. IESNA gives the limitation of surface brightness, while the CIE150 report gives the limits of the brightness and vertical illumination of the sign. We all know that the surface brightness limit term adjusts the brightness of a single sign, while vertical illuminations are used to prevent outdoor light from entering a room [11]. Although the latter is more suitable for evaluating the light intrusion status of advertising signs, Shanghai has not ignored the limitation of surface brightness and provides two limits.

In advertising lighting, Shanghai not only gives the limit values for surface brightness and vertical illumination, but also limits the LED display. In recent years, with the widespread use of LED displays in China, the LED advertising screens arranged in the city have seriously affected the normal life of residents. However, current international standards cannot be fully applied to the pollution status of Chinese cities. Therefore, research on LED display pollution in various cities in China is urgent [47]. LED displays consume 12 times more energy per day than common signage lighting and severely increase the vertical illumination of the building façades in commercial areas, greatly increasing light intrusion [48]. In addition, high-brightness dynamic picture LED displays create visual interference for drivers [49].

In summary, Shanghai has the most comprehensive limits on light pollution, followed by Guangzhou. However, the specifications of Guangzhou City are only drafts and do not have legal benefits. On the official website of the Guangzhou Municipal Government, to communicate with the people in a timely manner and solve problems, the government has a leadership mailbox. Some citizens have asked whether the regulations on environmental radiation management in Guangzhou have been officially promulgated and implemented. What is the basis? The government replied that it does not specifically regulate light pollution. It gives the Guangzhou building glass curtain wall management measures and the Guangzhou outdoor advertising and signboard management methods as measures related to light pollution [50]. However, in these two regulations, only the relevant restrictions of LED display screens and glass curtain walls on second floors are specified in the relevant buildings [28,51]. Finally, it can easily be seen from Table 6 that Beijing and Tianjin have not paid special attention to the relevant regulations on light pollution. Therefore, the relevant specifications given by Shanghai for the light pollution problem are the most comprehensive.

On the other hand, Seoul gives limits not only for decorative lighting, but also for lighting in the overall space. China's local laws and regulations are mainly reflected in one aspect, such as landscape lighting or decorative lighting, which lacks operability. On the contrary, this single mode has given some inspiration to Seoul, such as the ULOR proposed by Shanghai, the intensity of lighting, the brightness of building surfaces, the surface brightness of advertising signs, and the hard regulations related to light pollution. Seoul can improve the effectiveness of its laws and regulations according to the actual situation and the above noted provisions.

6. Recommendations

The authors believe that improving China's light pollution laws and regulations requires improvements to the legislative model, such as special legislation on light pollution. Depending on the actual situation of each city, light pollution impact assessment should be performed according to clear criteria. For example, Seoul proposes that the mayor should strive to maintain the Korean industrial standard street lighting as the standard for light pollution environmental impact assessment and can

seek expert advice accordingly. In addition, special department supervision is needed. For example, Seoul clearly stipulates that the mayor should formulate and implement policies to prevent light pollution and establish a light pollution committee. There should be clear accountability and incentive mechanisms, such as in Seoul, and the mayor may choose to reward those who contribute to the prevention of light pollution [16].

Furthermore, in the actual control, data analysis is needed, and the night sky brightness of different cities is collected to conduct a comparative analysis, and the results are obtained and then controlled point-to-point. For example, Wei Jiang et al. [52] used the Luojia 1–01 satellite to analyze and compare the night sky brightness with the brightness of different degrees in Wuhan, Seoul, Haifa and Mexico.

On the other hand, in future research of laws and regulations, the brightness of the night sky should be compared before and after the data in a range of years, so that the practicability of the current rules can be confirmed—for example, Wei Jiang et al. [53] used the Defense Meteorological Satellite Program Operational Linescan System (DMSP/OLS) for data collection from 1992 to 2012 in assessing light pollution in China based on nighttime light imagery and analyzed the degree of light pollution in various regions of China. It was concluded that China's light pollution has significantly expanded in provincial capital cities in the past 21 years. Therefore, by analyzing this, we can see that the degree of light pollution is on the rise when no relevant light pollution regulations are proposed. In the future, it is necessary to continue collecting proper data to compare and analyze the practicability of current rules on light pollution.

At the same time, in future research, the ecosystem needs to be paid attention to in light pollution. We can also conduct data comparison analysis. For example, Jonathan et al. [54] used DMSP/OLS in combination with GLC2000 to collect nighttime lights from 1992 to 2012 and evaluated the latest changes in nighttime artificial illumination for 43 global ecosystem types. The results indicated that the Mediterranean climate–ecosystem has experienced an enormous increase in exposure and that all terrestrial ecosystem types have experienced a certain degree of artificial light exposure and that this exposure is increasing. Through the analysis of the ecosystem, the relevant laws and regulations can be strengthened in the future.

In the era of big data, we not only need to use data collection but also need to listen to the opinions of the public—for example, the public's views on light pollution and its impact on the environment. Lyytimaki et al. [55] investigated the public's views on light pollution as an environmental problem using a questionnaire survey. Of the 2053 responses to the study, 84.6% said light pollution had spread to all areas. A total of 82.9 per cent of the respondents said it was essential to be dark. Various light pollution sources were found in the problem of light pollution sources. The most commonly mentioned sources were street lamps, courtyard lamps, commercial lights, and outdoor decorative lights. Therefore, the author believes that only by combining a questionnaire survey, interviews, and DMSP/OLS data collection, etc. can the occurrence of light pollution be effectively controlled, and the effectiveness of laws and regulations be improved in the future.

7. Conclusions

In the present study, we collected information pertaining to the control of local and national light pollution in Korea and four Chinese cities. We found that although both countries have relatively robust light pollution control policies, there are still many problems that need to be addressed. For instance, local light pollution laws in China seem too simple and lack specificity for a complex issue such as light pollution. For example, many local light pollution policies in China do not provide lighting standards for decorative and advertisement lighting, and yet these two forms of artificial lighting are major contributors to local light pollution. The issue of generalization is also seen in light pollution policies in Korea; for example, the lighting limits provided for advertisement lighting in the Korean "Light Pollution Prevention Law" are intended to control luminance levels emitted by a single signboard instead of the net luminance radiated by all the signboards on a building façade. As such, given that the two countries share a similar socio-economic background, they can learn from each other's specific

approaches to tackling light pollution. The current study, therefore, provides the basis for discussing this exchange of ideas between Korea and China on the issue of light pollution control and policy.

Author Contributions: Conceptualization, methodology, resources, compare analysis, W.G., J.N. and K.G.; investigation, writing—original draft preparation W.G.; writing—review and editing, supervision, J.N. and K.G.

Conflicts of Interest: The authors declare no conflict of interest.

References and Notes

1. Rybnikova, N.A.; Haim, A.; Portnov, B.A. Is prostate cancer incidence worldwide linked to artificial light at night exposures? Review of earlier findings and analysis of current trends. *Arch. Environ. Occup. Health* **2017**, *72*, 111–122. [CrossRef] [PubMed]
2. James, P.; Bertrand, K.A.; Hart, J.E.; Schernhammer, E.S.; Tamimi, R.M.; Laden, F. Outdoor light at night and breast cancer incidence in the nurses' health study II. *Environ. Health Perspect.* **2017**, *125*, 087010. [CrossRef] [PubMed]
3. Hu, C.; Jia, W. Linking MTNR1B Variants to Diabetes: The Role of Circadian Rhythms. *Diabetes* **2016**, *65*, 1490–1492. [CrossRef] [PubMed]
4. Weinert, D.; Waterhouse, J. *Interpreting Circadian Rhythms, in Biological Timekeeping: Clocks, Rhythms and Behaviour*; Springer: Berlin, Germany, 2017; pp. 23–45.
5. Liu, M.; Zhang, B.G.; Li, W.S.; Guo, X.W.; Pan, X.H. Measurement and distribution of urban light pollution as day changes to night. *Lighting Res. Technol.* **2018**, *50*, 616–630. [CrossRef]
6. Kyba, C.C.M.; Kuester, T.; De Miguel, A.S.; Baugh, K.; Jechow, A.; Hölker, F.; Bennie, J.; Elvidge, C.D.; Gaston, K.J.; Guanter, L. Artificially lit surface of Earth at night increasing in radiance and extent. *Sci. Adv.* **2017**, *3*, e1701528. [CrossRef] [PubMed]
7. Gaston, K.J.; Davies, T.W.; Bennie, J.; Hopkins, J. REVIEW: Reducing the ecological consequences of night-time light pollution: Options and developments. *J. Appl. Ecol.* **2012**, *49*, 1256–1266. [CrossRef] [PubMed]
8. Ko, T.K.; Kim, I.T.; Choi, A.S.; Sung, M.K. Quantitative assessment methods for determining luminous environmental zones in Korea. *Lighting Res. Technol.* **2016**, *48*, 307–322. [CrossRef]
9. Morgan-Taylor, M. *Regulating Light Pollution in Europe: Legal Challenges and Ways Forward*; Routledge: Abingdon, UK, 2015.
10. Cha, J.; Lee, J.; Lee, W.; Jung, J.; Lee, K.; Han, J.; Gu, J. Policy and status of light pollution management in Korea. *Light. Res. Technol.* **2014**, *46*, 78–88. [CrossRef]
11. Ho, C.; Lin, H. Analysis of and control policies for light pollution from advertising signs in Taiwan. *Lighting Res. Technol.* **2015**, *47*, 931–944. [CrossRef]
12. Taylor, M.M. Light pollution and nuisance: The enforcement guidance for light as a statutory nuisance. *JPL* **2006**, *8*, 1114–1127.
13. Zitelli, V.; Di Sora, M.; Ferrini, F. Local and national regulations on light pollution in Italy. In *Symposium-International Astronomical Union*; Cambridge University Press: Cambridge, UK, 2001.
14. Ngarambe, J.; Kim, G. Sustainable Lighting Policies: The Contribution of Advertisement and Decorative Lighting to Local Light Pollution in Seoul, South Korea. *Sustainability* **2018**, *10*, 1007. [CrossRef]
15. Cook, T.D.; Leviton, L.C. Reviewing the literature: A comparison of traditional methods with meta-analysis 1. *J. Personal.* **1980**, *4*, 449–472. [CrossRef]
16. Seoul Metropolitan Government Ordinance on the Prevention of Light Pollution and Management of Formation of Good Light. Available online: http://legal.seoul.go.kr/legal/english/front/page/law.html?pAct=lawView&pPromNo=1442 (accessed on 24 January 2018).
17. Taylor, A.E.F. *Illumination Fundamentals*; Lighting Research Center: Troy, New York, NY, USA, 2000.
18. China, T.N.P.s.C.o.t.P.s.R.o. Constitution of the People's Republic of China. Available online: http://www.npc.gov.cn/englishnpc/Constitution/node_2825.htm (accessed on 14 October 2018).
19. Congress, S.N.P.s. General Principles of the Civil Law of the People's Republic of China. Available online: http://www.npc.gov.cn/englishnpc/Law/2007-12/12/content_1383941.htm (accessed on 13 April 1986).
20. Congress, F.S.o.t.T.N.P.s. Property Law of the People's Republic of China. Available online: http://www.npc.gov.cn/englishnpc/Law/2009-02/20/content_1471118.htm (accessed on 1 October 2007).

21. Environmental Protection Law of the People's Republic of China. Available online: http://www.npc.gov.cn/englishnpc/Law/2007-12/12/content_1383917.htm (accessed on 26 December 1989).
22. l'éclairage, C.i.d. *Guide on the Limitation of the Effects of Obtrusive Light from Outdoor Lighting Installations*; Technical Report; CIE: Vienna, Austria, 2003.
23. Association, S.M.B.O.Q.A.T.S.S.l. *Specifications on Urban Environment (Decoration) Lighting*; Municipal Bureau of Quality and Technical Supervision: Shanghai, China, 2012.
24. Bureau, G.E.P. *Guangzhou Light Radiation Environment Management Specifications (Draft for Comment)*; Legal Office of Guangzhou Municipal People's Government: Shanghai, China, 2014.
25. Beijing Municipal Administration of Quality and Technology Supervision. *Technical Specification of Urban Landscape Lighting*; Beijing Municipal Administration of Quality and Technology Supervision: Beijing, China, 2015.
26. Xingguo, M.h. *Tianjin City Lighting Management Regulations*; Tianjin Municipal People's Government: Tianjin, China, 2012; pp. 2–6.
27. Shanghai Municipal Bureau of Quality and Technical Supervision; Shanghai Information System Quality Technology Association; Shanghai Landscape Affairs Center; Shanghai Sansi Technology CO., L. *Limits and Measure Methods of Maximum Visible Brightness for Public Places Light Emitting Diode (LED) Panels*; Shanghai Municipal Bureau of Quality and Technical Supervision: Shanghai, China, 2013.
28. Jianhua, M.C. *Guangzhou Outdoor Advertising and Signboard Management Methods*; G.m.p.s.: GuangZhou, China, 2014.
29. Cinzano, P. Light pollution by luminaires in roadway lighting. *CIE Div. TC4* **2003**, *21*, 1–8.
30. Falchi, F.; Cinzano, P. Measuring and modelling light pollution. *Mem. Soc. Astron. Ital.* **2000**, *71*, 139–152.
31. Falchi, F.; Cinzano, P.; Elvidge, C.D.; Keith, D.M.; Haim, A. Limiting the impact of light pollution on human health, environment and stellar visibility. *J. Environ. Manag.* **2011**, *92*, 2714–2722. [CrossRef] [PubMed]
32. Brüning, A.; Hölker, F.; Franke, S.; Preuer, T.; Kloas, W. Spotlight on fish: Light pollution affects circadian rhythms of European perch but does not cause stress. *Sci. Total. Environ.* **2015**, *511*, 516–522. [CrossRef] [PubMed]
33. Chauvel, P.; Perraudeau, M. Daylight as a source of visual discomfort-Daylighting Atlas. *Lyon Joule* **1995**, *2*, 17.
34. Collins, J.; Dogniaux, R.; Chauvel, P.; Longmore, J. Glare from windows: Current views of the problem. *Light. Res. Technol.* **1982**, *14*, 31–46.
35. Nazzal, A.; Oki, M. Could Daylight Glare Be Defined Mathematically? *J. Light Vis. Environ.* **2007**, *31*, 44–53. [CrossRef]
36. Osterhaus, W. Discomfort glare from daylight in computer offices: How much do we really know. In Proceedings of the LUX Europa, Reykjavik, Iceland, 18–20 June 2001; pp. 448–456.
37. Briggs, W.R. Physiology of plant responses to artificial lighting. *Ecol. Conseq. Artif. Night Lighting* **2006**, 389–411.
38. Rogge, E.; Dessein, J.; Gulinck, H. Stakeholders perception of attitudes towards major landscape changes held by the public: The case of greenhouse clusters in Flanders. *Land Use Policy* **2011**, *28*, 334–342. [CrossRef]
39. Knight, A.L.; Weiss, M.; Weissling, T. Diurnal patterns of adult activity of four orchard pests (Lepidoptera: Tortricidae) measured by timing trap and actograph. *J. Agric. Entomol.* **1994**, *11*, 125–136.
40. Svensson, M.G.E.; Rydell, J.; Brown, R. Bat Predation and Flight Timing of Winter Moths, Epirrita and Operophtera Species (Lepidoptera, Geometridae). *Oikos* **1999**, *84*, 193. [CrossRef]
41. Jetz, W.; Steffen, J.; Linsenmair, K.E. Effects of light and prey availability on nocturnal, lunar and seasonal activity of tropical nightjars. *Oikos* **2003**, *103*, 627–639. [CrossRef]
42. Moser, J.C.; Reeve, J.D.; Bento, J.M.S.; Della Lucia, T.M.C.; Cameron, R.S.; Heck, N.M.; Bento, J.M.S. Eye size and behaviour of day- and night-flying leafcutting ant alates. *J. Zoöl.* **2004**, *264*, 69–75. [CrossRef]
43. Żagan, W. *Iluminacja Obiektów*; OWPW: Warszawa, Poland, 2003; ISBN 83-7207-360-0.
44. Kubiak, K. About the necessity of break of the stagnation in illumination lighting equipment. *Prz. Elektrotechniczny* **2012**, *88*, 108–114.
45. Skarżyński, K. An attempt at controlling the utilisation factor and light pollution within the context of floodlighting. *Prz. Elektrotechniczny* **2016**, *1*, 180–183. [CrossRef]
46. Illuminating Engineering Society of North—The Lighting Authority; I.R.L. Committee. *IESNA Technical Memorandum on Light Trespass: Research, Results and Recommendations*; Illuminating Engineering Society of North—The Lighting Authority: I.R.L. Committee: New York, NY, USA, 2000.

47. Na, L. *Simulation Study on Typical Colour Light Trespass around Residential Buildings caused by LED Advertising Screens*; Tianjin University: Tianjin, China, 2017.
48. Ho, C.Y.; Lin, H.T.; Huang, K.Y. A Study on Energy Saving and Light Pollution of LED Advertising Signs. In *Applied Mechanics and Materials*; Trans Tech Publications: Zurich, Switzerland, 2012.
49. Farbry, J.; Wochinger, K.; Shafer, T.; Owens, N.; Nedzesky, A. *Research Review of Potential Safety Effects of Electronic Billboards on Driver Attention and Distraction*; Science Applications International Corporation: Reston: VA, USA, 2001.
50. Guangzhou Light Pollution Law Basis; 2018.
51. Wen, G.H. Guangzhou Building Glass Curtain Wall Management Measures. 2017. Available online: https://www.gz.gov.cn/gzgov/s8263/201706/2de15a795c2a4fcea73de0d25453c98e.shtml (accessed on 23 July 2019).
52. Jiang, W.; He, G.; Long, T.; Guo, H.; Yin, R.; Leng, W.; Liu, H.; Wang, G. Potentiality of Using Luojia 1-01 Nighttime Light Imagery to Investigate Artificial Light Pollution. *Sensors* **2018**, *18*, 2900. [CrossRef]
53. Jiang, W.; He, G.; Long, T.; Wang, C.; Ni, Y.; Ma, R. Assessing Light Pollution in China Based on Nighttime Light Imagery. *Remote. Sens.* **2017**, *9*, 135. [CrossRef]
54. Bennie, J.; Duffy, J.P.; Davies, T.W.; Correa-Cano, M.E.; Gaston, K.J. Global Trends in Exposure to Light Pollution in Natural Terrestrial Ecosystems. *Remote. Sens.* **2015**, *7*, 2715–2730. [CrossRef]
55. Lyytimäki, J.; Rinne, J. Voices for the darkness: Online survey on public perceptions on light pollution as an environmental problem. *J. Integr. Environ. Sci.* **2013**, *10*, 127–139. [CrossRef]

sustainability

MDPI

Article

Italian Road Tunnels: Economic and Environmental Effects of an On-Going Project to Reduce Lighting Consumption

Laura Moretti [1,*], Giuseppe Cantisani [1], Luigi Carrarini [2], Francesco Bezzi [2], Valentina Cherubini [2] and Sebastiano Nicotra [2]

[1] Department of Civil, Construction and Environmental Engineering, Sapienza University of Rome, 00184 Rome, Italy
[2] Operation e Territorial Coordination Management, Anas S.p.A., 00185 Rome, Italy
* Correspondence: laura.moretti@uniroma1.it; Tel.: +39-06-4458-5114

Received: 3 August 2019; Accepted: 20 August 2019; Published: 26 August 2019

Abstract: Tunnel lighting represents a major cost item for road managers, and particularly in Italy owing to its specific geomorphological and orographic features. In 2018, ANAS, the Italian government-owned road company launched an ambitious program to rehabilitate the lighting systems of more than 700 tunnel tubes across Italy. The Greenlight plan aims to reduce consumption and improve the management of lighting systems while minimizing the impact of works. Outdated high-pressure sodium (HPS) luminaries will be substituted with state-of-the-art light emitting diode (LED) luminaries without modifying the position and the number of the existing luminaires. The project involves an amount of 155 million euros and provides a total return over a less than seven-year period. The first phase of the project involves 147 tubes and is still on-going: 28 GWh (on average 55% of the current consumption) will be saved every year against a 30 million euro investment. More importantly, the economic benefits also have a direct impact on the environment for citizens and safety levels for road users—every year more than 17,000 t of CO_2 eq. and 230 TJ from combustion of fossil fuels will be saved. The lighting quality of the artificial lighting inside the tunnel will be enhanced thanks to better uniformity and the color temperature of the luminaries. The experience presented here could be useful since other road managers may pursue a similar approach in order to balance often-conflicting environmental, economic and safety goals.

Keywords: road tunnel; lighting; LED; road management

1. Introduction

According to the European Commission, improving energy efficiency is a broad term. Improvements in energy efficiency and energy saving are the two key targets [1]. An effective energy efficiency policy could contribute to EU competitiveness and encourage eco-innovation, on the other hand, energy saving is the first option for improving energy efficiency and is undoubtedly the quickest, most cost-effective way to reduce environmental impacts [2]. In the public sector, more efficient lighting can contribute to improving environmental sustainability of our lifestyle [3]. In 2009, 14% of the total electricity consumption in Europe was for lighting, and more than half of this was for public spaces and non-residential applications [4]. In particular, over 70% of existing light sources are based on obsolete technologies that have poor energy performance, and for which a better alternative is available [5].

Public lighting is 2% of the overall value [6] of energy consumption in Italy, however, both renewal of technologies and energy rationalization processes could contribute to meeting the three key targets set by EU on climate and energy (i.e., 20% cut in greenhouse gas emissions, 20% of EU from renewables,

and 20% improvement in energy efficiency). Among the various and important functions of public lighting is ensuring safety for the movement of traffic and pedestrians. In order to ensure the minimum safety illumination values on roads, specific standards have been set to define minimum luminance and illuminance levels according to the area to be illuminated. In Europe, the updated standard CEN/TR 13201-1:2014 [7] on road lighting provides far greater potential for dynamic control then the previous standard CEN/TR 13201-1:2004 [8], which results in significant energy saving [9,10]. Lighting costs represent up to 25% of the total budget for management of the road network [11], therefore both energy performance indicators and environmental criteria should be adopted when designing smart public lighting systems [12,13]. In particular, safety measures for tunnels and their overall equipment involve a high-energy consumption [14]. The aim of tunnel lighting is to allow traffic to enter, pass through and exit the enclosed section safely. This goal implies that drivers drive into the tunnel without reducing their vehicle speed and are able to see unexpected hazards on the carriageway and stop if necessary [15]. During day time, adequate illumination avoids the "black-hole effect" (i.e., a decrease of the drivers' visual perception) while passing from the outside into the tunnel [16,17]. Therefore, different methods and technologies have been adopted to reduce lighting energy and costs, especially in road tunnels [18–21].

Recently, research has focused on the use of sunlight to reduce energy consumption [22] and related environmental impacts [23]. In some cases, it is possible to use the natural light in an open stretch of the road before the tunnel entrance, that is, a pre-tunnel lighting (PTL) structure is positioned before the access to the "natural" tunnel [24,25]. A PTL is a reticular structure that reduces the luminance in the access zone [26,27]. Tension structures at the tunnel entrance shift the zones with the highest energy consumption; their effectiveness depends on the geometry and orientation, latitude and longitude of the tunnel [28,29]. The construction of these structures implies significant design and construction costs, but the life cycle cost analysis has revealed their economic advantage with respect to the "zero option". Pergolas imply lower energy savings and easier maintenance than tension structures [30]. The introduction of sunlight inside the tunnel with light-pipes [31] or optical fibers [32] is another option for more sustainable tunnels, but this strategy is difficult to use because of the relative position between the sun and light-pipes matrix [33]. When it is not possible to use natural light, the inner surfaces of the tunnel play a crucial role in the tunnel lighting design [34]. For this purpose, the pavement reflection coefficient in the visible spectrum has been recently analyzed as a saving strategy. Salata et al. [16] analyzed four alternative solutions to optimize road tunnel lighting systems with two asphalt pavements with different reflection coefficients and two lighting systems (high-pressure sodium (HPS) luminaries, or HPS and light emitting diode (LED) luminaries). Special asphalts with a high-reflection coefficient reduce the power required, and the energy savings balance their higher installation costs. On the other hand, concrete (light) pavements result in 29% less road tunnel lighting costs compared to traditional asphalt (or black) surfaces; calculations for Italian road tunnel pavements performed by Moretti and Di Mascio [35] have confirmed this. Moreover, the use of concrete instead of bituminous pavements implies a higher level of safety in both ordinary and emergency conditions. Indeed, compared to a flexible pavement, a rigid pavement requires less maintenance activities (which interfere with the traffic flow) [36] and it is not combustible in case of fire [23].

Recently, extensive interest in LED has given rise to new lighting systems in tunnels. LED is the most efficient available technology. Its main characteristics are long life, energy efficiency, environmental friendliness, and zero UV emissions; also, LED illumination produces little infrared light and close to no UV emissions, and excellent color rendering [37]. This technology has been adopted by the Italian government-owned road company ANAS (acronym for Azienda Nazionale Autonoma delle Strade—National Autonomous Roads Corporation, Rome, Italy) to rehabilitate lighting systems in its managed tunnels. In 2018, it launched the Greenlight project, which involves more than 700 tunnel tubes where HPS will be replaced by LED luminaries.

2. The Greenlight Project

The Greenlight project provides for rehabilitation works on road tunnel lighting systems, which consist of replacing outdated high-pressure sodium (HPS) luminaries with state-of-the-art light emitting diode (LED) luminaries. The new devices are equipped in order to wirelessly control the light flow and the energy consumption. The implemented remote control allows adjusting the luminous flux with a point-to-point regulation for each LED luminaire. The wireless management and control system aims to adapt the luminance curve to the different conditions of external brightness, and to diagnose the functional status of the individual projectors. Therefore, the luminous flux can be continuously adjusted according to the external luminance for the reinforcement circuits, and according to the daily time bands for the permanent lighting circuits. LED technology makes it possible to optimize the dimming levels up to 15–20% of their initial flow while maintaining the required perceptive conditions and ensuring a significant reduction in consumption. During the night-time hours, the required visibility conditions inside the tunnel are comparable to those of the open-air sections [16]; only the permanent lighting system is necessary to guarantee the required luminance level. To further reduce consumption, a luminous flux regulation system is also installed to manage permanent lighting according to the reduction in traffic at night.

Compared to SAPs, which only allow a step adjustment for homogeneous groups of fixtures, this technical difference ensures considerable savings for the road manager as it reduces costs and allows for operation flexibility in case of the addition or removal of new elements.

Moreover, the project aims not only to reduce consumption and optimize of tunnel lighting systems, but also to raise safety levels. Indeed, the new luminaries enhance the visibility and quality of the diffusion of artificial lighting inside the tunnel. This is due to the higher color-rendering index (CRI) of LED compared to HPS. CRI is a measure of a light source's ability to show object colors realistically or naturally: the higher the CRI, the better the color perception. Statistically LEDs have CRI values between 70 and 90 or more, while HPS have CRI values not higher than 70 [38]. Road lighting can use lighting systems that have a CRI below 70 because color rendering is not a major issue. However, LEDs offer significant color advantages over HPS, eliminating the monochromatic black appearance of objects illuminated by sodium-bulbs. Therefore, LEDs allow a further reduction in the electricity used for lighting in addition to their longer service life (LED devices have warranty coverage up to 11 years of continuous operation).

Of a total of 1900 tunnels under management, the project involves about 700 tunnel tubes in Italian territory. Greenlight has been divided into eight geographical areas (Figure 1) and two phases with the overall cost estimated as € 155 million (Table 1).

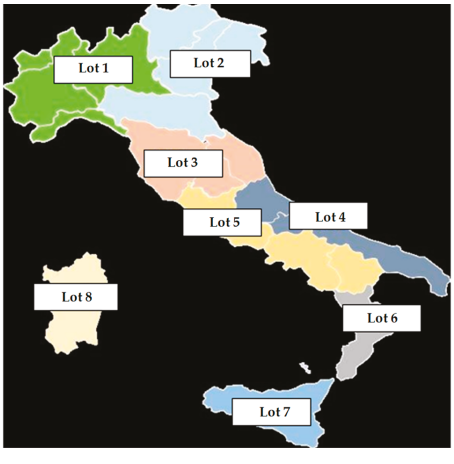

Figure 1. Greenlight project locations.

Table 1. Characteristics of Greenlight.

Lot	Number of Tubes	Overall Length of Tubes (km)	Amount of Estimated Cost (€)
L1	92	70	22,900,000
L2	65	45	13,500,000
L3	145	85	23,800,000
L4	89	75	21,000,000
L5	112	80	23,500,000
L6	117	74	22,300,000
L7	49	58	16,900,000
L8	39	45	11,700,000
Total	708	532	155,000,000

The first phase started in 2018 and is still ongoing: it involves the 147 tubes with the highest energy consumption per unit of length and the overall estimated cost is € 30 million at the end of 2020. Data and the allotted amounts for phase 1 are listed in Table 2.

Table 2. Characteristics of phase 1 Greenlight.

Lot	Number of Tubes	Overall Length of Tubes (km)	Amount Allotted (€)
L1	11	20.37	3,667,000
L2	11	22.22	3,333,000
L3	21	29.41	5,000,000
L4	19	22.22	4,000,000
L5	20	26.67	4,000,000
L6	40	24.07	4,333,000
L7	16	20.00	3,000,000
L8	9	17.78	2,667,000
Total	147	182.74	30,000,000

All works consists of:

- Substitution of old and inefficient lighting HPS systems with more recent and better performing LED ones
- Substitution of the power supply cables
- Substitution of switchboard systems in enclosures
- Installation of control units and brightness probes.

Therefore, there are no modifications, substitutions, or alterations of the existing position and number of luminaries, in both the interior zone and the adaptation zone. Energy-efficient equipment and technologies have been planned in order to monitor the systems and to control the functionality of the equipment during its service life.

3. Methods

The new lighting systems comply with the Italian standard UNI 11095:2011 Lighting of road tunnels [39]. It divides the longitudinal section of a road tunnel into five zones with different levels of required luminance [40,41] as follows:

- Access zone: the stretch of road just before the entrance portal. Its length is equal to the stopping distance at the relevant driving speed. The required luminance value ensures the early and safe detection of an obstacle without reduction in driving speed.
- Threshold zone: the first tunnel section is equal in length to the stopping distance at design speed. The required luminance value is affected by external luminance, which must remain constant and

equal to the outside luminance through half the length of the threshold zone, and it is reduced in a linear manner to 40% at the end of the second part of the section.

- Transition zone: this is the second tunnel section in which luminance values decrease to support the luminance perceived by the driver's eye.
- Interior zone: the internal stretch with a constant luminance value. Its minimum value depends on the design speed and the expected traffic flow. The luminance value of the interior zone is the major difference between European legislated levels of tunnel lighting CIE 88:2004 [42] and the Italian standard UNI 11095 [39]. The former does not set an objective luminance value while the Italian standard establishes a minimum value.
- Exit zone: the final stretch where it is possible to increase the luminance level close to the exit. Such reinforcement/adaptation lighting is not a design constraint for the UNI 11095 standard.

Each zone requires different minimum luminance values as a consequence of the design speed, the meteorological visibility distance, the horizontal lighting in the access zone, the natural luminance, and the optics type, and are calculated using Equations (1)–(3)

$$L_e = c \times L_v = c\ (L_{seq} + L_{atm} + L_{par} + L_{cru}) \quad (1)$$

$$L_t = L_e/(1.9 + t)^{1.4} \quad (2)$$

$$L_t \geq 2 \times L_r \quad (3)$$

where L_e is the maximum luminance value of L_v; c is a coefficient, which depends on the optics; L_v is the veiling luminance; L_{seq} is the equivalent veiling luminance; L_{atm} is the atmospheric luminance; L_{par} is the luminance of the windshield; L_t is the average luminance value in the transition zone; L_{cru} is the luminance of the dashboard; t is the travel time in the transition zone; L_i is the minimum luminance of the permanent lighting circuit; and L_r is the reference luminance value according to [39]. L_{seq} is calculated according to the L20 method, which considers the average value of the luminance in a visual cone of 20°, centred on the line of sight of the driver from the beginning of the access zone.

Since the project involves existing tunnels, no modifications were made to the input data with regard to design speed, meteorological visibility distance, horizontal lighting in the access zone, and natural luminance. Therefore, the stopping distance and the threshold luminance remained the same. The lighting system of each tunnel is composed of one permanent and several reinforcement installations. All devices are arranged in a quincunx geometric pattern in both systems. Counter beam optics create the maximum contrast between existing objects and the road because luminaires are placed above the traffic lanes. The minimum luminous efficacy of each LED luminaire was 105 lm/W and its correlated colour temperature (CCT) was 4000 K; for existing HPS luminaries these average characteristics were 95 lm/W and 2000 K, respectively.

Uniformity performances were settled in agreement with UNI 11095 [39] and UNI EN 13201-2 [43]; these standards require parameters for night-time and daytime, and for each regulation state of the lighting system, which are:

U_0 and $U_l \geq 0.50$ over the carriageway or over one-way lanes;
U_0 and $U_l \geq 0.40$ over all other surfaces and over bi-directional lanes

In areas with constant level of luminance, the standards required are:

$U_l \geq 0.70$ over the carriageway
$U_l \geq 0.60$ over all other surfaces

where:

U_0 is the general luminance uniformity, that is, the ratio between the minimum and the average of luminance values [43].

U_l is the longitudinal luminance uniformity, that is, the ratio between the minimum and the maximum of luminance values [43] determined along the median axle of a lane for the carriageway.
U_t is the transversal luminance uniformity, that is, the ratio between the minimum and the average of luminance values in the same calculus surface section [39].

The software LITESTAR 4D Litecalc [44] was used to design the new lighting systems. It models and verifies the lighting design of road tunnels, and provides numeric and rendered solutions simulating the effects of lighting (shadows, reflections, colour vision and rendering volumes) and obtains a picture of the lighted environment. According to the Italian standard UNI 10439:2001 [45], the assumed maintenance coefficient is equal to 0.8 and the average luminance coefficient is 0.7. These values coincide with those adopted for designing HPS systems.

The adopted software was proven to be suitable for lighting design, since it has an open database where the operator can save product data, do product research, process photometries and spectra or update data automatically; the software was used to realize a real simulation of the results obtained by means of the designed lighting system.

With regard to the lighting design criteria, as previously stated, the luminaires that constitute the permanent lighting system were placed in the same position of the ones previously installed in the tunnel. Each luminaire is equipped with a luminous flux regulation system (transmission module), which communicates with a control unit placed in the cabin. The reinforcement circuits are managed through the veil sensors placed on the external side of the portals, while the permanent lighting circuits are managed through pre-established time cycles. All lighting devices can be modulated to maximize the energy saving performances.

In spite of the design constraints (especially the fixed position of the luminaires), the results of the simulation were satisfying and met all the standard requirements; in particular, with regard to the uniformity, the calculated values generally vary between 0.80 and 0.95 for U_l and between 0.60 and 0.90 for U_0.

Lighting energy and cost calculation take into account the power regulation during the day and the year, for both variations in external luminance and for energy saving.

4. Results

Having referenced the current energy consumption to light the tunnels involved in the first phase of Greenlight, Table 3 summarizes the calculated yearly energy savings for each lot and its overall value. The listed values take into account the switching control and the variable absorbed power during the day (day and night hours) and during the year (sunny, cloudy, or rainy days).

Table 3. Yearly energy savings—first phase.

Lot	Yearly Energy Saving (MWh)
L1	3423
L2	3111
L3	4667
L4	3733
L5	3733
L6	4044
L7	2800
L8	2489
Total	28,000

For each tunnel, the yearly energy saving represents up to 65% of the current yearly energy consumption related to lighting; the value depends on geographical, traffic, and meteorological conditions. At present, the yearly overall consumption for lighting all tunnels managed by ANAS is

about 220 GWh, of which 51 GWh is used for the tunnels involved in phase 1 of Greenlight. Therefore, the average energy saving is 55%: this result has both economic and environmental consequences.

Given the average Italian electricity price is 0.16 €/kWh, the economic results and savings obtained in the first phase of Greenlight are listed in Table 4. Moreover, these savings have environmental implications: the saved tons of oil equivalent (TOE) were calculated. According to the Italian Authority for Energy and Gas, the conversion factor of electric energy into primary energy is 0.187 TEP/MWh, and this is the reference value that was adopted to evaluate the effectiveness of the energy efficiency measures.

Table 4. Economic and environmental results—first phase.

Lot	Yearly Saving from Electricity Consumption (€)	Yearly Saved TOE (t of Oil Equivalent)
L1	3,667,000	640.01
L2	3,333,000	781.72
L3	5,000,000	872.67
L4	4,000,000	698.13
L5	4,000,000	698.13
L6	4,333,000	756.25
L7	3,000,000	523.6
L8	2,667,000	465.48
Total	4,480,000	5236.00

Taking into account the expected rebates in the tender phases, ANAS estimated that the actual investment is 30 million euro. Therefore, the economic gains from saving electricity consumption ensure a breakeven point at 7 years after the rehabilitation works, when the project will return its initial investment.

In regard to the environmental issue, the saved impacts from energy non-consumption were calculated using the software package SimaPro 8.0.5.13 [46]. A Life Cycle Impact Assessment was implemented to evaluate the saved environmental impacts in relation to the electricity savings listed in Table 3. The database Ecoinvent 3 was used to assess the parameters describing environmental impacts according to the characterization factors listed in EN 15804:2012+A1:2013 [47]. The examined environmental impact categories (ICs) were: Global Warming Potential (GWP), Ozone layer Depletion Potential (ODP), Acidification Potential (AP), Eutrophication Potential (EP), Photochemical oxidation Potential (POCP), Abiotic depletion-elements (ADP-e), and Abiotic depletion-fossil fuels (ADP-f).

The processes included in the environmental analysis of the transmission of high voltage electricity were electricity production in Italy and from imports, the transmission network and the electricity losses. In order to obtain reliable results consistent with the Italian energy market, the production mix was composed of 36.6% of renewable primary energy and 63.4% of non-renewable primary energy (Table 5).

Table 5. Electricity production mix in Italy [48].

Source	Production Share (%)
Coal	13.75
Natural gas	42.34
Oil and other	7.31
Hydro	14.64
Solar	7.68
Wind	5.86
Biomass	6.22
Geothermic	2.20

Table 6 lists the impact categories that were avoided annually due to the total yearly energy saving listed in Table 3.

Table 6. Avoided impact categories—first phase.

IC	Amount	Units
GWP	1.78×10^7	kg CO_2 eq.
ODP	1.35×10^0	kg CFC-11 eq.
AP	6.18×10^4	kg SO_2 eq.
EP	1.51×10^4	Kg $(PO_4)^{3-}$ eq.
POCP	1.84×10^4	kg C_2H_4 eq.
ADP-e	1.93×10^1	kg Sb eq.
ADP-f	2.32×10^8	MJ
GWP	1.78×10^7	kg CO_2 eq.

The Greenlight project represents a big effort on the part of ANAS, the Italian government-owned road company to rehabilitate and improve the lighting systems in its tunnels. The investments are significant, for example, for the rehabilitation works completed in 2018, the total cost was 6 million euros (Figure 2), and in 2019, works worth 13.5 million euros are in progress or planned (Table 7).

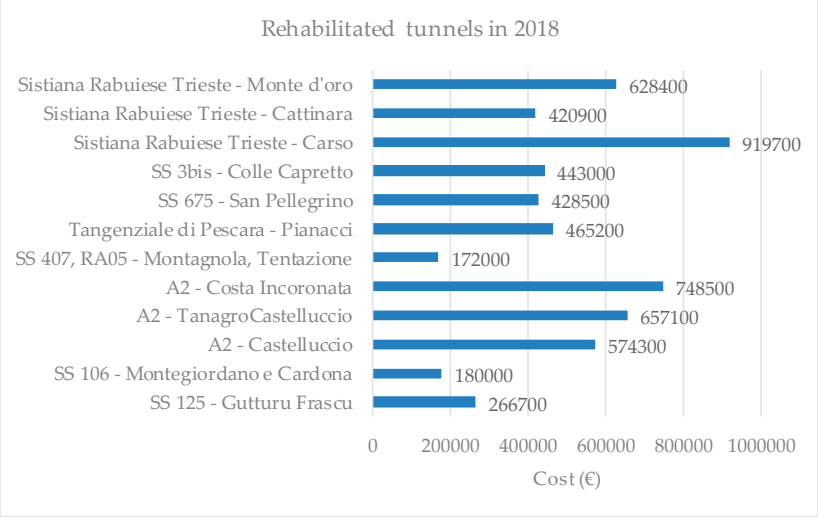

Figure 2. Completed works in 2018.

Table 7. Planned and on-going works in 2019.

Lot	Planned and On-Going Works (€)
L1	1,177,750
L2	1,869,690
L3	3,059,210
L4	2,573,350
L5	1,330,420
L6	2,857,680
L7	0
L8	687,270
Total	13,555,370

Data in Table 7 were also analyzed in order to correlate the required investment to the tunnel length (L): Figure 3 shows the results obtained for 32 tunnels (their overall length is 39,663 m) of phase 1.

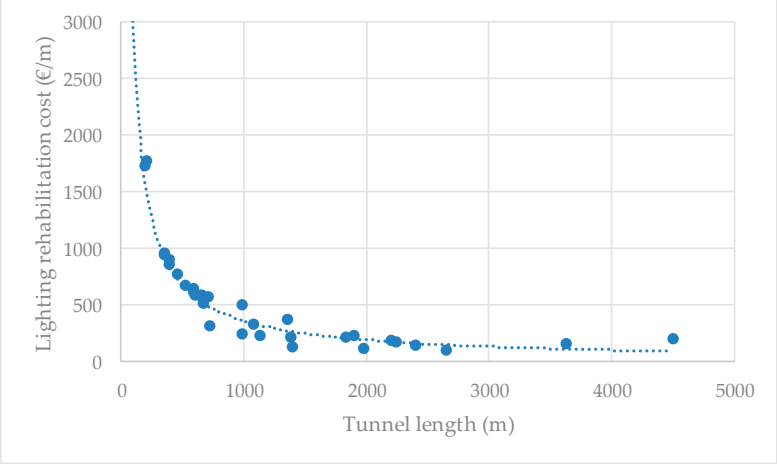

Figure 3. Tunnel length vs. rehabilitation lighting costs per unit length.

As shown in Figure 3, a correlation curve between L and the lighting rehabilitation cost per unit length (c_l) was identified (Equation (4)):

$$c_l = 182339\ \mathrm{L}^{-0.901} \tag{4}$$

where L is expressed in m and c_l is in €/m.

The coefficient of determination R^2 of the dashed trend line is 0.87. The obtained curve is valid under two important hypotheses about the cost of luminaries and the layout of the lighting systems.

With regard to the cost, the unit prices comply with those currently valid in Italy [49]; the price of each luminaire ranges between € 395 for elements with less than 3000 lm luminous flux and € 1798 for elements with more than 41,500 lm luminous flux. Regarding the layout of the lighting systems, the number and the position of LED luminaries coincide with those of existing HPS luminaries. Thus, the distance between LEDs could be less without the restriction of having to replace the HPS at the same distance, and the total initial cost of the luminaires in the interior zones could be higher.

5. Discussion

For ANAS, tunnel lighting is the principal cost item in the energy budget expenditure: at present, the yearly consumption for tunnel lighting is about 230 GWh. Therefore, the Greenlight multi-year project aims to reduce energy consumption for lighting in its road tunnels. It consists of using equipment and technologies characterized by high energy efficiency (i.e., LED luminaries) and balancing environmental-economic needs and the operational limits due to pre-existing structures.

Greenlight aims to improve and standardize safety standards and service to road customers, as well as to optimize energy consumption, especially in more energy-intensive lighting systems. The high CRI, the luminous efficiency and the high visual comfort of LED luminaries allow for significant reductions in the energy consumption with the same luminance on the road surface. For each luminaire considered in the project, the minimum CRI is 80, the minimum luminous efficacy is 105 lm/W, and its CCT is 4000 K. Furthermore, the installation of luminance sensors at tunnel entrances permits the internal luminance to be monitored continuously and verifies the state of efficiency and reliability of the

system. Lighting monitoring is ensured by specific latest-generation software and its results are dealt with in real time. Moreover, in contrast to the HPS luminaries, during day hours this type of luminaire permits point-by-point adjustment of the internal illumination in accordance to the external luminance, in order to optimize the luminous flux. Therefore, the wireless management and control system diagnoses the functional status of the individual projectors, and also adapts the brightness of each luminaire to different conditions. During night hours, only permanent lighting remains in operation to guarantee the required luminance level. In order to further reduce consumption, a luminous flux adjustment system is also installed for permanent lighting, which takes into account the reduction of vehicular traffic at night.

The benefits arising from Greenlight are related to users' safety, road management savings, and environmental protection. ANAS estimates that the return on investment is 7 years, this has been calculated considering only energy savings, without the cost of maintenance. Therefore, the return on investment could be a shorter time because of the durability of LED which is greater than HPS. Considering the costs and the effectiveness of the investment, it should also be noted that the knowledge gained to date suggests there is a correlation between the lighting rehabilitation cost and the length of the tunnel. This analysis was presented above (see Figure 3) and this finding might help to expedite the assessment of the cost of road tunnel LED lighting systems: it fits with the variability in lighting rehabilitation costs per unit length that is caused by the luminance requirements laid down by the reference standard UNI 11095.

6. Conclusions

Renewal of technologies and energy rationalization processes could contribute to meeting the sustainability targets set by the European Union on climate and energy. Within this framework, ANAS, the Italian government-owned road company launched the Greenlight project to replace HPS tunnel lighting systems with state-of-the-art LED luminaries. The new systems will reduce electricity consumption by up to 50% of the current values; additionally, the lighting quality inside the tunnel will be enhanced thanks to better uniformity and color temperature of the new luminaries.

The initiative is composed of two phases: the first one will account for 45 million euros and the second one for about 110 million euros. Until now, the on-going first phase involves 147 tubes: their new lighting systems cost 30 million euros (allotment volume) and ensure 28 GWh saved energy every year (on average 55% of the current consumption). The economic saving provides a total return over less than seven years and has direct environmental effects. According to the European standard EN 15804, the avoided yearly emissions of greenhouse gases are 17,000 t of CO_2 eq., while saved abiotic and fossil resources are 19.3 kg of Sb and 230 TJ, respectively.

The presented on-the-field experience permitted us to correlate the tunnel length to the rehabilitation cost per unit length; the high value of the coefficient of determination corroborated the result, which could be useful to road managers pursuing environmental, economic and safety goals with tunnel LED lighting.

Author Contributions: Conceptualization, L.M. and G.C.; Data curation, L.C., F.B., V.C. and S.N.; Formal analysis, L.M. and G.C.; Investigation, L.M. and G.C.; Methodology, L.M. and G.C.; Project administration, L.C.; Software, F.B., V.C. and S.N.; Supervision, L.C.; Validation, F.B.; Visualization, V.C. and S.N.; Writing—original draft, L.M. and G.C.; Writing—review & editing, L.M. and G.C.

Funding: This research received no external funding.

Conflicts of Interest: The authors declare no conflict of interest.

References

1. European Commission. *Green Paper on Energy Efficiency or Doing More with Less*; European Commission: Brussels, Belgium, 2005.
2. Miccoli, S.; Finucci, F.; Murro, R. Assessing project quality: A multidimensional approach. *Adv. Mater. Res.* **2014**, *1030–1032*, 2519–2522. [CrossRef]

3. Miccoli, S.; Finucci, F.; Murro, R. Measuring shared social appreciation of community goods: An experiment for the east elevated expressway of Rome. *Sustainability* **2015**, *7*, 15194–15218. [CrossRef]
4. European Commission. *Green Paper Lighting the Future Accelerating the Deployment of Innovative Lighting Technologies*; European Commission: Brussels, Belgium, 2011.
5. European Technology Platform Photonics21. *Lighting the Way Ahead Photonics21 Strategic Research Agenda*; Photonics21: Susseldorf, Germany, 2010.
6. Terna. Consumi Energia Elettrica per Settore Merceologico Italia. 2018. Available online: https://www.terna.it/it-it/sistemaelettrico/statisticheeprevisioni/consumienergiaelettricapersettoremerceologico.aspx (accessed on 17 May 2019).
7. CEN. CEN/TR 13201-1:2014. In *Road Lighting—Part 1: Guidelines on Selection of Lighting Classes*; Technical Report; European Commitee for Standardization: Brussels, Belgium, 2014.
8. CEN. CEN/TR 13201-1:2004. In *Road Lighting. Selection of Lighting Classes*; Technical Report; European Committee for Standardization: Brussels, Belgium, 2004.
9. Wojnicki, I.; Komnata, K.; Kotulski, L. Comparative study of road lighting efficiency in the context of CEN/TR 13201 2004 and 2014 lighting standards and dynamic control. *Energies* **2019**, *12*, 1524. [CrossRef]
10. Wojnicki, I.; Kotulski, L. Empirical study of how traffic intensity detector parameters influence dynamic street lighting energy consumption: A case study in Krakow, Poland. *Sustainability* **2018**, *10*, 1221. [CrossRef]
11. Löfsjögård, M.; Silfwerbrand, J. Proposal for improvement of road lighting design for concrete roads. *Road Mater. Pavement Des.* **2004**, *5*, 193–213. [CrossRef]
12. Doulos, T.; Sioutis, I.; Kontaxis, P.A.; Zissis, G.; Faidas, K. A decision support system for assessment of street lighting tenders based on energy performance indicators and environmental criteria: Overview, methodology and case study. *Sustain. Cities Soc.* **2019**, *51*, 101759. [CrossRef]
13. Pasolini, G.; Toppan, P.; Zabini, F.; Castro, C.D.; Andrisano, O. Design, deployment and evolution of heterogeneous smart public lighting systems. *Appl. Sci.* **2019**, *9*, 3281. [CrossRef]
14. Doulos, T.; Sioutis, I.; Tsangrassoulis, A.; Canale, L.; Faidas, K. Minimizing lighting consumption in existing tunnels using a no-cost fine-tuning method for switching lighting stages according revised luminance levels. In Proceedings of the IEEE International Conference on Environment and Electrical Engineering and 2019 IEEE Industrial and Commercial Power Systems Europe (EEEIC/I&CPS Europe), Genova, Italy, 11–14 June 2019; pp. 1–6. [CrossRef]
15. Wenchenga, C.; Zhengb, H.; Lipinga, G.; Yandana, L.; Dahua, C. Performance of induction lamps and HPS lamps in road tunnel lighting. *Tunn. Undergr. Space Technol.* **2008**, *23*, 139–144. [CrossRef]
16. Salata, F.; Golasi, I.; Bovenzi, S.; de Lieto Vollaro, E.; Pagliaro, F.; Cellucci, L.; Coppi, M.; Gugliermetti, F.; de Lieto Vollaro, A. Energy optimization of road tunnel lighting systems. *Sustainability* **2015**, *7*, 9664–9680. [CrossRef]
17. Salata, F.; Golasi, I.; Poliziani, I.; Futia, A.; de Lieto Vollaro, E.; Coppi, M.; de Lieto Vollaro, A. Management optimization of the luminous flux regulation of a lighting system in road tunnels. A first approach to the exertion of predictive control systems. *Sustainability* **2016**, *8*, 1092. [CrossRef]
18. Maheswari, C.; Jeyanthi, R.; Krishnamurthy, K.; Sivakumar, M. Implementation of energy management structure for street lighting systems. *Modern Appl. Sci.* **2009**, *3*, 31–37. [CrossRef]
19. Sunky, Z.; Mohit, P. Lighting design of an urbanized tunnel. Present at the Seminar Series 2012 Part 4 Research Projects, The University of Auckland, Auckland, New Zealand, 6–7 September 2012.
20. Rabazan, O.; Peña-García, A.; Pérez-Ocón, F.; Gómez-Lorente, D. A simple method for designing efficient public lighting, based on new parameter relationships. *Exp. Syst. Appl.* **2013**, *40*, 7305–7315. [CrossRef]
21. Peña-García, A.; López, J.C.; Grindlay, A.L. Decrease of energy demands of lighting installations in road tunnels based in the forestation of portal surroundings with climbing plants. *Tunn. Undergr. Space Technol.* **2015**, *46*, 111–115. [CrossRef]
22. Peña-García, A. The SLT equation: A tool to predict and evaluate energy savings in road tunnels with sunlight systems. *Tunn. Undergr. Space Technol.* **2017**, *64*, 43–50. [CrossRef]
23. Cantisani, G.; Di Mascio, P.; Moretti, L. Comparative Life Cycle Assessment of lighting systems and road pavements in an Italian twin-tube road tunnel. *Sustainability* **2018**, *10*, 4165. [CrossRef]
24. Cantisani, G.; D'Andrea, A.; Moretti, L. Natural lighting of road pre-tunnels: A methodology to assess the luminance on the pavement—Part I. *Tunn. Undergr. Space Technol.* **2018**, *73*, 37–47. [CrossRef]

25. Cantisani, G.; D'Andrea, A.; Moretti, L. Natural lighting of road pre-tunnels: A methodology to assess the luminance on the pavement—Part II. *Tunn. Undergr. Space Technol.* **2018**, *73*, 170–178. [CrossRef]
26. Drakou, D.; Celucci, L.; Burattini, C.; Nardecchia, F.; Gugliermetti, F. Study of a daylight "filter" in a pre-tunnel structure. In Proceedings of the International Conference on Environment and Electrical Engineering, Rome, Italy, 10–13 June 2015; pp. 649–652.
27. Drakou, D.; Celucci, L.; Burattini, C.; Nardecchia, F.; Gugliermetti, F. Study for optimizing the daylight "filter" in a pre-tunnel structure. In Proceedings of the IEEE Conference 2016, Florence, Italy, 6–10 June 2016.
28. Peña-García, A.; Gil-Martín, L.M.; Escribano, R.; Espín-Estrella, A. A scale model of tension structures in road tunnels to optimize the use of solar light for energy saving. *Int. J. Photoenergy* **2011**, *2011*, 9. [CrossRef]
29. Peña-García, A.; Escribano, R.; Gil-Martín, L.M.; Espín-Estrella, A. Computational optimization of semi-transparent tension structures for the use of solar light in road tunnels. *Tunn. Undergr. Space Technol.* **2012**, *32*, 127–131. [CrossRef]
30. Peña-García, A.; Gil-Martín, L.M. Study of pergolas for energy savings in road tunnels. Comparison with tension structures. *Tunn. Undergr. Space Technol.* **2013**, *35*, 172–177. [CrossRef]
31. Gil-Martín, L.M.; Peña-García, A.; Jimenez, A.; Hernández-Montes, E. Study of light-pipes for the use of sunlight in road tunnels: From a scale model to real tunnels. *Tunn. Undergr. Space Technol.* **2014**, *41*, 82–87. [CrossRef]
32. Qin, X.; Zhang, X.; Qi, S.; Han, H. Design of solar optical fiber lighting system for enhanced lighting in highway tunnel threshold zone: A case study of Huashuyan tunnel in China. *Int. J. Photoenergy* **2015**, *2015*, 10. [CrossRef]
33. Peña-García, A.; Gil-Martín, L.M.; Hernández-Montes, E. Use of sunlight in road tunnels: An approach to the improvement of light-pipes' efficacy through heliostats. *Tunn. Undergr. Space Technol.* **2016**, *60*, 135–140. [CrossRef]
34. Fotios, S.; Boyce, P.; Ellis, C. The effect of pavement material on road lighting performance. *Light. J.* **2005**, *71*, 35–40.
35. Di Mascio, P.; Moretti, L. Concrete vs. asphalt: Pavement and lighting costs in Italian road tunnels. In *ACI Special Publication SP-326 Durability and Sustainability of Concrete Structures, Proceedings of the 2nd Workshop on Durability and Sustainability of Concrete Structures, Moscow, Russia, 6–7 June 2018*; American Concrete Institute: Farmington Hills, MI, USA, 2018.
36. Jung, Y.; Freenman, T.J.; Zollinger, D.G. *Guidelines for Routine Maintenance of Concrete Pavement*; FHWA/TX-08/0-5821-1; Federal Highway Administration: Austin, TX, USA, 2008.
37. Peña-García, A.; Lai Nguyen, T.P. A global perspective for sustainable highway tunnel lighting regulations: Greater road safety with a lower environmental impact. *Int. J. Environ. Res. Public Health* **2018**, *15*, 2658. [CrossRef]
38. Rodrigues, C.R.; Almeida, P.S.; Soares, G.M.; Jorge, J.M.; Pinto, D.P.; Braga, H.A. An experimental comparison between different technologies arising for public lighting: LED luminaires replacing high pressure sodium lamps. In Proceedings of the IEEE International Symposium on Industrial Electronics, Gdansk, Poland, 27–30 June 2011; pp. 141–146.
39. Ente Nazionale Italiano di Normazione [UNI]. *UNI 11095:2011: Illuminazione Delle Gallerie Stradali*; UNI: Milan, Italy, 2011. (In Italian)
40. Moretti, L.; Cantisani, G.; Di Mascio, P. Management of road tunnels: Construction, maintenance and lighting costs. *Tunn. Undergr. Space Technol.* **2016**, *51*, 84–89. [CrossRef]
41. Moretti, L.; Cantisani, G.; Di Mascio, P.; Caro, S. Technical and economic evaluation of lighting and pavement in Italian road tunnels. *Tunn. Undergr. Space Technol.* **2017**, *65*, 42–52. [CrossRef]
42. Commission Internationale de l'Eclairage [CIE]. *Guide for the Lighting of Road Tunnels and Underpasses*; CIE 88-2004; Commission Internationale de l'Eclairage: Vienna, Austria, 2004.
43. Ente Nazionale Italiano di Normazione [UNI]. *UNI EN 13201:2016: Illuminazione Stradale—Parte 2: Requisiti Prestazionali*; UNI: Milan, Italy, 2016. (In Italian)
44. Oxytech. Litestar 4D Litecalc. In *Manuale dell'Utente*; OxyTech srl: Milano, Italy, 2018.
45. Ente Nazionale Italiano di Normazione (UNI). *UNI 10439:2001: Illuminotecnica—Requisiti Illuminotecnici delle Strade Con Traffico Motorizzato*; UNI: Milan, Italy, 2001. (In Italian)
46. SimaPro 8.0.5.13. *Software SimaPro. Pré*; Consultants: Amersfoort, The Netherlands, 2016.

47. European Committee for Standardization (EN). *Sustainability of Construction Works—Environmental Product Declarations—Core Rules for the Product Category of Construction Products*; EN 15804:2012+A1:2013; European Committee for Standardization: Brussels, Belgium, 2013.
48. Gestione Servizi Energetici. *Fuel Mix, Determinazione del Mix Energetico per Gli Anni 2016–2017*; Gestore dei Servizi Energetici GSE S.p.A.: Rome, Italy, 2018; Available online: https://www.gse.it/servizi-per-te/fuel-mix-determinazione-del-mix-energetico-per-gli-anni-2016-2017 (accessed on 18 July 2019).
49. ANAS. *Elenco prezzi Nuove Costruzioni e Manutenzione Straordinaria*; ANAS: Rome, Italy, 2018.

sustainability

MDPI

Article

Application of Climate Based Daylight Modelling to the Refurbishment of a School Building in Sicily

Vincenzo Costanzo [1,*], Gianpiero Evola [2], Luigi Marletta [2] and Fabiana Pistone Nascone [2]

[1] School of the Built Environment, University of Reading, Whiteknights, Reading RG6 6AW, UK
[2] Department of Electric, Electronic and Computer Engineering, University of Catania, Viale A. Doria 6, 95125 Catania, Italy; gevola@unict.it (G.E.); luigi.marletta@dii.unict.it (L.M.); fabiana.pistonenascone@gmail.com (F.P.N.)
* Correspondence: v.costanzo@reading.ac.uk; Tel.: +44-1183-78-7379

Received: 29 June 2018; Accepted: 25 July 2018; Published: 28 July 2018

Abstract: This paper aims at promoting the use of Climate Based Daylight Modelling (CBDM) and related state-of-the-art metrics by discussing a range of design options to improve daylight fruition in rooms with different orientation, shape, function, and furniture of an elementary school that is located in the Mediterranean climate of Agira (Italy). The local climatic conditions, with clear skies for most of the year, require the integration of different shading and re-directing systems with the existing envelope and rooms' layout. Results show that the dynamic modelling is a powerful and 'creative' tool in the designer's hands, which helps to inform about the choice of the most appropriate technological solutions and on their architectural integration. Comparison with mostly used static daylight metrics, such as the average Daylight Factor (*aDF*) and the Uniformity Ratio (*UR*), reveals a contrast with what would be suggested if considering these metrics alone, as prescribed by the Italian legislation. These outcomes rebate the need of performing more accurate and dynamic daylight simulations using recorded (i.e., varying) rather than fixed sky conditions to correctly inform the design process.

Keywords: daylighting; school building; measurement campaign; building simulation; climate based daylight modelling

1. Introduction

The concept of Climate-Based Daylight Modelling (CBDM) was introduced around 20 years ago by two seminal papers [1,2] that defined it as the prediction of any luminous quantity—mainly illuminance time series on a grid of ideal horizontal sensors—by considering the intrinsic variability of the sun and sky conditions as derived from standard weather data.

According to this approach, the use of hourly—or even finer—time steps to describe the relevant climate variables, as recorded by meteorological stations spread throughout the globe, allows for understanding the daylight distribution in a space under different climates and times of the year. This has the potential to revolutionize the way that daylight is conceived and assessed by practitioners and building scientists, while also questioning the reliability of the traditional approach that is based on the use of the Daylight Factor (*DF*) (or its spatial average *aDF* [3]), as prescribed by many regulatory bodies. It does not appear fortuitous then that very recently the Leadership in Energy and Environmental Design (LEED) rating system introduced the use of two dynamic metrics, such as the spatial Daylight Autonomy (*sDA*) and the Annual Sunlight Exposure (*ASE*), for compliance purposes (Illuminating Engineering Society, LM-83 [4]), thus replacing the option of running simulations under fixed clear sky conditions. Furthermore, in 2013, the Education Funding Agency in the United Kingdom (UK) was the first public organization that made mandatory the use of the Useful Daylight Illuminance

(*UDI*) metrics [5] for the evaluation of design proposals that were submitted to the Priority Schools Building Programme [6].

However, despite the indisputable advances achieved by considering real (i.e., recorded) time series of irradiance/illuminance values from largely available weather datasets, there are some concerns to bear in mind when adopting CBDM.

First, the choice of the weather dataset should be based on the purposes of the modelling and the underlying characteristics of the dataset itself (e.g., location, measurement period, statistical techniques being employed for resembling typical or extreme weather conditions). In fact, as demonstrated by Bellia et al. [7], using the IWEC (International Weather for Energy Calculation), Meteonorm, Satel-Light, or TRY weather sources could lead to different results in terms of Annual Light Exposures (i.e., the amount of light falling onto a certain point throughout the year, measured in luxh), and of various dynamic metrics, such as the Daylight Availability (*DA*, [8]) and the *UDI*. This happens because usually the TRY datasets show lower values for the global horizontal irradiance than in other sources; however, these outcomes were only proven for a north-oriented room, while different exposures could lead to different results because of sunlight contribution [7].

Secondly, there is a lack of consensus around the choice of the metrics and of their thresholds to judge if a space is 'well daylit' or not. The variety of CBDM approaches employed for educational buildings, ranging from traditional illuminance and luminance distribution under fixed sky conditions to novel circadian metrics, has been documented in a recent review paper by Costanzo et al. [9].

As an example, in regards to the above-mentioned adoption of the *UDI* metrics for school buildings design in the UK, Littlefair noted that the way calculations are conducted, in terms of offset distance from the walls, grid size, operational hours, and threshold values, might affect the outcomes [10]. This does not allow for comparison among spaces that are used for different purposes (e.g., schools, offices, houses).

Does it mean we should neglect the advances in daylight modelling, and stick to the current 50 years old practice? According to Tregenza [11], the daylight factor would still play a role in daylighting mandatory standards when a simple, robust, meaningful, and easy to test metrics is required for compliance with building codes, provided that a mandatory standard is the best option to achieve a good design. Nonetheless, the same author stated that CBDM should be used creatively, to explore new design solutions driven by different space requirements, orientations, and climate conditions.

Mardaljevic has critically assessed all of these aspects during a recent CIBSE technical symposium [12], demonstrating that, apart from a (quite) understandable 'shock of the new' for everyone that is involved in the fields of daylighting and lighting design, some of the critics are neither well-founded nor would automatically assign a preference to the old practice based on static illuminance ratios.

For example, the care in choosing the 'right' weather file is commonly accepted for thermal simulations, where, except for specific purposes, such as complying with energy performance certification requirements or peak loads calculations, steady-state methods are already put aside in favour of dynamic ones. It seems then that the daylighting simulation community is just a step away from doing it as well.

Furthermore, there is evidence of overheating and glare issues recorded in buildings designed to comply with the minimum *DF* requirements, whose main rationale was to guarantee a minimum sufficient quantity of light for different visual tasks under the worst conditions of a standard overcast sky [13].

What appears more founded is rather the critique about the somehow subjective and arbitrary threshold values set for some of the CBDM metrics, such as *sDA*, *ASE*, and *UDI* (see the next section for their definition and calculation methods). In this sense, more case studies are needed to prove the concept and show their potentialities of informing on different design solutions when being 'creatively' used.

This paper contributes to advance the familiarity with the use of dynamic daylight simulations by presenting a range of design options fitting the needs of different users of a surveyed elementary school that is located in the Mediterranean climate of Agira (Sicily). The local climatic conditions, mostly sunny throughout the year, indeed require the integration of different shading and re-directing systems with the existing envelope and rooms' layout, a task that has been accomplished by employing several CBDM and static metrics. Results show that the dynamic modelling of the spaces is a powerful tool in the designer's hands, helping to inform about the choice of the most appropriate technological solutions and their architectural integration.

2. Methodology

In order to perform an accurate daylight analysis, in Section 2.1, state-of-the-art metrics are presented and commented to show their peculiarities and provide a rationale for their use. Then, in Section 2.2, the building and the experimental campaign are described; finally, the development of a model that is used for running daylight simulations is described in Section 2.3. The simulations were run for both the current configuration of the building and for a series of proposed interventions that are aimed to improve daylight fruition.

2.1. Static and Dynamic Metrics: Which Ones do Fit the Purpose?

As introduced in Section 1 and reported in ref. [9], a number of static and dynamic metrics have been employed in previous studies concerning daylight in schools. In this research, we chose to use both traditional 'static' and more recent 'dynamic' metrics to highlight the differences in terms of applicability and derived outcomes. Furthermore, standard metrics, such as the average Daylight Factor (*aDF*) and the Uniformity Ratio (*UR*) have been considered to inform about daylight distribution under the worst-case condition of an overcast sky. These static metrics are also prescribed by Italian regulations, which set the achievement of minimum thresholds for compliance purposes. The mathematical formulation for these metrics is reported in Equations (1)–(3):

$$DF = \frac{E_i}{E_o} \tag{1}$$

$$aDF = \frac{T \cdot W \cdot \theta \cdot M}{A \cdot (1 - R^2)} \tag{2}$$

$$UR = \frac{E_{\min}}{E_{avg}} \tag{3}$$

The first equation represents the classical definition of punctual Daylight Factor, expressed as the percent ratio of the indoor illuminance value E_i to the outdoor horizontal illuminance value E_o under a standard CIE overcast sky luminance distribution. The second equation expresses the spatial average *DF*, according to the simplified formulation proposed by Crisp and Littlefair [3] for a room of total enclosing surface area A (opaque and transparent), showing an average reflectance R and equipped with windows of effective transmittance T and area W. In Equation 2, θ is the angle subtended by the visible sky from the centre of a window in a vertical plane and M is the maintenance factor.

The Uniformity Ratio (*UR*) is instead defined as the ratio of the indoor minimum illuminance value E_{min} to the average value E_{avg}, under the same overcast sky conditions that are used for the *DF* calculations.

The CBDM metrics adopted are the Useful Daylight Illuminance (*UDI*), the spatial Daylight Autonomy (*sDA*), and the Annual Sunlight Exposure (*ASE*), all of which are defined with reference to an ideal horizontal grid of sensor points. The rationale behind their selection is that all of them are complimentary to each other and help in depicting both the temporal and spatial distribution of daylight in a comprehensive way. In fact, the *UDI* metrics informs about the percent of occupied hours in which the illuminance value in a specific point of the room falls within a specific illuminance bin;

in many cases, the *UDI* is also determined in relation to the spatial mean illuminance value. In this study, three different bins are considered for the illuminance: lower than 100 lux (insufficient daylight), between 100 and 2000 lux (appropriate daylight) and higher than 2000 lux (potential glare), as suggested in the original formulation of Nabil and Mardaljevic [5]. It is worth mentioning that a later study suggested increasing the upper threshold to 3000 lux [14]. On the other hand, the *sDA* metrics informs on the percentage of space achieving a target illuminance value for a specified amount of time in a year. According to the definitions that are given in the IES-LM-83-12 Standard [4], the target illuminance value for *sDA* is 300 lux and the amount of time above which this value should be retained is 50% of the occupied hours.

Finally, the *ASE* metrics expresses the percentage of space for which direct sunlight only (i.e., without considering any internal and exterior reflections and blinds operation) exceeds a threshold value for a fixed number of hours. The illuminance threshold is set to 1000 lux, while the number of annual hours exceeding this value should be lower than 250, otherwise discomfort glare may occur.

The mathematical formulation adopted for these metrics in this paper is reported in Equations (4) and (5):

$$UDI = \frac{\sum_{i=1}^{n} t_i x_i}{\sum_{i=1}^{n} t_i} \quad \text{with } x_i = \begin{cases} 1 \text{ if } E_{avg} \text{ is within the bin} \\ 0 \text{ if } E_{avg} \text{ is outside the bin} \end{cases} \tag{4}$$

$$sDA = \frac{\sum_{i=1}^{n}\sum_{j=1}^{p} x_{i,j}}{\sum_{j=1}^{p} p_j \cdot \sum_{i=1}^{n} t_i} \quad \text{with } x_{i,j} = \begin{cases} 1 \text{ if } E_{i,j} \geq E_{threshold} \\ 0 \text{ if } E_{i,j} < E_{threshold} \end{cases} \tag{5}$$

In Equation (4), the spatial average of the illuminance values is considered; here, t_i is the i-th occupied hour and x_i is a binary function that, according to the mean illuminance recorded in the i-th occupied hour, is $x_i = 1$ if this falls within the bin and $x_i = 0$ otherwise. In Equation 5, p_j is the generic j-th sensor node on the horizontal calculation grid, while the binary function becomes x_{ij} to account for a double summation over both the temporal and spatial domains being this metrics defined as a spatial average. The expression for the *ASE* metrics is the same as for the *sDA* metrics, with differences in the calculation method (i.e., only the direct sunlight contribution is considered for illuminance appraisal) and thresholds (see Table 1).

Finally, the risk of glare occurrence can be studied for some points of view by calculating the Daylight Glare Probability (*DGP*) index, which, according to Carlucci et al. and Pierson et al. [15,16], is one of the most robust approaches for glare assessment. In fact, it is able to account for both the saturation effect when the amount of light reaching the eye is too large, and the contrast effect when the contrast between the visual task and the field of view is too strong. These two aspects are considered in the vertical illuminance at eye level E_v and in the logarithmic term of Equation (6):

$$DGP = 5.87 \cdot 10^{-5} E_v + 0.0918 \cdot \log\left[1 + \sum_{i=1}^{n}\left(\frac{L_{s,i}^2 \cdot \omega_{s,i}}{E_v^{1.87} \cdot P_i^2}\right)\right] + 0.16 \tag{6}$$

Here, L_s is the luminance of the i-th glare source, ω_s is the solid angle through which the glare source is seen, and P_i is the position index. It is important to note that, unlike the other metrics, the *DGP* reports the probability that a person is disturbed by glare in a scale of 20% to 80% [17], rather than a percent of time or space achieving a target value (see Table 1).

Because of current computational limitations, most of the available daylight simulation tools make use of a simplified version of the *DGP*, defined by Wienold in [18,19] and known as *DGPs*:

$$DGPs = 6.22 \cdot 10^{-5} E_v + 0.184 \tag{7}$$

Table 1. Thresholds and target values of the metrics employed *.

Metrics	Space and Time Domain	Target/suggested Value	Source
aDF	Space average over a grid of points, Fixed sky luminance conditions	>3% for classrooms >2% for other rooms	[20,21]
UR	Space average over a grid of points, Fixed sky luminance conditions	>60% for classrooms Not specified for other rooms	[20,21]
UDI	Punctual or space average over a grid of points, Hourly sky luminance conditions	Not specified	[5]
sDA	Space average over a grid of points, Hourly sky luminance conditions	>55% for acceptance >75% for preference	[4]
ASE	Space average over a grid of points, Hourly sky luminance conditions	<10% for acceptance <7% for neutrality <3% for preference	[4]
DGPs	Observer's viewpoint dependent, Hourly sky luminance conditions	<0.35 imperceptible glare 0.35–0.40 perceptible glare 0.40–0.45 disturbing glare >0.45 intolerable glare	[18]

* Except for *aDF* and *UR*, all the metrics have been derived for office spaces.

Here, the influence of the single glare sources is neglected, an assumption that proved to provide reliable results in the absence of direct sunlight transmission and peak reflections through the façade in the observer's direction [19]. Within these validity constraints, four different bands are suggested for categorization purposes: imperceptible glare ($DGPs < 0.35$), perceptible glare ($0.35 \leq DGPs < 0.4$), disturbing glare ($0.4 \leq DGPs < 0.45$), and intolerable glare ($DGPs \geq 0.45$) [18]. In this way, numerical outcomes can directly be used as for the other metrics, since they do not refer any more to a probability distribution. For all these reasons, *DGPs* is used as a glare metrics in this study.

2.2. Case Study Building and the Experimental Campaign

The case study building is an elementary school located in Agira (Italy), a town that is characterized by the warm and sunny climate conditions of a typical Mediterranean island like Sicily. The building shows an E shape with the main façade and the two lateral wings hosting about 30 classrooms on two floors (rooms' height of 4.50 m, total floor area of around 4600 m^2), while the central wing is separated from the lateral ones by means of two courtyards and hosts the gym (see Figure 1). A long corridor running along the north side gives access to the different rooms, all of which are side lit by two or more double-glazed PVC windows that are equipped with external plastic roller shades. This configuration is different for the gym, which has windows placed on all three external walls and has no shading provision.

(**a**) (**b**)

Figure 1. Guglielmo Marconi elementary school in Agira. (**a**) External view of the main facade; and, (**b**) Aerial view.

For the sake of assessing the daylight availability inside the school, three rooms with different functions, orientations, and features have been surveyed: a typical classroom and a computer classroom facing south, and the gym with openings to the north, west, and east oriented facades (see Figure 2).

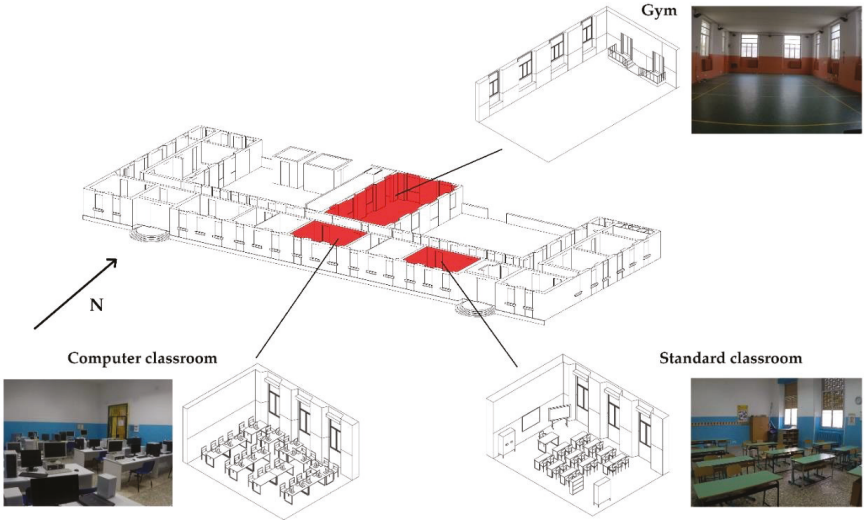

Figure 2. Axonometric views and pictures of the study rooms.

Unfortunately, by the time that the measurement campaign was carried out, the rooms on the west and east wings were not accessible. However, most of them are used for office purposes and not for teaching and learning activities.

Concerning the features of the selected rooms, the standard and computer classrooms have the same size ($8.8 \times 6.1 \times 4.5$ m^3), three openable windows of 1.6 m^2 size each exposed due to south, placed at 1.2 m from the floor, and equipped with a 0.9 m^2 wide clerestory. The interior finishing layer of the walls and the ceiling is of cement plaster painted with a white colour, except for a light blue belt at 2 m from the floor, while the floor itself is made up of granite tiles. In order to keep a high level of detail for modelling, the existing furniture has been considered as well. The standard classroom is furnished with a traditional blackboard and an interactive whiteboard on one of the shortest sides of the room, a closet on the opposite side and a number of desks to accommodate the pupils and the teacher (see Figure 2). The computer classroom instead presents a series of desks with 25 LCD screens and cases.

The gym shows an open plan layout ($18.5 \times 9.8 \times 4.5$ m^3), the walls and the ceiling have the same interior finishing layer of the standard and computer classrooms painted white but with a light pink coloured belt of 2 m height from the floor, which is finished with an anti-slip green coloured PVC layer. Ten windows (four on each of the long sides, two on the north oriented wall) that are placed at 2 m from the floor and equipped with a clerestory (for a resulting window area of 4.8 m^2) bring daylight inside.

The visible reflectance of all indoor opaque surfaces has been calculated through Equation (8), under the hypothesis that the opaque finishing layers behave as a Lambertian diffuser (i.e., equal reflectance for all directions). The luminance L to be used in Equation (8) is the mean value from three spot luminance measurements, which are gathered through a MINOLTA LS 100 luminance meter (measurement range 0.01–50 kcdm^{-2}, accuracy $\pm$ 0.2%). Similarly, the average of three illuminance measurements, collected through a MINOLTA T-10A lux meter (measurement range 0.01–300 klux, accuracy $\pm$ 3%), allows for assessing the illuminance value E in Equation (8).

The visible transmittance of the glazing is calculated at the center of the glass as the ratio of the recorded indoor vertical illuminance close to the windows (measured with the lux meter facing the glazing) to the outdoor vertical illuminance measured just outside the window with the lux meter facing outdoor, see Equation (9). The indoor and outdoor illuminance measurements have been taken simultaneously using tripods on 26 February under partly overcast sky conditions. The resulting values, which are used as an input to the software, are listed in Table 2.

$$\rho = \frac{\pi L}{E} \tag{8}$$

$$\tau = \frac{E_{indoor}}{E_{outdoor}} \tag{9}$$

Table 2. Optical properties of the surfaces in the selected rooms.

Material	Reflectance/Transmittance
White walls	0.78
Blue belt (walls)	0.35
Pink belt (walls)	0.38
Granite tiles	0.31
Green PVC layer	0.12
White ceiling	0.82
Desks finishing (green)	0.37
Blackboard	0.13
Interactive whiteboard	0.80
Wooden chairs	0.35
Blue plastic chairs	0.15
Wooden closet	0.26
Steel frames (desks and chairs)	0.21
PVC windows frames	0.48
PC screens	0.14
Computer and classrooms windows*	0.74
Gym windows*	0.65

* The transmittance is different despite the use of the same glazing type because of dirt deposition.

2.3. Daylighting Simulations and Calibration of the Model

The appraisal of daylight conditions has been conducted by means of dynamic simulations in DIVA [22], a tool that makes use of the well-validated backward ray-tracing method that was provided by Radiance [23]. Given the similarities between the standard classroom and the computer room, the calibration of the model has been carried out only for the standard classroom and the gym, by fine-tuning the more relevant radiance parameters, namely ambient bounces –ab, ambient accuracy–aa, ambient sample–as, ambient divisions–ad, and ambient resolution–ar. The reader can get a thorough understanding of these and other Radiance parameters by consulting [24].

The rooms are supposed to be occupied all year long from 8AM to 1PM on Monday to Friday, except from half of June to half of September (summer break) and for some weeks during the winter break, for a total of 1122 hours per year.

The grid of sensor points has been placed on an ideal 'work plane' identified at desks height in the standard and computer classrooms and at 1 m from the floor in the gym. In both cases, the grid has an offset of 0.5 m from the walls, as suggested by the Italian legislation [20], which also prescribes the use of a calculation grid whose maximum spacing p is defined as a function of the maximum room size d through Equation (10):

$$p = 0.2 \cdot 5^{\log d} \tag{10}$$

This computation results in a square grid of 0.8 m spacing in the case of the standard and computer classrooms, and of 1.8 m spacing in the gym.

For the sake of brevity, the results of the model calibration are presented in Figure 3 for the standard classroom only in the form of gradient contour lines, where the measured illuminance values

((a) panel) are compared to those that are resulting from the simulations ((b) panel). From this picture, it is easy to appreciate how well the simulated illuminance values follow the measured values in terms of both magnitude (illuminance differences are always lower than 12%) and spatial distribution. In both cases, the half of the classroom that is farther from the windows keeps below 500 lux, while in the other half, the illuminance values frequently keep between 500 lux and 1000 lux. The main differences are detected close to the windows, where the effects of direct sunlight is more evident in the measurements. As an example, the measurements pointed out a spot of direct sunlight close to the middle window that is not detected by the simulations. The main reason for this discrepancy is the approximation of climate conditions due to the lack of weather time series for the town of Agira (LAT. 37°39′ N, LON. 14°31′ E, altitude of 824 m above the sea level). Indeed, the closest weather dataset available, provided in the Typical Meteorological Year format (TMY, [25]) and used in this research, is that pertaining to the city of Catania (LAT. 37°30′ N, LON. 15°05′ E, altitude of 7 m above the sea level).

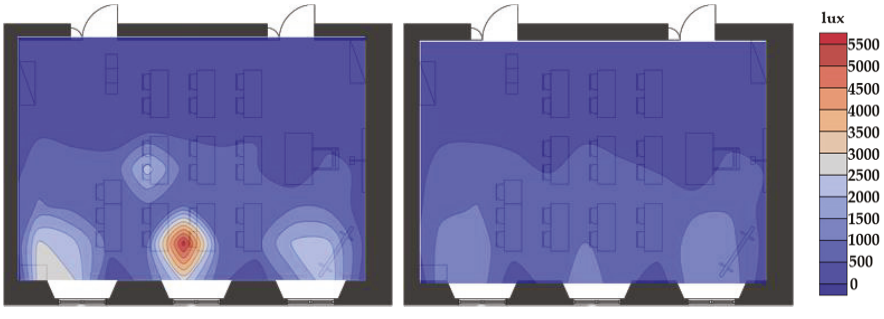

Figure 3. Comparison between measured (**a**) and simulated (**b**) illuminance levels for the standard classroom on 26 February at 11:30 a.m.

Notwithstanding this limitation, similar results are obtained for the gym (a maximum punctual difference of around 23% is reached for the points furthest away from the windows) and the model can be considered to be calibrated. The resulting Radiance parameters are listed in Table 3. Here, it is worth to discuss how the coarser values that are chosen for the gym derive mainly from its geometry and the absence of any furniture to be modelled. More in detail, the number of ambient bounces *-ab* (that is to say the maximum number of bounces of the diffuse indirect component) have been set to two instead of four because the vast amount of glazed surfaces, as well as their orientation and the room size, make the diffuse component lower than the direct one. For the same reasons, the ambient resolution value *-ar* has been set to 128 (that expresses the maximum density of ambient values used for interpolation). These parameters, together with the use of ambient super-samples *-as* and ambient divisions *–ad* values of 256 and 512, respectively, (that are mainly used for reducing noise effects when rendering), help keeping the simulation time reasonable without significantly affecting the simulation outcomes.

Table 3. Main Radiance parameters used for simulations.

Parameter	Standard and Computer Classrooms	Gym
-ab	4	2
-aa	0.12	0.15
-as	400	256
-ad	2200	512
-ar	300	128

3. Results

The outcomes of the simulations are presented first for the existing scenario, showing for each room peculiarities and issues in terms of the metrics that are described in Section 2.1. Based upon these results, specific design solutions for the different environments are proposed, and the metrics calculated again to show the improvements that is possible to achieve.

3.1. Existing Scenario

3.1.1. Standard Classroom and Computer Classroom

The standard and computer classrooms behave differently from the gym, but in a similar way to each other because of the same orientation and of the identical geometric layout and finishing materials. Only slight differences are recorded, imputable to the different furniture only, thus the results of both rooms are presented together for the sake of brevity.

As shown in Table 4, where the calculation of each metrics is reported for the existing configuration, in none of these spaces the statutory *aDF* and *UR* thresholds (amounting to 3% and 60%, respectively) are satisfied. In fact, the *aDF* values amount to 1.8% in the standard classroom and to 2.6% in the computer room, while the UR values are 37% and 24%, respectively.

Table 4. Daylight metrics for the existing scenario.

Metrics (%)	Standard Classroom	Computer Classroom	Gym
aDF	1.8	2.6	3.4
UR	37	24	68
sDA	90.4	96.5	97
ASE	53.4	49	68.2
UDI < 100 lux	4.8	0.3	0
UDI 100–2000 lux	72.5	76.3	93.6
UDI > 2000 lux	22.7	23.4	6.4

The *sDA* metrics suggests a good daylight availability in both cases, with around 90% and 96% of the room area that is daylit with more than 300 lux for at least half of the occupancy time. *ASE* values of 53.4% and 49% are predicted in the standard classroom and computer room in order, which are significantly lower than the 68.2% value that was recorded in the case of the gym (see next subsection) because of the lower amount of glazed surfaces and of the different orientation, which excludes the direct sunlight contribution for most of the time.

In terms of *UDI* distribution, the percent of time when daylight levels fall within the useful range is pretty much the same for these rooms, being around 72% for the classroom against 76% for the computer room, while the percent of occupied time within the *UDI* > 2000 lux bin is around 23% in both cases.

If looking at glare issues, the fisheye pictures that are reported in the Appendix A refer to the observers' point of view reported in the plans. The glare sources are highlighted as coloured patches, together with the instantaneous *DGPs* values achieved during a summer day (1 June at 10 a.m.) and a winter day (1 December at 10 a.m.). The observers' positions have been chosen by running the simulations under clear-sky conditions and identifying the points where the illuminance values were the highest at solstices and equinoxes. In the case of the standard and computer classrooms, very different instantaneous values of *DGPs* both in wintertime (0.48 for the standard classroom against 0.16 for the computer classroom) and in summertime (0.62 against 0.19, respectively) are predicted.

This different behavior is confirmed by the annual *DGPs* calculations for the same observers' position, as reported in Figure 4a,b through the "month-hour" diagrams, which was first introduced by Kambezidis et al. [26]. Here, the columns identify the month of the year, and the rows identify the hours of the day. The hourly *DGPs* values are reported using coloured patches: green patches stand for

imperceptible glare ($DGPs < 0.35$), yellow patches for perceptible glare ($0.35 \leq DGPs < 0.40$), orange patches for disturbing glare ($0.40 \leq DGPs < 0.45$), and red patches for intolerable glare ($DGPs \geq 0.45$).

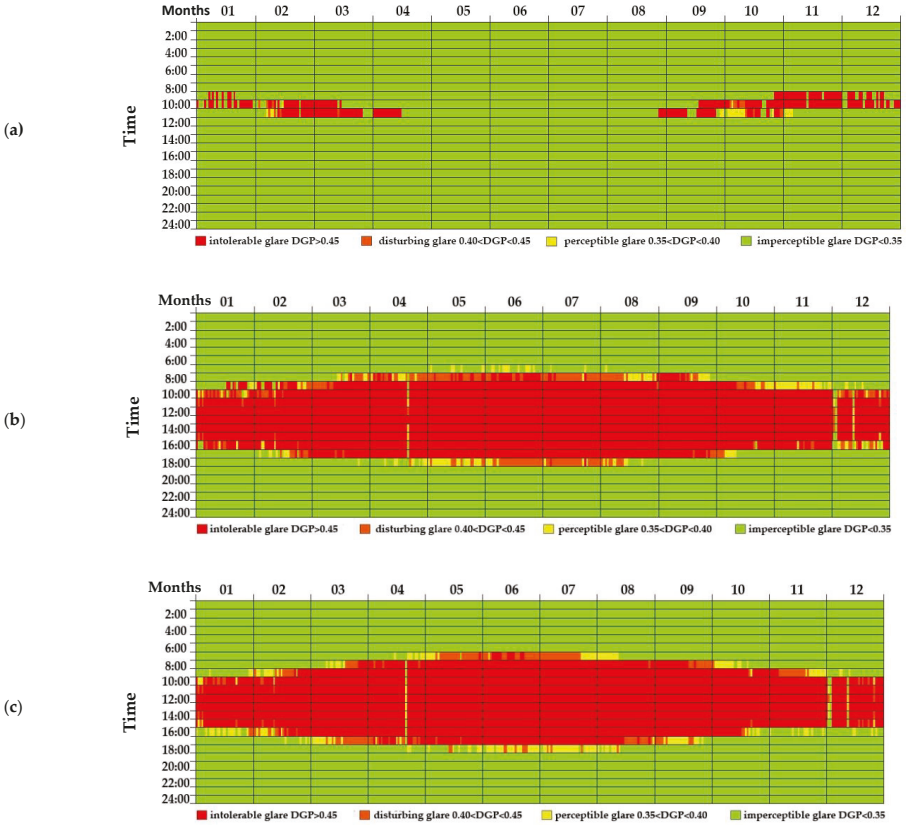

Figure 4. Annual Daylight Glare Probability (*DGPs*) calculation for the current configuration: (**a**) standard classroom; (**b**) computer classroom; and, (**c**) gym.

What emerges from these pictures is that intolerable glare is seldom predicted for the classroom, and this happens only for some hours during winter and transition seasons (January to April and September to December) from 10 a.m. to 11 a.m., when the sun's position is lower over the sky. On the other hand, intolerable glare is expected for the computer classroom for most of the occupancy time throughout the year, mainly because the selected observer is close to the window and it suffers from reflections of direct sunlight on the monitors.

3.1.2. Gym

The simulations run under the current room configuration show how only the gym comply with the prescriptions being set by the Italian building codes for schools in terms of achievement of the minimum *aDF* and *UR* values listed in Table 1. In fact, if looking at Table 4, *aDF* amounts to 3.4% and *UR* amounts to 68% respectively.

For the same room, the *sDA* metrics delineates good daylight availability (the indoor illuminance is higher than 300 lux in 97% of the space for at least 50% of the occupancy period) because of the large amount of windows that are placed on the west and east oriented walls. For the same reasons,

a high value of the *ASE* metrics (amounting to 68.2%) should be expected because of direct sunlight entering the gym both in the morning from the east exposed windows and in the afternoon from the west exposed windows.

However, this piece of information is not enough to support the occurrence of glare issues. In fact, if looking at the *UDI* distribution in Table 4, it is seen that illuminance values are for almost 94% of the time within the 'useful' range of 100 to 2000 lux, with just a few hours of the year (around 6%) being above the upper threshold. Furthermore, glare is a complex phenomenon to assess as it depends on several concurrent factors not yet fully understood [16,17,27]. From the fisheye pictures reported in the Appendix A, it appears that during the above-mentioned summer and winter days *DGPs* values as high as 0.24 should be expected, and thus an imperceptible glare condition is predicted for this observer's position irrespective of different sun's heights.

To have a long-term understanding of glare issues, a yearlong *DGPs* calculation has been carried out for the same observer's positions used for the instantaneous calculation. The corresponding results are presented in Figure 4c for the gym and shows that *DGPs* values are higher than 0.45 for most of the occupied hours (from 8 a.m. to 1 a.m.), thus highlighting the need for implementing some shading provision on the west and east oriented windows.

Furthermore, exemplary hourly luminance patterns during 7 December from 7 a.m. to 5:30 p.m. are reported in the supplementary materials section by using animated GIF pictures of the three rooms discussed so far. Although rather qualitative, this representation makes easy to identify the presence of direct sunlight patches falling within the observer's field of view at different times of the year, thus helping to inform the design of the various shading and re-directing devices discussed in the next subsection.

3.2. Retrofit Scenario

3.2.1. Standard Classroom

The analysis of the current daylight fruition in the standard classroom revealed, on the whole, good daylight availability, as pointed out by the *sDA* and useful *UDI* metrics amounting to 90.4% and 72.5%, respectively. On the other hand, daylight is unevenly distributed within the room (*UR* = 37%), with peak illuminance values being achieved close to the windows and rapidly declining if moving away from them. These issues are fairly typical for single-sided daylit spaces [28,29], and a range of design options can be implemented for reducing daylight levels close to the windows, while also improving those at the bottom of the room and thus increasing the overall uniformity. In particular, the refurbished scenario first aimed at reducing direct sunlight contribution by adding an external horizontal overhang at the top of the clerestory. Secondly, the bottom of the clerestory has been provided with a light shelf with internal and external protrusions, in order to bring daylight in and reflect it further inside through a highly reflective false ceiling.

Different geometrical solutions have been analyzed for the overhang and the light shelf (both internal and external sections) by varying their depth (more insights on this aspect can be found in parametric studies, such as ref. [30]), while in the case of the false ceiling, a planar and a double-curve configuration declining towards the bottom of the room have been investigated.

Various optical properties combinations for the glazing (namely the visible transmittance), the light shelf and the false ceiling (their diffuse and specular reflectance components in order) have been explored as well. The optimal combination resulted in:

- depth of the external overhang: 0.4 m;
- width of the light shelf: 1 m externally + 0.8 m internally; and,
- double-curve false ceiling, with the lowest height set at 1 m from the ceiling, with 0.85 diffuse reflectance and 0.2 specular reflectance.

Reflective glazing (visible transmittance = 0.65) has been used for the biggest panes below the clerestory (see Figure 5), while the light shelf exhibits a diffuse reflectance of 0.85 and a specular

component of 0.5. The use of light shelves and ceilings with a specular component, aimed to enhance the amount of light re-directed towards the bottom of the room, has been described by other researchers [31,32] and it is actually observed in real products that are available on the market. In particular, a specular behaviour has been found to improve illuminance levels and their uniformity in winter and in the mid-seasons, while diffuse lightshelves perform better at high solar altitudes (in summer) [28].

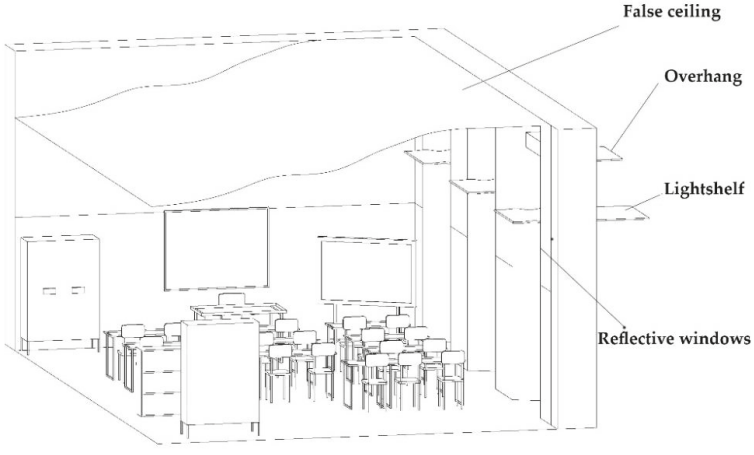

Figure 5. Design solutions for the standard south-oriented classroom.

The use of these design solutions allowed for improving all of the metrics except for the *aDF*, which dropped from 1.8% to 0.8%, and for the *sDA* that dropped from 90.4% to 74.1%. These results sound reasonable, since the amount of light entering the room has been reduced by the combined action of the external overhang, the light shelf, and the reflective glazing. On the other hand, daylight is more evenly distributed thanks to the internal light shelf that re-directs the sunlight to the highly-reflective ceiling, which in turn conveys the light deep to the end of the room. This leads to a reduction in the *UDI* over 2000 lux metrics from the original value of 22.7% to the new one of 3.4%, and to an increase of the useful *UDI* (i.e., that in the range of 100 to 2000 lux) from 72.5% to 89.2%, respectively.

These improvements can be appreciated if looking at Table 5, where all of the values are summarized for both the existing and refurbished scenario, and where a column named 'effect' identifies if a metrics improves (better) or worsens (worse) the corresponding daylight performance if compared to its original value. In terms of annual *DGP* values, Figure 6 shows only minor improvements, meaning that glare is not an issue for the chosen observer's position.

Table 5. Daylight metrics for the standard classroom: existing and refurbished scenario.

Metrics (%)	Existing Scenario	Refurbished Scenario	Effect
aDF	1.8	0.8	Worse
UR	37	55	Better
sDA	90.4	74.1	Worse
ASE	53.4	6.3	Better
UDI < 100 lux	4.8	7.4	Better
UDI 100–2000 lux	72.5	89.2	Better
UDI > 2000 lux	22.7	3.4	Better

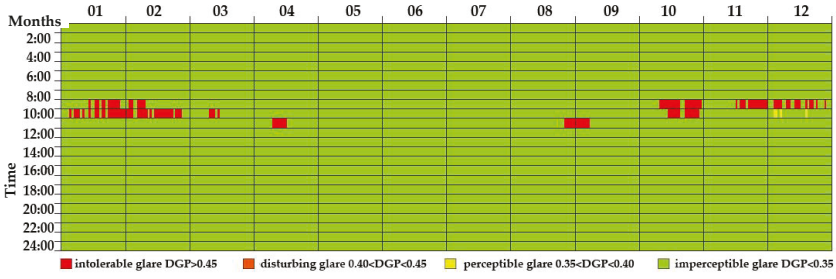

Figure 6. Annual *DGPs* calculation for the standard classroom. Refurbished scenario.

3.2.2. Computer Classroom

As discussed in Section 3.1, the computer classroom differs from the standard classroom only in terms of the furnishing layout, so theoretically it would be possible to apply the same measures that are discussed above. However, the discontinuous use of this room suggests to implement different and more flexible solutions, with lower impact on room geometry and possibly on construction costs as well.

Accordingly, the focus was on reducing the high illuminance values in proximity of the windows, where approximately one-third of the desks are accommodated. To this aim, the benefits of using reflective glazing with visible transmittance as high as 0.5 and internal blinds (curtains) with diffuse reflectance equal to 0.45 have been analysed as two different options (see Figure 7).

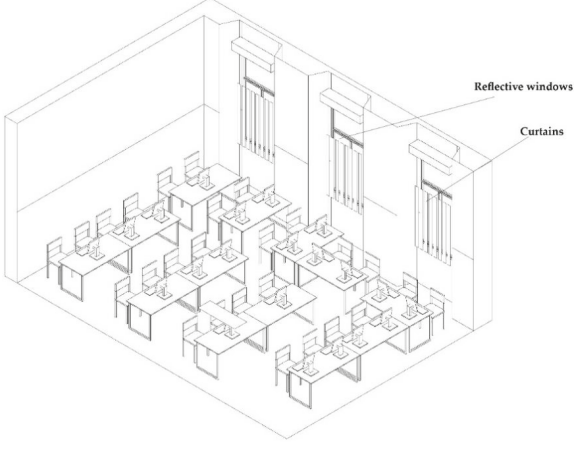

Figure 7. Design solutions for the computer room.

Both of the alternatives behave rather similarly, but a preference is given to the installation of curtains because of the costs and the higher flexibility of use over reflective windows.

By comparing the metrics for the existing and the refurbished cases (Table 6), it can be observed that the main contribution of the curtains is the reduction of the amount of light entering the room, as demonstrated by the lower *sDA* (81.6% against 96.5%) and *UDI* exceeded values (3.6% against 23.4%). Nonetheless, the reduced incoming light brings some benefits in terms of useful *UDI*, since now the average illuminance value is expected to be in the range of 100 lux to 2000 lux for 96.1% of the time against the original 76.3% value. The *UR* also improves, increasing from 24% to 33%, but it still keeps below the threshold of 60% prescribed by the Italian regulations.

Table 6. Daylight metrics for the computer classroom: existing and refurbished scenario.

Metrics (%)	Existing Scenario	Refurbished Scenario	Effect
aDF	2.6	2.4	Slightly worse
UR	24	33	Better
sDA	96.5	81.6	Worse
ASE	49	49	=
UDI < 100 lux	0.3	0.3	=
UDI 100-2000 lux	76.3	96.1	Better
UDI > 2000 lux	23.4	3.6	Better

Negligible differences are expected in terms of *aDF* (2.4% of the refurbished case against 2.6% of the base case), while it is worth noticing how the *ASE* value keeps constant at 49%, just because this is calculated without accounting for the operation of movable shading devices, according to the IES definition [4].

Finally, the annual *DGPs* calculation reported in Figure 8 shows no glare occurrence at every time of the year. This happens because curtains are supposed to be used whenever the *DGPs* calculation for the observer's viewpoint is expected to be above 0.40; different activation strategies would likely perform differently, but they have not been further explored because of the discontinuous use of this room.

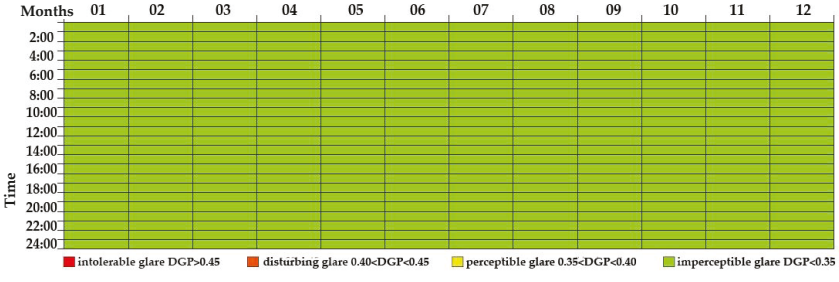

Figure 8. Annual *DGPs* calculation for the computer classroom. Refurbished scenario.

3.2.3. Gym

In the case of the gym, the main issue to be tackled is the rather high illuminance values due to direct sunlight only, as expressed by an *ASE* = 68.2%. When considering that this room presents large glazed surfaces exposed both due to east and west, which are hit from direct sunlight during the morning and the afternoon, respectively, when the sun height is low on the horizontal, the proposed intervention aimed at excluding this contribution by applying louvers on both sides.

The optimal configuration, achieved by running several simulations, was found when using aluminium blades of 0.25 m width, separated from each other by 0.25 m, and showing a diffuse reflectance that is equal to 0.5 and a specular component equal to 0.2.

Moreover, a double-curved false ceiling is proposed, hanging down by approximately 1 m from the centreline of the roof and showing the same optical properties as the false ceiling being applied to the standard classroom (0.85 diffuse reflectance and 0.2 specular reflectance). This is expected to raise the *UR* from the original 68% value (see Figure 9 for an axonometric representation of the proposed interventions).

Simulation results show that, despite that the gym is almost entirely lit with more than 300 lux for at least 50% of its occupancy time (*sDA* = 99.2%), the ASE value is now as low as 12.1% and the time during which illuminance is higher than 2000 lux is only 5.7% of the occupancy period against the original 6.4% value. Moreover, even if the *aDF* drops down from 3.4% to 1.8%, the useful *UDI* metrics

has slightly improved (from 93.6% to 94.3%), meaning that indoor lighting conditions are improved rather than worsened (Table 7).

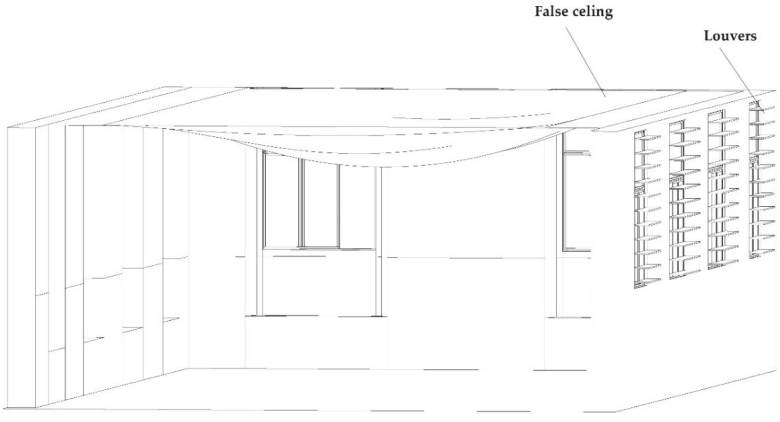

Figure 9. Design solutions for the gym.

Table 7. Daylight metrics for the gym: existing and refurbished scenario.

Metrics (%)	Existing Scenario	Refurbished Scenario	Effect
aDF	3.4	1.8	Worse
UR	68	91	Better
sDA	97	99.2	Slightly better
ASE	68.2	12.1	Better
UDI < 100 lux	0	0	=
UDI 100–2000 lux	93.6	94.3	Slightly better
UDI > 2000 lux	6.4	5.7	Slightly better

Finally, the annual *DGPs* calculation reported in Figure 10 for the observer's position depicted in the Appendix A clearly indicates that with the proposed interventions intolerable glare is expected only for very few hours in a year (around 11AM in February and September and around 5PM in April and September). In the remaining of the year, glare conditions are tagged as imperceptible (i.e., with *DGPs* < 0.35); this represents a strong improvement if compared with the annual *DGPs* calculation of the existing case reported in Figure 4c.

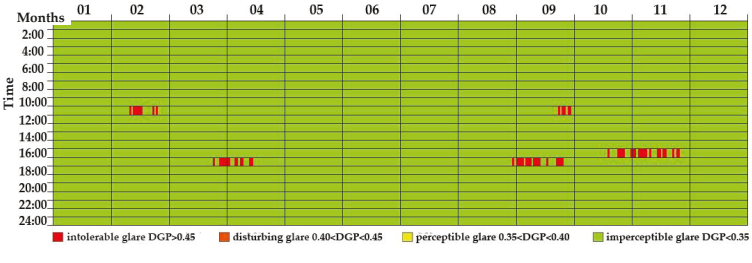

Figure 10. Annual *DGPs* calculation for the gym. Refurbished scenario.

4. Discussion

The outcomes of the daylight simulations presented in the previous section helped inform the design of a retrofit intervention for a school building that is located in the sunny climate of Sicily (Italy).

Three rooms with different orientation, shape, function, and furniture arrangement have been considered for designing the most suitable shading and re-directing devices.

What clearly emerges from the analysis of the different metrics is that, if following the current practice of simply complying with the statutory *aDF* and *UR* values, these devices would likely not be installed. In fact, both the standard and computer classrooms show an *aDF* that is lower than 3%, suggesting that more daylight would be desirable, e.g., by installing larger windows. However, the use of the *sDA* and *ASE* metrics suggests that there is already a good daylight availability throughout the year, and, on the other hand, direct sunlight may cause glare issues.

Further analyses that were conducted with the help of the *UDI* metrics allow for binning of the illuminance values achieved on the work plane (i.e., the ideal surface assumed to host the main visual task) under different sky conditions, pointing out that for more than 20% of the occupancy time illuminance seems to be excessive, especially close to the windows. This information is supported by glare calculations that are carried out in terms of instantaneous and yearlong *DGPs* values for observers that are placed in proximity of the windows.

Given the different orientation and amount of glazed surfaces already available, the gym appears the only room complying with the statutory requirements in terms of *aDF* (above 3%) and *UR* values (above 60%). Nonetheless, the high value that is achieved by the *ASE* metrics (almost 70%) suggests considering the implementation of some shading device in order to reduce or completely cut out direct sunlight contribution.

These results consolidate the existing knowledge about the use of CBDM simulations for informing the design process of school buildings [33,34], and further the understanding of dynamic daylight metrics by using a wide range of illuminance- and luminance-based metrics in a comprehensive way. The comparison with the results of traditional and commonly adopted static metrics shows that the messages coming from these static metrics can be deceiving. It is thus reaffirmed that static metrics are not solid enough to support the appraisal of daylight exploitation, at least under mostly sunny and clear sky conditions. Further, it is not possible to use just one metrics (static or dynamic) to judge if and for how long a space is 'well' daylit, but rather different metrics are needed to consider both the spatial and temporal variability of daylight.

What still appears to be critical is the assessment of glare, which depends on several human-related and room-related factors, and how well-established metrics, such as the *DGPs*, could inform the design process. In fact, the calculation of this metrics is strongly dependent on the field of view, so there could be observers suffering from glare for most of the time while others would not. Moreover, as reported by Berardi and Wang in a paper dealing with daylight conditions in an atrium house [35], inconsistencies in the prediction of glare—and of its intensity—should be expected if comparing different glare indexes. When also considering the long simulation times that are required to carry out year *DGPs* calculations (up to four hours for the standard classroom using an i7 2670QM processor), a criterion to carefully select the worst observer's position before running these simulations would be needed.

5. Conclusions

The introduction of the Climate Based Daylight Modelling (CBDM) concept has questioned the robustness of the traditional practice of relying on static (i.e., fixed) sky conditions to appraise daylight levels within buildings. This paper advanced the knowledge about the use of recently developed CBDM metrics by proposing a detailed daylight analysis of a school building located in Agira (Italy), a town that experiences sunny and clear-sky conditions for most of the year.

Hourly simulations, run using the Radiance-based DIVA software for a calibrated daylight model, allowed to identify the main issues of rooms presenting different orientation, shape, function, and furniture, and helped to inform the design of the required shading and re-directing devices.

More in detail, the calculation of the spatial Daylight Autonomy (*sDA*) metrics revealed good daylight availability for all of the rooms analysed (with values always higher than 90%), but on the other hand the Annual Sunlight Exposure (*ASE*) calculation evidenced a risk of glare occurrence

especially for the gym (*ASE* = 68.2%). This happens because of the large glazed surfaces that are oriented due to both west and east, since they expose the room to direct sunlight in the morning (from east) and in the afternoon (from west). Glare risks have been confirmed by the calculation of the simplified Daylight Glare Probability (*DGPs*) metrics for some observers' position and by the number of hours when the Useful Daylight Illuminance (*UDI*) metric is above the upper threshold of 2000 lux (which happens for around 23% of the occupied hours in the standard and computer classrooms).

Based on these outcomes, retrofit solutions that are aimed at reducing and re-directing direct sunlight, such as external overhangs, light shelves, louvers, and reflective ceilings, have been designed and their efficacy tested by calculating all of the static and dynamic metrics again. The results showed that, despite a reduction in daylight levels in proximity of the windows, as shown by lower *sDA* values than in the base case, higher illuminance values were expected at the bottom of the rooms.

In this way, the useful *UDI* metrics keeps above 90% in all rooms, the *ASE* metrics is close to the threshold of acceptability of 10% (except for the computer classroom) and the *UR* significantly improves in all rooms.

However, it must be pointed out that a design that was carried out using CBDM metrics appears in contrast with what would be suggested if considering the average Daylight Factor (*aDF*) metrics alone, as it is usually done in common design practice. In fact, all of the proposed design solutions lower the *aDF* values if compared to the existing scenario, which are already below the minimum threshold, as prescribed by the Italian regulations for classrooms. This would likely suggest a designer to bring in more daylight by increasing the glazed surfaces; however, such a choice would actually be wrong in relation to the sunny hours, which are much more frequent than cloudy hours in Southern Italy.

These outcomes rebate the need of performing more accurate and dynamic daylight simulations using recorded (i.e., varying) rather than fixed sky conditions to correctly inform the design process.

Supplementary Materials: The following are available online at http://www.mdpi.com/2071-1050/10/8/2653/s1, Figure S1: Hourly luminance distribution for a typical user of the standard classroom, computer classroom and gym, respectively, during 7 December from 7 a.m. to 5:30 p.m.

Author Contributions: Conceptualization, Methodology and Writing, V.C.; Writing—review and editing and Data Curation, G.E.; Supervision and Resources, L.M.; Investigation and Visualization, F.P.N.

Acknowledgments: The authors would like to warmly thank all the teachers and pupils of the 'Guglielmo Marconi' elementary school in Agira (Italy) for their kind support throughout the measurement campaign.

Conflicts of Interest: The authors declare no conflict of interest.

Appendix

This appendix reports the instantaneous *DGPs* values achieved by the observers' positions depicted on the left column for every room analyzed during a typical summer day (1of June at 10 a.m., middle column) and winter day (1 December at 10 a.m., right column) respectively.

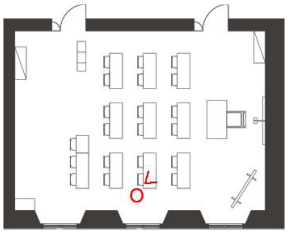

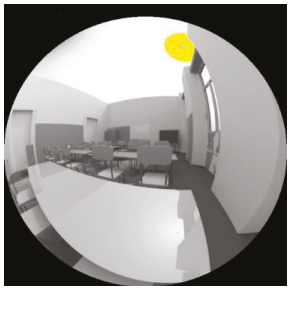

STANDARD CLASSROOM *DGPs = 0.48* *DGPs = 0.62*

COMPUTER CLASSROOM *DGPs = 0.16* *DGPs = 0.19*

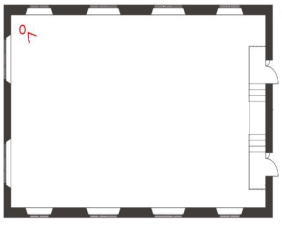

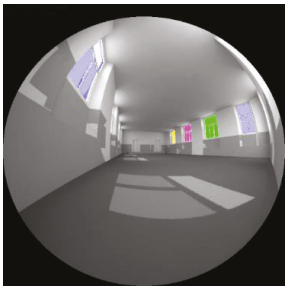

GYM *DGPs = 0.24* *DGPs = 0.21*

References and Notes

1. Mardaljevic, J. Simulation of annual daylighting profiles for internal illuminance. *Light. Res. Technol.* **2000**, *32*, 111–118. [CrossRef]
2. Reinhart, C.F.; Herkel, S. The Simulation of annual daylight illuminance distributions—A state-of-the-art comparison of six RADIANCE-based methods. *Energy Build.* **2000**, *32*, 167–187. [CrossRef]
3. Crisp, V.H.C.; Littlefair, P.J. Average laborious procedure prediction. In Proceedings of the National Lighting Conference (CIBSE), London, UK; 1984.
4. Illuminating Engineering Society. *Approved Method: IES Spatial Daylight Autonomy (sDA) and Annual Sunlight Exposure (ASE)*; IES: New York, NY, USA, 2012.
5. Nabil, A.; Mardaljevic, J. Useful daylight illuminances: A replacement for daylight factors. *Energy Build.* **2006**, *38*, 905–913. [CrossRef]
6. Education and Skills Funding Agency. Priority School Building Programme (PSBP). Available online: https://www.gov.uk/government/collections/priority-school-building-programme-psbp (accessed on 26 June 2018).
7. Bellia, L.; Pedace, A.; Fragliasso, F. The role of weather data files in Climate-based Daylight Modeling. *Sol. Energy* **2015**, *112*, 169–182. [CrossRef]
8. Reinhart, C.F.; Mardaljevic, J.; Rogers, Z. Dynamic daylight performance metrics for sustainable building design. *LEUKOS—J. Illum. Eng. Soc. North Am.* **2006**, *3*, 7–31.
9. Costanzo, V.; Evola, G.; Marletta, L. A Review of Daylighting Strategies in Schools: State of the Art and Expected Future Trends. *Buildings* **2017**, *7*, 41. [CrossRef]
10. Littlefair, P. Opinion: Climate-based daylighting modelling in practice. *Light. Res. Technol.* **2015**, *47*, 512. [CrossRef]
11. Tregenza, P. Opinion: Climate-based daylight modelling or daylight factor? *Light. Res. Technol.* **2014**, *46*, 618. [CrossRef]

12. Mardaljevic, J. Climate-Based Daylight Modelling And Its Discontents. In Proceedings of the CIBSE Technical Symposium, London, UK, 16–17 April 2015; pp. 1–12.
13. Wu, W.; Ng, E. A review of the development of daylighting in schools. *Light. Res. Technol.* **2003**, *35*, 111–125. [CrossRef]
14. Lindelöf, D.; Morel, N. Bayesian estimation of visual discomfort. *Build. Res. Inf.* **2008**, *36*, 83–96. [CrossRef]
15. Carlucci, S.; Causone, F.; De Rosa, F.; Pagliano, L. A review of indices for assessing visual comfort with a view to their use in optimization processes to support building integrated design. *Renew. Sustain. Energy Rev.* **2015**, *47*, 1016–1033. [CrossRef]
16. Pierson, C.; Wienold, J.; Bodart, M. Review of Factors Influencing Discomfort Glare Perception from Daylight. *LEUKOS—J. Illum. Eng. Soc. North Am.* **2018**, *14*, 111–148. [CrossRef]
17. Wienold, J.; Christoffersen, J. Evaluation methods and development of a new glare prediction model for daylight environments with the use of CCD cameras. *Energy Build.* **2006**, *38*, 743–757. [CrossRef]
18. Wienold, J. Dynamic daylight glare evaluation. In Proceedings of the IBPSA 2009 Conference, Glasgow, Scotland, 27–30 July 2009; pp. 944–951.
19. Wienold, J. Dynamic simulation of blind control strategies for visual comfort and energy balance analysis. In Proceedings of the IBPSA 2007 Conference, Beijing, China, 3–6 September 2007; pp. 1197–1204.
20. Luce e illuminazione—Illuminazione dei posti di lavoro—Parte 1: Posti di lavoro in interni. UNI EN 12461-1:2011, 2011. (In Italian)
21. Luce e illuminazione—Locali scolastici—Criteri generali per l'illuminazione artificale e naturale. UNI 10840:2007, 2007. (In Italian)
22. Reinhart, C.; Rakha, T.; Weissman, D. Predicting the Daylit Area—A Comparison of Students Assessments and Simulations at Eleven Schools of Architecture. *Leukos* **2014**, *10*, 193–206. [CrossRef]
23. Ward, G.J.; Rubinstein, F.M. A new technique for computer simulation of illuminated spaces. *J. Illum. Eng. Soc.* **1988**, *17*, 80–91. [CrossRef]
24. Ward, G.L.; Shakespeare, R. *Rendering with Radiance: The Art and Science of Lighting Visualization*; Booksurge Llc: Charleston, SC, USA, 2007; ISBN 0-9745381-0-8.
25. Wilcox, S.; Marion, W. *Users Manual for TMY3 Data Sets*; Technical Report; National Renewable Energy Laboratory: Lakewood, CO, USA, May 2008.
26. Kambezidis, H.D.; Muneer, T.; Tzortzis, M.; Arvanitaki, S. Global and diffuse horizontal solar illuminance: Month-hour distribution for Athens, Greece in 1992. *Light. Res. Technol.* **1998**, *30*, 69–74. [CrossRef]
27. Cantin, F.; Dubois, M.C. Daylighting metrics based on illuminance, distribution, glare and directivity. *Light. Res. Technol.* **2011**, *43*, 291–307. [CrossRef]
28. Pellegrino, A.; Cammarano, S.; Savio, V. Daylighting for Green schools: A resource for indoor quality and energy efficiency in educational environments. *Energy Procedia* **2015**, *78*, 3162–3167. [CrossRef]
29. Korsavi, S.S.; Zomorodian, Z.S.; Tahsildoost, M. Visual comfort assessment of daylit and sunlit areas: A longitudinal field survey in classrooms in Kashan, Iran. *Energy Build.* **2016**, *128*, 305–318. [CrossRef]
30. Berardi, U.; Anaraki, H.K. The benefits of light shelves over the daylight illuminance in office buildings in Toronto. *Indoor Built Environ.* **2018**, *27*, 244–262. [CrossRef]
31. Meresi, A. Evaluating daylight performance of light shelves combined with external blinds in south-facing classrooms in Athens, Greece. *Energy Build.* **2016**, *116*, 190–205. [CrossRef]
32. Ho, M.C.; Chiang, C.M.; Chou, P.C.; Chang, K.F.; Lee, C.Y. Optimal sun-shading design for enhanced daylight illumination of subtropical classrooms. *Energy Build.* **2008**, *40*, 1844–1855. [CrossRef]
33. Zomorodian, Z.S.; Korsavi, S.S.; Tahsildoost, M. The effect of window configuration on daylight performance in classrooms: A field and simulation study. *Int. J. Archit. Eng. Urban Plan* **2016**, *26*, 15–24.
34. Zomorodian, Z.S.; Tahsildoost, M. Assessment of window performance in classrooms by long term spatial comfort metrics. *Energy Build.* **2017**, *134*, 80–93. [CrossRef]
35. Berardi, U.; Wang, T. Daylighting in an atrium-type high performance house. *Build. Environ.* **2014**, *76*, 92–104. [CrossRef]

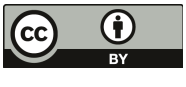

sustainability

MDPI

Review

Compatibility between Crops and Solar Panels: An Overview from Shading Systems

Raúl Aroca-Delgado [1], José Pérez-Alonso [1], Ángel Jesús Callejón-Ferre [1,*] and Borja Velázquez-Martí [2]

[1] Department of Engineering, University of Almería, Agrifood Campus of International Excellence (CeiA3), s/n, 04120 La Cañada, Almería, Spain; raul.aroca.edu@juntadeandalucia.es (R.A.-D.); jpalonso@ual.es (J.P.-A.)

[2] Departamento de Ingeniería Rural y Agroalimentaria, Universitat Politècnica de València, Camino de Vera s/n, 46022 Valencia, Spain; borvemar@dmta.upv.es

* Correspondence: acallejo@ual.es; Tel.: +34-950-214-236

Received: 14 January 2018; Accepted: 6 March 2018; Published: 8 March 2018

Abstract: The use of alternative energy in agricultural production is desired by many researchers, especially for protected crops that are grown in greenhouses with photovoltaic panels on the roofs. These panels allow for the passage of varying levels of sunlight according to the needs of each type of crop. In this way, sustainable and more economic energy can be generated than that offered by fossil fuels. The objective of this work is to review the literature regarding the applications of selective shading systems with crops, highlighting the use of photovoltaic panels. In this work, shading systems have been classified as bleaching, mesh, screens, and photovoltaic modules. The search was conducted using Web of Science Core Collection and Scopus until February 2018. In total, 113 articles from scientific journals and related conferences were selected. The most important authors of this topic are "Yano A" and "Abdel-Ghany AM", and regarding the number of documents cited, the most important journal is Biosystems Engineering. The year 2017 had the most publications, with a total of 20, followed by 2015 with 14. The use of shading systems, especially of photovoltaic panels, requires more crop-specific research to determine the optimum percentage of panels that does not reduce agricultural production.

Keywords: sunlight; shading; greenhouse; solar panels; renewable energy

1. Introduction

Depending on the latitude, the weather conditions (temperature, humidity, and CO_2) often are not optimal for crops. For this reason, crops are usually protected by structures (greenhouses). Even so, climate control becomes necessary—in winter/fall due to low temperatures during the night and in spring/summer due to high temperatures during the day (Callejón-Ferre et al. [1]; Castilla [2]). A clear example of this situation occurs in Mediterranean countries.

To correct high and low temperatures, several shading systems in greenhouses are available: bleaching, mesh, screens, and photovoltaic panels (Figure 1).

Bleaching is the simplest and most economical technique that is used as a shading system. It consists of applying a solution of water and calcium carbonate to the roof of the greenhouse [1]. The other systems that were used (mesh and screens) can be used inside or outside of the greenhouse, and can be permanent (fixed) or mobile (displaceable; Figure 1).

Recently, photovoltaic panels have been used on the roofs of the greenhouses. These can be opaque, semi-transparent, or transparent, allowing for less solar radiation to pass through, which can intentionally affect or not affect the crop development. This situation, supposedly, would allow for the compatible generation of electrical energy and agricultural production (Ureña-Sánchez et al. [3]).

The integration of semi-transparent photovoltaic panels can decrease the solar irradiation and the internal air temperatures, as well as generate electric energy for environmental control systems (Hassanien et al. [4]).

Some concern remains about the impact that solar panels could have on crop yield and fruit quality, as a direct relation exists between the solar radiation that is received by the plants and decreased crop yields ($kg \cdot m^{-2}$) and smaller fruit sizes [5].

The objective of this work is to review the literature for applications of selective shading systems on crops, highlighting the use of photovoltaic panels.

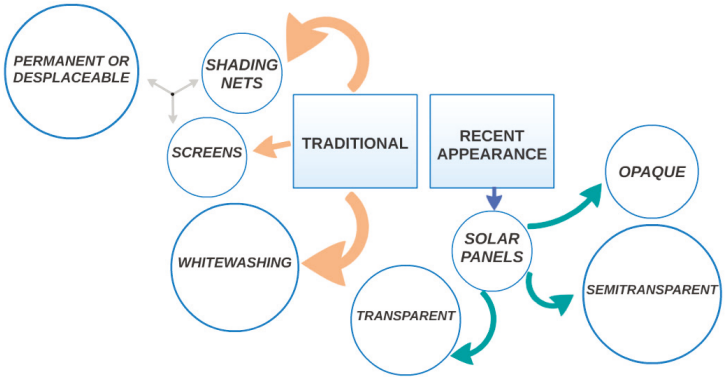

Figure 1. Shading systems in greenhouses typical of Mediterranean countries.

2. Material and Methods

The analysed articles were obtained electronically from the Library of the University of Almeria with a license from the Spanish Foundation for Science and Technology (FECYT) of Web of Science Core Collection (Wos) provided by Clarivate Analytics [6] and Scopus [7]. Through the 'Advanced search' option, terms such as 'greenhouse', 'solar', 'roof', 'energy', 'covering material', and 'shading' were used. A total of 113 articles (articles from scientific journals and conferences) that were directly or indirectly related to the previous terms have been analysed in the period from January 1990 to February 2018.

Only two databases have been used, which could limit the number of bibliographic citations obtained. Likewise, because only articles and congresses were considered, information from books, book chapters, and other similar formats is excluded.

3. Shading, Mesh, Screens and Others

Shading produced by different systems and used in greenhouses has been investigated by numerous authors, mainly from the 1990s to the present (Table 1).

Table 1. Studies related to shading in greenhouses.

Authors	Location	Observations
Cockshull et al. (1992) [5]	United Kingdom	Shading nets and whitewashing on tomato
Abdel-Mawgoud et al. (1996) [8]	Egypt	Effects of shading
Papadopoulos y Pararajasingham (1997) [9]	Canada	Plant spacing
Klaring (1998) [10]	Germany	Shading on broccoli
Kittas et al. (1999) [11]	Greece	Shading on the spectral distribution of light
Araki et al. (1999) [12]	Belgium	Shading nets on spinach
Abreu y Meneses (2000) [13]	Portugal	Effects of whitewashing on tomato
Kittas et al. (2003a) [14]	Greece	Aluminized thermal shading screen on roses

Table 1. *Cont.*

Authors	Location	Observations
Kittas et al. (2003b) [15]	Greece	Aluminized thermal shading screen on roses
Sandri et al. (2003) [16]	Brazil	Effects of shading screen on tomato
Medrano et al. (2004) [17]	Spain	Mobile shading on tomato
Bartzanas y Kittas (2005) [18]	Greece	Shading and evaporative cooling system
Lorenzo et al. (2006) [19]	Spain	Mobile shading on tomato
Rosales et al. (2006) [20]	Spain	Temperature and solar radiation
Gent (2007) [21]	United States	Reflective-aluminized shading screen on tomato
Callejón-Ferre et al. (2009) [1]	Spain	Reflective-aluminized shading screen on tomato
Abdel-Ghany y Al-Helal (2010) [22]	Saudi Arabia	Shading nets
Sato et al. (2010) [23]	Japan	Effects of shading
Aberkani et al. (2010) [24]	Canada	Shading using a retractable liquid foam on tomato and pepper
Abdel-Ghany y Al-Helal (2011) [25]	Saudi Arabia	Shading nets
Al-Helal y Abdel-Ghany (2011) [26]	Saudi Arabia	Shading nets
Chen et al. (2011) [27]	Taiwan	Shading nets
García et al. (2011) [28]	Spain	Mobile shading and fog system
Abdel-Ghany y Al-Helal (2012) [29]	Saudi Arabia	Shading nets
Holcman y Sentlhas (2012) [30]	Brazil	Shading screens of different colors
Ilic et al. (2012) [31]	Serbia	Shading nets
Abdel-Ghany et al. (2015) [32]	Saudi Arabia	Shading nets
Hernández et al. (2015) [33]	Spain	Shading and increased N doses
Ahmed et al. (2016) [34]	Saudi Arabia	Shading nets and whitewashing on tomato and pepper
Nagy et al. (2017) [35]	Hungary	Shading nets on pepper
Murakami et al. (2017) [36]	Japan	Shading nets on melon
Yasin et al. (2017) [37]	Denmark	Shading nets on Grass Weeds
Costa et al. (2017) [38]	Brazil	Reflective-aluminized shading screen on tomato
Holcman et al. (2017) [39]	Brazil	Thermo-reflective shading screen on tomato
Priarone et al. (2017) [40]	Italy	Benefits of shading

3.1. Mesh

Cockshull et al. [5] explain that shading can reduce the average tomato size, but in turn favours a more homogeneous ripening in summer.

Araki et al. [12], in a plantation of spinach, observed that shading of 45% is optimal for growth in the months of June, August, and September, but 60% is optimal for the month of July.

Abdel-Ghanyand Al-Helal [22] claim that the diffusion of solar radiation occurring with shading mesh is related to the colour, texture, and porosity of the mesh; however, they caution that the methods used to measure the porosity of shading mesh may have an estimated error of 14% to 38% [25]. In addition, they revealed that shading mesh behaves like translucent materials, and the colour and solidity of the mesh influence heat transfer [26]. Later, they confirmed that the temperature and porosity of the mesh are more relevant parameters than texture and colour when radiative transmission and reflection are measured [29].

Chen et al. [27] developed a model to evaluate the performance of shading mesh and to predict air temperature in greenhouses.

In Serbia, Ilic et al. [31] observed that shading with coloured mesh in a tomato plantation reduced the amount of fruit with cracked skin and increased the commercial production by 35%, although the fruits had a lower beta-carotene content.

Abdel-Ghany et al. [32] compared upper exterior shading of the greenhouse with interior shading, finding that interior shading increases the thermal radiation by 147% and daytime air temperatures, whereas this increase is not seen with exterior shading.

Ahmed et al. [34] claim that shading methods reduce energy and water consumption, and increase fruit productivity and quality.

Nagy et al. [35] conducted a study of the production of pepper plants grown in a greenhouse under white, red and green shading and determined that the content of ascorbic acid increased even more in the fruits of plants grown with white shading.

Murakami et al. [36] state that the use of mesh in a melon crop reduced the leaf temperature of greenhouse plants by approximately 5 °C, and the size of the fruit was not affected, although the sugar accumulation in the fruit did increase.

3.2. Screens

In rose cultivations in glass greenhouses in Greece, Kittas et al. [14,15] reported that the aluminized thermal screens achieved a more homogeneous microclimate and increased the winter air temperature, thus achieving energy savings of approximately 15%.

Sandri et al. [16] verified that the number of fruits per square metre did not differ in shaded tomato plantations (52%) when compared with those that were unshaded.

Medrano et al. [17] found that the use of external mobile shading reduced the transpiration rate in tomato plants.

Lorenzo et al. [19] explained that, in hot climates with sparse water sources, mobile shading can improve tomato quality and water-use efficiency.

In the north-eastern United States, Gent [21] achieved 9% more commercial tomato production with a 50% shade based on aluminized cloth; the shade only reduced the size of the fruits one of the five years that were studied; in addition, the amount of tomatoes with cracked skin was reduced by 10%.

Callejón-Ferre et al. [1] found that tomatoes have less °Brix when aluminized screens with 60% shading are used instead of traditional bleaching, but no difference was observed with a lower percentage shading.

García et al. [28] explain that mobile shading and misting are equally efficient in reducing high air temperatures.

Yasin et al. [37] studied how the use of greenhouse climate screens affected the growth and development of three common weeds; shade substantially reduced the height of the plant, the number of leaves, and the index of foliar chlorophyll content.

Costa et al. [38] evaluated the growth parameters of the tray seedlings, as well as the growth and production of plants in pepper pots in greenhouses with three different types of shading—transparent low-density polyethylene and reflective aluminized screen under the film, black filament with 50% shade, and aluminized screen—with better yields being obtained with the first method.

Holcman et al. [30] comment that in cherry tomato crops, a greater yield of the plant and greater average weight of the fruits are obtained with a diffusive plastic than with the use of a thermoreflective shading screen.

3.3. Others

Klaring [10] found that broccoli yield is reduced by 1% for every 1% reduction in irradiation by shading.

Abdel-Mawgoud et al. [8] found that, in tomatoes with 30% shade, the yield was not reduced, although the total dry matter did decrease; the shade can serve to improve the commercial quality of the fruit by reducing burns.

Rosales et al. [20] comment that the increase in temperature and solar radiation in the cherry tomato during May in Spain diminishes the nutritional quality of the fruits.

Sato et al. [23] claim that as the shading level increases, the dry weights of tomato plants decrease, but no differences occur in the distribution of the organic dry matter.

Hernández et al. [33] state that in tomatoes with 50% of the sunlight attenuated by shading, a higher yield, as well as a higher concentration of lycopene, was obtained with lower doses of irrigated nitrogen (7 mM of N), regardless of the doses of N to tomatoes without shade.

Papadopoulos and Pararajasingham [9] explored the consequences of spacing between plants and light penetration for tomato productivity.

Kittas et al. [11] evaluated the quality of light that is received by plants by comparing three types of shading: bleaching, external mesh, and internal aluminized screens. Their results indicate the need to better control the characteristics of the light that is caused by the shading system used.

Abreu and Meneses [13] assert that roof bleaching reduces radiation transmission by 50%, which in turn reduces periods with temperatures above 30 °C.

Bartzanas and Kittas [18] took different measurements in a partially shaded greenhouse with a cooling system, finding that in the shaded part, greater transpiration occurred.

Aberkani et al. [24] comment that differences in air temperature of up to 6 °C, a humidity increase of 10% and reduction in the need for ventilation are possible when polyethylene liquid foam is used in greenhouse ceilings.

Holcman and Sentelhas [39] maintain that the lowest transmission of solar radiation is achieved with black polyethylene sheets ascompared with the use of red or blue sheets or with thermo-reflective sheets; the highest temperatures are reached with blue sheets.

Priarone et al. [40] investigated the selection of the most favourable solutions for ventilation, heating, cooling and thermo-hygrometric control of a greenhouse, and they propose, as optimal, the shading of the glazed surfaces, the natural ventilation and the forced convection of the external air.

4. Photovoltaic Modules in Greenhouses

The application of photovoltaic modules (PM) to agricultural environments has been analysed by a large number of authors (Table 2).

Table 2. Studies related to photovoltaic modules in agriculture.

Authors	Location	Observations
Kozai et al. (1999) [41]	Japan	Electricity generated using photovoltaic cells
Yano et al. (2007) [42]	Japan	Applications of photovoltaic power systems
Campiotti et al. (2008) [43]	Italy	Prototype of photovoltaic greenhouse
Yano et al. (2009) [44]	Japan	Photovoltaic modules mounted inside the roof
Minuto et al. (2009) [45]	Italy	Semi-transparent photovoltaic systems
Yano et al. (2010) [46]	Japan	Configuration of photovoltaic modules
Qoaider y Steinbrecht (2010) [47]	Germany	The economic feasibility of photovoltaic technology
Carlini et al. (2010) [48]	Italy	Performance analysis of greenhouses with PV
Sonneveld et al. (2010) [49]	Netherlands	Hybrid system with PV and thermal energy
Dupraz et al. (2011) [50]	France	Agrivoltaic system
Campiotti et al. (2011) [51]	Italy	Photovoltaic system on tomato
Pérez-Alonso et al. (2011)[52]	Spain	Flexible solar panels and shading
Ganguly et al. (2011) [53]	India	Floriculture greenhouse by solar photovoltaic
Carlini et al. (2012) [54]	Italy	Photovoltaic system on tomato
Kadowaki et al. (2012) [55]	Japan	Configuration of photovoltaic modules on onions
Marucci et al. (2012) [56]	Italy	Semi-transparent photovoltaic systems
Pérez-Alonso et al. (2012)[57]	Spain	Evaluation of a photovoltaic system
Poncet et al. (2012) [58]	France	Agrivoltaic system
Klaring y Krumbein (2013) [59]	Germany	PM and permanent shading
Marrou et al. (2013) [60]	France	Agrivoltaic system
Castellano (2014) [61]	Italy	Configuration of photovoltaic modules
Juang y Kacira (2014) [62]	South Corea	PM in an arid environment
Cossu et al. (2014) [63]	Italy	PM and shading
Tani et al. (2014) [64]	Japan	PM and light diffusion on lettuce
Pérez-Alonso et al. (2014) [65]	Spain	PM and shading on tomato
Pérez-García et al. (2014) [66]	Spain	Evaluation of a photovoltaic system
Serrano et al. (2014) [67]	Spain	PM and shading
Yano et al. (2014) [68]	Japan	Semi-transparent photovoltaic systems
Fatnassi et al. (2015) [69]	France	Configuration of photovoltaic modules
Marucci et al. (2015) [70]	Italy	Prototype of dynamics photovoltaic greenhouse
Bulgari et al. (2015) [71]	Italy	PM and shading on tomato
Yang et al. (2015) [72]	China	Transparent photovoltaic systems
Castellano y Tsirogiannis (2015) [73]	Italy	Configuration of photovoltaic modules
Cossu et al. (2016) [74]	Japan	Semi-transparent photovoltaic systems
Marucci y Capuccini (2016a) [75]	Italy	PM and energy efficiency

Table 2. *Cont.*

Authors	Location	Observations
Marucci y Capuccini (2016b) [76]	Italy	PM and energy efficiency
Hassanien et al. (2016) [77]	Egypt	The challenges for photovoltaic systems
Buttaro et al. (2016) [78]	Italy	Semi-transparent photovoltaic systems
Castellano et al. (2016a) [79]	Italy	PM and photosynthetic photon flux
Castellano et al. (2016b) [80]	Italy	PM and shading
Cuce et al. (2016) [81]	United Kingdom	PM and energy consumption
Saifultah et al. (2016) [82]	South Corea	Semi-transparent photovoltaic systems
Dinesh y Pearce (2016) [83]	United States	Agrivoltaic system
Cossu et al. (2017) [84]	Japan	PM and radiation
Cossu et al. (2017) [85]	Japan	Configuration of photovoltaic modules
Carreño-Ortega et al. (2017) [86]	Spain	Environmental and socioeconomic development
Marucci et al. (2017) [87]	Italy	Photovoltaic greenhouse tunnel
Valle et al. (2017) [88]	France	Agrivoltaic system
Trypanagnostopoulos et al. (2017) [89]	Greece	PM and shading
Loik et al. (2017) [90]	United States	PM and energy balance
Yildirim et al. (2017) [91]	Turkey	PM and economic and environmental evaluation
Trypanagnostopoulos et al. (2017) [92]	Greece	Electricity generated using photovoltaic cells
Kavga et al. (2017) [93]	Greece	PM and shading
Marucci et al. (2018) [94]	Italy	Photovoltaic greenhouse tunnel
Liu et al. (2018) [95]	China	PM and shading

Kozai et al. [41] explain that considerable amounts of electricity can be generated without significantly affecting the transmission of solar radiation if the number of photovoltaic modules and the orientation of the greenhouse are correctly chosen for the latitude and the time of year.

Yano et al. [42] made use of the energy that is generated by photovoltaic modules to operate an autonomous lateral ventilation system. Later, Yano et al. [44] verified that when photovoltaic modules are mounted on the interior surface of greenhouses in Japan, greater energy efficiency is obtained with inclination angles of 20 degrees than with angles of 28 degrees.

Campiotti et al. [43] describe a prototype photovoltaic greenhouse being built in southern Italy.

Yano et al. [46] and Fatnassi et al. [69] found that the arrangement of panels in the form of a chessboard compared to panels placed in other arrangements improves the distribution of sunlight within the greenhouses. Kadowaki et al. [55] found that the placement of photovoltaic modules in this arrangement is desired to reduce the effects of shading. Additionally, Cossu et al. [85] suggest new design criteria for PV greenhouses, concerning the decrease of the PV array coverage and different installation patterns of the PV panels on the roof.

Qoaider and Steinbrecht [47] demonstrated that providing power for entire farming populations is feasible with photovoltaic energy.

Carlini et al. [48] used TRNSYS 16 software to simulate temperatures and humidity in a greenhouse with photovoltaic modules in order to determine the performance of the greenhouse.

Sonneveld et al. [49] developed a hybrid system of photovoltaic and thermal panels together with the reflection of near infrared radiation to improve climate conditions in a greenhouse and avoid the use of fossil fuels.

Dupraz et al. [50] propose that an agrovoltaic system (using agricultural land for the generation of solar energy) may be the best solution in countries with few areas conducive to agriculture. One year later, Poncet et al. [58] stated that the main challenge for the agrovoltaic systems is to achieve higher productivity and quality, while reducing the environmental impact. However, Marrou et al. [60] note that moving from an open crop to an agrovoltaic system requires small modifications focused on the mitigation of shaded areas and the selection of plants adapted to fluctuating shadows. More recently, Dinesh and Pearce [83] affirmed that the value of electricity that is generated by solar energy and the production of shade-adapted crops creates an increase of more than 30% of the economic value of the lands that deploy an agrovoltaic system.

Campiotti et al. [51], in an experiment that was carried out in southern Italy with a greenhouse with rooftop photovoltaic panels, found that the energy requirements of 21 tomato plants for 120 days were 19.48 kW·h, and the modules produced a total of 333.6 kW·h from September to December. Later, Pérez-Alonso et al. [57] and Pérez-García et al. [66] conducted two experiments in south-eastern Spain, in which an annual energy yield of 8.25 $kW \cdot h \cdot m^{-2}$ was achieved through 24 flexible modules.

Pérez-Alonso et al. [52] did not obtain significant differences between tomatoes shaded by flexible photovoltaic panels and non-shaded tomatoes; however, Klaring and Krumbein [59] maintain that restricting the intensity of solar radiation through permanent shading leads to a reduction in the growth and yield of the tomato plant but not the quality of the fruit.

Ganguly et al. [53] managed to maintain an optimum temperature for the cultivation of flowers in a greenhouse in India from energy provided by panels installed in the roof and a support system for critical hours, providing a clear example of agronomic compatibility.

Carlini et al. [54] proved that solar greenhouses with photovoltaic modules manage to save energy in both cooling and heating tasks.

Castellano [61] discusses different configurations for the placement of photovoltaic modules in greenhouses and analyses some parameters with Autodesk Ecotect Analysis software.

In South Korea, Juang and Kacira [62] propose adding integrated photovoltaic systems to the structure of greenhouses to alleviate the energy and food problems of certain populations that have difficulty accessing electricity, fertilizers, or good quality water.

Cossu et al. [63], in a greenhouse with 50% of the roof surface being occupied by photovoltaic modules, included supplementary lighting with the energy that was generated by the modules, but the plantation was too shaded and did not obtain benefits.

Tani et al. [64] claim that light diffusion films can be applied to improve productivity in crops shaded by photovoltaic panels.

Pérez-Alonso et al. [65] state that the commercial production of tomatoes is compatible with 9.8% shading that is produced by flexible photovoltaic modules. Tripanagnostopoulos et al. [92] propose that a PV system covering only 6.5% of the roof surface could be enough to completely cover the electricity needs for the auxiliary processes of a greenhouse. Liu et al. [95] have developed new types of photovoltaic sheets that shade on the field can be reduced.

Serrano et al. [67] made use of flexible panels to supply energy to autonomous systems and to replace the shading elements, thus achieving normal crop development.

Marucci et al. [70] used dynamic panels, which move along the longitudinal axis, in order to vary the degree of shading.

Bulgari et al. [71] reveal that the efficiency of the use of solar radiation by tomato plants is greater in greenhouses with solar panel shading, but the fruit tends to have lower lycopene, beta-carotene, sucrose, reducing sugars, and total sugar content.

Castellano and Tsirogiannis [73] performed an analysis of different photovoltaic configurations in the greenhouse to determine the effects of shading and energy efficiency.

Marucci and Capuccini [75] reported that it is possible to combine the production of electricity and agricultural production if the type of crop, the latitude, and the characteristics of the greenhouse are taken into account. That same year, Marucci and Capuccini [76] affirmed that the use of photovoltaic panels is a viable alternative both for shading greenhouses and for electricity production in warm areas.

Hassanien et al. [77] conducted a small discussion on photovoltaic technology and the challenges it faces in the agricultural environment.

Castellano et al. [79] used a model that predicts the density distribution of photosynthetic photons in photovoltaic greenhouses with an error of 19%. That same year, Castellano et al. [80] developed a model to predict the effect of shading within a photovoltaic greenhouse.

Cuce et al. [81] managed to save up to 80% in energy consumption in greenhouses by combining solar and thermal energy with new insulation materials.

Cossu et al. [84] developed an algorithm to estimate the global radiation that had accumulated within photovoltaic greenhouses to aid in the selection of the most suitable plant species according to their light needs.

Carreño-Ortega et al. [86] estimated that the use of photovoltaic modules in the agricultural environment can increase the profitability of the farms up to 52.78% and that environmental and economic improvements would also be obtained.

Marucci et al. [87,94] analysed the shading variation produced by the application of flexible and semi-transparent photovoltaic panels in a tunnel-type greenhouse, where the percentage of shading during the year never exceeded 40%.

Valle et al. [88] demonstrated that an agrivoltaic system achieved high productivity per unit of land area using solar trackers instead of stationary photovoltaic panels, whereas the production of lettuce biomass was maintained close to or even similar to that obtained under full sun conditions.

Trypanagnostopoulos et al. [89,93] explained that the use of photovoltaic panels in a lettuce crop produced a 20% shading of the greenhouse, and plant growth was the same as that of the reference greenhouse, without photovoltaic panels on the roof.

Loik et al. [90] reported that in a trial conducted on a tomato crop, the wavelength-selective photovoltaic systems produced a small decrease in water use, whereas minimal effects were observed on the number and fresh weight of the fruit for several commercial species.

Yildirim et al. [91] conducted an economic and environmental assessment for tomato, cucumber and lettuce crops using photovoltaic solar panels on the roof of the greenhouse and connected to the grid to support a heat pump and generate electricity.

Minuto et al. [45] conducted an experiment with semi-transparent photovoltaic panels on a glass greenhouse and did not find large differences in the behaviour of the tomato plants due to shade.

Marucci et al. [56] explored the possibility of using semi-transparent photovoltaic materials to avoid the loss of solar radiation by shading.

Yano et al. [68] revealed that the electrical energy produced by semi-transparent modules with a cell density of 39% is sufficient for regions with high demand in summer and low demand in winter.

Yang et al. [72] optimized the use of sunlight by manipulating the photonic crystals in transparent organic photovoltaic cells.

Buttaro et al. [78], in a greenhouse arugula plantation, found that semi-transparent modules can satisfy all of the required electricity demand and that the yield of the plantation decreases if traditional modules are used.

Cossu et al. [74] claim that semi-transparent photovoltaic technology with spherical microcells can be used to contribute to the sustainability of greenhouses.

Saifultah et al. [82] conducted a review of materials used for manufacturing semi-transparent modules.

5. Other Related Studies

Table 3 shows articles that are related to greenhouses, renewable energies and/or shading but do not fit into the categories described above.

Table 3. Other related studies.

Authors	Location	Observations
Bot et al. (2005) [96]	Netherlands	Energy saving
Marcelis et al. (2006) [97]	Netherlands	Effects of light quantity
Hemming et al. (2006) [98]	Netherlands	Effects of diffuse light
Suri et al. (2007) [99]	Italy	Solar energy in the European Union
Hemming et al. (2008) [100]	Netherlands	Effects of diffuse light
Sonneveld et al. (2010b) [101]	Netherlands	The feasibility of solar energy
Abdel-Ghany y Al-Helal (2011) [102]	Saudi Arabia	Thermal model

Table 3. *Cont.*

Authors	Location	Observations
Abdel-Ghany (2011) [103]	Saudi Arabia	Solar energy and heat
Bibi et al. (2012) [104]	Pakistan	Effects of diffuse light
Verheul (2012) [105]	Norway	Light Intensity
Schuch et al. (2014) [106]	Germany	Solar energy and heating
Klaring et al. (2015) [107]	Germany	Heating and carbon dioxide emissions
Bian et al. (2015) [108]	China	Effects of light quality
El-Maghlany et al. (2015) [109]	Egypt	Solar energy and heating cost savings
Cakir y Sahin (2015) [110]	Turkey	Analysis of types greenhouses
Attar y Farhat (2015) [111]	Tunisia	Heating and costs
Shyam et al. (2015) [112]	India	Greenhouse dryer
Elkhadraoui (2015) [113]	Tunisia	Greenhouse dryer
Reca et al. (2016) [114]	Spain	The profitability of photovoltaic systems
Ziapour y Hashtroudi (2017) [115]	Iran	Solar energy and saving energy process
Arabkooshar et al. (2017) [116]	Iran	Hybrid solar-geothermal heating system
Xue (2017) [117]	China	Solar energy and costs
Anifantis et al. (2017) [118]	Italy	Heating

Reca et al. [114] verified that the profitability and energy efficiency of a photovoltaic system for irrigation is relatively low, although it can be improved by using excess energy for other tasks.

Bot et al. [96] developed Dutch-type greenhouses that do not use fossil fuels, thus improving the insulation value of the roofs and capturing solar energy for storage.

Marcelis et al. [97] showed that light has a positive effect on the yield and quality of greenhouse crops, but this effect is more noticeable when the amount of light is lower.

Verheul [105] states that an increase in the intensity of the light increases the tomato yield, but not the quality.

In Holland, Hemming et al. [98] observed that covering greenhouses with light-diffusing materials led to increases in production in the summer months by 6%. Later, in Dutch greenhouses, Hemming et al. [100] and Bibi et al. [104] obtained great results in cucumbers, proving that diffuse light improves photosynthesis in the middle zones of plants.

Suri et al. [99] state that photovoltaic energy is already in a position to make a significant contribution to the European Union's energy landscape.

Sonneveld et al. [101] presented the possibility of taking advantage of excess solar energy in summer to convert it into high-grade electricity and use it for cooling or heating.

Abdel-Ghanyand Al-Helal [102] developed an improved thermal model for greenhouses.

Abdel-Ghany [103] states that at a density of plants corresponding to a leaf area index of 3, 54% of the solar radiation used by the greenhouse is converted into sensible heat and 46% into latent heat through evapotranspiration.

Schuch et al. [106] reduced the consumption of fossil fuels by 81% with a system to capture solar thermal energy in a tomato greenhouse.

Klaring et al. [107] reported that carbon dioxide emissions from tomato crops can be reduced by lowering the heating temperature without affecting the fruit, but harvest times are increased.

Bian et al. [108] discussed the advantages of LED technology to modify the accumulation of phytochemicals with light.

El-Maghlany et al. [109] performed an efficiency analysis of solar energy capture and energy savings according to the type of greenhouse.

Cakir and Sahin [110] analysed different greenhouse types and found the elliptical greenhouse to be the most appropriate for the cold climate and latitude of Bayburt, Turkey.

Attar and Farhat [111] explain that the cost of heating in a 1000-m^3 greenhouse can be reduced by 51.8% if a heated water system is integrated.

Shyam et al. [112] and Elkhadraoui et al. [113] developed greenhouses as biomass dryers with electricity that is supplied from solar panels.

Ziapour and Hashtroudi [115] modified the roof of a greenhouse to partially reflect sunlight in a collector, and thus save on energy expenditure.

Arabkooshar et al. [116] used thermal panels and geothermal wells for heating, thus reducing the diesel consumption in winter.

Xue [117] states that photovoltaic greenhouses that occupy a large area of land require large outlays, which are not available to farmers or even to large companies.

Anifantis et al. [118] analyses the performance of an independent renewable energy system for greenhouse heating by using photovoltaic panels that are connected to an electrolyser, which produces hydrogen by electrolysis during the day and stores it in a pressure tank.

6. Studies Related to Shading and Photovoltaic Panels in Greenhouses by Country

The country of the main author of each of the publications analysed has been used to create Figure 2.

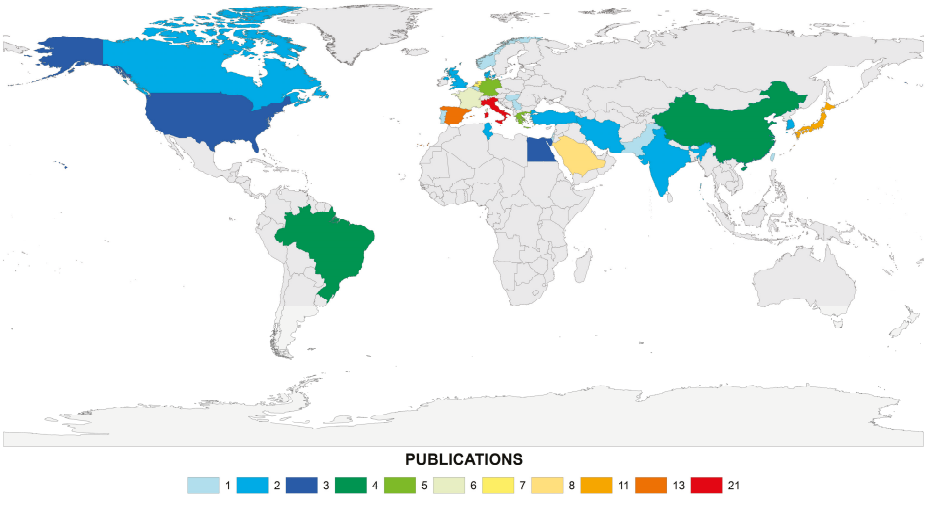

Figure 2. Publications by country.

The 113 publications analysed, which were related in some way to greenhouses, solar panels, tomato, and/or shade, represent 27 countries. If we look at the number of investigations in each country, the one with the most publications is Italy, with a total of 21, followed by Spain with 13; Japan with 12; Saudi Arabia with 8; Greece with 7; Holland with 6; France and Germany with 5; Brazil and China with 4; Egypt and the United States with 3; Canada, South Korea, India, Iran, United Kingdom, Tunisia, and Turkey with 2, and Belgium, Denmark, Hungary, Norway, Pakistan, Portugal, Serbia, and Taiwan with 1 (Figure 2).

In Figure 3, the research carried out in each section of the review by each country is indicated.

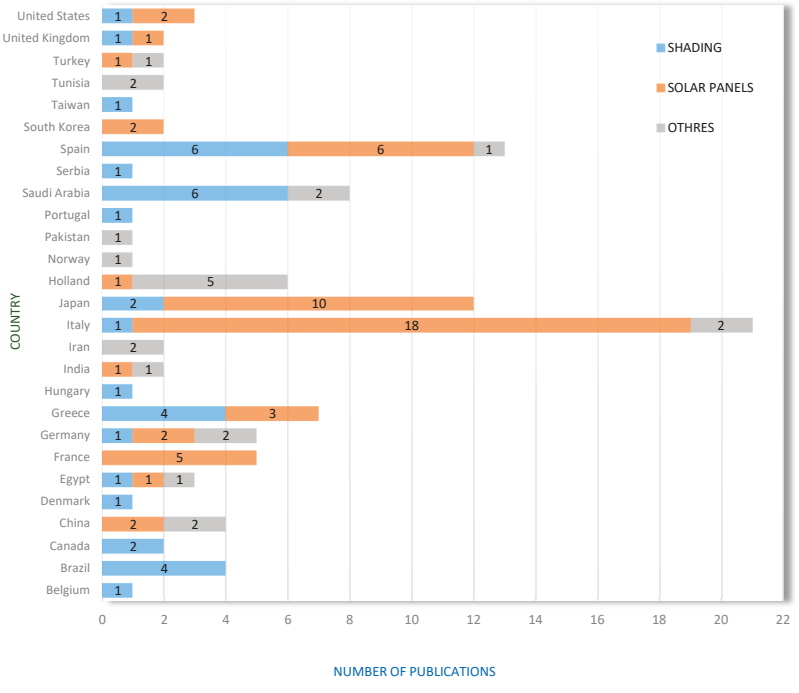

Figure 3. Number of publications in each field per country.

7. Studies Related to Shading and Photovoltaic Modules in Greenhouses by Year

Figure 4 shows the number of studies per year, as well as the fields studied.

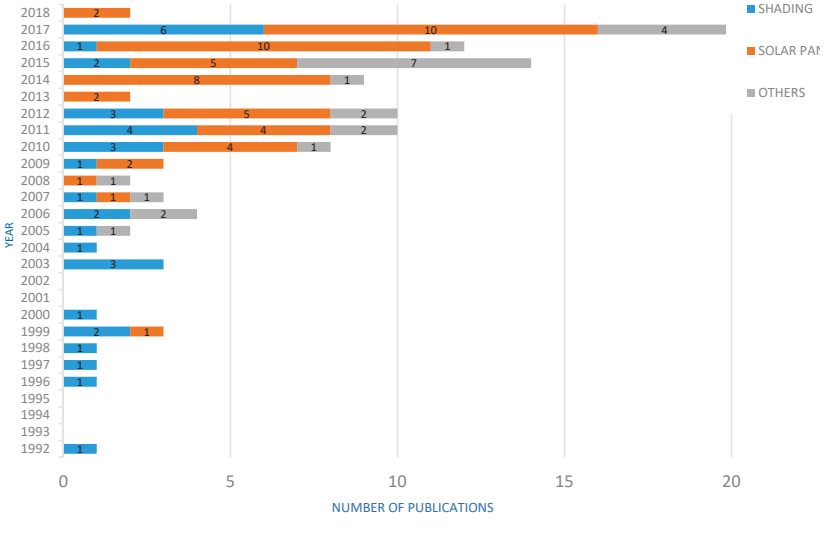

Figure 4. Number of publications in each field of knowledge per year.

A clear tendency to increase the number of publications can be observed. A notable difference is apparent in the number of studies that have carried out since 2010, with the exception of 2013, when only two studies that were related to the subject were analysed; however, 2017 had the most publications, with a total of 20, followed by 2015 with 14.

8. Studies Related to Authors and the Number of Citations

Table 4 shows the authors that appear in at least two citations.

Table 4. Authors and the number of documents.

Authors	Documents	Authors	Documents
Yano A	8	Onoe M	2
Abdel-Ghany AM	8	Cecchini M	2
Al-Helal IM	6	Trypanagnostopoulos G	2
Marucci A	6	Chessa F	2
Colantoni A	5	Deligios PA	2
Callejón-Ferre AJ	5	Marrou H	2
Kittas C	5	Murakami K	2
Pérez-Alonso J	5	Poncet C	2
Castellano S	4	Hiraki E	2
Monarca D	4	Caparrós I	2
Pérez-García M	4	Giménez M	2
Cossu M	4	Brun R	2
Serio F	3	Bibbiani C	2
Santamaria P	3	Incrocci L	2
Sánchez-Guerrero MC	3	Holcman E	2
García ML	3	Furue A	2
Pazzona A	3	Sentelhas PC	2
Sirigu A	3	Carlini M	2
Ledda L	3	Fatnassi H	2
Murgia L	3	Sonneveld PJ	2
Noda S	3	Alonzo G	2
Cappuccini A	3	Campiotti C	2
Klaring HP	3	Farhat A	2
Carreño-Ortega A	3	Krumbein A	2
Baille A	3	Dufour L	2
Katsoulas k	3	Swinkels GLAM	2
Ishizu F	3	Bot GPA	2
Medrano E	3	Cabrera FJ	2
Lorenzo P	3	Dueck T	2
Tripanagnostopoulos Y	3	Li M	2
Kadowaki M	3	Kavga A	2
Hemming S	3	Dondi F	2
Tanaka T	3	Capuccini A	2

If we observe the number of documents per each author, the ones with the most publications are "Yano A" and "Abdel-Ghany AM", with a total of 8, followed by "Al-Helal IM" and "Marucci A" with 6 (see Table 4).

9. Studies Related to Journals and the Number of Citations

Table 5 shows the journals that appear in at least two articles.

Table 5. Journals/Conferences and the number of documents.

Journals/Conferences	Documents
Acta Horticulturae	19
Biosystems Engineering	8
Renewable Energy	6
Solar Energy	5
Renewable & Sustainable Energy Reviews	5
Applied Energy	5
Journal of Agricultural Engineering	5
ScientiaHorticulturae	4
Energy Conversion and Management	3
Solar Energy Materials and Solar Cells	3
Energies	2
Agricultural and Forest Meteorology	2
Journal of Renewable and Sustainable Energy	2
Mathematical Problems in Engineering	2

The most important conference document is Acta Horticulturae with 19 documents. The most important journal is Biosystems Engineering, with a total of eight documents, followed by Renewable Energy with 6; Solar Energy, Renewable & Sustainable Energy Reviews, Applied Energy and Journal of Agricultural Engineering with five. It should be noted that Acta Horticulturae is not a journal in the true sense of the word.

10. Conclusions of the Review

The countries with the highest number of publications concerning solar panels and crops were Italy, with a total of 21; Spain with 13; and Japan with 12. During the past decade, the number of relevant publications has increased. These three countries are in the same latitude range, although the studies are very different depending on the type of crop selected and the type of greenhouse structure.

The most important authors of this topic are "Yano A" and "Abdel-Ghany AM", and regarding the number of documents that are cited, the most important journal is Biosystems Engineering.

Most of the studies justify the use of photovoltaic panels alongside agricultural production, although others cast general doubt on the economics of using these panels. Further technological development of photovoltaic panels with respect to transparency and energy efficiency could make their coexistence with greenhouse crops more economically viable. The trend of research on this subject is the search for the percentage of shading that makes the shading compatible for each type of crop.

Acknowledgments: To the 'Consejería de Innovación, Ciencia y Empresa de la Junta de Andalucía (Spain)' and the 'Ministerio de Ciencia e Innovación del Gobierno de España' as well as to the 'Fondos Europeos de Desarrollo Regional (FEDER)' for financing the present work through the research projects P08-AGR-04231 and AGL2006-11186, respectively.

Author Contributions: All authors contributed equally to the manuscript, and have approved the final manuscript.

Conflicts of Interest: The authors declare no conflict of interest.

References and Notes

1. Callejón-Ferre, A.J.; Manzano-Agugliaro, F.; Díaz-Pérez, M.; Carreño-Ortega, A.; Pérez-Alonso, J. Effect of shading with aluminised screens on fruit production and quality in tomato (*Solanumlycopersicum* L.) under greenhouse conditions. *Span. J. Agric. Res.* **2009**, *7*, 41–49. [CrossRef]
2. Castilla, N. *Invernaderos de Plástico: Tecnología y Manejo*; Mundi-Prensa: Madrid, Spain, 2005.
3. Ureña-Sánchez, R.; Callejón-Ferre, A.J.; Pérez-Alonso, J.; Carreño-Ortega, A. Greenhouse tomato production with electricity generation by roof-mounted flexible solar panels. *Sci. Agric.* **2012**, *69*, 233–239. [CrossRef]

4. Hassanien, R.H.E.; Ming, L. Influences of greenhouse-integrated semi-transparent photovoltaics on microclimate and lettuce growth. *Int. J. Agric. Biol. Eng.* **2017**, *10*, 11–22. [CrossRef]
5. Cockshull, K.E.; Graves, C.J.; Cave, C.R.J. The influence of shading on yield of glasshouse tomatoes. *J. Hortic. Sci.* **1992**, *67*, 11–24. [CrossRef]
6. Web of Science (Wos). *Electronic Access to the University of Almería Library with the License of the Spanish Foundation for Science and Technology (FECYT) of the 'Web of Science' (Wos) Provided by 'Clarivate Analytics'*; Foundation for Science and Technology (FECYT), Library of the University of Almería: Almería, Spain, 2018.
7. Scopus. *Electronic Access to the University of Almería Library with the License of the Spanish Foundation for Science and Technology (FECYT) of the 'Scopus' Provided by 'Scopus'*; Foundation for Science and Technology (FECYT), Library of the University of Almería: Almería, Spain, 2018.
8. Abdel-Mawgoud, A.M.R.; El-Abd, S.O.; Singer, S.M.; Hsiao, T.C. Effect of shade on the growth and yield of tomato plants. *Acta Hortic.* **1996**, *434*, 313–320. [CrossRef]
9. Papadopoulos, A.P.; Pararajasingham, S. The influence of plant spacing on light interception and use in greenhouse tomato (Lycopersiconesculentum Mill): A review. *Sci. Hortic.* **1997**, *69*, 1–29. [CrossRef]
10. Klaring, H.P. Growth of broccoli as affected by global radiation and air temperature. *Gartenbauwissenschaft* **1998**, *63*, 116–122.
11. Kittas, C.; Baille, A.; Giaglaras, P. Influence of covering material and shading on the spectral distribution of light in greenhouses. *J. Agric. Eng. Res.* **1999**, *73*, 341–351. [CrossRef]
12. Araki, Y.; Inoue, S.; Murakami, K. Effect of shading on growth and quality of summer spinach. *Acta Hortic.* **1999**, *483*, 105–110. [CrossRef]
13. Abreu, P.E.; Meneses, J.F. Influence of soil covering, plastic ageing and roof whitening on climate and tomato crop response in an unheated plastic Mediterranean greenhouse. *Acta Hortic.* **2000**, *534*, 343–350. [CrossRef]
14. Kittas, C.; Katsoulas, N.; Baille, A. Influence of an aluminized thermal screen on greenhouse microclimate and canopy energy balance. *Trans. ASAE* **2003**, *46*, 1653–1663. [CrossRef]
15. Kittas, C.; Katsoulas, N.; Baille, A. Influence of aluminized thermal screens on greenhouse microclimate and night transpiration. *Acta Hortic.* **2003**, *614*, 387–392. [CrossRef]
16. Sandri, M.A.; Andriolo, J.L.; Witter, M.; Dal Ross, T. Effect of shading on tomato plants grown under greenhouse. *J. Hortic. Bras.* **2003**, *4*, 642–645. [CrossRef]
17. Medrano, E.; Lorenzo, P.; Sánchez-Guerrero, M.C.; García, M.L.; Caparrós, I.; Giménez, M.J. Influence of an external greenhouse mobile shading on tomato transpiration. *Acta Hortic.* **2004**, *659*, 195–199. [CrossRef]
18. Bartzanas, T.; Kittas, C. Heat and mass transfer in a large evaporative cooled greenhouse equipped with a progressive shading. *Acta Hortic.* **2005**, *691*, 625–631. [CrossRef]
19. Lorenzo, P.; García, M.L.; Sánchez-Guerrero, M.C.; Medrano, E.; Caparrós, I.; Giménez, M. Influence of mobile shading on yield, crop transpiration and water use efficiency. *Acta Hortic.* **2006**, *719*, 471–478. [CrossRef]
20. Rosales, M.A.; Ruiz, J.M.; Hernández, J.; Soriano, T.; Castilla, N.; Romero, L. Antioxidant content and ascorbate metabolism in cherry tomato exocarp in relation to temperature and solar radiation. *J. Sci. Food Agric.* **2006**, *86*, 1545–1551. [CrossRef]
21. Gent, M.P.N. Effect of degree and duration of shade on quality of greenhouse tomato. *HortScience* **2007**, *42*, 514–520.
22. Abdel-Ghany, A.M.; Al-Helal, I.M. Characterization of solar radiation transmission through plastic shading nets. *Sol. Energy Mater. Sol. Cell.* **2010**, *94*, 1371–1378. [CrossRef]
23. Sato, H.; Yanagi, T.; Hirai, H.; Ueda, Y.; Oda, Y. Effects of Shading on Growth, Fruit Yield and Dry Matter Partitioning of Single Truss Tomato Plants. *Environ. Control Biol.* **2010**, *32*, 231–237. [CrossRef]
24. Aberkani, K.; Hao, X.M.; de Halleux, D.; Dorais, M.; Vineberg, S.; Gosselin, A. Effects of Shading Using a Retractable Liquid Foam Technology on Greenhouse and Plant Microclimates. *Horttechnology* **2010**, *20*, 283–291.
25. Abdel-Ghany, A.M.; Al-Helal, I.M. Analysis of solar radiation transfer: A method to estimate the porosity of a plastic shading net. *Energy Convers. Manag.* **2011**, *52*, 1755–1762. [CrossRef]
26. Al-Helal, I.M.; Abdel-Ghany, A.M. Measuring and evaluating solar radiative properties of plastic shading nets. *Sol. Energy Mater. Sol. Cell.* **2011**, *95*, 677–683. [CrossRef]
27. Chen, C.; Shen, T.; Weng, Y. Simple model to study the effect of temperature on the greenhouse with shading nets. *Afr. J. Biotechnol.* **2011**, *10*, 5001–5014. [CrossRef]

28. García, M.L.; Medrano, E.; Sánchez-Guerrero, M.C.; Lorenzo, P. Climatic effects of two cooling systems in greenhouses in the Mediterranean area: External mobile shading and fog system. *Biosyst. Eng.* **2011**, *108*, 133–143. [CrossRef]
29. Abdel-Ghany, A.M.; Al-Helal, I.M. A method for determining the long-wave radiative properties of a plastic shading net under natural conditions. *Sol. Energy Mater. Sol. Cell.* **2012**, *99*, 268–276. [CrossRef]
30. Holcman, E.; Sentelhas, P.C. Microclimate under different shading screens in greenhouses cultivated with bromeliads. *Rev. Bras. Eng. Agric. Ambient.* **2012**, *16*, 858–863. [CrossRef]
31. Ilic, Z.S.; Milenkovic, L.; Stanojevic, L.; Cvetkovic, D.; Fallik, E. Effects of the modification of light intensity by color shade nets on yield and quality of tomato fruits. *Sci. Hortic.* **2012**, *139*, 90–95. [CrossRef]
32. Abdel-Ghany, A.M.; Picuno, P.; Al-Helal, I.; Alsadon, A.; Ibrahim, A.; Shady, M. Radiometric Characterization, solar and thermal radiation in a greenhouse as affected by shading configuration in an arid climate. *Energies* **2015**, *8*, 13928–13937. [CrossRef]
33. Hernández, V.; Hellín, P.; Fenoll, J.; Garrido, I.; Cava, J.; Flores, P. Impact of Shading on Tomato Yield and Quality Cultivated with Different N Doses Under High Temperature Climate. *Procedia Environ. Sci.* **2015**, *29*, 197–198. [CrossRef]
34. Ahemd, H.A.; Al-Faraj, A.A.; Abdel-Ghany, A.M. Shading greenhouses to improve the microclimate, energy and water saving in hot regions: A review. *Sci. Hortic.* **2016**, *201*, 36–45. [CrossRef]
35. Nagy, Z.; Daood, H.; Nemenyi, A.; Ambrozy, Z.; Pek, Z.; Helyes, L. Impact of Shading Net Color on Phytochemical Contents in Two Chili Pepper Hybrids Cultivated Under Greenhouse Conditions. *Hortic. Sci. Technol.* **2017**, *35*, 418–430. [CrossRef]
36. Murakami, K.; Fukuoka, N.; Noto, S. Improvement of greenhouse microenvironment and sweetness of melon (Cucumismelo L.) fruits by greenhouse shading with a new kind of near-infrared ray-cutting net in mid-summer. *Sci. Hortic.* **2017**, *218*, 1–7. [CrossRef]
37. Yasin, M.; Rosenqvist, E.; Andreasen, C. The Effect of Reduced Light Intensity on Grass Weeds. *Weed Sci.* **2017**, *65*, 603–613. [CrossRef]
38. Costa, E.; Santo, T.L.E.; Batista, T.B.; Curi, T.M.R.C. Different type of greenhouse and substrata on pepper production. *Hortic. Bras.* **2017**, *35*, 458–466. [CrossRef]
39. Holcman, E.; Sentelhas, P.C.; Mello, S.D. Cherry tomato yield in greenhouses with different plastic covers. *Cienc. Rural* **2017**, *47*, 10. [CrossRef]
40. Priarone, A.; Fossa, M.; Paietta, E.; Rolando, D. Energy demand hourly simulations and energy saving strategies in greenhouses for the Mediterranean climate. *J. Phys. Conf. Ser.* **2017**, *796*, 796. [CrossRef]
41. Kozai, T.; He, D.; Ohtsuka, H. Simulation of solar radiation transmission into a lean-to greenhouse with photovoltaic cells on the roof-Case study for a greenhouse with infinite longitudinal length. *Environ. Control Biol.* **1999**, *37*, 101–108. [CrossRef]
42. Yano, A.; Tsuchiya, K.; Nishi, K.; Moriyama, T.; Ide, O. Development of a greenhouse side-ventilation controller driven by photovoltaic energy. *Biosyst. Eng.* **2007**, *96*, 633–641. [CrossRef]
43. Campiotti, C.; Dondi, F.; Genovese, A.; Alonzo, G.; Catanese, V.; Incrocci, L.; Bibbiani, C. Photovoltaic as Sustainable Energy for Greenhouse and Closed Plant Production System. *Acta Hortic.* **2008**, *797*, 373–378. [CrossRef]
44. Yano, A.; Furue, A.; Kadowaki, M.; Tanaka, T.; Hiraki, E.; Miyamoto, M.; Ishizu, F.; Noda, S. Electrical energy generated by photovoltaic modules mounted inside the roof of a north-south oriented greenhouse. *Biosyst. Eng.* **2009**, *2*, 228–238. [CrossRef]
45. Minuto, G.; Bruzzone, C.; Tinivella, F.; Delfino, G.; Minuto, A. Photovoltaics on greenhouse roofs to produce more energy. *Inf. Agrar. Suppl.* **2009**, *65*, 16–19.
46. Yano, A.; Kadowaki, M.; Furue, A.; Tamaki, N.; Tanaka, T.; Hiraki, E.; Kato, Y.; Ishizu, F.; Noda, S. Shading and electrical features of a photovoltaic array mounted inside the roof of an east-west oriented greenhouse. *Biosyst. Eng.* **2010**, *4*, 367–377. [CrossRef]
47. Qoaider, L.; Steinbrecht, D. Photovoltaic systems: A cost competitive option to supply energy to off-grid agricultural communities in arid regions. *Appl. Energy* **2010**, *87*, 427–435. [CrossRef]
48. Carlini, M.; Villarini, M.; Esposto, S.; Bernardi, M. Performance Analysis of Greenhouses with Integrated Photovoltaic Modules. *Lect. Notes Comput. Sci.* **2010**, *6017*, 206–214. [CrossRef]

49. Sonneveld, P.J.; Swinkels, G.L.A.M.; Campen, J.; van Tujil, B.A.J.; Janssen, H.J.J.; Bot, G.P.A. Performance results of a solar greenhouse combining electrical and thermal energy production. *Biosyst. Eng.* **2010**, *106*, 48–57. [CrossRef]
50. Dupraz, C.; Marrou, H.; Talbot, G.; Dufour, L.; Nogier, A.; Ferard, Y. Combining solar photovoltaic panels and food crops for optimising land use: Towards new agrivoltaic schemes. *Renew. Energy* **2011**, *36*, 2725–2732. [CrossRef]
51. Campiotti, C.; Dondi, F.; Di Carlo, F.; Scoccianti, M.; Alonzo, G.; Bibbiani, C.; Incrocci, L. Preliminary Results of a PV Closed Greenhouse System for High Irradiation Zones in South Italy. *Acta Hortic.* **2011**, *893*, 243–250. [CrossRef]
52. Pérez-Alonso, J.; Callejón-Ferre, A.J.; Ureña-Sánchez, R.; Carreño-Ortega, A.; Vázquez-Cabrera, F.J.; Pérez-García; Marti, B.V. PAR assessment within an Almeria-type greenhouse in integrating a photovoltaic roof. In Proceedings of the 69th International Conference on Agricultural Engineering LAND TECHNIK AgEng, Hannover, Germany, 11–12 November 2011; Volume 2124, p. 343.
53. Ganguly, A.; Ghosh, S. Performance Analysis of a Floriculture Greenhouse Powered by Integrated Solar Photovoltaic Fuel Cell System. *J. Sol. Energy Eng.-Trans. ASME* **2011**, *133*, 041001. [CrossRef]
54. Carlini, M.; Honorati, T.; Castellucci, S. Photovoltaic Greenhouses: Comparison of Optical and Thermal Behaviour for Energy Savings. *Math. Probl. Eng.* **2012**, *2012*, 743–764. [CrossRef]
55. Kadowaki, M.; Yano, A.; Ishizu, F.; Tanaka, T.; Noda, S. Effects of greenhouse photovoltaic array shading on Welsh onion growth. *Biosyst. Eng.* **2012**, *111*, 290–297. [CrossRef]
56. Marucci, A.; Monarca, D.; Cecchini, M.; Colantoni, A.; Manzo, A.; Cappuccini, A. The semitransparent photovoltaic films for Mediterranean greenhouse: a new sustainable technology. *Math. Probl. Eng.* **2012**, *14*. [CrossRef]
57. Pérez-Alonso, J.; Pérez-García, M.; Pasamontes-Romera, M.; Callejón-Ferre, A.J. Performance analysis and neural modelling of a greenhouse integrated photovoltaic system. *Renew. Sustain. Energy Rev.* **2012**, *16*, 1675–4685. [CrossRef]
58. Poncet, C.; Muller, M.M.; Brun, R.; Fatnassi, H. Photovoltaic Greenhouses, Non-Sense or a Real Opportunity for the Greenhouse Systems? *Acta Hortic.* **2012**, *927*, 75–79. [CrossRef]
59. Klaring, H.P.; Krumbein, A. The Effect of Constraining the Intensity of Solar Radiation on the Photosynthesis, Growth, Yield and Product Quality of Tomato. *J. Agron. Crop Sci.* **2013**, *199*, 351–359. [CrossRef]
60. Marrou, H.; Guilioni, L.; Dufour, L.; Dupraza, C.; Wery, J. Microclimate under agrivoltaic systems: Is crop growth rate affected in the partial shade of solar panels? *Agric. For. Meteorol.* **2013**, *177*, 117–132. [CrossRef]
61. Castellano, S. Photovoltaic greenhouses: Evaluation of shading effect and its influence on agricultural performances. *J. Agric. Eng.* **2014**, *45*, 168–174. [CrossRef]
62. Juang, P.; Kacira, M. System Dynamics of a Photovoltaic Integrated Greenhouse. *Acta Hortic.* **2014**, *1037*, 107–112. [CrossRef]
63. Cossu, M.; Murgia, L.; Ledda, L.; Deligios, P.A.; Sirigu, A.; Chessa, F.; Pazzona, A. Solar radiation distribution inside a greenhouse with south-oriented photovoltaic roofs and effects on crop productivity. *Appl. Energy* **2014**, *133*, 89–100. [CrossRef]
64. Tani, A.; Shiina, S.; Nakashima, K.; Hayashi, M. Improvement in lettuce growth by light diffusion under solar panels. *J. Agric. Meteorol.* **2014**, *70*, 139–149. [CrossRef]
65. Pérez-Alonso, J.; Callejón-Ferre, A.J.; Pérez-García, M.; Sánchez-Hermosilla, J. Evaluation of the tomato crop production under exterior selective shading in "raspa y amagado" greenhouses. In Proceedings of the 7th IberianCongress of AgriculturalEngineering and Horticultural Sciences, Madrid, Spain, 26–29 August 2013; pp. 470–475.
66. Pérez-García, M.; Cabrera, F.J.; Pérez-Alonso, J.; Callejón-Ferre, A.J. Electricity production of flexible photovoltaic modules integrated on the roof of a "raspa y amagado" type greenhouse. In Proceedings of the 7th Iberian Congress of Agricultural Engineering and Horticultural Sciences, Madrid, Spain, 26–29 August 2013; pp. 907–912.
67. Serrano, I.; Muñoz-García, M.A.; Alonso-García, M.C.; Vela, N. Evaluation of the use of solar panels as a shade in greenhouses. In Proceedings of the 7th Iberian Congress of Agricultural Engineering and Horticultural Sciences, Madrid, Spain, 26–29 August 2013; pp. 2056–2061.
68. Yano, A.; Onoe, M.; Najata, J. Prototype semi-transparent photovoltaic modules for greenhouse roof applications. *Biosyst. Eng.* **2014**, *122*, 62–73. [CrossRef]

69. Fatnassi, H.; Poncet, C.; Bazzano, M.M.; Brun, R.; Bertin, N. A numerical simulation of the photovoltaic greenhouse microclimate. *Sol. Energy* **2015**, *120*, 575–584. [CrossRef]
70. Marucci, A.; Monarca, D.; Cecchini, M.; Colantoni, A.; Capuccini, A. Analysis of internal shading degree to a prototype of dynamics photovoltaic greenhouse through simulation software. *J. Agric. Eng.* **2015**, *46*, 144–150. [CrossRef]
71. Bulgari, R.; Cola, G.; Ferrante, A.; Franzoni, G.; Mariani, L.; Martinetti, L. Micrometeorological environment in traditional and photovoltaic greenhouses and effects on growth and quality of tomato (*Solanumlycopersicum L.*). *Ital. J. Agrometeorol.* **2015**, *20*, 27–38.
72. Yang, F.; Zhang, Y.; Hao, Y.Y.; Cui, Y.X.; Wang, W.Y.; Ji, T.; Shi, F.; Wei, B. Visibly transparent organic photovoltaic with improved transparency and absorption based on tandem photonic crystal for greenhouse application. *Appl. Opt.* **2015**, *54*, 10232–10239. [CrossRef] [PubMed]
73. Castellano, S.; Tsirogiannis, I.L. Daylight analysis inside photovoltaic greenhouses. In Proceedings of the 43rd International Symposium on Agricultural Engineering, Actual Tasks on Agricultural Engineering, Opatija, Croatia, 24–27 February 2015; pp. 703–712.
74. Cossu, M.; Yano, A.; Li, Z.; Onoe, M.; Nakamura, H.; Matsumoto, T.; Nakata, J. Advances on the semi-transparent modules based on micro solar cells: First integration in a greenhouse system. *Appl. Energy* **2016**, *162*, 1042–1051. [CrossRef]
75. Marucci, A.; Cappuccini, A. Dynamic photovoltaic greenhouse: Energy efficiency in clear sky conditions. *Appl. Energy* **2016**, *170*, 362–376. [CrossRef]
76. Marucci, A.; Capuccini, A. Dynamic photovoltaic greenhouse: Energy balance in completely clear sky condition during the hot period. *Energy* **2016**, *102*, 302–312. [CrossRef]
77. Hassanien, R.H.E.; Li, M.; Lin, W.D. Advanced applications of solar energy in agricultural greenhouses. *Renew. Sustain. Energy Rev.* **2016**, *54*, 989–1001. [CrossRef]
78. Buttaro, D.; Renna, M.; Gerardi, C.; Blando, F.; Santamaria, P.; Serio, F. Soilles production of wild rocket as affected by greenhouse coverage with photovoltaic modules. *Acta Sci. Pol.-Hortic. Cultus* **2016**, *15*, 129–142.
79. Castellano, S.; Santamaria, P.; Serio, F. Photosynthetic photon flux density distribution inside photovoltaic greenhouses, numerical simulation, and experimental results. *Appl. Eng. Agric.* **2016**, *32*, 861–869. [CrossRef]
80. Castellano, S.; Santamaria, P.; Serio, F. Solar radiation distribution inside a monospan greenhouse with the roof entirely covered by photovoltaic panels. *J. Agric. Eng.* **2016**, *47*, 1–6. [CrossRef]
81. Cuce, E.; Harjunowibowo, D.; Cuce, P.M. Renewable and sustainable energy saving strategies for greenhouse systems: A comprehensive review. *Renew. Sustain. Energy Rev.* **2016**, *64*, 34–59. [CrossRef]
82. Saifultah, M.; Gwak, J.; Yun, J.H. Comprehensive review on material requirements, present status, and future prospects for building-integrated semitransparent photovoltaics (BISTPV). *J. Mater. Chem. A* **2016**, *4*, 8512–8540. [CrossRef]
83. Dinesh, H.; Pearce, J.M. The potential of agrivoltaicsystems. *Renew. Sustain. Energy Rev.* **2016**, *54*, 299–308. [CrossRef]
84. Cossu, M.; Ledda, L.; Urracci, G.; Sirigu, A.; Cossu, A.; Murgia, L.; Pazzona, A.; Yano, A. An algorithm for the calculation of the light distribution in photovoltaic greenhouses. *Sol. Energy* **2017**, *141*, 38–48. [CrossRef]
85. Cossu, M.; Yano, A.; Murgia, L.; Ledda, L.; Deligios, P.A.; Sirigu, A.; Chessa, F.; Pazzona, A. Effects of the photovoltaic roofs on the greenhouse microclimate. *Acta Hortic.* **2017**, *1170*, 461–468. [CrossRef]
86. Carreño-Ortega, A.; Galdeano-Gómez, E.; Pérez-Mesa, J.C.; Galera-Quiles, M.C. Policy and Environmental Implications of Photovoltaic Systems in Farming in Southeast Spain: Can Greenhouses Reduce the Greenhouse Effect? *Energies* **2017**, *10*, 761. [CrossRef]
87. Marucci, A.; Monarca, D.; Colantoni, A.; Campiglia, E.; Cappuccini, A. Analysis of the internal shading in a photovoltaic greenhouse tunnel. *J. Agric. Eng.* **2017**, *48*, 154–160. [CrossRef]
88. Valle, B.; Simonneau, T.; Sourd, F.; Pechier, P.; Hamard, P.; Frisson, T.; Ryckewaert, M.; Christophe, A. Increasing the total productivity of a land by combining mobile photovoltaic panels and food crops. *Appl. Energy* **2017**, *206*, 1495–1507. [CrossRef]
89. Trypanagnostopoulos, G.; Kavga, A.; Souliotis, M.; Tripanagnostopoulos, Y. Greenhouse perfomance results for roof installed photovoltaics. *Renew. Energy* **2017**, *111*, 724–731. [CrossRef]
90. Loik, M.E.; Carter, S.A.; Alers, G.; Wade, C.E.; Shugar, D.; Corrado, C.; Jokerst, D.; Kitayama, C. Wavelength-Selective Solar Photovoltaic Systems: Powering Greenhouses for Plant Growth at the Food-Energy-Water Nexus. *Earth Future* **2017**, *5*, 1044–1053. [CrossRef]

91. Yildirim, N.; Bilir, L. Evaluation of a hybrid system for a nearly zero energy greenhouse. *Energy Convers. Manag.* **2017**, *148*, 1278–1290. [CrossRef]
92. Tripanagnostopoulos, Y.; Katsoulas, N.; Kittas, C. Potential energy cost and footprint reduction in Mediterranean greenhouses by means of renewable energy use. *Acta Hortic.* **2017**, *1164*, 461–466. [CrossRef]
93. Kavga, A.; Trypanagnostopoulos, G.; Zervoudakis, G.; Tripanagnostopoulos, Y. Growth and Physiological Characteristics of Lettuce (*Lactuca sativa* L.) and Rocket (*Eruca sativa* Mill.) Plants Cultivated under Photovoltaic Panels. *Not. Bot. Horti Agrobot. Cluj-Napoca* **2017**, *46*, 206–212. [CrossRef]
94. Marucci, A.; Zambon, I.; Colantoni, A.; Monarca, D. A combination of agricultural and energy purposes: Evaluation of a prototype of photovoltaic greenhouse tunnel. *Renew. Sustain. Energy Rev.* **2018**, *82*, 1178–1186. [CrossRef]
95. Liu, W.; Liu, L.; Guan, C.; Zhang, F.; Li, M.; Lv, H.; Yao, P.; Ingenhoff, J. A novel agricultural photovoltaic system based on solar spectrum separation. *Sol. Energy* **2018**, *162*, 84–94. [CrossRef]
96. Bot, G.; van de Braak, N.; Challa, H.; Hemming, S.; Rieswijk, T.; Von Straten, G.; Verlodt, I. The solar greenhouse: State of the art in energy saving and sustainable energy supply. *Acta Hortic.* **2005**, *691*, 501–508. [CrossRef]
97. Marcelis, L.F.M.; Broekhuijsen, A.G.M.; Meinen, E.; Nijs, E.M.F.M.; Raaphorst, M.G.M. Quantification of the growth response to light quantity of greenhouse grown crops. *Acta Hortic.* **2006**, *711*, 97–103. [CrossRef]
98. Hemming, S.; Van der Braak, N.; Dueck, T.; Jongschaap, R.; Marissen, N. Filtering natural light by the greenhouse covering using model simulations-More production and better plant quality by diffuse light? *Acta Hortic.* **2006**, *711*, 105–110. [CrossRef]
99. Suri, M.; Huld, T.A.; Dunlop, E.D.; Ossenbrink, H.A. Potential of solar electricity generation in the European Union member states and candidate countries. *Sol. Energy* **2007**, *81*, 1295–1305. [CrossRef]
100. Hemming, S.; Dueck, T.; Janse, J.; van Noort, F. The Effect of Diffuse Light on Crops. *Acta Hortic.* **2008**, *801*, 1293–1300. [CrossRef]
101. Sonneveld, P.J.; Swinkels, G.L.A.M.; Bot, G.P.A.; Flamand, G. Feasibility study for combining cooling and high grade energy production in a solar greenhouse. *Biosyst. Eng.* **2010b**, *105*, 51–58. [CrossRef]
102. Abdel-Ghany, A.M.; Al-Helal, I.M. Solar energy utilization by a greenhouse: General relations. *Renew. Energy* **2011**, *36*, 189–196. [CrossRef]
103. Abdel-Ghany, A.M. Solar energy conversions in the greenhouses. *Sustain. Cities Soc.* **2011**, *1*, 219–226. [CrossRef]
104. Bibi, B.; Sajid, M.; Rab, A.; Shah, S.T.; Ali, N.; Jan, I.; Haq, I.; Wahid, F.; Haleema, B.; Ali, I. Effect of partial shade on growth and yield of tomato cultivars. *Glob. J. Biol. Agric. Health Sci.* **2012**, *1*, 22–26.
105. Verheul, M.J. Effects of Plant Density, Leaf Removal and Light Intensity on Tomato Quality and Yield. *Acta Hortic.* **2012**, *956*, 365–372. [CrossRef]
106. Schuch, I.; Dannehl, D.; Miranda-Trujillo, L.; Rocksch, T.; Schmidt, U. ZINEG Project—Energetic Evaluation of a Solar Collector Greenhouse with Above-Ground Heat Storage in Germany. *Acta Hortic.* **2014**, *1037*, 195–201. [CrossRef]
107. Klaring, H.P.; Klopotek, Y.; Krumbein, A.; Schwarz, D. The effect of reducing the heating set point on the photosynthesis, growth, yield and fruit quality in greenhouse tomato production. *Agric. For. Meteorol.* **2015**, *214*, 178–188. [CrossRef]
108. Bian, Z.H.; Yang, Q.C.; Liu, W.K. Effects of light quality on the accumulation of phytochemicals in vegetables produced in controlled environments: a review. *J. Sci. Food Agric.* **2015**, *95*, 869–877. [CrossRef] [PubMed]
109. El-Maghlany, W.M.; Teamah, M.A.; Tanaka, H. Optimum design and orientation of the greenhouses for maximum capture of solar energy in North Tropical Region. *Energy Convers. Manag.* **2015**, *105*, 1096–1104. [CrossRef]
110. Cakir, U.; Sahin, E. Using solar greenhouses in cold climates and evaluating optimum type according to sizing, position and location: A case study. Comput. *Electron. Agric.* **2015**, *117*, 245–257. [CrossRef]
111. Attar, I.; Farhat, A. Efficiency evaluation of a solar water heating system applied to the greenhouse climate. *Sol. Energy* **2015**, *119*, 212–224. [CrossRef]
112. Shyam;Al-Helal, I.M.; Singh, A.K.; Tiwari, G.N. Performance evaluation of photovoltaic thermal greenhouse dryer and development of characteristic curve. *J. Renew. Sustain. Energy* **2015**, *7*, 033109. [CrossRef]

113. Elkhadraoui, A.; Kooli, S.; Hamdi, I.; Farhat, A. Experimental investigation and economic evaluation of a new mixed-mode solar greenhouse dryer for drying of red pepper and grape. *Renew. Energy* **2015**, *77*, 1–8. [CrossRef]
114. Reca, J.; Torrente, C.; López-Luque, R.; Martínez, J. Feasibility analysis of a standalone direct pumping photovoltaic system for irrigation in Mediterranean greenhouses. *Renew. Energy* **2016**, *85*, 1143–1154. [CrossRef]
115. Ziapour, B.M.; Hashtroudi, A. Performance study of an enhanced solar greenhouse combined with the phase change material using genetic algorithm optimization method. *Appl. Therm. Eng.* **2017**, *110*, 253–264. [CrossRef]
116. Arabkooshar, A.; Farzaneh-Gord, M.; Ghezelbash, R.; Koury, R.N.N. Energy consumption pattern modification in greenhouses by a hybrid solar-geothermal heating system. *J. Braz. Soc. Mech. Sci. Eng.* **2017**, *39*, 631–643. [CrossRef]
117. Xue, J.L. Economic assessment of photovoltaic greenhouses in China. *J. Renew. Sustain. Energy* **2017**, *9*. [CrossRef]
118. Anifantis, A.S.; Colantoni, A.; Pascuzzi, S. Thermal energy assessment of a small scale photovoltaic, hydrogen and geothermal stand-alone system for greenhouse heating. *Renew. Energy* **2017**, *103*, 115–127. [CrossRef]

sustainability

MDPI

Article

Comparisons of Different Lighting Systems for Horticultural Seedling Production Aimed at Energy Saving

Pedro Garcia-Caparros [1], Rosa María Chica [2], Eva María Almansa [1], Antonio Rull [1], Lara Alicia Rivas [1], Antonio García-Buendía [2], Francisco Javier Barbero [3] and María Teresa Lao [1,*]

[1] Agronomy Department of Superior School Engineering, University of Almeria, Agrifood Campus of International Excellence ceiA3, Carretera Sacramento s/n, 04120 La Cañada de San Urbano, Almería, Spain; pedrogar123@hotmail.com (P.G.-C.); almansaeva@gmail.com (E.M.A.); a.rull.rodriguez@gmail.com (A.R.); lararivasona@gmail.com (L.A.R.)

[2] Engineering Department of Superior School Engineering, University of Almeria, Agrifood Campus of International Excellence ceiA3, Carretera. Sacramento s/n, 04120 La Cañada de San Urbano, Almería, Spain; rmchica@ual.es (R.M.C.); abuendia@ual.es (A.G.-B.)

[3] Applied Physics Department of Superior School Engineering, University of Almeria, Agrifood Campus of International Excellence ceiA3, Carretera. Sacramento s/n, 04120 La Cañada de San Urbano, Almería, Spain; jbarbero@ual.es

* Correspondence: mtlao@ual.es Tel.: +34-950-015876; Fax: +34-950-015939

Received: 30 August 2018; Accepted: 17 September 2018; Published: 19 September 2018

Abstract: Nowadays, the evaluation of sustainability is an important aspect in the study of agricultural systems and the number of projects and methods for impact assessment of food production systems is increasing. In this work, we initially carried out a survey to know the status of the artificial lighting establishment in horticultural seedling nurseries in southern Spain. Taking into account the data obtained in the survey, we conducted an experiment with different types of fluorescent lamps (TLD-18, CF, TL5, TLD-56), light-emitting diodes (LEDs) and their combinations along with the novelty white LEDs lamps and XTRASUN LEDs to evaluate their technical parameters and spectral light qualities. In addition, the effectiveness of light irradiance (ELI_{plant}) and the use of irradiance (UI) by cucumber and tomato seedling plants were estimated considering their light absorbance capacity previously analyzed. The results showed that TLD-18 lamps and their combinations, CF and XTRASUN LEDs, had a limited value of energy efficiency (VEEI) ≤ 2. The lamps essayed with the lowest total irradiance were LEDs (B, R, V, W) and the ones with the highest values were TLD58-6 lamps. The effectiveness of light irradiance (ELI_{plant}) and the UI were slightly higher in the case of cucumber than that of the tomato for all essayed lamps. Considering the effectiveness of the light irradiance (ELI_{plant}), TL5-6 lamps showed the highest values. On the other hand, considering the use of irradiance, XTRASUN LEDs on the mode of vegetative growth (VG) showed the highest values.

Keywords: artificial light; electric power; morphogenetically active radiation; nurseries; photosynthetically active radiation; spectral irradiance

1. Introduction

Light is one of the most important environmental regulators for the growth of crop species since it provides essential energy input and triggers various signaling pathways for the dynamic growth regulation of crops [1]. In this sense, plant species have evolved photoreceptors to sense the light environment and adjust to changing environmental conditions through the modulation of cellular processes [2]. Unique plant photoreceptors respond to changing light quality and quantity

through developmental and physiological responses commonly referred to as photomorphogenesis [3]. For instance, blue light is involved in a wide range of plant processes such as phototropism, photomorphogenesis, stomatal opening, photosynthesis, and flowering [4,5]; meanwhile, red light participates in stem elongation, root to shoot ratio, chlorophyll content, and photosynthetic apparatus [6].

Among traditional artificial lighting systems, high-pressure sodium (HPS) and fluorescent lamps (FL) have been most commonly used in plant growth systems [7]. Nevertheless, these lighting systems have several drawbacks such as non-uniformity in spectral quality and an excessive heating that may result in tissue damage when lamps are placed near plants [8].

In this sense, the evolution and performance of LEDs in plant growth systems plays an essential role since they emit wavelengths close to those needed by plant photoreceptors, ultimately achieving an optimal production due to the influence in plant morphology and metabolism [9]. Light-emitting diodes (LEDs) are more energy efficient and versatile than traditional lighting systems but their cost is higher. Nevertheless, the improvement of LEDs production and its maintenance reduce their costs and have all contributed to its establishment as a lighting source [10]. The use of LED light in horticulture has been established in plant tissue or cuttings, culture rooms and growth chambers, greenhouses, and nurseries [11].

The establishment of LEDs instead of traditional artificial lighting systems results in energy saving. For instance, while comparing LEDs with traditional lighting systems, Macias et al. [12] reported that there was a great energy saving, between 41% and 73% of power consumption, compared with the technology of that period such as HPS lamps. Similarly, Serrano-Tierz [13] concluded that the replacement of metal halide lights by LEDs luminaries resulted in a high energy saving and an increase of the life span of the luminaires. Moreover, the use of LEDs reduces the disposal of toxic elements such as mercury to the environment [14].

Nowadays, the production of horticultural seedlings in southern Spain totals to around 1,800,000,000 seedling plants [15]. To produce horticultural seedlings, supplementary artificial lighting has been considered as economically practical since it allows growers to improve profits mainly due to a faster development of plants, therefore improving their sales [16]. In one experiment, Almansa et al. [17] reported that tomato producers in the Mediterranean area used growth chambers with artificial light to reduce the period of production and to achieve better quality plants due to the increase of the root/shoot ratio.

In a recent review concerning the achievement in the field of horticulture with the use of different types of LEDs [8], it can be highlighted that these artificial lighting systems are being used as a complementary source of light in growth chambers and greenhouses, vertical farming systems and in the maintenance of postharvest fruit quality of fruits and vegetables. In addition, there are different studies worldwide regarding the use of LEDs during healing and acclimatization in seedlings in different crops such as tomato [18] and pepper [19]. Nevertheless, there are few references about this topic under nurseries as productions systems in southern Spain; therefore, the aims of this work are: (1) to evaluate technical and spectral irradiance of the different types of FL (TLD, TL5 and CF) commonly used in nurseries, LEDs lamps (blue (B), red (R) and red + blue (violet) (V)) with a high saving energy and their different combinations with FL due to the spectral enrichment, and novel types of LEDs such as white LEDs (W) and XTRASUN LEDs; and (2) to theoretically estimate the potential growth of tomato and cucumber seedlings under the lamps assessed.

2. Materials and Methods

2.1. Survey Concerning Lighting Sources in Horticultural Nurseries

Before conducting the experiment, we carried out a survey in local horticultural seedling nurseries (50 enterprises) (Figure 1) in southern Spain to determine which was the degree of lighting establishment in these nurseries as well as the main spectral characteristics of the lamps used for

horticultural seedling production. The spectral quality data of each nursery was registered using a luxometer (GOSSEN MAVOLUX model 5032C USB; Casella., Madrid, Spain).

Figure 1. Local horticultural seedling nurseries surveyed in Almería (Spain).

2.2. Technical Parameters of the Lamps

The characterization of the lamps assessed in this experiment are shown in Table 1.

Table 1. Types of lamps, characteristics, model, and company of the lamps assessed in the experiment.

Lamps	Characteristics	Model and Company
TLD	Fluorescent TLD (Standard lamps with reduced size tubes of 26 mm diameter) of 18 W and 58 W	Light Philips TCS097, Philips Lighting Spain, Madrid, Spain
TL5	Standard long tubes with a nominal diameter of 5/8 inch	High Efficiency Fluorescent TL5 35 W, MAXOS 4M691, Philips Lighting Spain, Madrid, Spain
CF	Compact fluorescent lamps, PL Electronic 23 W/840	Philips Lighting Spain, Madrid, Spain
LEDs	ALUM luminaire 40·25 LED SMD RGB controlled with a DN-RGB FIBER LIGHT console	
White LEDs	ALUM luminaire 40·25 LED SMD RGB	
XTRASUN LEDs	2 LEDs conversion antennas, 140 W	Prohydroponics, Greensburg, PA, USA.

Twenty-seven combinations between FL and LEDs (blue, red, and violet) were assessed. On the other hand, the choice of white LEDs and XTRASUN LEDs was mainly due to the novelty of these lighting systems sources. In the case of XTRASUN LEDs, it is an equipment that allows the combination of LEDs in order to satisfy the need for light established for plant development in different phenological stages which are set up as programs and also the equipment set-definition program related to the use of five channels: general growth (GG), vegetative growth (VG), flowering period (FP), ultraviolet (UV) and infrared (IR) (Table 2).

For each lighting source of the 27 combinations, white LEDs and XTRASUN LEDs, luminous flux (Φ) (expressed in lm) and the total electric power (P) (expressed in W) were all recorded. Then, with these measurements we determined the luminous efficacy (η) (expressed in lm W^{-1}) using Equation (1). The minimum illumination level (Ev) was calculated dividing the value of Φ by the surface (S) (1.2 m^2) (expressed in lx) and the limit value of energy efficiency (VEEI) (expressed in W m^{-2}) was then calculated using Equation (2) following the methodology established by Hidalgo et al. [20].

$$\eta = \phi / P \quad (1)$$

$$VEEI = (P * 100)/(S * Em) \quad (2)$$

2.3. Spectral Irradiance of Lamps

The spectral distribution scans were recorded at 300–1100 nm with 1-nm steps of the different lamps tested with a calibrated spectroradiometer (LI-COR 1800, Lincoln, NE, USA) at the distance of 45 cm below to the lamps. With these measurements, the spectral irradiance of each lamp was assessed following the methodology established by Baille et al. [21].

2.4. Absorbance of Seedling Plants

Seedling plants of three cultivars of tomato (Mayoral, Creativo and Torry) and three cultivars of cucumber (Jungla, Litoral, and Valle) were grown in a local horticultural seedling nursery (average temperature of 26 °C and relative humidity of 70% during the growing period). The radiometric determinations of transmittance (%Tr) and reflectance (%Re) of leaves of both seedling plants were measured by an integrating sphere using a calibrated spectroradiometer (LI-COR 1800, Lincoln, NE, USA) in a laboratory in the University of Almeria (36°49′ N, 2°24′ W). Measurements were taken in six plants (one replication per plant) per cultivar and species.

The percentage of leaf absorbance (%Ab) at each wavelength of leaves was obtained using Equation (3):

$$\%Ab(\lambda) = 100 - (\%Tr(\lambda) + \%Re(\lambda)) \quad (3)$$

Then, the effectiveness of light irradiance (ELI_{plant}) of the different types of lamps assessed on cucumber and tomato leaves was calculated using Equation (4):

$$ELI_{plant} = I(\lambda) \times \%Ab(\lambda) \quad (4)$$

where I(λ): irradiance at λ (W m^{-2}).

Finally, the use of irradiance (UI) in tomato and cucumber was calculated using Equation (5):

$$UI = ELI_{plant} \times 100/Itotal \quad (5)$$

where Itotal is total irradiance (W m^{-2}).

3. Results and Discussion

3.1. Current Status of Lighting Establishment in Horticultural Seedling Production

The different enterprises assessed (50) were located in four different areas with the following geographic coordinates: La Curva (36.75, −2.97), El Ejido (36.77, −2.81), Níjar (36.89, −2.10) and Pulpí (37.40, −1.75). The facilities of the nurseries were multi-tunnel greenhouses and the horticultural crops were the following: tomato, pepper, cucumber, zucchini, eggplant, green beans, melon, watermelon, and lettuce. The data obtained revealed that only 8% of the total nurseries surveyed used artificial lighting in the first culture period in crop chamber, to improve the uniform and increase growth of the seedling plants. The artificial lighting systems used were FL model TLD (36/58 W) (standard lamps with reduced size tubes of 26 mm diameter) with an average light intensity from 1600 to 4000 lux. The

assessment of the data obtained in the survey allow us to give recommendations about the sorts of lamps and spectral quality needed in this horticultural technology.

The low level of establishment of complementary lighting sources in nurseries in southern Spain can be due to the high level of sunny hours in this area as reported by Castilla and Prados [22]. On the other hand, the use of FL model TLD by nurseries was related to the low cost of these lighting sources and the ease handling as reported the owners of the nurseries surveyed, although the efficiency of these lighting sources was very low. Moreover, the lack of information between nursery growers about the possibilities of the establishment of other lighting sources resulted in the use of the same lighting systems between them. To improve the knowledge of the effects of TLD lamps in horticultural seedlings, Almansa et al. [23] carried out an experiment with these light sources in tomato seedlings reporting a growth enhancement and uniformity.

3.2. Technical Parameters of the Lamps

The use of LEDs as complementary light sources did not result in significant changes of luminous flux (Φ) and minimum illumination level (Em) values in all the lamps assessed. Nevertheless, the addition of LEDs in all the lamps resulted in an increase of the total electric power (P). This increase of total electric power resulted in a decrease of the luminous efficacy (η) and an increase of the limit value of energy efficiency (VEEI) compared to the case of lamps without LEDs incorporation. Lamps of TL5-2 with the addition of LEDs showed the highest values of VEEI. Regarding LEDs, it is necessary to point out that white LEDs (new lighting sources) showed the highest values of Φ and η compared to the other LEDs assessed in the experiment and the lowest value of VEEI. Moreover, the combination of red and blue LEDs (LEDs V) resulted in a higher value of luminous efficacy (η) and a lower limit value of energy efficiency (VEEI) compared with the red and blue LEDs separately. The main technical parameters of XTRASUN LED were a luminous efficacy (η) around 50 and a VEEI value of 2.0. From an energy efficiency point of view, it is necessary to highlight that TLD-18 lamps and their combinations, CF and XTRASUN LEDs were the most effective among the sources of light assessed with lower values of VEEI (Table 2), with values lower than 3.5 as proposed by the Spanish Technical Building Code (CTE) (2006) [24].

The range of luminous efficacy in all the lighting sources assessed in our experiment ranged from 1.3 to 75 lm W^{-1}, being lower than the values reported by other researchers who obtained luminous efficacies greater than 130 lm W^{-1} in different experiments with different lighting sources [25,26]. Similarly, the values of luminous efficacy in LEDs in our experiment were very low compared to the values reported by other researchers in different experiments [27,28].

As far as the limit values of energy efficiency were concerned, it is necessary to point out that the values registered in lamps combined with LEDs in our experiment were lower than the values reported by Almansa [7], with values around 9. Moreover, the high values of VEEI in LEDs can be related to the increase of light technology during the last ten years.

Table 2. Technical parameters of the lamps tested: luminous flux (Φ), total electric power (P), luminous efficacy (η), minimum illumination level (Em) and limit value of energy efficiency (VEEI).

Test	Lamp Type	Lamp Description	Φ (lm)	P (W)	η (lm W^{-1})	Em (lx)	VEEI (W m^{-2})
T1:TLD-18	TLD 18 W/830	6	8100	108	75.0	6750	1.3
T2:TLD-18LED-B	TLD 18 W/830 + LED-B	6 + 4Blue LEDs modules	8148	144	56.6	6790	1.8
T3:TLD-18LED-R	TLD 18 W/830 + LED-R	6 + 4Red LEDs modules	8207	144	57.0	6839	1.8
T4:TLD-18LED-V	TLD 18 W/830 + LED-V	6 + 4Violet LEDs modules	8239	144	57.2	6865	1.7
T5:CF	CF 23 W/840	4	5300	92	57.6	4417	1.7
T6:CF-LED-B	CF 23 W/840 + LED-B	4 + 4Blue LEDs modules	5348	128	41.8	4457	2.4
T7:CF-LED-R	CF 23 W/840 + LED-R	4 + 4Red LEDs modules	5407	128	42.2	4506	2.4
T8:CF-LED-V	CF 23 W/840 + LED-V	4 + 4Violet LEDs modules	5439	128	42.5	4532	2.4
T9:TL5-6	TL5-35 W/830	6	9900	210	47.1	8250	2.1
T10:TL5-6-LED-B	TL5-35 W/830 + LED-B	6 + 4Blue LEDs modules	9948	246	40.4	8290	2.5
T11:TL5-6-LED-R	TL5-35 W/830 + LED-R	6 + 4Red LEDs modules	10,007	246	40.7	8340	2.5
T12:TL5-6-LED-V	TL5-35 W/830 + LED-V	6 + 4Violet LEDs modules	10,039	246	41.2	8365	2.5
T13:TL5-2	TL5-35 W/830	2	3300	70	47.1	2750	2.1
T14:TL5-2-LED-B	TL5-35 W/830 + LED-B	2 + 4Blue LEDs modules	3348	106	31.6	2790	3.2
T15:TL5-2-LED-R	TL5-35 W/830 + LED-R	2 + 4Red LEDs modules	3407	106	32.1	2840	3.1
T16:TL5-2-LED-V	TL5-35 W/830 + LED-V	2 + 4Violet LEDs modules	3439	106	32.4	2865	3.1
T17:TLD-58-2	TLD 58 W/840	2	5200	116	44.8	4333	2.2
T18:TLD-58-2LED-B	TLD 58 W/840 + LED-B	2 + 4Blue LEDs modules	5248	152	34.5	4373	2.9
T19:TLD-58-2LED-R	TLD 58 W/840 + LED-R	2 + 4Red LEDs modules	5307	152	34.9	4423	2.9
T20:TLD-58-2LED-V	TLD 58 W/840 + LED-V	2 + 4Violet LEDs modules	5339	152	35.1	4449	2.8
T21:TLD-58-6	TLD 58 W/840	6	15,600	348	44.8	13,000	2.2
T22:TLD-58-6LED-B	TLD 58 W/840 + LED-B	6 + 4Blue LEDs modules	15,648	384	40.8	13,040	2.5
T23:TLD-58-6LED-R	TLD 58 W/840 + LED-R	6 + 4Red LEDs modules	15,707	384	40.9	13,090	2.4
T24:TLD-58-6LED-V	TLD 58 W/840 + LED-V	6 + 4Violet LEDs modules	15,738	384	41.0	13,115	2.4
T25:LED-B	LED-RGB-28	4Blue LEDs modules	48	36	1.3	40	74.9
T26:LED-R	LED-RGB-28	4Red LEDs modules	107	36	3.0	90	33.5
T27:LED-V	LED-RGB-28	4Violet LEDs modules	139	36	3.8	115	26.0
T28:LED-W	LED-RGB-28	4White LEDs modules	254	36	7.1	1017	3.0
T29:XTRASUN LED			6938	140	49.6	5781.8	2.0

3.3. Spectral Irradiance of Lamps

FL assessed showed common peaks at the following wavelengths: 436, 486, 544, 580, 612, 704 and 1010 nm. In addition, in some lamps, there was a pick in ultraviolet region (364 nm). Regarding LEDs, blue LEDs showed a peak at 470 nm, red LEDs at 636 and blue + red and white LEDS at 470 and 636 nm, respectively. The different stages in XTRASUN LEDs assessed were characterized as follows: GG showed two main peaks at 450 and 660 nm, VG at 430 and 660 nm, FP at 660 nm, whereas the ultraviolet (UV) had three main peaks at 405, 460 and 590 nm and the infrared (IR) at 660 and 745 nm (Figure 2).

The main peaks observed in the different combinations of lamps and LEDs assessed revealed that they were in the photosynthetically active radiation (PAR) range, so they might affect the photomorphological aspects of the plant along with its development [29].

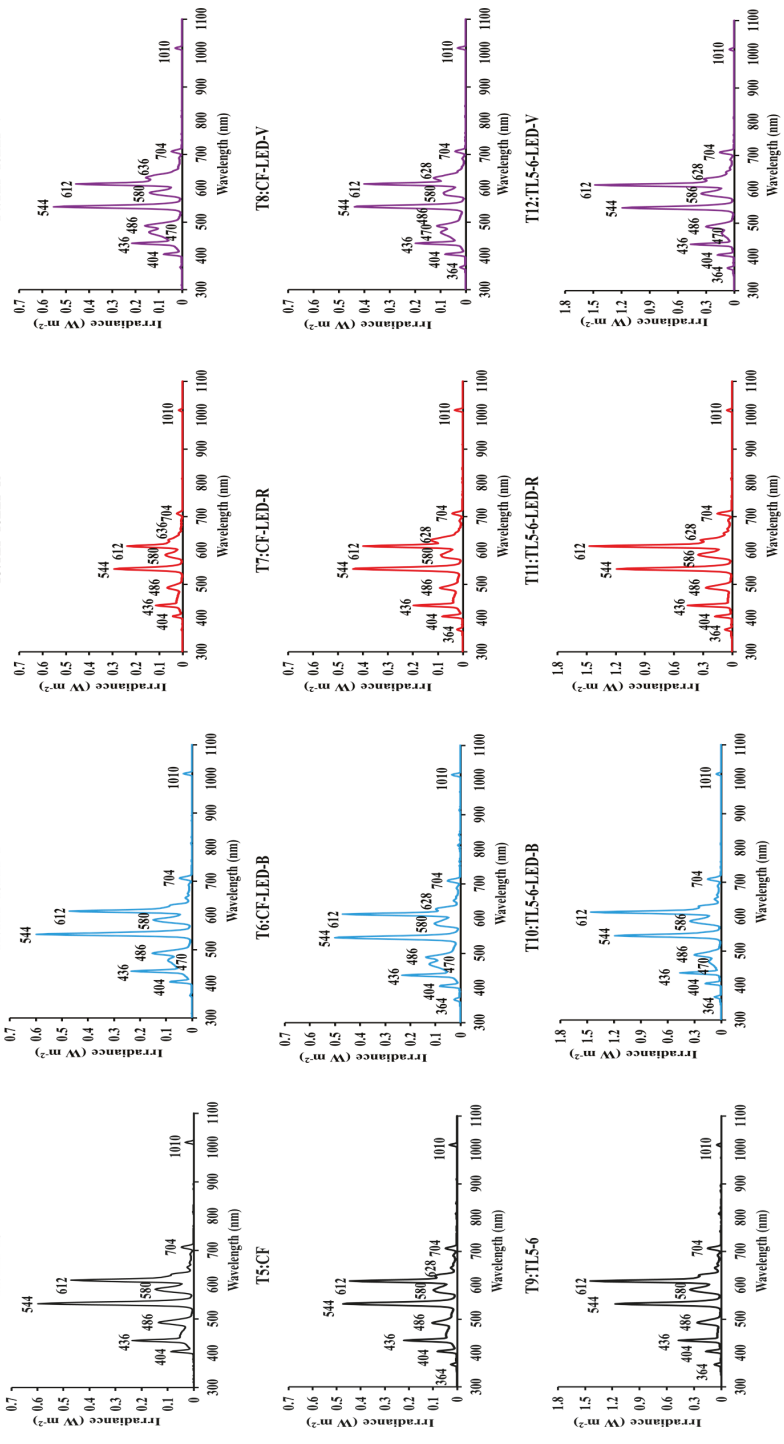

Figure 2. *Cont.*

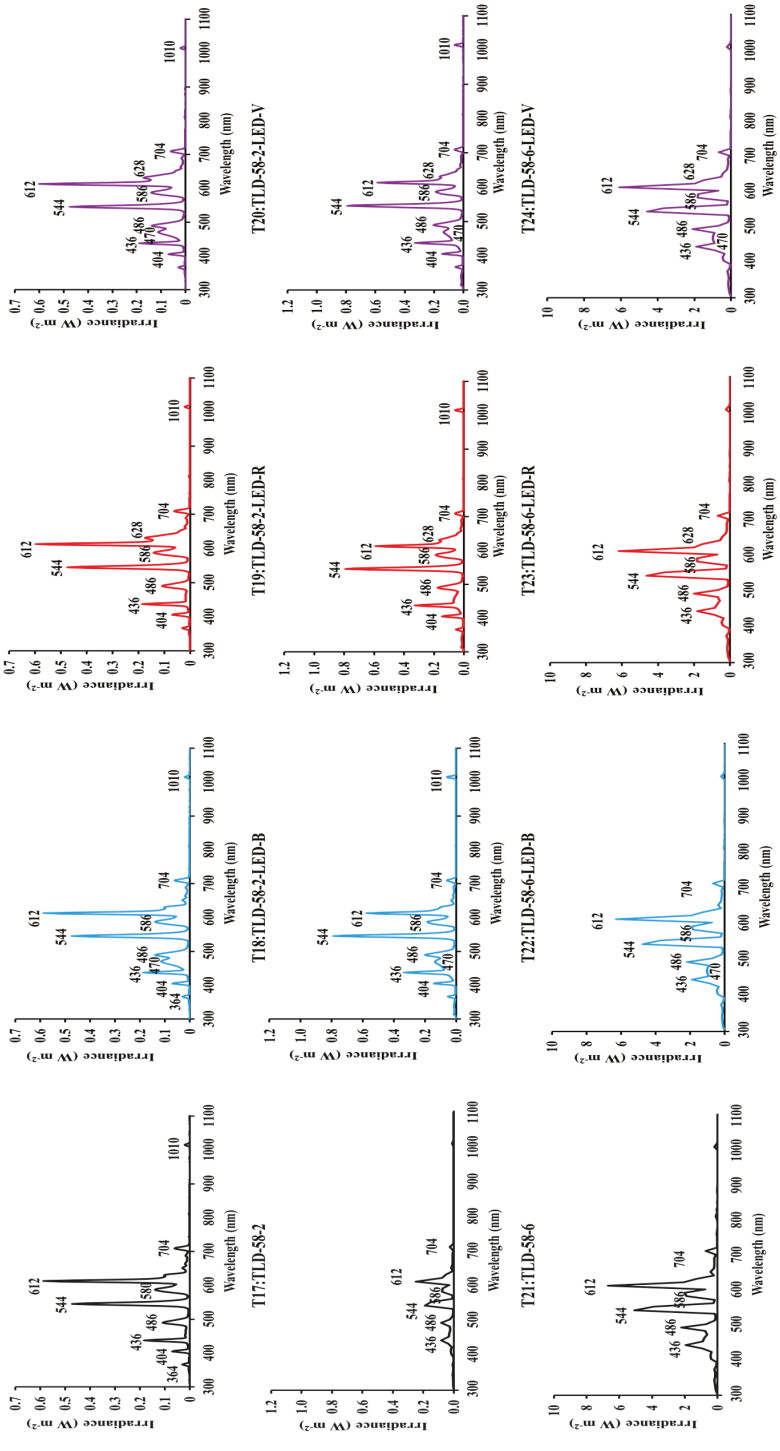

Figure 2. *Cont.*

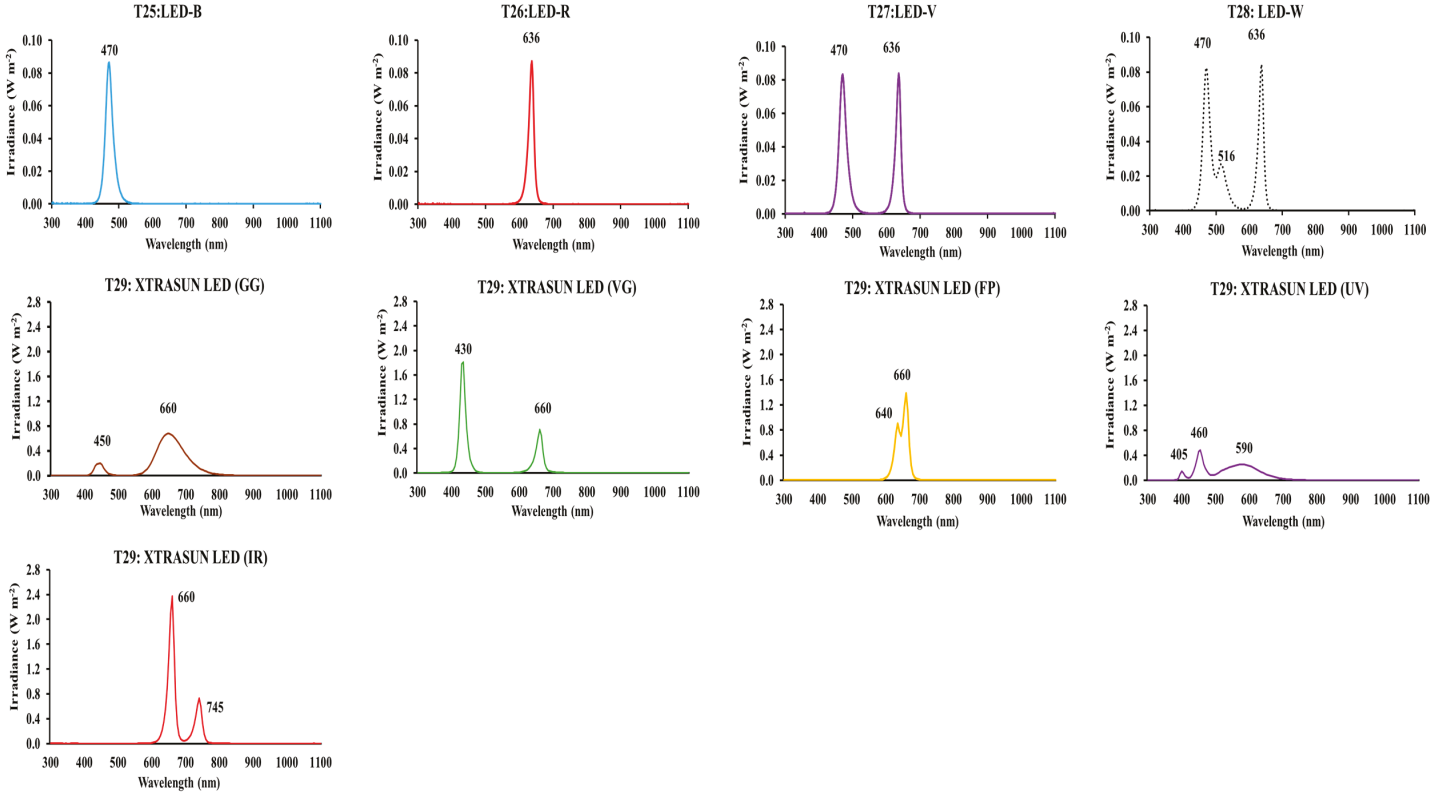

Figure 2. Spectral irradiance of different fluorescent lamps and LED (X axis: wavelength (nm), Y-axis: Irradiance (W m^{-2})).

The spectral irradiance of the different lamps assessed was recorded in Table 3. The addition of LEDs in lamps resulted in an increase of total irradiance in all the lamps assessed except for TLD58-6 lamps. The lamps with the highest total irradiance were TLD58-6 lamps with values around 75 W m^{-2} and with the lowest value were LEDs with values around 3 W m^{-2}.

The spectral irradiance in the different regions such as ultraviolet (UV), blue (B), red (R), far-red (FR) and their ratios are very important since they affect the morphogenetic responses of the plant growth under lamps, because plants have evolved other specialized photoreceptors to regulate responses to these physiologically important wavelengths. This region of the light spectrum is well known as morphogenetically active radiation (MAR) [30]. Phytochromes are primarily red-light photoreceptors and distinguish between red and far-red wavelengths to control physiological responses such as seed germination and flowering [31,32]. Cryptochromes, phototropins, and F-box proteins (a specific structural motif associated with signal transduction and regulation of the cell cycle) are blue-light receptors responding to blue/ultraviolet (UV) light wavelengths. Cryptochromes trigger signaling molecules that regulate responses such as circadian rhythms and stem elongation, whereas phototropins control chloroplastic movements to maximize absorption of light [3,33].

Phytochromes and cryptochromes have also been reported to act as green light photoreceptors [34].

The incorporation of blue and red LEDs increased the irradiance in their respective regions (R and B) in all the lamps assessed but the use of combination of red and blue (V) LEDs did not show the same results in all the lamps assessed since in TL5-6, TL5-2 and TLD58-2 lamps, the values of B and R were similar to the values obtained considering the use of red and blue LEDs separately; whereas in TLD18, CF and TLD 58-6 lamps, the values of B and R were different. The use of complementary lighting sources did not generate changes in FR region mainly due to the values of zero found in LEDs. Nevertheless, there was an enrichment in UV region using red and blue LEDs as complementary lighting sources.

Morrow [35] reported that the incorporation of LEDs resulted in an increase in irradiance in their respective regions (R and B) mainly due to their energy efficiency and spectral specificity. Nevertheless, the combination of red and blue LEDs did not result in a clear increase of the regions R and B in all the lamps assessed in our experiment which can be due to a possible interaction between the different types of wavelength emitted by each type of LEDs.

Near infrared radiation (NIR) is mainly related to heat and energy balance. Nevertheless, in a culture chamber with light near to the crop, NIR could result in plant overheating and the possibility of damaging tissues [36]. Therefore, the results obtained in LEDs with NIR values of 0 corroborate the high degree of applicability of these lighting systems for seedling plant growth.

As far as PAR was concerned, it was necessary to point out that the results obtained in this experiment revealed that TLD 58-6 lamps showed the highest values of PAR of all the lamps assessed. The use of LEDs separately as a source of lighting provided lower values of PAR around 5 W m^{-2}. Considering the different stages analyzed in XTRASUN LEDs, the highest values of PAR were in GG and VG respectively. Moreover, the use of LEDs in combination with the lamps assessed increased the value of PAR except for TLD58-6. Another important feature in light spectrum was the ratio of PAR/Total in the lamps. In our experiment, the ratio PAR/Total showed the highest value in LEDS and in the stages of VG and FP analyzed in XTRASUN LEDs. The ratios B/R, B/FR and R/FR analyzed in the experiment showed different trends according to the type of lamps assessed.

The PAR (400–700 nm) has a higher importance than the other wavebands of the solar spectrum because of its fundamental role in photosynthesis [30]. Therefore, the lamps assessed in our experiment with the highest values of PAR should be the most efficient for the growth of plants mainly due to the role of the PAR in the photosynthetic process. The values of the ratio PAR/Total around 1 in LEDs involves a higher photosynthetic efficiency radiation as reported by Almansa et al. [36].

Table 3. Spectral irradiance of the lamps and ratios between different regions of the radiation spectrum.

Lamps	Irradiance (Wm^{-2}) in Spectral Regions							Ratios				
	UV	B	R	FR	PAR	NIR	TOTAL	PAR:TOTAL	PAR:NIR	B:R	B:FR	R:FR
T1:TLD-18	0.12	6.52	6.80	0.58	22.66	0.92	23.74	0.95	24.63	0.96	11.24	11.72
T2:TLD-18LED-B	0.16	8.00	6.78	0.58	24.22	0.90	25.28	0.96	26.91	1.18	13.79	11.68
T3:TLD-18LED-R	0.16	6.36	7.88	0.56	23.48	0.88	24.52	0.96	26.68	0.81	11.35	14.07
T4:TLD-18LED-V	0.16	9.00	8.68	0.54	23.56	0.86	27.58	0.96	30.88	1.04	16.66	16.07
T5:CF	0.28	5.00	6.66	0.60	20.10	0.80	20.80	0.96	25.12	0.75	8.33	11.10
T6:CF-LED-B	0.32	8.26	6.66	0.68	23.84	1.16	25.34	0.94	20.50	1.24	12.12	9.76
T7:CF-LED-R	0.30	5.02	7.06	0.52	21.74	0.84	22.86	0.95	23.69	0.71	9.62	13.52
T8:CF-LED-V	0.28	6.88	7.04	0.52	21.66	0.82	22.78	0.95	26.32	0.98	13.23	13.52
T9:TL5-6	0.94	10.22	19.58	1.84	49.30	2.72	52.96	0.93	18.18	0.52	5.56	10.65
T10:TL5-6-LED-B	0.92	12.94	19.86	1.78	52.74	2.34	55.98	0.94	22.62	0.65	7.27	11.15
T11:TL5-6-LED-R	0.92	10.20	21.98	1.78	52.04	2.34	55.30	0.94	22.18	0.46	5.70	12.30
T12:TL5-6-LED-V	0.94	12.92	22.00	1.80	54.98	2.36	58.26	0.94	23.33	0.59	7.19	12.26
T13:TL5-2	0.36	4.04	7.94	0.72	19.86	0.94	21.14	0.94	21.34	0.51	5.67	11.12
T14:TL5-2-LED-B	0.36	6.82	7.94	0.72	22.80	0.94	24.08	0.95	24.50	0.86	9.57	11.14
T15:TL5-2-LED-R	0.36	4.08	10.04	0.72	22.06	0.94	22.34	0.94	23.53	0.41	5.68	13.98
T16:TL5-2-LED-V	0.38	6.76	10.02	0.72	24.88	0.94	26.18	0.95	26.28	0.68	9.37	13.88
T17:TLD-58-2	1.28	7.56	9.26	0.72	27.74	1.08	29.72	0.93	25.93	0.82	10.50	12.86
T18:TLD-58-2-LED-B	1.10	11.22	8.18	0.68	31.60	1.18	33.88	0.93	26.79	1.37	16.51	12.04
T19:TLD-58-2-LED-R	1.12	8.84	10.08	0.70	31.18	1.20	33.48	0.93	26.19	0.88	12.82	14.61
T20:TLD-58-2-LED-V	1.14	11.22	10.06	0.70	33.70	1.22	36.06	0.93	27.76	1.12	16.15	14.47
T21:TLD-58-6	3.28	19.42	24.60	2.00	72.24	2.98	77.70	0.93	24.21	0.79	9.69	12.27
T22:TLD-58-6-LED-B	3.18	20.94	23.18	1.84	71.08	2.68	76.12	0.93	26.60	0.90	11.42	12.64
T23:TLD-58-6-LED-R	3.08	17.96	24.42	1.78	68.74	2.60	73.56	0.93	26.46	0.74	10.07	13.68
T24:TLD-58-6-LED-V	3.12	20.34	24.02	1.78	70.62	2.60	75.46	0.94	27.20	0.85	11.48	13.56
T25:LED-B	0.02	2.42	0	0	2.56	0	2.58	0.99	-	-	-	-
T26:LED-R	0.02	0	1.80	0	1.82	0	1.82	1	-	-	-	-
T27:LED-V	0	2.34	1.74	0	4.24	0	4.24	1	-	1.34	-	-
T28:LED-W	0.02	2.38	1.74	0	5.10	0	5.10	1	-	1.37	-	-
T29:XTRASUN LED GG	0.02	1.45	10.87	2.25	13.06	2.71	15.44	0.85	4.83	0.13	0.64	4.83
T29:XTRASUN LED VG	0.10	8.60	3.87	0.10	12.55	0.12	12.72	0.99	107.23	2.22	90.06	40.53
T29:XTRASUN LED FP	0.01	0.00	9.87	0.03	9.93	0.04	9.97	1.00	242.10	-	0.03	340.19
T29:XTRASUN LED UV	0.30	3.48	2.28	0.15	9.83	0.18	10.14	0.97	54.92	1.53	23.64	15.50
T29:XTRASUN LED IR	0.01	0.00	11.25	3.80	11.27	3.85	15.08	0.75	2.92	-	-	2.96

3.4. Absorbance of Seedlings Plants

The leaf absorbance from 490 to 700 nm was slightly higher in the case of cucumber than in tomato seedlings plants although from 700 to 1100 nm there were no differences in leaf absorbance between both crops. Considering the values of leaf absorbance obtained in our experiment, it can be highlighted that there were different trends taking into account the range of the wavelength studied. For instance, from 490 to 555 nm there was a clear decline of leaf absorbance reaching values around 65% but from 555 nm until 700 nm, leaf absorbance in both crops increased until values of 92%. On the same hand, there was a significant decline in leaf absorbance from 700 to 745 nm in both crops reaching values of 5% which remained constant from 745 to 1100 nm (Figure 3).

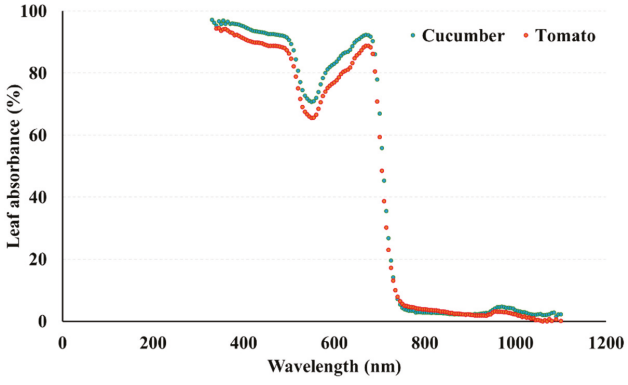

Figure 3. Leaf absorbance expressed in percentage of tomato and cucumber seedling plants.

While reviewing previous literature, we observed that there were references concerning the degree of absorbance in leaves in different crops. For instance, Schurer [37] evaluated this optical parameter in species such as Fuchsia sp., Geranium sp., Hibiscus sp. Similarly, in another experiment, Paradiso et al. [38] evaluated the absorbance of rose leaves reporting a decrease of transmittance and reflectance.

The alteration of spectral properties in leaves in the visible wavelengths can be related to the loss in chlorophyll content. In addition, the arrangement of cells within a leaf can be involved in the increase and/or decrease transmitted light by adjustment of the optical pathlength through the leaf [39].

The effectiveness of light irradiance $ELI_{cucumber}$ was slightly higher than ELI_{tomato} for all essayed lamps. The addition of complementary LEDs resulted in an increase of ELI_{plant} in TLD-18, TL5-6 and TL5-2 lamps. TLD-18 lamps and the combination with LEDs showed the lowest values of ELI_{plant} while TL5-6 lamps and the combination with LEDs showed the highest values of ELI_{plant} in both crops. The addition of LEDs in CF lamps only resulted in a significant increase in the UI (expressed in percentage) in both crops. The UI showed the highest values in LEDs in both crops except for white LEDs with values around 35%. Concerning XTRASUN LED, GG showed the highest values of ELI_{plant} in both species whereas in VG, UI was found at maximum levels in both crops (Table 4). No references have been found regarding this topic. These results are in accordance with Lin et al. [40] who considered that the use of LEDs could optimize the spectral quality for various plants and different physiological processes, and that they could also create a digitally controlled and energy efficient lighting system. Although the value of VEEI for white LEDs was within the range established by CTE, the UI was really low for both species essayed. Therefore, it is necessary to consider both parameters for the choice of the lamps for their use in horticulture.

Table 4. Effectiveness of light irradiance (ELI_{plant}) and the use of irradiance (UI) in each species.

Lamps	ELI_{tomato} (Wm^{-2})	$ELI_{cucumber}$ (Wm^{-2})	UI_{tomato} (%)	$UI_{cucumber}$ (%)
T1:TLD-18	9.38	9.52	79	80
T2:TLD-18LED-B	10.08	10.23	80	81
T3:TLD-18LED-R	19.49	19.76	79	81
T4:TLD-18LED-V	11.16	11.33	81	82
T5:CF	16.79	17.07	66	67
T6:CF-LED-B	20.06	20.42	79	81
T7:CF-LED-R	16.53	16.78	79	80
T8:CF-LED-V	18.27	18.56	80	81
T9:TL5-6	41.34	41.94	78	79
T10:TL5-6-LED-B	44.33	45.01	79	80
T11:TL5-6-LED-R	43.65	44.26	79	80
T12:TL5-6-LED-V	46.28	46.96	79	81
T13:TL5-2	16.62	16.86	79	80
T14:TL5-2-LED-B	19.26	19.58	80	81
T15:TL5-2-LED-R	18.54	18.78	79	80
T16:TL5-2-LED-V	21.07	21.39	80	82
T17:TLD-58-2	26.77	27.19	79	80
T18:TLD-58-2-LED-B	26.33	26.69	79	80
T19:TLD-58-2-LED-R	28.60	29.03	79	81
T20:TLD-58-2-LED-V	11.80	11.96	79	80
T21:TLD-58-6	30.72	31.15	79	80
T22:TLD-58-6-LED-B	30.29	30.73	80	81
T23:TLD-58-6-LED-R	29.24	29.64	80	81
T24:TLD-58-6-LED-V	30.11	30.54	80	81
T25:LED-B	2.30	2.37	89	92
T26:LED-R	1.60	1.60	88	88
T27:LED-V	3.76	3.83	89	91
T28:LED-W	1.72	1.81	34	35
T29:XTRASUN LED GG	11.35	12.05	73	78
T29:XTRASUN LED VG	11.19	11.69	88	92
T29:XTRASUN LED FP	8.43	8.91	85	89
T29:XTRASUN LED UV	8.07	8.55	80	84
T29:XTRASUN LED IR	10.16	10.69	67	71

4. Conclusions

The previous survey carried out allows us to discern which were the main technical parameters of the artificial lighting systems used in horticultural nurseries in southern Spain as well as the degree of their implementation. The results obtained in this experiment reported that the most efficient systems with a high value of η and low value of VEEI were XTRASUNLED and TLD-18 lamps. Regarding the level of irradiance, the lamps with the lowest total irradiance were CF but the combination with LEDs increased the value of the total irradiance. The lamps with the highest values of total irradiance were TLD58-6 lamps and the stage of GG in XTRASUN LEDs. Nevertheless, while considering the use of lamps in seedling production, two parameters have been proposed (ELI_{plant} and UI_{plant}) relating the power light emission of the lamp with the light absorption by leaves. The effectiveness of light irradiance (ELI_{plant}) was slightly higher in the case of cucumber than that of tomato for all essayed lamps. It can be found in our experiment that LEDs showed the lowest values, while TL5-6 lamps presented the highest values. Nevertheless, the use of irradiance was similar in both species and higher for blue, red, and violet (around 90%) LEDs, medium for FL and their combinations (around

80%) and lower for CF, LEDs-W and XTRASUN LEDs GG and infrared (IR). In this sense, novelty lamps (XTRASUN LEDs) supposed an improvement of the limit value of energy efficiency and the UI for plants as well as a high versatility related to MAR effects. The advantage of artificial lighting systems in nurseries is mainly related to the technological development of this industry that allows nursery growers to produce quality seedling plants in a shorter growing period. Nevertheless, the lack of knowledge among nursery growers concerning the accurate light requirements in horticultural nurseries involves a delay to the implantation of this technology. In this sense, this work shows the current extent of knowledge of artificial lighting systems, showing different alternatives of light sources that can be used in the growth of seedling plants, and the implementation of specific agronomic indexes such as ELI_{plant} and UI to choose the light sources which are more suitable for use in nursery growing systems, ultimately allowing energy saving and the improvement of quality in seedling plants.

Author Contributions: The authors contributed equally to this work.

Funding: This research received no external funding.

Acknowledgments: The authors thank Dimitrios Tsokanos for his English style corrections.

Conflicts of Interest: The authors declare no conflict of interest.

Abbreviations

The following abbreviations are used in this manuscript:

Ab	Absorbance
B	Blue
CF	Compact Fluorescent
ELI_{plant}	Effectiveness of light irradiance
FR	Far-Red
FL	Fluorescent Lamps
FP	Flowering Period
GG	General Growth
HPS	High-Pressure Sodium
IR	Infrared radiation
I	Irradiance
E	Light irradiance
VEEI	Limit Value of Energy Efficiency
LED	Light-emitting diode
MAR	Morphogenetically Active Radiation
NIR	Near Infrared Radiation
P	Electric Power
PAR	Photosynthetically Active Radiation
R	Red
Re	Reflectance
Tr	Transmittance
UI	Use of Irradiance
UV	Ultraviolet
V	Violet
VG	Vegetative Growth
W	White

References

1. Yang, B.; Zhou, X.; Xu, R.; Wang, J.; Lin, Y.; Pang, J.; Wu, S.; Zhong, F. Comprehensive analysis of photosynthetic characteristics and quality improvement of purple cabbage under different combinations of monochromatic light. *Front. Plant Sci.* **2016**, *7*, 1788. [CrossRef] [PubMed]

2. Kopsell, D.A.; Sams, C.E.; Morrow, R.C. Blue wavelengths from LED lighting increase nutritionally important metabolites in specialty crops. *Hortscience* **2015**, *50*, 1285–1288.
3. Christie, J.M. Phototropin blue-light receptors. *Annu. Rev. Plant Biol.* **2007**, *58*, 21–45. [CrossRef] [PubMed]
4. Inoue, S.I.; Kinoshita, T.; Matsumoto, M.; Nakayama, K.I.; Doi, M.; Shimazaki, K.I. Blue light-induced autophosphorylation of phototropin is a primary step for signaling. *Proc. Natl. Acad. Sci. USA* **2008**, *105*, 5626–5631. [CrossRef] [PubMed]
5. Wang, H.; Gu, M.; Cui, J.; Shi, K.; Zhou, Y.; Yu, J. Effects of light quality on CO_2 assimilation, chlorophyll-fluorescence quenching, expression of Calvin cycle genes and carbohydrate accumulation in *Cucumis sativus*. *J. Photochem. Photobiol. B Biol.* **2009**, *96*, 30–37. [CrossRef] [PubMed]
6. Sæbø, A.; Krekling, T.; Appelgren, M. Light quality affects photosynthesis and leaf anatomy of birch plantlets in vitro. *Plant Cell Tissue Organ Cult.* **1995**, *41*, 177–185. [CrossRef]
7. Almansa, E.M. Sistema Híbrido de Iluminación para el Desarrollo de Plantas. Aplicación en Invernaderos. Ph.D. Thesis, University of Almería, Almería, Spain, 2011.
8. Bantis, F.; Smirnakou, S.; Ouzounis, T.; Koukounaras, A.; Ntagkas, N.; Radoglou, K. Current status and recent achievements in the field of horticulture with the use of light-emitting diodes (LEDs). *Sci. Hortic.* **2018**, *235*, 437–451. [CrossRef]
9. Hernández, R.; Kubota, C. Tomato seedling growth and morphological responses to supplemental LED lighting red:blue ratios under varied daily solar light integrals. *Acta Hortic.* **2012**, *956*, 187–194. [CrossRef]
10. Currey, C.J.; Lopez, R.G. Cuttings of Impatiens, Pelargonium, and Petunia propagated under light-emitting diodes and high-pressure sodium lamps have comparable growth, morphology, gas exchange, and post-transplant performance. *Hortscience* **2013**, *48*, 428–434.
11. Cocetta, G.; Casciani, D.; Bulgari, R.; Musante, F.; Kołton, A.; Rossi, M.; Ferrante, A. Light use efficiency for vegetables production in protected and indoor environments. *Eur. Phys. J. Plus* **2017**, *132*, 43. [CrossRef]
12. Macias, H.A.; Ulianov, Y.; Ramos, Y. Illumination benefits using LED high brightness bulb compare to traditional illumination systems. In Proceedings of the 2012 IEEE International Symposium on Alternative Energies and Energy Quality (SIFAE), Barranquilla, Colombia, 25–26 October 2012; pp. 1–5.
13. Serrano-Tierz, A.; Martínez-Iturbe, A.; Guarddon-Muñoz, O.; Santolaya-Sáenz, J.L. Análisis de ahorro energético en iluminación LED industrial: Un estudio de caso. *Dyna* **2015**, *82*, 231–239. [CrossRef]
14. Lim, S.R.; Kang, D.; Ogunseitan, O.A.; Schoenung, J.M. Potential environmental impacts of light-emitting diodes (LEDs): Metallic resources, toxicity, and hazardous waste classification. *Environ. Sci. Technol.* **2010**, *45*, 320–327. [CrossRef] [PubMed]
15. ASEHOR (Asociacion de Semilleros Horticolas). 2018. Available online: http://pitalmeria.es/empresas/asehor/ (accessed on 16 August 2018).
16. Almansa, E.M.; Espín, A.; Chica, R.M.; Lao, M.T. Bioassimilation behaviour of tomato seedling cultivars under different sources of artificial light. *Aust. J. Crop Sci.* **2014**, *8*, 873–880.
17. Almansa, E.M.; Chica, R.M.; Espín, A.; Lao, M.T. Study on the use of supplementary artificial light in greenhouse production systems in the province of Almeria. Presented at the IV National Congress and I Agronomy Iberian Congress, Albacete, Spain, 2007.
18. Vu, N.T.; Kim, Y.S.; Kang, H.M.; Kim, I.S. Effect of red LEDs during healing and acclimatization process on the survival rate and quality of grafted tomato seedlings. *Prot. Hortic. Plant Fact.* **2014**, *23*, 43–49. [CrossRef]
19. Jang, Y.; Mum, B.; Seo, T.; Lee, J.; Oh, S.; Chun, C. Effects of light quality and intensity on the carbon dioxide exchange rate, growth and morphogenesis of grafted pepper transplants during healing and acclimatization. *Korean J. Hortic. Sci. Technol.* **2013**, *31*, 14–23. [CrossRef]
20. Hidalgo, A.; Villacrés, L.; Hechavarría, R.; Moya, D. Proposed integration of a photovoltaic solar energy system and energy efficient technologies in the lighting system of the UTA-Ecuador. *Energy Proc.* **2017**, *134*, 296–305. [CrossRef]
21. Baille, A.; González-Real, M.M.; López, J.C.; Cabrera, J.; Pérez-Parra, J. Characterization of the solar diffuse component under "Parral" plastic greenhouses. *Acta Hortic.* **2003**, *614*, 341–346. [CrossRef]
22. Castilla, N.; Prados, N.C. *Invernaderos de Plástico: Tecnología y Manejo*; Mundi-Prensa Libros: Madrid, Spain, 2007.
23. Almansa, E.M.; Chica, R.M.; Lao, M.T. Influence of the quality of artificial light on grafting tomato. *Aust. J. Crop Sci.* **2018**, *12*, 318–325. [CrossRef]

24. Spanish Technical Building Code (CTE). Basic Document of Energy Saving (DB-HE). 2006. Available online: http://www.buildup.eu/en/practices/publications/spanish-technical-building-code-royaldecree-3142006-17th-march-2006 (accessed on 16 August 2018).
25. Pimputkar, S.; Speck, J.S.; Den Baars, S.P.; Nakamura, S. Prospects for LED lighting. *Nat. Photonics* **2009**, *3*, 180–182. [CrossRef]
26. Landis, T.D.; Pinto, J.R.; Dumroese, R.K. Light emitting diodes (LED): Applications in forest and native plant nurseries. *For. Nurs. Notes* **2013**, *33*, 5–13.
27. Narukawa, Y.; Ichikawa, M.; Sanga, D.; Sano, M.; Mukai, T. White light emitting diodes with super-high luminous efficacy. *J. Phys. D Appl. Phys.* **2010**, *43*, 354002. [CrossRef]
28. Nakamura, S. Nobel lecture background story of the invention of efficient blue InGaN light emitting diodes. *Rev. Mod. Phys.* **2015**, *87*, 1139–1151. [CrossRef]
29. Sundström, V. Light in elementary biological reactions. *Prog. Quantum Electron.* **2000**, *24*, 187–238. [CrossRef]
30. Pérez, M.; Teixeira da Silva, J.A.; Lao, M.T. Light management in ornamental crops. *Floric. Ornam. Plant Biotech.* **2006**, *4*, 683–695.
31. Chaves, I.; Pokorny, R.; Byrdin, M.; Hoang, N.; Ritz, T.; Brettel, K.; Essen, L.O.; van der Horst, G.T.J.; Batschauer, A.; Ahmad, M. The cryptochromes: Blue light photoreceptors in plants and animals. *Annu. Rev. Plant Biol.* **2011**, *62*, 335–364. [CrossRef] [PubMed]
32. Fraikin, G.Y.; Strakhovskaya, M.G.; Rubin, A.B. Biological photoreceptors of light-dependent regulatory processes. *Biochemistry* **2013**, *78*, 1238–1253. [CrossRef] [PubMed]
33. Briggs, W.R.; Christie, J.M. Phototropins 1 and 2: Versatile plant blue-light receptors. *Trends Plant Sci.* **2002**, *7*, 204–210. [CrossRef]
34. Folta, K.M.; Maruhnich, S.M. Green light: A signal to slow down or stop. *J. Exp. Bot.* **2007**, *58*, 3099–3111. [CrossRef] [PubMed]
35. Morrow, R.C. LED lighting in horticulture. *Hortscience* **2008**, *43*, 1947–1950.
36. Almansa, E.M.; Espín, A.; Chica, R.M.; Lao, M.T. Changes in endogenous auxin concentration in cultivars of tomato seedlings under artificial light. *Hortscience* **2011**, *46*, 698–704.
37. Schurer, K. Leaf Absorbance and Photosynthesis. NASA-CP-95-3309. In Proceedings of the International Lighting in Controlled Environments Workshop, Madison, WI, USA, 27–30 March 1994.
38. Paradiso, R.; Meinen, E.; Snel, J.F.; De Visser, P.; Van Ieperen, W.; Hogewoning, S.W.; Marcelis, L.F. Spectral dependence of photosynthesis and light absorptance in single leaves and canopy in rose. *Sci. Hortic.* **2011**, *127*, 548–554. [CrossRef]
39. Bauerle, W.L.; Weston, D.J.; Bowden, J.D.; Dudley, J.B.; Toler, J.E. Leaf absorptance of photosynthetically active radiation in relation to chlorophyll meter estimates among woody plant species. *Sci. Hortic.* **2004**, *101*, 169–178. [CrossRef]
40. Lin, K.H.; Huang, M.Y.; Huang, W.D.; Hsu, M.H.; Yang, Z.W.; Yang, C.M. The effects of red, blue, and white light-emitting diodes on the growth, development, and edible quality of hidroponically grown lettuce (*Lactuca sativa* L. var. capitata). *Sci. Hortic.* **2013**, *150*, 86–91. [CrossRef]

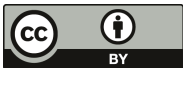

sustainability

MDPI

Article

Users' Awareness, Attitudes, and Perceptions of Health Risks Associated with Excessive Lighting in Night Markets: Policy Implications for Sustainable Development

Thi Phuoc Lai Nguyen [1,*] and Antonio Peña-García [2,3]

[1] Department of Development and Sustainability, School of Environment, Resources and Development, Asian Institute of Technology, Pathum Thani 12120, Thailand
[2] Department of Civil Engineering, University of Granada, 18071 Granada, Spain; pgarcia@ugr.es
[3] Reserarch Group "Lighting Technology for Safety and Sustainability", 18071 Granada, Spain
* Correspondence: phuoclai@ait.asia

Received: 5 September 2019; Accepted: 25 October 2019; Published: 1 November 2019

Abstract: The introduction of artificial lighting has dramatically transformed nighttime activities, becoming a very positive but also disruptive factor that must be optimized and adapted according to the guidelines of sustainable policies. In this framework, night markets in Thailand are definitely popular destinations among locals and tourists that are found in every town and city in the whole country, being the source of livelihoods for many people. It is well-known that shops in night markets frequently use colorful light sources, emitting high levels of illumination to attract customers. Since previous research has shown environmental risks of inappropriate lighting on human health and well-being, as well as on ecosystems, excessive lighting in night markets could have adverse effects on vendors' health if they are exposed to high illumination levels during long hours every night. This is a risk for people, but also for their attachment to their lands, traditions, culture, and way of life. This study was designed to explore whether excessive illumination of night markets has impacts on vendors' health and well-being. The research was conducted through an empirical study in a night market in the center of Surin province (Thailand), using observations and a questionnaire survey of 205 vendors and clients (non-vendors). The results show that night markets' vendors were more likely to suffer from eye- and sleep-related problems than non-vendors. Women were affected more than men. The results also revealed that the majority of both vendors and non-vendors tended to have awareness about excessive lighting impacts on human health, with more vendors tending to agree with the fact than non-vendors. Although night markets' are their main source of income, the majority of vendors were more unlikely to agree about the contribution of night markets to local livelihoods and development than non-vendors. These findings have implications for the Thai Authority in setting up appropriate lighting policies and regulations for night markets. The target is not only energy savings, but also to protect the public's health, culture, and traditional livelihoods, in a way that supports sustainable development.

Keywords: sustainable development; lighting policy; public health; energy savings; Thailand

1. Introduction

Nowadays, there is wide agreement that many of the most dramatic problems of humankind directly deal with sustainable development. Although the sustainable use of energy and natural resources, as well as the decrease in the emissions of contaminant and greenhouse gases, are major concerns, fostering the well-being of people and sustainable progress, without substantial disruptions to traditional ways of life, are key factors to grant a fair distribution of resources and ensure their

availability to future generations. Appropriate lighting has proven to be a transversal factor of sustainable development, with a high importance in human activities, granting safety, well-being, efficacy, profitability, and a healthy environment. Although the primary target of lighting should be to grant the safety of people and their goods [1], its impact on other activities, like commerce, leisure, or both, is also essential for personal well-being, as well as economic and social development. In spite of this positive influence on human life, the impact of night lighting, from other perspectives, also has negative aspects. Thus, light pollution [2], or the very high consumption in terms of energy, raw materials for the manufacture of luminaries, CO_2 emissions due to the production of electrical energy, and the manufacture of the luminaries, auxiliary devices, wiring, etc. are major concerns for public administrations [3–5]. Although the massive introduction of LED lighting has resulted in a lower consumption per luminary, the continuous growth of cities and population makes lighting a main challenge for sustainable development.

Furthermore, the effects of no-appropriate lighting during nighttime on human health are proven [6–10], as well as its effects on animal life [11–13], plants [14–18], and astronomical observations [19,20]. More specifically, the effects of light on human physiology and psychology have been well-known for ages. For the purposes of this research, the most important effects of lighting are those produced on the circadian rhythms (oscillations in some rhythms of our body lasting about a day, such as the sleep–wake cycle, the cycle of body temperature) [21].

In summary, all the advantages and shortcomings of lighting must be carefully considered when planning all kinds of facilities and installations [22], with special attention to sustainable development, when considered from its wider perspective. Night markets are a good example of necessary facilities in many countries of the world where inappropriate lighting can be a source of problems in spite of other benefits.

Night Markets and Excessive Illumination in Thailand

Night markets are typical opencast facilities for both local inhabitants and tourists to shop and spend time working during the night. They are very popular and indispensable to people in many Asian countries.

Thailand is home to some of the biggest and best ones across South East Asia. This country has a long history of night markets, which are teeming all over the country, in every corner of cities and villages, and usually on every night of the week. Thus, night markets of all shapes, sizes, and types of businesses are present in every village and town in Thailand, and they are open on a daily basis. These facilities are sources of livelihoods for many Thai people, especially for the poor, women, and unskilled people, as the vending activities in the night markets require low capital and investment.

For instance, the Talad Neon market in Bangkok (Figure 1) is open during the whole night. Food, clothes, and other goods are sold, and there are also stands to have a drink and chill out. Jumbo Klongsam market in Pathum Thani province (Figure 2) is open from 5:00 p.m. to 12:00 a.m. and mainly sells food. Night markets provide jobs and income for a large Thai population and are also considered to be a platform for creating new entrepreneurs [23].

Shops in night markets in Thailand are easily recognizable for their neon signs and intense illumination, which are used to attract customers. The reason is that shop owners perceived that more illumination is better, and, in addition, the lighting of night markets is not regulated in that country. However, continuous exposure to high levels and/or types of lighting during nighttime could have adverse effects on vendors' health, as mentioned above.

The dimensions of a standard shop are around 1.0–1.5 m x 2.0–2.5 m, and the number of lamps range from 4 to 12, depending on the shop's size and power of light sources. The majority of them use LED lamps, in order to save energy.

This study aims to understand people's perceptions of night markets' lighting and the impact of its excessive use on vendors' health and well-being. Its results and conclusions are expected to

contribute to important aspects of sustainable development, such as local policy, rural development, and attachment to the traditional economy.

Figure 1. Talad neon market (Bangkok).

Figure 2. Jumbo Klongsam market (Pathumthani).

2. Research Design

2.1. Study Location

A survey was conducted in a night market in Surin province, in Thailand (Figure 3). Surin is one of the northeastern provinces in Thailand, and it is considered one of the poorest areas. It covers a total area of 8124 km^2 and borders Oddar Meancheay of Cambodia. For centuries, northeastern provinces were considered to be isolated from the rest of the country. However, like other rural provinces in Thailand, Surin is also undergoing urbanization and becoming a tourist attraction, and many night markets have emerged and become popular destinations that can be easily found in almost every district along the province. Night markets there mainly sell food, clothes, and accessories. The vendors usually use an arbitrary number of any kind of lamp and different levels of illumination, without following a strict regulation. The market opened from 5:00 p.m. to 12:00 a.m.

Figure 3. Study case: Surin province night market.

2.2. Questionnaire Design

The survey instrument was created in Thai language. The survey (Appendix A) was composed of four parts:

1. Respondents' background and demographic information.
2. Respondents' circadian-rhythm and eye-related problems. Yes/no questions were used to inquire if respondents suffered circadian-rhythm and eye-related problems, and then open-ended questions were asked, in order to explore which specific problems the respondents had and how long they suffered with them.
3. Respondents' attitude toward night markets. It was composed of 5 items (i.e., contribution of night markets to income generation, poverty reduction, urbanized landscape, efficient use of public spaces, and community connection), on a five-point Likert scale (strongly disagree; disagree; uncertain; agree; and strongly agree).
4. Respondents' awareness of the effects of excessive light on human health. A five-point Likert scale (strongly disagree; disagree; uncertain; agree; strongly agree) was also used to see the level of respondents' awareness on effects of excessive light on human health (i.e., changes in biological clock, reduction in vision capacity, disturbances of sleep, and increases in other health problems).

2.3. Sampling Method

The survey was conducted with a total of 205 respondents, in which 103 night-market vendors and 102 non-night-market vendors (night-market clients), in order to test the differences between the 2 groups—vendors and non-vendors. The vendor and non-vendor groups were determined by using a random sampling method. The vendor population of the Surin province night market is approximately 142 people (information was given by the market authority). Therefore, the number of surveyed vendors was 103, which was calculated by using the modified Cochran Formula for sample size in smaller populations, desiring a 95% confidence level and ±5% precision. However, other criteria were also set to select the vendor group, including equal representatives of both men and women, as well as age ranges. To make the sample design balanced, the same number of respondents and the same characteristics (i.e., gender and age ranges) were also determined for the non-vendor group.

2.4. Survey Procedure

The survey took place within two days in March 2019 and was administered in paper format via a face-to-face interview method. The interviews of the vendor group were conducted in the first day, and the second day was for the non-vendor group, by selecting randomly among night-market clients, ensuring the non-vendor sample had equal representatives of men and women and all age groups, like the vendor respondents. In total, 103 night-market vendors and 102 non-night-market vendors were surveyed, providing a total size of 205 respondents. A group of 10 assistants coming from Surin University administered the surveys, supervised by the author. The survey was administered in the Thai language, and each interview took around 10–15 min.

2.5. Data Analysis

Descriptive and inferential statistical analyses were subsequently performed. Chi-square (χ^2) was applied to compare the distribution of responses to the discrete outcome variable among two or more independent comparison groups. The χ^2 test provides information not only on the significance of any observed differences, but also provides detailed information on exactly which categories account for any differences found. The χ^2 test was performed to compare demographic characteristics between vendor and non-vendor groups, as well as the difference in percentages of vendors/non-vendors' and male/females' responses, in terms of health problems associated with excessive lighting. Fisher's exact test was instead used in cases where there were cells with a frequency less than 5 and/or with small group sizes, as the Fisher's exact test has no sample-size restriction.

Two sample T-tests were performed with continuous data and Likert data to compare the difference in means between the two independent groups' responses, i.e., between vendors and non-vendors, and between male and female, regarding respondents' demographic characteristics, awareness of excessive light impacts on human health, and attitude toward the contribution of night markets to local development. Similarly, the one-way analysis of variance (ANOVA) was used to explore the differences in means among more than two groups (i.e., age groups).

Some statistical notations used in the paper are reported in Table 1.

Table 1. Statistical notations.

N	Number of Members of Sample
χ^2	Chi-Square statistic
t	*t* score
df	Degree of freedom
SD	Standard deviation
$\bar{x}$	Mean of sample
F	F ratio
p	*p*-value

3. Results and Discussion

3.1. Sample Socioeconomic Demographics

There was no difference in number of male and female respondents in both groups of vendors and clients, and the populations of vendors and clients differed in number of socioeconomic and demographic parameters (Table 2). Overall, 103 night-market vendors and 102 non-night-market vendors were surveyed, providing a total size of 205. However, 11 respondents (eight vendors and three non-vendors) did not fully answer all questions; therefore, the number of respondents used for data analysis was 194 (95 vendors and 99 non-vendors).

Concerning the ages of both groups, there was a slight difference between two respondent groups' ages: more surveyed non-vendors fell into the age range from 30 to 40 than surveyed vendors. Respondents of the vendor group were more likely to have higher education (70.5% vs. 42.4% having university, $p < 0.001$), because working in night markets is usually a source of income in additional to a main occupation, so vendors had a higher overall income (1423.57 ± 899.38 vs. 661.609 ± 588.0 Baht/day, $p < 0.001$), but more exposure to artificial light (7.78 ± 2.63 vs. 5.17 ± 1.21 h/night, $p < 0.001$), and they stayed closer to lamps (around 103.89 ± 61.48 cm vs. 195.53 ± 96.09, $p < 0.001$).

Both groups (67.4% for vendors and 73.7% for clients) applied energy-saving measures, but around half of both two groups didn't know about lamp and lighting regulations (43.2% for vendors and 57.6% for non-vendors). The majority in both groups perceived light color of the environment around them as "white".

Table 2. Sample demographics and comparisons among respondents of two groups of night-market vendors and non-vendor participants.

		Vendors	Non-Vendors	Statistic	df	*p*-Value
Number of surveys (n)	194	*95*	99			
Gender (%)	Female	52.6%	50.5%	$\chi^2 = 0.023$	1	0.87
	Male	47.4%	49.5%			
Age (%)	<30	16.8%	8.1%	$\chi^2 = 7.89$	3	0.048
	30–40	38.9%	56.6%			
	40–50	28.4%	19.2%			
	>50	15.8%	16.2%			
Education (%)	Primary	6.3%	7.1%			< 0.001 *
	Secondary	4.2%	18.2%			
	High school	17.9%	31.3%			
	Graduate	70.5%	42.4%			
	Post-graduate	1.1%	1.0%			
Income per day (Thai Baht) ($\bar{x} \pm SD$)		1423.57 ± 899.38	661.609 ± 588.0	$t = -6.81$	163.34	< 0.001
Perception of night light colors (%)	White	72.6%	69.7%			
	Yellow	3.2%	6.1%			
	Amber	13.7%	4.0%			
	Red	0.0%	2.0%			
	Multi-colors	10.5%	18.2%			
Exposure to artificial light per day (h) ($\bar{x} \pm SD$)		7.78 ± 2.63	5.17 ± 1.21	$t = 7.75$	92.66	<0.001
Distance to artificial light (cm) ($\bar{x} \pm SD$)		103.89 ± 61.48	195.53 ± 96.09	$t = 5.96$	65.22	<0.001
Apply energy-saving regulations (%)	Yes	67.4	73.7	$\chi^2 = 0.67$	1	0.415
	No	32.6	26.3			
Knowing about lamp and light-system regulations (%)	Yes	56.8	42.4	$\chi^2 = 4.54$	2	0.103
	No	43.2	57.6			

* Note: Fisher's exact test.

3.2. Public Perception of Excessive-Light-Related Health Problems

Our result showed that night-market vendors reported suffering from more health problems than non-vendors. The main problems of the vendors were eye-related, including eyestrain, sensitivity, burning, squinting, impaired vision, etc. They also suffered from difficulty initiating sleep, difficulty maintaining sleep, and daytime sleepiness, which is in agreement with the disruptions of circadian rhythms caused by lighting reported in the literature. In general, more night-market vendors have these problems than non-vendors (Figure 4).

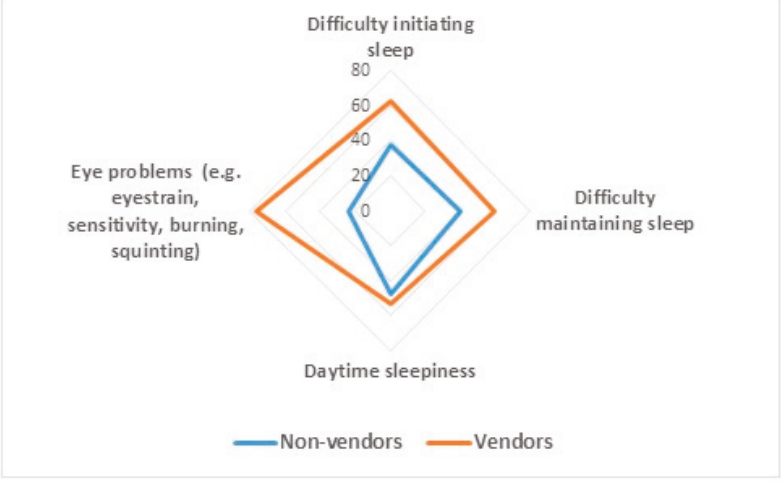

Figure 4. Percentages of vendors and non-vendors reporting health problems they perceived as being associated with excessive lighting.

The calculated χ^2 revealed a significant difference between non-vendors and vendors in terms of eye problems ($\chi^2 = 12.52$, $p < 0.001$, df = 1). There is a much higher number of vendors reporting eyestrain and sleeping problems associated with excessive lighting in the market than non-vendors.

The χ^2 was also performed to compare the difference in percentages between male and female respondents reporting health problems they perceived as being associated with excessive lighting. The results revealed that women seem to report these problems more than men. Female respondents had difficulty initiating sleep (χ^2 =3.73, p-value = 0.05, df = 1), experienced daytime sleepiness ($\chi^2 = 15.13$, p-value < 0.001, df = 1), and suffered from eye-related problems (χ^2 =6.31, p-value = 0.01, df = 1) more than male respondents. These results may be due to the remarkable hormonal differences between men and women.

3.3. Public Awareness of the Impact of Excessive Light on Human Health

The results indicated that the majority of survey respondents were aware of the excessive-lighting impacts on human health (Figure 5). Both vendors and non-vendors tended to be neutral about or agree with the proposal that excessive lighting levels are linked to circadian-rhythm-related problems. T-test data showed that vendors tended to agree more and agree strongly than non-vendors on how excessive light can change a human's biological clock ($t = 3.75$, df = 185.8, $p < 0.001$), disturb human sleep ($t = 2.55$, df = 191.26, $p = 0.012$) and increase health problem ($t = 2.10$, df = 189.96, $p = 0.04$), while there was no difference of awareness about the impact of excessive lighting on vision between two groups.

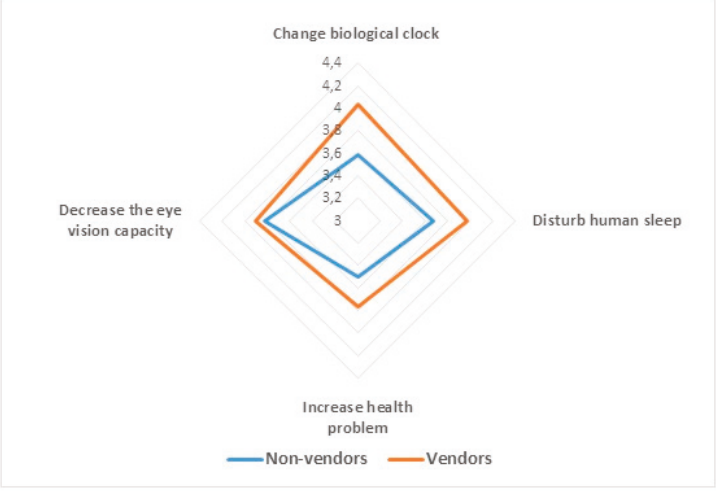

Figure 5. Excessive lighting impacts on human health. Mean values calculated from individual scores (1 = strongly disagree; 2 = disagree; 3 = uncertain; 4 = agree; 5 = strongly agree) (N = 194).

3.4. Public Attitude Toward the Contribution of Night Market to Local Development

Table 3 shows that vendors tended to be neutral about the contribution of night markets to local development, while non-vendors were more likely to agree with that. T-test data revealed the difference of attitudes between the two groups for all aspects of night markets' contributions to local livelihoods, local development, and community cohesion.

Table 3. Difference between vendors' and non-vendors' attitudes toward the contribution of night markets to local development. Mean values calculated from individual scores (1 = strongly disagree; 2 = disagree; 3 = uncertain; 4 = agree; 5 = strongly agree) (N = 194).

	Vendors ($\bar{x} \pm$ SD)	Non-Vendors ($\bar{x} \pm$ SD)	*t*-Statistic	df	*p*-Value
Income generation	3.30 ± 0.67	3.95 ± 0.83	5.98	186.89	<0.001
Poverty reduction	3.07 ± 0.88	4.04 ± 0.76	8.21	185.23	<0.001
Landscape urbanized and modernized	3.20 ± 0.85	3.84 ± 0.86	5.29	191.9	<0.001
Efficient use of public space	3.37 ± 1.00	3.85 ± 0.87	3.55	186.21	<0.001
Community interaction and connection	3.41 ± 0.96	3.91 ± 0.81	3.90	183.74	<0.001

T-test was also performed to see the difference of attitudes between females and males within the vendor group. The results in Table 4 revealed that men were more likely to disagree or be neutral about the role of night markets in poverty reduction, urbanization, efficient use of public space, and community connection.

ANOVA was performed to see the differences of attitude toward the contribution of night markets to local development among four age groups. The results revealed no significant difference among these groups.

The study results show that night markets are a source of livelihoods and incomes for local populations. The income per day gained from selling in the night market is higher than the daily salary of an ordinary worker. That is the reason why many university graduates choose to be vendors in the night markets as their main or second job. One of the reasons behind this success can be in their very striking lighting. This is in agreement with other studies, like the one of Johnstone et al., in 2019 [24], which showed that LED lighting impacts night-market businesses' prosperity in Kenya because of its attractiveness to customers.

However, the findings also depicted that more night-market vendors suffered from circadian-rhythm-related problems than non-vendors, including vision problems, difficulty initiating sleep, and difficulty maintaining sleep. The experience with health problems made vendors unlikely to have positive attitudes toward the contribution of night markets to local development, in spite of their dependence on night markets and the higher incomes they received from them, when compared to other jobs.

Table 4. Difference between female and male attitudes toward the contribution of night market to local development within vendors' group. Mean values calculated from individual scores (1 = strongly disagree; 2 = disagree; 3 = uncertain; 4 = agree; 5 = strongly agree) (N = 194).

	Female ($\bar{x}$ ± SD)	Male ($\bar{x}$ ± SD)	*t*-Statistic	df	*p*-Value
Income generation	3.44 ± 0.79	3.18 ± 0.52	1.91	75.34	0.059
Poverty reduction	3.27 ± 0.94	2.90 ± 0.79	2.05	86.36	0.043
Landscape urbanized and modernized	3.51 ± 0.84	2.92 ± 0.75	3.59	88.72	<0.001
Efficient use of public space	3.37 ± 0.86	3.04 ± 1.01	3.61	92.77	<0.001
Community interaction and connection	3.78 ± 0.77	3.08 ± 1.01	3.82	90.55	<0.001

Because individuals' own experiences and environments often influence their awareness and attitude [25,26], both vendors and clients were aware of lighting impacts on vision, as lighting's impacts on the eyes are more perceptible than other problems. Vendors were more likely to accept that excessive light can alter the human biological clock, disturb human sleep, and increase health problem, because many of them had experienced the health problems related to high levels of illumination.

This is the first field study up to date demonstrating these effects and perceptions in real conditions applicable to the topic under consideration: people developing their activities under too intensive or spectrally inaccurate lighting in night markets.

4. Conclusions

This study analyzed both the real and perceived impact of lighting among vendors and non-vendors in night markets. The methodology was based on a field survey in one typical night market in Surin province (Thailand).

Given the importance of night markets as a source of complementary income and even as unique livelihood, and their critical role in maintaining the traditional economy in many urban and rural environments around Asia, the health and well-being of both vendors and visitors is a key factor to achieving sustainable development in such a quickly growing zone like Southeast Asia and, in general, in the whole continent. Hence, the higher the sense of well-being among people making their living from night markets, the higher their attachment to their land and way of life. This is especially critical to avoid depopulation in rural zones and uncontrolled shifts to unsustainable economies and massive migrations toward big cities.

On the other hand, the extremely important role of lighting as a transversal factor in every human activity, and the necessity to keep it in mind when talking about sustainable development, is without doubt. Thus, the need for accurate policies for lighting, in order to grant health and well-being to the users of lighting installations, as well as the need to design and maintain these installations with the minimum consumption of energy, raw materials, and financial resources, makes it necessary to apply the current knowledge on this matter to night markets.

From the well-known perspective of installations, excessive levels of lighting, spectral distribution producing scattering toward the sky, or emission of light beams toward inaccurate directions, disturbing people, is considered light pollution. Night markets are outdoor places, and, hence, they can produce light pollution, but they are also places where people work. Most countries in Europe and North America regulate light pollution and also lighting levels in work places.

The results of this work, proving more health problems among vendors, confirm the necessity of regulating the lighting of night markets in Thailand and most countries in Southeast Asia.

This higher impact among vendors can be explained by their more continuous exposure to higher levels of illumination during inappropriate hours, at night. This impact is real (higher incidence of eye- and sleep-related problems) and also perceived.

Besides the considerations above, a careful analysis of the results leads to some very interesting conclusions:

(1) The incidence of health-related problems and circadian-rhythm issues among the vendors is proven. Given the direct relationship between high levels of illumination during nighttime and these kinds of problems, policies requesting lower levels, especially in the late night, could result in a clear improvement in their health and well-being, as well as a decrease in sanitary expenses and increase in productivity. This increase in productivity could be especially important for the vendors who have other occupations and use night markets as a supplementary source of income.
(2) Vendors are aware of the impact of intensive lighting on their health, but do not seem to look for alternatives. They just go on with their activities. They are probably afraid of losing customers if they individually decrease the levels of lighting in their shops. This makes it even more necessary to reach agreements with the support of the local authorities.
(3) The relatively low mood of vendors toward the impact of night markets seems to be motivated by their health problems and their awareness about the causes, directly related to intensive lighting at inappropriate times of the night. This attitude can influence new generations to abandon night markets as a main source of income or, at least, as a complementary source of incomes. This lack of attachment can become a source of migration and the search for less-sustainable ways of life outside their homelands.
(4) Lower levels of lighting result in a decrease in energy consumption and number of light sources, as well as the maintenance and operations related to daily life, like recycling. It has a positive impact on both the economy and environment.

In summary, night markets are key sources of incomes and traditional economy at local levels, in many Asian countries, like Thailand. The impact of their peculiar lighting on vendors' health, well-being, and perceived problems is a real threat for their long-term survival, with a consequent influence on sustainable development.

Although this study was conducted with a small vendor population from a seven-hour night-market in a remote province, it provided the first empirical insight into the health impacts caused by excessive lighting in night markets in Thailand. It is suggested that further research should be conducted in other types of night markets (i.e., 24-h night markets, e.g., in Bangkok) and/or integrated with medical statistics reporting vendors with circadian-rhythm disturbances and other health problems associated with excessive illumination, in order to provide more accurate evidence. These research findings speak to the need for policies regulating sustainable lighting in night markets to not only ensure livelihoods for local vendors and save energy, but also to reduce the lighting impacts on vendors and health-care costs.

Author Contributions: T.P.L.N. designed the research, conducted the survey, and analyzed the data. Both T.P.L.N. and A.P.-G. equally contributed to the writing and revision of the paper.

Funding: This research received no external funding.

Acknowledgments: This research was conducted during the field activity of a Master regular course "Regional and Rural Development Planning Workshops" of Asian Institute of Technology. The authors thank vendors and clients of Surin province night market who participated in this survey. Special thanks are given to Wilawan, B. Prathaithep, and students from Rajamanjala University of Technology Isan Surin Campus who supported the implementation of the survey, Nitchakan Inkong and Vu Thanh Bien, AIT Master students for their assistance in data input and analysis.

Conflicts of Interest: The authors declare no conflict of interest.

Appendix A Questionnaire Survey (Thai Language was the Original Language of the Survey)

Survey on awareness, attitude, and perception of excessive lighting effects on human health.

Dear participants, This is a survey regarding users' awareness, attitude, and perception of excessive lighting effects on human health. It is implemented by Dr. Thi Phuoc Lai Nguyen, Assistant Professor at the Department of Development and Sustainability, School of Environment, Development, and Resources, Asian Institute of Technology (Thailand). Your participation is voluntary and may be discontinued at any time. Your responses are anonymous, and the individual study results will be confidential and only used for the research purpose. Data will not be traceable to you and will not be shared with anyone.

Thank you for your time. If you have any questions, or if you want the study's final report, please contact me at phuoclai@ait.asia.

I. Respondent's general information

1. What is your gender? □ Female □ Male	2. How old are you? _____
3. What is your highest education? □ Primary □ Secondary □ High school □ University □ Post-university	4. How much is your average income a day? _____ Baht
5. What is the color of lamps around you? □ White □ Yellow □ Amber □ Red □ Multicolor	6. How many hours a night are you exposed to artificial light? _____ hours
	7. How far is approximately the distance between your post and the lamps? _____ cm
8. Do you apply any energy saving regulation? □ Yes □ No	9. Do you know any lamp and light system regulations? □ Yes □ No
10. At what time do you go to bed in the night? _____-	11. How many hours do you sleep a day? _____ hours

II. Information on Respondent's circadian rhythm and eye health

1. Do you suffer any problems with sleeping associated with excessive lighting?

□ Yes

□ No

If yes, what are the problems and how long have you suffered with this problem?

Problems **When**

_____ _____

_____ _____

_____ _____

_____ _____

2. Do you have any eye related problem associated with excessive lighting?

□ Yes

□ No

If yes, what are the problems and how long have you suffered with this problem?

Problems **When**

_____ _____

_____ _____

_____ _____

_____ _____

III. Respondent's attitude toward night markets

To what extend to you agree with the following statement?	Strongly disagree	Disagree	Neutral	Agree	Strongly agree
1. Night markets are a source of income generation and employment of many people in your area					
2. Night markets contribute to poverty reduction in your area					
3. Night markets have made your town more urbanized and modernized					
4. Night markets have contributed to the efficient use of public space					
5. Night markets have contributed to community interaction and connection					

IV. Respondent's awareness of excessive light effects on human health

To what extend to you agree with the following statement?	Strongly disagree	Disagree	Neutral	Agree	Strongly agree
Exposure to excessive illumination during the night can change your biological clock					
Exposure to excessive illumination during the night can trouble your sleep					
Exposure to excessive illumination can cause health problems					
Exposure to excessive illumination can decrease vision capacity					

References

1. Peña-García, A.; Hurtado, A.; Aguilar-Luzón, M.C. Impact of public lighting on pedestrians' perception of safety and well-being. *Saf. Sci.* **2015**, *78*, 142–148. [CrossRef]
2. Peña-García, A.; Sedziwy, A. Optimizing lighting of rural roads and protected areas with white light: A compromise among light pollution, energy saving and visibility. *LEUKOS* **2019**, *15*, 10. [CrossRef]
3. Montoya, F.G.; Peña-García, A.; Juaidi, A.; Manzano-Agugliaro, F. Indoor Lighting Techniques: An overview of evolution and new trends for energy saving. *Energy Build.* **2017**, *140*, 50–60. [CrossRef]
4. Jones, B.A. Measuring Externalities of Energy Efficiency Investments using Subjective Well-Being Data: The Case of LED Streetlights. *Resour. Energy Econ.* **2018**, *52*, 18–32. [CrossRef]
5. Beccali, M.; Bonomolo, M.; Leccese, F.; Lista, D.; Salvadori, G. On the impact of safety requirements, energy prices and investment costs in street lighting refurbishment design. *Energy* **2018**, *165*, 739–759. [CrossRef]
6. Davis, S.; Mirick, D.K.; Stevens, R.G. Night shift work, light at night, and risk of breast cancer. *J. Natl. Cancer Inst.* **2001**, *93*, 1557–1562. [CrossRef]
7. Schernhammer, E.S.; Rosner, B.; Willett, W.C.; Laden, F.; Colditz, G.A.; Hankinson, S.E. Epidemiology of urinary melatonin in women and its relation to other hormones and night work. *Cancer Epidemiol. Biomark. Prev.* **2004**, *13*, 936–943.
8. Jung-Hynes, B.; Reiter, R.J.; Ahmad, N. Sirtuins, melatonin and circadian rhythms: Building a bridge between aging and cancer. *J. Pineal Res.* **2010**, *48*, 9–19. [CrossRef]
9. Chepesiuk, R. Missing the dark: Health effects of light pollution. *Environ. Health Perspect.* **2009**, *117*, A20–A27. [CrossRef]
10. Contín, M.A.; Benedetto, M.M.; Quinteros-Quintana, M.L.; Guido, M.E. Light pollution: The possible consequences of excessive illumination on retina. *Eye* **2016**, *30*, 255–263. [CrossRef]
11. Davies, T.W.; Bennie, J.; Gaston, K.J. Street lighting changes the composition of invertebrate communities. *Biol. Lett.* **2012**, *8*, 764–767. [CrossRef] [PubMed]
12. Rich, C.; Longcore, T. *Ecological Consequences of Artificial Night Lighting*; Island Press: Washington, DC, USA, 2005.
13. Van Geffen, K.G.; van Grunsven, R.H.A.; van Ruijven, J.; Berendse, F.; Veenendaal, E.M. Artificial light at night causes diapause inhibition and sex-specific life history changes in a moth. *Ecol. Evol.* **2014**, *4*, 2082–2089. [CrossRef] [PubMed]
14. Bennie, J.; Davies, T.W.; Cruse, D.; Gaston, K.J. Ecological effects of artificial light at night on wild plants. *J. Ecol.* **2016**, *104*, 611–620. [CrossRef]
15. Bennie, J.; Davies, T.W.; Cruse, D.; Bell, F.; Gaston, K.J. Artificial light at night alters grassland vegetation species composition and phenology. *J. Appl. Ecol.* **2018**, *55*, 442–450. [CrossRef]
16. Blanchard, M.G.; Runkle, E.S. Intermittent light from a rotating high-pressure sodium lamp promotes flowering of long-day plants. *HortScience* **2010**, *45*, 236–241. [CrossRef]
17. Garcia-Caparros, P.; Chica, R.M.; Almansa, E.M.; Rull, A.; Rivas, L.A.; García-Buendía, A.; Barbero, F.J.; Lao, M.T. Comparisons of Different Lighting Systems for Horticultural Seedling Production Aimed at Energy Saving. *Sustainability* **2018**, *10*, 3351. [CrossRef]

18. García-Caparrós, P.; Almansa, E.M.; Chica, R.M.; Lao, M.T. Effects of Artificial Light Treatments on Growth, Mineral Composition, Physiology, and Pigment Concentration in Dieffenbachia maculata "Compacta" Plants. *Sustainability* **2019**, *11*, 2867. [CrossRef]
19. Falchi, F.; Cinzano, P. Measuring and Modeling Light Pollution. *Mem Soc. Astron. Ital.* **2000**, *71*, 139.
20. Rabaza, O.; Galadí, D.; Espín-Estrella, A.; Aznar Dols, F. All-Sky brightness monitoring of light pollution with astronomical methods. *J. Environ. Manag.* **2010**, *91*, 1278–1287. [CrossRef]
21. Saper, C.B.; Scammell, T.E.; Lu, J. Hypothalamic regulation of sleep and circadian rhythms. *Nature* **2005**, *437*, 1257–1263. [CrossRef]
22. Peña-García, A.; Nguyen, T.P.L. A Global Perspective for Sustainable Highway Tunnel Lighting Regulations: Greater Road Safety with A Lower Environmental Impact. *Int. J. Environ. Res. Public Health* **2018**, *15*, 2658. [CrossRef]
23. Chin, O.; Harun, M.Z.M.B. Night Market: A Platform for Creating New Entrepreneurs. *Humanit. Soc. Sci.* **2015**, *3*, 35–36. [CrossRef]
24. Johnstone, P.; Jacobson, A.; Mills, E.; Maina, M. *Self-reported Impacts of LED Lighting Technology Compared to Fuel-Based Lighting on Night Market Business Prosperity in Kenya*; Lawrence Berkeley National Lab.: Berkeley, CA, USA, 2009. [CrossRef]
25. O'Toole, P. *Knowing About Knowledge. How Organizations Remember: Retaining Knowledge through Organizational Action*; O'Toole, P., Ed.; Springer: New York, NY, USA, 2011; pp. 7–32.
26. Nguyen, T.P.L.; Seddaiu, G.; Roggero, P.P. Declarative or procedural knowledge? Knowledge for enhancing farmers' mitigation and adaptation behaviour to climate change. *J. Rural Stud.* **2019**, *67*, 46–56. [CrossRef]

sustainability

MDPI

Article

Lighting Features in Historical Buildings: Scientific Analysis of the Church of Saint Louis of the Frenchmen in Sevilla

Jose-Manuel Almodovar-Melendo [1,*], Joseph-Maria Cabeza-Lainez [1] and Inmaculada Rodriguez-Cunill [2]

[1] School of Architecture and the Faculty of East Asian Studies, University of Seville, 41012 Sevilla, Spain; crowley@us.es
[2] Faculty of Fine Arts, University of Sevilla, 41003 Sevilla, Spain; irodrigu8@gmail.com
* Correspondence: jmalmodovar@us.es; Tel.: +34-954-556556

Received: 18 July 2018; Accepted: 14 September 2018; Published: 19 September 2018

Abstract: Heritage issues have increased significantly in recent years. However, they tend to remain in the cultural sphere and are often resistant to scientific analyses. If we have to deal with the contradictory matter of sustainability in design for ancient buildings, such hindrances appear frequently. A crucial aspect in Architecture has always been its capacity to dispose internal spaces and apertures in a manner that enhances the balance of light and thus provides attuned perception and well-being. Poor performance in that respect raised objections against the prestige of admirable works and famed artists. If we reject the absurd idea of accurately reproducing identical buildings in the same place repeatedly, how are we supposed to benefit from the said knowledge without the help of any objective design tools? It is easy to agree that at least we would need some scientific support to transmit such proper effects. Aware of the former notions, authors have developed a novel simulation software called DianaX, which is based on mathematical models and equations produced and expanded by Joseph Cabeza-Laïnez, from roughly 1990 to 2018. This non-commercial software deals with radiative exchanges in all kinds of surfaces (for instance domes, vaults, cylinders, hyperboloids and curves in general). It also includes direct sun in the simulations unlike most programs. Therefore, it is ideally suited for the analysis of heritage architecture and especially that which identifies with the Renaissance, baroque and neoclassical epochs. The case of temples from the baroque period resumes the conflict expressed in the first paragraph and the Jesuit Church of Saint Louis (1699–1731) is one of the most relevant examples of efficient illumination found in Mediterranean latitudes, having been recently restored. In this article, we would like to discuss the subtle and interesting implications of employing our simulation software for lighting in such a complex baroque temple. The methodology would be to identify the main energy sources within the church in order to construct a suitable model for simulation. Subsequently we apply the said software DianaX to such model and establish the most significant results trying to compare them with available on-site measurements. Finally, a strategy to enhance day-lighting and supplement it with other light sources in the church is proposed.

Keywords: daylighting; architectural simulation; monitoring; Saint Louis of the Frenchmen; iconography

1. Introduction

Famous buildings from the past and the present have brandished their excellence in the respect of lighting control. Their thresholds were praised from an artistic point of view for the way in which solar radiation penetrated their interiors [1]. It is said that these buildings scattered the light when it was excessive or augmented it if scarce. Inside their vaults the light itself has been termed by poets or

architects as quaint, bland, dim, uplifting, ruthless or even monosyllabic. Consequently, knowledge of daylighting has interested many architectural theorists including Siegfried Giedion, Le Corbusier's colleague, who pointed out:

> "It is light that induces the sensation of space. Space is annihilated by darkness. Light and space are indissolubly summoned." [2] (p. 445)

Even though architectural theoreticians have celebrated the excellence of daylighting in relevant buildings, they carried out very few assessments of such illumination. In fact, the architectural literature has usually shown a high degree of inaccuracy regarding its most revered buildings (Figures 1 and 2). Consequently, they have produced an undesired effect, the inability to preserve or transmit the benefits of daylighting in historic halls, thus provoking inadequacy of environmental measures and supplementary means of lighting.

We would agree that we require objective evaluation of performance in ancient buildings. However, such evaluation of lighting is difficult and cumbersome due to the unpredictable behaviour of visitors and personnel and the variability of weather conditions. Henceforth simulation is an appropriate tool to evaluate the potential of the building in sustainability terms, given that we take certain caveats into account [3].

Following such concern, we have been involved, for a number of years, in the development of a mathematical model to simulate the radiation or more specifically illumination in a physical or architectural medium. To this end, the authors expand a series of algorithms stemming from the algebra of configuration factors [4]. This mathematical model extends the radiation properties of diffuse sources to all kinds of luminous exitance from building surfaces irrespective of their shape (a significant novelty to our knowledge) and including the reflected component, even for curved geometries, for the first time in history. The surfaces are therefore treated as radiative emitters by virtue of the generalized law of the projected solid angle [5,6]. The concept of surface source allows for the inclusion of direct solar radiations since it is independent of the sky condition. The simulation of the aforementioned objectives can be fulfilled by entirely geometric or formal factors and thus appropriate to the architectural profession.

When we are discussing a radiant phenomenon in which a sufficiently diffuse energy is transmitted, we intend to know how the energy will be propagated or distributed so we can improve our architectural design with respect to such distribution. In this regard, illumination manifests itself through fields of a fundamentally vector nature [7]. Therefore, our main objective is to discern the behaviour of these fields in their unaltered state. On this topic, we have incorporated important contributions by Yamauchi [8], Moon and Spencer [9,10] among others.

Nevertheless, modifications of architectural features have the potential to alter substantially the field of study. In this regard, one of the main problems in environmental sciences applied to architecture has been to determine in which ways the existing physical fields are transformed due to buildings' features and towards which direction our design should be oriented in the search for a sounder transmission of climatic events [11]. In other words, how the design and architectural forms could be improved to achieve an optimal and coherent distribution of natural energies or at least of supplementary energy in the case of retrofit of heritage.

In this regard, the proposed mathematical model allows us to determine the illuminance vector at every point of the space under study and hence to immediately obtain the flux lines in the radiant field caused by any architecturally conceived form. This procedure has been validated in dozens of projects and hundreds of radiation measurements around the world [12–23], see Figure 3. Among them, we would like to present some random cases of the following: in Rome (Italy), the Church of Sant'Andrea by Bernini, Sant'Ivo by Borromini and the Pantheon. In Paris (France) the National Library by Henri Labrouste. In Kyoto (Japan), the Buddhist temple of Ryoanji. In Salvador (Brazil) the Church of Sao Bento, in India the temples of Ajanta and Modhera and in Korea the temple of Seokguram (Gyeongju). These field works have been completed roughly between 1996 and 2018.

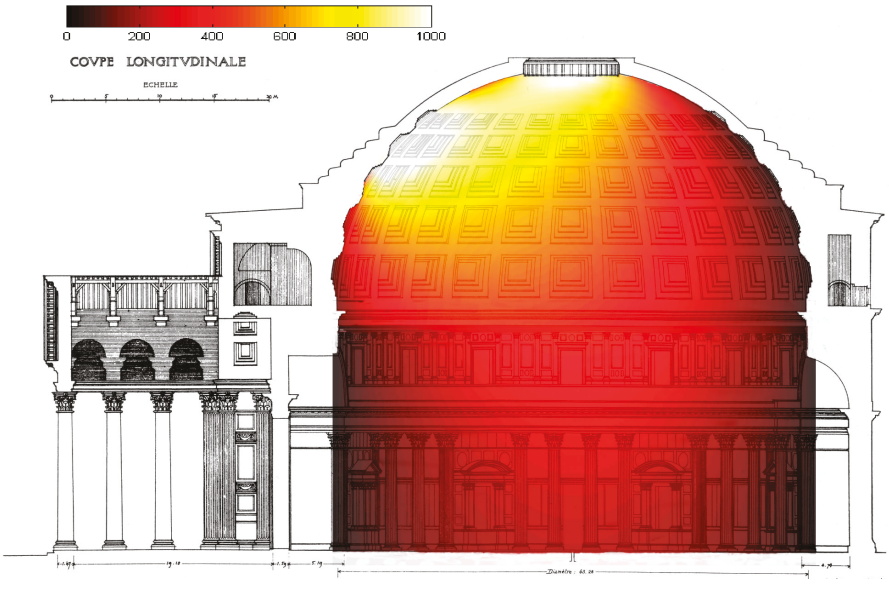

Figure 1. The Roman Pantheon, lighting simulation conducted and validated by Joseph Cabeza-Laïnez.

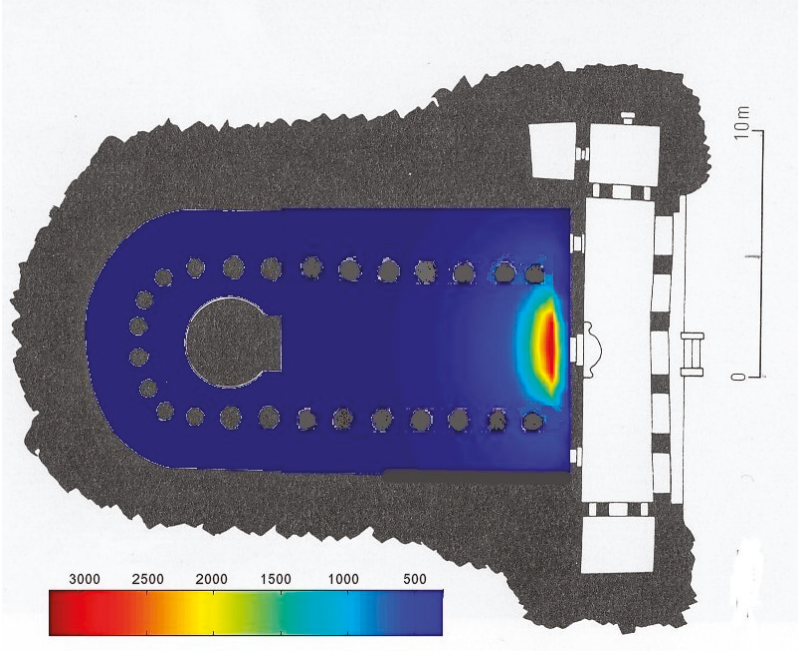

Figure 2. Plans and Views of Chaitya number 26 at Ajanta (India) showing illuminance levels. (3000–50 lux). Simulation conducted and validated by Joseph Cabeza-Laïnez.

In this manner, such remarkable spaces for Universal Architectural History have been thoroughly and painstakingly analysed and we ought to say that with the encouragement of no one.

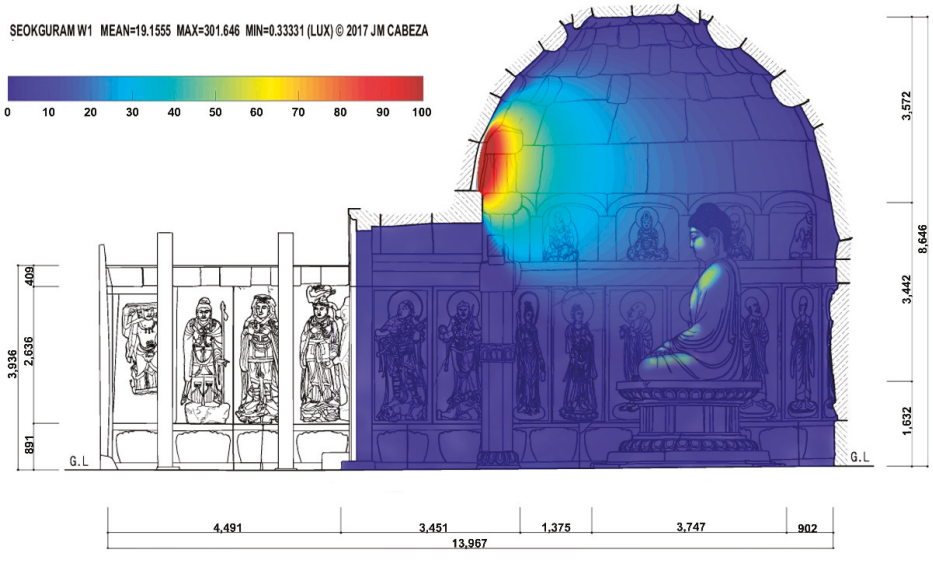

Figure 3. The Seokguram Buddha temple at Gyeongju (Korea). Simulation of a hypothetical aperture conducted and validated by Joseph Cabeza-Laïnez.

2. A Brief Outline of the History of the Church

The Church of Saint Louis lies in Sevilla in the southernmost point of Spain (latitude 37°22′ N), (Figure 4). It was erected by local builders between 1699 and 1731 under the guidance of Jesuit architects and hypothetically among them Angelo Italia. The building was so influential in the urban layout that the former King's Street, in which the church is located, changed its name to the current denomination of Saint Louis' Street.

Figure 4. View of the Dome decorated with frescoes from the inside and the lantern and main eight windows. Source: Almodovar-Melendo.

Despite the discussion on the authorship of the project, an important participation in the works of the famous Sevillian master Leonardo de Figueroa has been reported, albeit in collaboration with other artists. Its Greek-cross disposition is rare in Spain and probably relates to the Italian tradition showing a clear parallel with the church of S. Francesco Saverio (St. Francis Xavier) in Palermo (Sicily), where the Jesuit Angelo Italia was the chief architect. In fact, resemblances can be traced to other important religious constructions, featuring designs by Carlo Fontana, Bernini, Rainaldi or Borromini, like the church of Santa Maria in Monte Santo or Santa Agnese in Piazza Navona. The church has been considered as one of the most outstanding temples erected by the Society of Jesus of all times and comparable to the ancient wonders of antiquity as ziggurats et cetera [24].

This church is oriented according to the four cardinal points in a way that the main entrance is located to the east and the main altar to the west and, in this manner, revolves the usual Christian disposition where the main façade must face west. Many artworks manufactured by great masters of the Sevillian Baroque can be found in the interior of the church [25]. The altarpieces, which exhibit a great profusion of gilt surfaces and other glistening and reflective details, were mainly carved by Pedro Duque Cornejo and the author of the majority of the frescoes was Domingo Martinez. The iconographic program refers to relevant evangelizers and founders of the Society of Jesus like Xavier depicted in his arrival to the shores of Japan and Loyola. An altarpiece dedicated to Saint Stanislaus Kostka was carved in the south wall, while another dedicated to Saint Francis Borgia appears in the north side of the temple (Figure 5).

Figure 5. Altarpiece dedicated to Saint Francis Borgia, detail of the church. Source: Almodovar-Melendo.

Referring to the girth and typology of the building, the width of the cupola is of 13.5 m and it rests on a drum 14.85 m high, that presents eight tall windows with a total area of 6.3 square meters each. It is interesting to notice that the ratio of glazing to lateral enveloping area is lesser than 10% and incomparable to modern buildings made of curtain walls or even fully glazed (Figure 6).

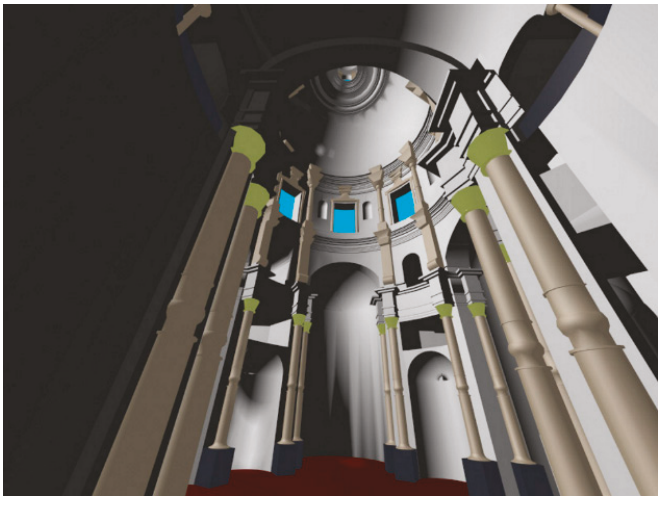

Figure 6. Virtual reality depiction of the central nave of the Church. Source: Gonzalo Pulido.

3. Description of the Mathematical Model

3.1. Fundamentals

A variety of mathematical models has been employed to determine the potential of the physical components at the nave of the church and to simulate its daylighting fields. The basic operations involve a configuration factor algebra newly developed by the authors. Another important innovation of the method proposed is that it incorporates both the direct and reflected component of light for curved surfaces, as we will discuss in more detail below. This procedure, a further advance of the research of Yamauchi and the American engineers H. Higbie and Levine [26], completes Lambert's corollary of reciprocity [27], representing a more generalized version of the form factors concomitant with those used in heat transfer for radiometric systems [28].

The model extends the radiation properties of diffuse sources to luminous exitance of all kinds of building surfaces that are subsequently considered as radiative emitters. Once the initial intensity of each surface is known and the primary shape of the exchangers is fixed, successive interchanges are obtained until a balance of the required accuracy is achieved.

The configuration factor is a dimensionless fraction (varying from zero to one) that originated in the work of J. Lambert (1760). It expresses the amount of radiant flux E_b that arrives from a given surface to others directly exposed to the first, if both are perfectly diffuse emitters. It depends solely on the position, size and form of the given surfaces. Therefore, we could term it as geometrical and the corresponding domain of study of these matters is geometric optics [29]. Mathematically speaking, we can define it by the following integral equation whose terms appear in Figure 7.

$$F_{12} = \frac{1}{A_1}\left[\int_{A_2}\int_{A_1}\frac{\cos\theta_1\cos\theta_2}{\pi r^2}dA_1dA_2\right], \quad (1)$$

where E_{bi} is the radiant power emitted by the corresponding surface 1 or 2 (lumen/m^2). A_i is the area of surface, dA_i is the differential of area (m^2); r is the distance radio-vector (m). θ_i is the angle between

radio-vector at differential element i and the normal to the surface (radians), $d\Phi_{1-2}$ is the differential of radiant flux from surface 1 to 2 (lumen).

The previous expression states that radiant interchange for every given form depends on its shape and its relative position in the three-dimensional space. From the times of Lambert to our days, researchers and scientists in the fields of geometric optics and radiative transfer have sought to provide solutions to the canonical equation in the figure for a variety of forms [6]. This implies no minor feat, since the said equation leads, in most cases, to a quadruple integration and the fourth degree primitive of even simple mathematical expressions often entails lengthy calculations [4].

The configuration factors F_{ij} possess the well-known property by virtue of which,

$$\sum_{j=i}^{n} F_{ij} = 1, \tag{2}$$

For any surface A_i and this implies within an enclosure of n surfaces,

$$F_{11} + F_{12} + F_{13} + \ldots + F_{1n} = 1.0, \tag{3}$$

If only planar surfaces are considered $F_{11} = 0$ (a flat surface does not see itself). But in the particular case of baroque churches with many curved surfaces like spheres and cylinders, the factors with repeated sub-indexes tend to have values which have not been described in the literature in an exact formulation. Such is a significant part of the novelty and opportunity of our approach and simulation program, one of the main reasons behind this article.

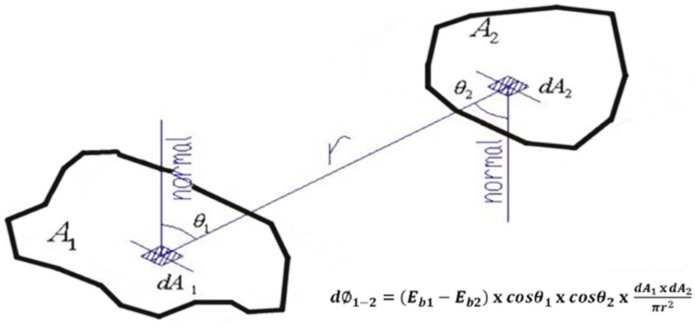

Figure 7. Equation parameters. Source: Joseph Cabeza-Laïnez.

The authors have devoted more than a decade of their careers to solve the former integral equation in an exact manner and the main outcome is that both the accuracy and speediness of computational time with these procedures are radically enhanced.

The second fundamental property of configuration factors is lack of symmetry. Since, due to Lambert's law, $A_1F_{12} = A_2F_{21}$ consequently, $F_{12} \neq F_{21}$, unless both surfaces have the same size.

The authors have established based on these two principle axioms a complete algebra for the first time in the literature that includes not only addition but also scalar product. We judge that to delve on this product exceeds the scope of the present article. Suffice to say that it permits the analysis of concatenated curved surfaces (previously untreated).

For the particular case of rectangular windows, if we are discussing their effects in the daylighting performance of a building, we should be utterly aware of how and where and especially under which conditions the light reaches the inner spaces. With this objective in mind, expressions for the configuration factor between rectangular inclined surfaces have been integrated at several angles to be used for daylighting simulation (Figure 8).

The window is considered to be, a uniform diffuse luminous source (its luminance L in lumen is constant for a given instant of time). As a result, we can obtain the following and more general expression for its illuminance E (lumen/m^2):

$$E = \frac{L}{2}\left[\begin{array}{c} \frac{a\cos\varphi - y}{\sqrt{a^2+y^2-2ay\cos\varphi}}\text{arctg}\frac{b}{\sqrt{a^2+y^2-2ay\cos\varphi}} + \\ + \frac{b\cos\varphi}{\sqrt{b^2+y^2\sin^2\varphi}}\text{arctg}\frac{a\sqrt{b^2+y^2\sin^2\varphi}}{b^2+y^2-ay\cos\varphi} + arctg\frac{b}{y} \end{array}\right], \quad (4)$$

Angle φ defines the relation with the normal to the considered work-plane. If $\varphi = 90^\circ$, cosine is 0 and the expression equates the formula for vertical rectangles to a point-source.

$$E = \frac{L}{2}\left[\text{arctg}\frac{b}{y} - \frac{y}{\sqrt{a^2+y^2}}\text{arctg}\frac{b}{\sqrt{a^2+y^2}}\right], \quad (5)$$

The above expression (4) alters if we are trying to find the illuminance of the perpendicular surface; consequently, the solving equation would be in this case,

$$E = \frac{L}{2}\left[\begin{array}{c} \frac{a\sin\varphi}{\sqrt{a^2+y^2-2ay\cos\varphi}}\text{arctg}\frac{b}{\sqrt{a^2+y^2-2ay\cos\varphi}} + \\ + \frac{b\sin\varphi}{\sqrt{b^2+y^2\sin^2\varphi}}\text{arctg}\frac{a\sqrt{b^2+y^2\sin^2\varphi}}{b^2+y^2-ay\cos\varphi} \end{array}\right], \quad (6)$$

It is easy to notice in this situation that if $\varphi = 90^\circ$, this would give $\cos\varphi = 0$ and $\sin\varphi = 1$, substituting these values in the former equation:

$$E = \frac{L}{2}\left[\frac{a}{\sqrt{a^2+y^2}}\text{arctg}\frac{b}{\sqrt{a^2+y^2}} + \frac{b}{\sqrt{b^2+y^2}}\text{arctg}\frac{a}{\sqrt{b^2+y^2}}\right], \quad (7)$$

This expression represents the exchange between a horizontal rectangle and a point-source parallel surface.

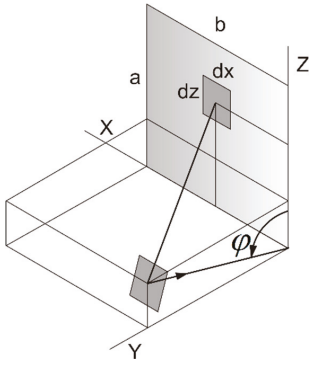

Figure 8. Configuration factor between a rectangle and a point that belongs to a tilted plane by the angle φ. Source: authors.

3.2. The Projected Solid Angle Principle

The former calculations allow us to find configuration factors that consist of geometric parameters or proportions. Thus, it seems reasonable that the desired values can also be determined through graphic procedures like those employed in geometry. In science, something that may sound reasonable is not always easy to prove but after some time researching we could arrive at the proper demonstrations.

The advantages for architects and researchers are obvious compared with formulas because if during the calculations doubts appear due to the difficulty of the lighting problem, this mathematical model provides fast and easy visualization and it is suitable for BIM protocols.

In order to obtain the flux transfer between a surface and a point, we could simply draw a cone whose vertex is the study-point and its base the surface. The intersection of the said cone with a sphere of unit radius ($r = 1$) is then projected onto the reference plane (horizontal, vertical, etc.). The area inside this projection, divided by the projected area of the whole sphere on the same plane (i.e., π), gives the value of the configuration factors much in the same way as with the analytical methods already described (Figure 9) [30].

To summarize, view factors are dimensionless quantities or ratios that we can expressed as a relation of areas. The first area is a projection and the second is the total surface area expressed in circular terms π.

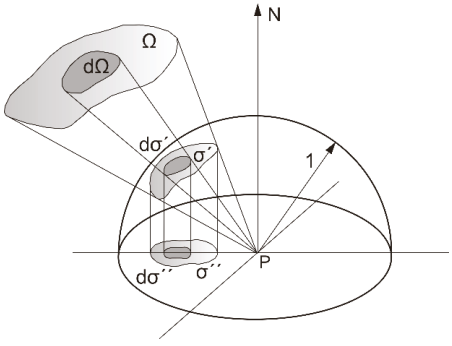

Figure 9. The light-cone in this figure cuts the area σ' from the unit sphere. Orthogonal projection of σ' onto the illuminated or irradiated plane gives the area σ'', this surface divided by $\pi r^2 = \pi$ equates the value of the configuration factor. Source: authors.

The main consequence that we can draw from this fact is that the problem of finding the configuration factor will have a unique solution regardless of its complexity because the area of a projection always produces a definite value.

Moreover, the factors can be understood as projections and thus they possess the additive property, only recently we have defined the scalar product of configuration factors (see above). Addition is useful when dealing with several light sources, if we can add their effects or under special conditions multiply them. The average of this geometric proportion extended over the corresponding surface equates the configuration factor, which in some cases it is non-trivial to find with analytical expressions, due to calculus constraints.

The useful corollary is that we can alternately use graphic or analytical methods. In either way, we assume that we are able to solve one of the fundamental problems in radiative transfer by means of geometric procedures. This signifies that the geometric form is very important in this type of problem and not all building shapes may receive the same performance from a radiation standpoint.

In this regard, the centralized plan of Saint Louis' church contributes to increase the radiative transfers between the interior surfaces. This type of geometry with axial symmetry generates greater configuration factors than a parallelepiped surface. Theretofore, higher daylighting levels are obtained with the same reduced proportion of windows to total surface area.

3.3. Internal Reflections

We have dealt with the question of primary or direct radiative transfer but in order to solve the problem completely, we have to consider secondary energy sources produced by reflections that may hold fair significance in some particular cases such as in this church. In a closed space, the main

components of secondary transfer are those produced by the limiting surfaces that, depending on their properties, re-emit some of the light that reaches them. This phenomenon may be treated with the help of a procedure similar to the so-called "radiosity" (or balancing infinite rebounds) in the technical literature, see below [28,29].

Within the process of analysis of an architectural space, it is important to qualify adequately this component of inter-reflections because direct light may not be satisfactory or even wanted and secondary sources may add the required surplus to compensate for such decrement.

All cultures have been aware of the phenomena of reflection at some point or another in their history and they have furnished the interior renderings of their buildings to produce more brightness and to serve better their spatial purposes and dwelling aims. In that way, their chambers consistently enjoyed the boons of nature.

In the case of Saint Louis, the inner surfaces present a lavish decoration enriched by innumerable artworks, including, gilt pads, mirrors, engravings and frescoes. Beyond the liturgical symbolism of these decorations underlies a univocal aim to enhance illumination of the space. Such "enlightenment" undoubtedly refers to spiritual and territorial domains other than the European. Oriental and American pre-Hispanic cultures accrue in the forge of the transition to a baroque era, as we have shown, a period very much informed by the Jesuits as the present authors have studied in other treatises [31].

Particularly, some of the most significant events of the Jesuit mission in Japan feature in this church. Saint Xavier appears in his arrival to the shores of Kagoshima (Kyushu, Japan) in a niche with numerous mirrors, precious stones and other glistening devices. Moreover, presiding the altarpiece of Saint Stanislaus Kotska in the south wall, there is a representation of the three martyrs of Japan (Pablo Miki, Juan Soan de Goto and Diego Kisai) holding palms and embracing the Cross symbol of their faith and torment (Figure 10). Naturally, news of the great martyrdom of Nagasaki soon diffused in Spain. Most of the missionaries who travelled to the Asia departed from the ports of Seville and the maritime city of Cadiz. A rather curious phenomenon related with the former is that the medallion representing the three martyrs of Japan always remains in backlight.

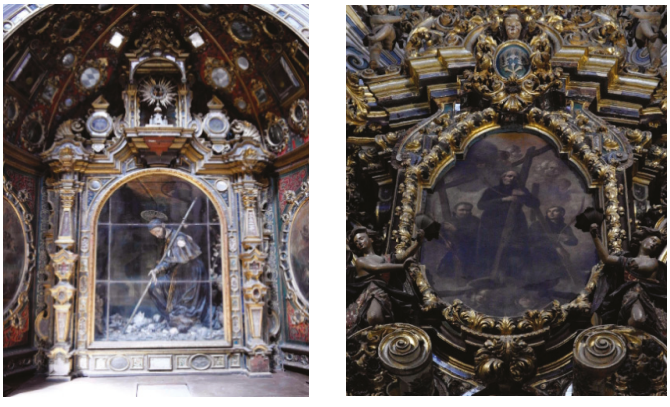

(**a**) (**b**)

Figure 10. Interior of Saint Louis of the Frenchmen: (**a**) niche of St. Xavier; (**b**) representation of the three martyrs of Japan. Source: Almodovar-Melendo.

Returning to technical matters in discussion, we have made a summary of the necessary algebra to treat this complex problem. In the first stage, we have considered the illuminance of each surface as a final average, acquired after a high number of reflections (Figure 11). As we mentioned earlier, this procedure is akin to the procedure of balancing infinite rebounds of radiation in an enclosed volume and is amply used for thermal problems though not so often in lighting, where more detailed distributions of energy may be required.

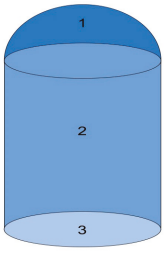

Figure 11. Typical volume of the central space in churches composed of a cylinder and a spherical cap used to find the reflected component in illuminance exchanges. Source: Cabeza-Laïnez.

For a given set of surfaces as defined in the figure above, the involved mathematics summarizes as follows: the total component is made of the direct light plus the reflected light.

$$E_{tot} = E_{dir} + E_{ref}, \tag{8}$$

Thus, if we are able to create two matrices F_d and F_r with the elements described as follows:

$$F_r = \begin{bmatrix} 1 & -F_{12}\rho_2 & -F_{13}\rho_3 \\ -F_{21}\rho_1 & 1 & -F_{23}\rho_3 \\ -F_{31}\rho_1 & -F_{32}\rho_2 & 1 \end{bmatrix}, \tag{9}$$

$$F_r = \begin{bmatrix} F_{11}\rho_1 & F_{12}\rho_2 & F_{13}\rho_3 \\ F_{21}\rho_1 & F_{22}\rho_2 & F_{23}\rho_3 \\ F_{31}\rho_1 & F_{32}\rho_2 & 0 \end{bmatrix}, \tag{10}$$

On the understanding that surface 3 represents the floor plane. F_{ij} are the corresponding configuration factors from surface i to surface j and ρ_i is the coefficient of reflection of surface i.

Then we could easily establish a relationship between reflected and direct illuminance.

$$F_r E_r = F_d E_d, \tag{11}$$

For instance, the first line of the matrix product above gives:

$$E_{r1} - E_{r2}F_{12}F\rho_2 - E_{r3}F_{13}\rho_3 = E_{d1}F_{11}\rho_1 + E_{d2}F_{12}\rho_2 + E_{d3}F_{13}\rho_3, \tag{12}$$

And extracting the reflected component at surface 1, we would obtain,

$$E_{r1} = \rho_1 F_{11} E_{d1} - \rho_2 F_{12}(E_{d2} + E_{r2}) + \rho_3 F_{13}(E_{d3} + E_{r3}), \tag{13}$$

Expressed in worlds the former means that, the light reflected on surface 1 is the total received from surfaces 1, 2 and 3 multiplied by their reflection coefficients and their configuration factors (in the case of 1 being curved we would deal with F_{11}, an auto-factor). As we have seen that total light is the sum of direct and reflected light or once again,

$$F^{-1}{}_r F_r E_r = F^{-1}{}_r F_d F_d, \text{ , } \tag{14}$$

$$E_r = F_{rd} E_d; \; where \; F_{rd} = F^{-1}{}_r F_d, \tag{15}$$

In this situation, the resultant component of illuminance is a sum of a direct component and a reflected one. That is, the amount of light, which a particular surface receives from the primary source and a second component consisting of the reflections, received from all the other surfaces in unison. In this way, the problem is solved from a mathematical point of view.

Thus, if we know the direct illuminance for each surface we are able to predict all possible reflections and add them to the first one.

The reflective coefficients are often difficult to find in ancient veneers. In some cases, we had to determine them at our laboratory by constructing several replicas of the wall materials and measuring it by means of spectroscopic procedures.

Such coefficients were checked in situ whenever possible by direct monitoring (bearing in mind that the church has been closed and restored for ten years). The richer decorations correspond with the lower part of the church and do not add much quantitatively to the illumination of the space, their effect is mainly qualitative and so to say subjective.

In addition, it is interesting to notice that, the former expressions discussed, give the average value of illuminance for the whole surface (the entire drum of the church for instance), thus minimizing errors.

In the unlikely event that we would need to know a point-by-point field distribution, minor adjustments would be required for each case or usually we could divide the problem into an adequate number of sub-surfaces.

3.4. Sky Model

We should employ direct measurements if available from the meteorological institute, which we have proved fare well with the algorithm proposed by Pierpoint et al. [32] to obtain daylighting intensities for vertical and horizontal surfaces depending on the latitude of the place. Such clear sky-model regulates the vertical component of illuminance (in lux) as a function of the solar altitude (α) and the azimuth (β), by virtue of the equation below.

$$E_v = 4000\alpha^{1.3} + 12,000 \sin^{0.3}\alpha \cos^{1.3}\alpha \left[\frac{2+\cos\beta}{3-\cos\beta}\right], \tag{16}$$

If we have to deal with the CIE standard overcast sky, the former equation simplifies to:

$$E_v = 8500 \sin\alpha, \tag{17}$$

4. Monitoring

In parallel, the authors have conducted a thorough monitoring campaign to modulate the range of the simulations and at the same time to check the usefulness of their outputs. We have to outline that the objective validation of our simulation program has taken place beforehand in other controlled experiments and test chambers [12–23].

To perform the evaluation, we installed data loggers in Saint Louis to monitor the dry bulb temperature, mean radiant temperature and relative humidity. The sensors were Onset models U12-012, UX 120-006 M and TMC6-HD, with data recorded every ten minutes. Temperature sensors had a measuring range from 0 to +100 °C and an accuracy of ±0.5 °C. The calibration before taking the measurements guaranteed the proper functionality of the setup.

Accumulative measures of light are not helpful from a spatial point of view, one-time measurements conducted simultaneously at a ground-floor grid work usually better. To that end, we have used a lux-meter PCE-170A with ISO calibration, a measuring range from 0 to 40,000 lux and an accuracy of ±0.3%. Of those, we present a comparison with simulated values for partly cloudy sky, which correspond well by not showing relevant discrepancies (Figures 12 and 13). The correlation coefficient of east-west and north-south main axis are 0.93 and 0.92, respectively.

The slight differences registered between simulated and measured data are presumably due to the event that on the days of performance of the experiments, as the sky was partly cloudy, some sunlight filtered from the southern fenestration increasing the levels on the north niche (bottom side in the graph). Besides, the main façade of the church faces east and through the upper choir perceptible intensities appear around midday but these were deliberately taken out of the simulation. The latter would explain minor augments of level near the entrance area to the east (left side of the figure).

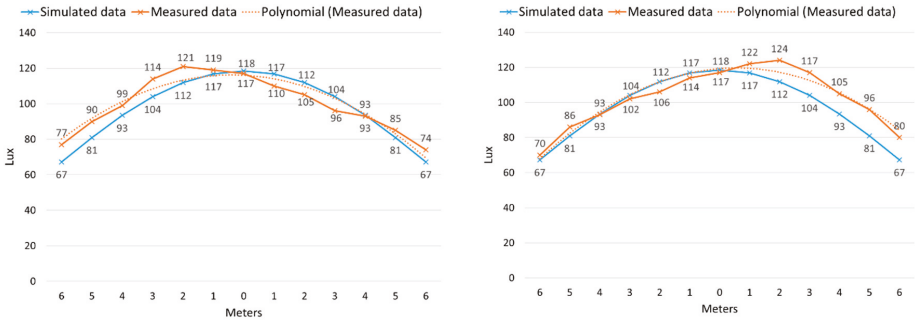

Figure 12. Comparison of measured and simulated data for partly cloudy sky at midday on 21 December. 0 m corresponds to the central point of the church: (**a**) east-west axis, from entrance (left) to the altar (right). (**b**) south-north axis, from right to left respectively. Source: Almodovar-Melendo.

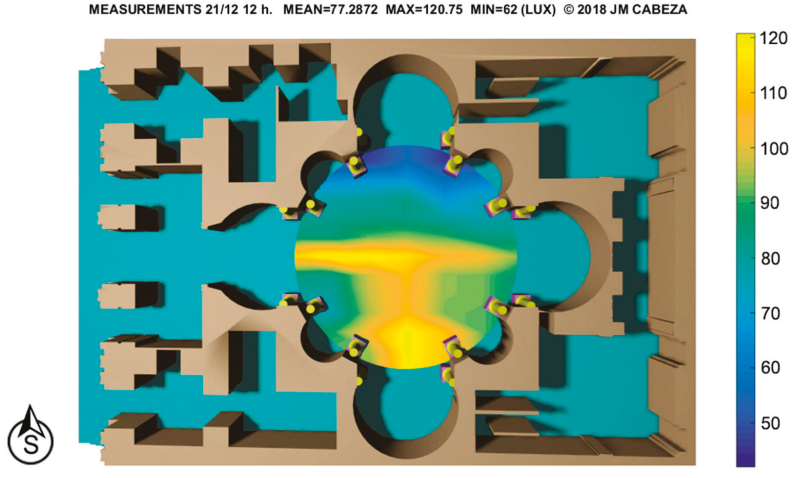

Figure 13. Extension of Figure 12, measurements effected at the ground floor in winter solstice at 12 h. Source: Cabeza-Laïnez.

We investigated other sky plus sun conditions with occasional registers, these showing the reliability of the simulations. As stated above, the model has been validated in previous campaigns of projects with straight parallelepiped shapes in laboratory-like conditions and for that reasons we are not in the position here to offer a full-range validation for such unusual architecture, as is this church.

In order to discuss the environmental performance of the building, measured daylighting values have been correlated to other environmental parameters such as temperature and relative humidity, relevant for the IEQ of the building [33,34]. Measurement data registered during the summer show that the lighting values are in a range of 200 to 400 lux, by all standards a steady level of lighting apt for the majority of visual tasks. On the other hand, we identified consistent temperatures nearing 25 °C in the floor level of the nave, at a time in which external shade temperature can reach 45 °C or even more on the north face of the cylindrical drum (Figure 14). This means that such adequate illumination is not attained by means of discomfort or excessive overheating, as is the case of so many contemporary buildings, fully glazed. Shading devices are generally not required in this kind of structure. However, we found photographs of late 1920s in which the tall windows were shaded from the inside with

fabrics, a curiosity which may attest to the significant amount of light that impinges on the lower levels of the compound.

Theretofore, the property of the capacitive mass of this masonry and tile (ceramics) building is noticeable. Moreover, the low ratio of window to total surface area (under 10% as previously mentioned) averts excessive solar gains and contributes to obtain an optimal thermal performance. In this regard, we have to remind that daylight is the lighting source with the best light to heat ratio (up to 160 lumen/W).

The indoor relative humidity remained around 50% during the daily cycle though it could increase slightly at night.

Similar monitoring results were obtained by the authors at another baroque paradigm, the church of San Lorenzo in Turin (Italy) by Guarino Guarini (Figure 15). However, this temple is located almost 10 degrees more to the north than Saint Louis and markedly receives less solar radiation.

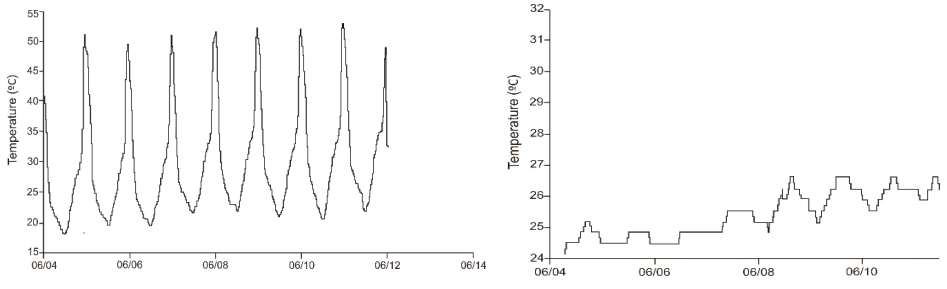

(**a**) (**b**)

Figure 14. Temperature measured at the Church in summer to check overheating effects: (**a**) external temperature at the dome, (**b**) internal temperature at floor level near the altar. Notice that when external temperature in the north face of the drum reaches a scorching 50 °C, at the altar zone we measured a much cooler maximum of 26 °C. Source: authors.

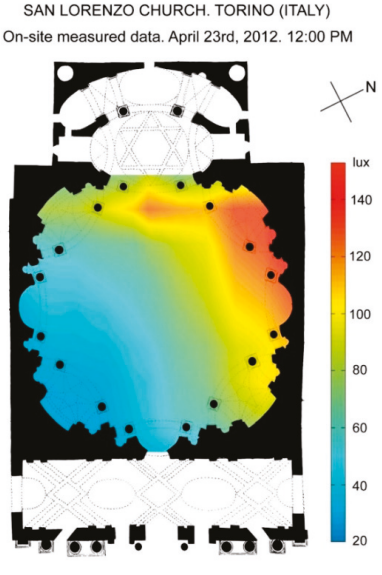

Figure 15. Clear Sky monitoring in April at the famous church by C. G. Guarini. Turin. Lat. 45°6′ N. Source: Cabeza-Laïnez.

5. Discussion of the Results

Due to the particular orientation of the church that defies the postulate of the longitudinal West-East axis from entrance to altar, which presided over European architecture until late Renaissance; the solar events like solstices and equinoxes are critical to define the performance of the central space under consideration. In fact, the fenestrated cylindrical drum allows the capture of solar radiation impinging from every solar position and suppresses the absolute necessity of offering a southern façade to achieve solar gains for natural heating and lighting, especially in winter, as was the case of Gothic architecture in England, France and Germany. The inner cylinder so to speak funnels direct solar radiation and due to its considerable height, it seldom permits the sunrays from reaching the floor level avoiding visual discomfort to the visitors.

In each case, we have investigated two situations: overcast conditions (isotropic but with hourly and monthly variation (Figure 16) and clear sky with sun (where orientation and hourly/monthly variations are mandatory). The first condition refers to conventional models for cold climates while the second condition is more innovative and typical of warmer regions but many simulation programs are unable to deal with it not to mention with the occurrence of curved surfaces (Figures 17–19). The daylighting levels have been calculated in a plane located 1 m above the floor, a position deemed for a sitting person.

Spectroscopy analyses were necessary to evaluate the reflective coefficients for this simulation. To this aim the authors conducted several on site tests. Such values tend to differ from those suggested by conventional colour charts, because ageing, candle fumes or inadequate refurbishments may have altered the original condition of the veneers.

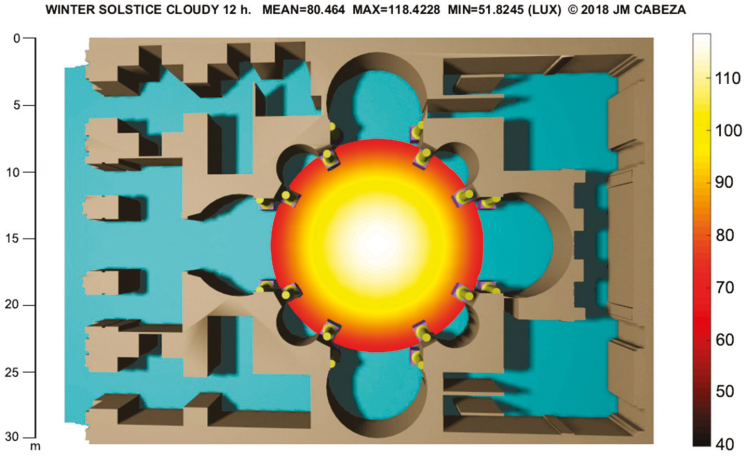

Figure 16. Cloudy Sky at midday in winter. Source: Almodovar-Melendo and Cabeza-Laïnez.

One of the most unfavourable cases occurs in winter under cloudy sky condition. Even so, the average value is more than 80 lux (Figure 16) which is considered sufficient to perform basic tasks even with modern standards. The light field is rather homogeneous (from 120 to 80 lux) in the central nave and presents a marked axial symmetry appropriate for the liturgy and reinforcement of the design intentions. The minimum levels remain well over 50 lux.

In spring, the situation is much enhanced, as even in the mornings or afternoons the mean illuminance is about 150 lux and values lying in the range from 200 to 300 lux are easily reached (Figure 17). At noon (Figure 18) the average level is over 200 lux and a maximum of circa 1000 lux can be found in several points, the light is more varied but without abrupt contrasts in a soft progression from 200 to 500 lux towards the north niche where the sun impinges during the equinox.

The cloudy sky condition is slightly lower in its intensities but we have not presented that here since it is untypical of Seville in spring and autumn, its probability of occurrence is of 18% according to meteorological data; even so minimum values remain over 50 lux.

In summer, the mean illuminance lies in the range of 150 lux in early morning and late afternoon (Figure 19) and reaches 250 lux at noon.

If, following with the discussion on the simulations, we refer below to the vertical component of the radiation vector; the simulations show an interesting performance of light in the more likely event in Seville of enjoying a clear sky with direct sun (Figure 20). According to a TMY (typical meteorological year) of Seville provided in the software Energy Plus and derived from the Spanish Weather for Energy Calculations (SWEC), the probability of occurrence of non-clear skies in spring, autumn and summer combined is of 11%.

The illumination sectional vector keeps at an angle of around 45 degrees (which means it is not too steep), this clearly allows for distinct perception of artworks and wall decorations unlike Roman pantheon and derived churches like San Bernardo alle Terme (built under the dome of an ancient thermal bath).

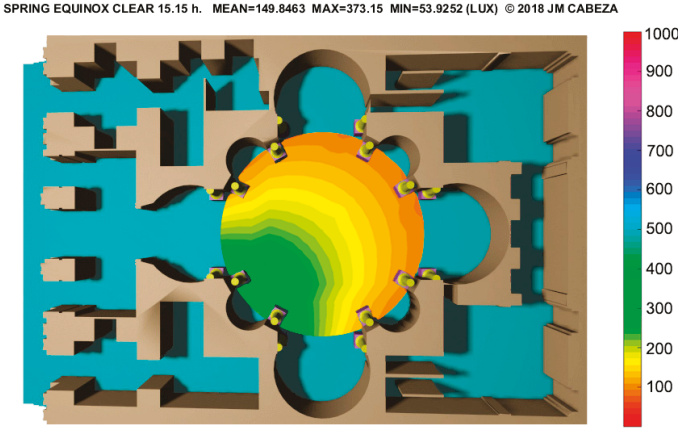

Figure 17. Spring clear sky with sun. Probability of 74% (76% in autumn). The graph is symmetric at 15.15 h. Source: Almodovar-Melendo and Cabeza-Laïnez.

Figure 18. Spring clear sky with sun at midday, at some spots values of 1000 lux are registered. Source: Almodovar-Melendo and Cabeza-Laïnez.

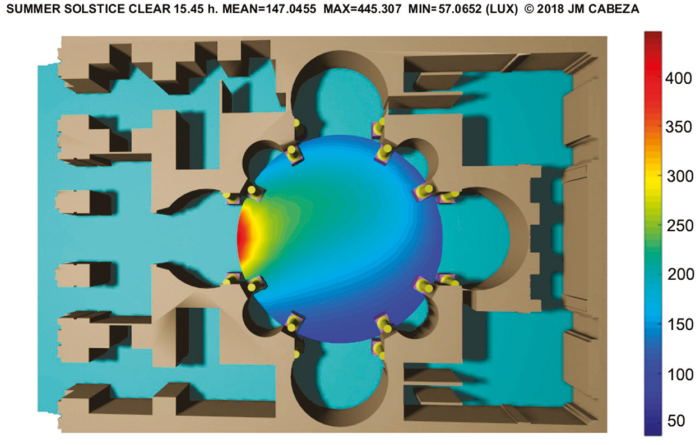

Figure 19. Summer Clear Sky with sun. Symmetric with 8.45 h. Source: Almodovar-Melendo and Cabeza-Laïnez.

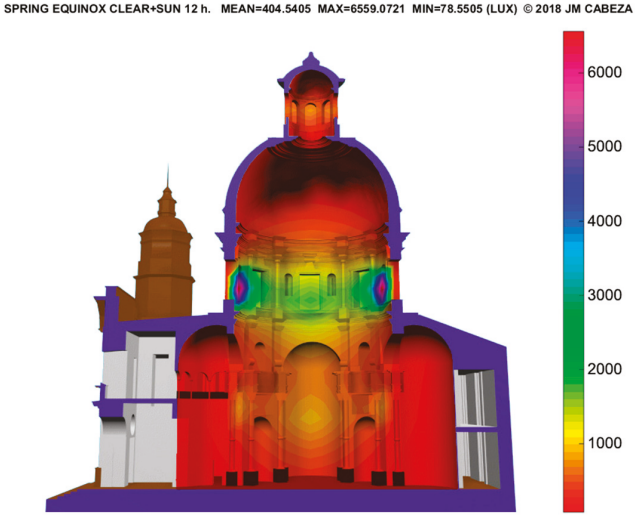

Figure 20. Daylight Section at the spring equinox with sun, midday. Values reach 300 lux at floor level. Source: Cabeza-Laïnez and Almodovar-Melendo.

Such character is less pronounced for the infrequent case of cloudy skies but can still be perceived and it has been checked against monitoring (Figure 21).

To sum up, the results examined from Figures 16–21 show that the daylighting field is balanced; with a range of around 100 lux in plan for cloudy sky in winter. In other sky conditions, values exceeding 300 lux can be amply found and over 200 lux are guaranteed in the central circle of the nave for a 56% of the total daytime. To clarify the results, we have compared in Figure 22 simulated data in Summer, Spring and Winter for clear sky with sun.

The vertical situation of lighting also facilitates orientation and perception of the space and adds variety or spark in the disposition of liturgical spaces for Southern Spain. In a famous poem (by Angel Camacho), dating from 1733 the church of Saint Louis was compared, precisely for its lighting features, to the temples of Jerusalem and Zorobadel in ancient Babylon.

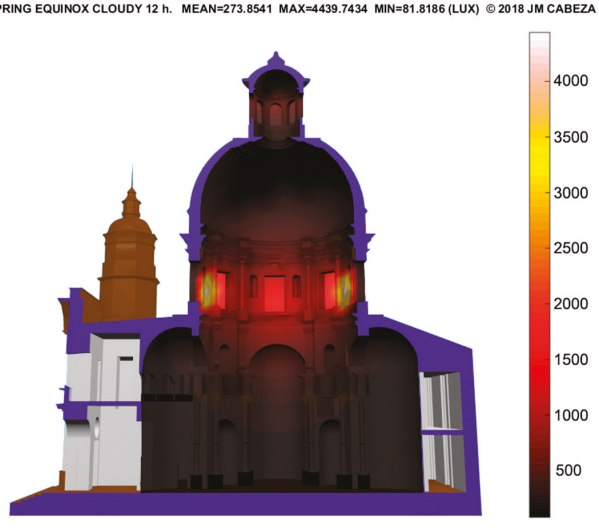

Figure 21. Daylight Section at the spring equinox in a cloudy situation. Maximum values of 200 lux on the ground. Source: Cabeza-Laïnez and Almodovar-Melendo.

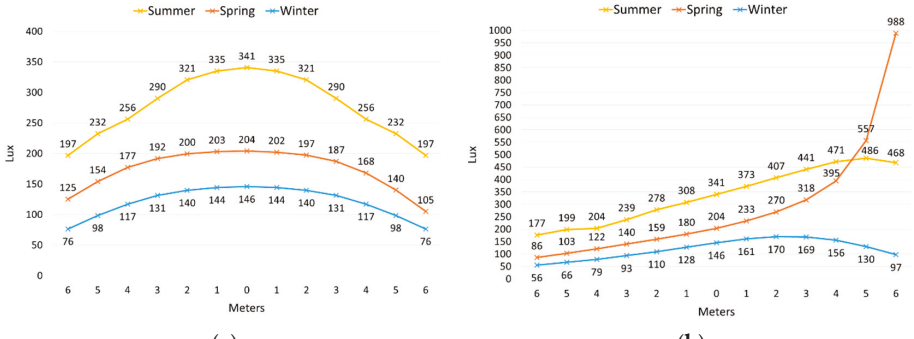

Figure 22. Comparison of simulated data for a clear sky with sun at midday: (**a**) east-west axis, from entrance (left) to the altar (right). (**b**) south-north axis, from right to left respectively. Source: Almodovar-Melendo.

Coming back on the figures to describe this considerable success of religious architecture, the small proportion of window to total surface area (less than 10%) alongside with the low latitude of Seville (37°22′ N) may lead to such admirable results. We should notice that the values in this church are comparatively less than at its earlier baroque counterparts, which were mostly built in temperate north-central Italy and thus using wider fenestration in disregard of the heat.

Such could be the upfront explanation for the subdued illuminance levels attained on the inside of the Saint Louis temple. Especially if we compare them with some jewels of Roman Baroque (Figure 23), like Sant'Ivo by Borromini, the church at the site of ancient University of Rome and mainly Sant'Andrea by Bernini (Figure 24), an oval shaped masterpiece and not casually commissioned by the Jesuits as well.

So far, the analysis performed by the authors permit to trace a sure-handed line in the evolution of centralized temples pertaining to the baroque era. Such line is deeply chiselled in what we may call a proto-scientific artisanship of light within space.

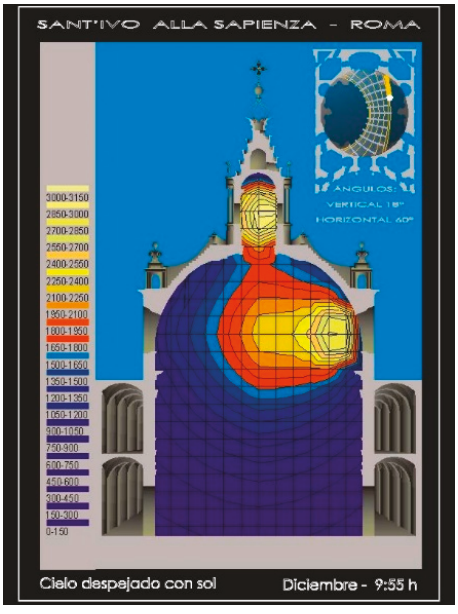

Figure 23. Simulations at Sant'Ivo by Borromini in Rome. December at 9:55 am. Clear sky plus sun. Source: Almodovar-Melendo.

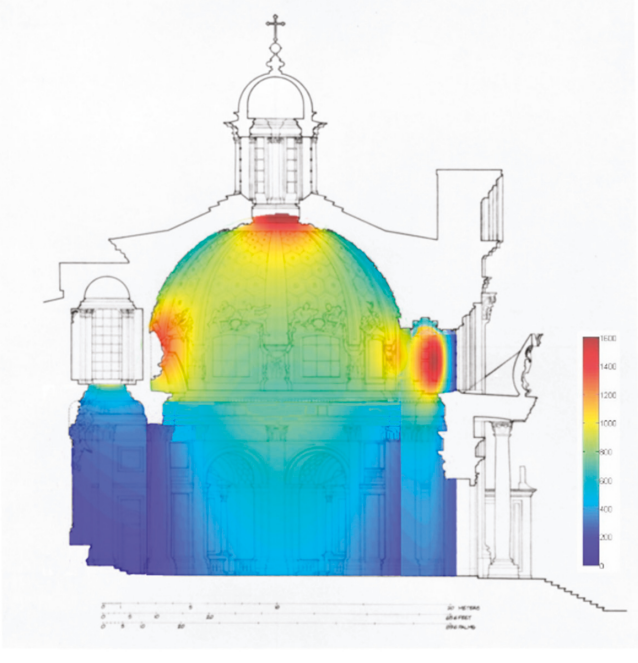

Figure 24. Simulations at Sant'Andrea by Bernini in Rome. Summer solstice. Source: Cabeza-Laïnez.

As we have clearly seen, sundry environmental and historical design strategies such as lighting, thermal comfort, et cetera, do intertwine in this analysis whilst at the same time they recall human

and cultural nuances of architecture. For instance, the introduction of gilding and reflective specular veneers is critical in maintaining an acceptable visual perception with a restrained glazed surface. Such design features contribute to overcoming a situation perhaps created by an excessive seclusion from external climatic conditions.

Moreover, we confirm that the hypothesis by which the galleries of the nave were used as a place of study for the novices is plausible given the bright atmosphere that is achieved at the upper levels and the accuracy in which the educational and liturgical details of the interior of the dome cum drum are perceived from above.

6. Conclusions

In correspondence with all the former, the conservative distribution of light in the church in winter under cloudy sky starts at a dim range (around 80–100 lux) but it suffices to perform basic tasks due to its homogeneity and character as shown in the simulations and surveys. For the most part of the year, with sunny conditions, illumination is adequate though not excessive (200–400 lux) thereby avoiding overheating or solar discomfort. Thus, it leads to acceptable thermal conditions, as demonstrated by the data recorded and presented in Figures 11–14 and elsewhere. Therefore, we are reinforced in the belief that the project of this church was designed outside Spain by Father Angelo Italia, after his own experiences in a harsh warm climate in Sicily, 1699 (Figure 25).

The diverse strategies for sustainability be it thermal, luminous, acoustic and so forth, do accumulate in search of an architectural opportunity, encompassing a wealth of cultural nuances. Now and then, sustainable architecture demands an inclusive methodology to provide for the physical and aesthetic improvement of intercultural societies [35].

For instance, the whole previous analysis together with other considerations developed in the references, lead us to conclude that the Jesuit builders had been carefully summoning an ecumenical model of church. A model that could be exported outside Italy and precisely because of its environmental character, it was somewhat more encompassing for the believers of diverse cultures, be it American, Asian or African (Figure 26). Nevertheless, ignorant of the climate variations to be faced, they were unsure of the real effects of their works and consequently their success was limited outside Europe arguably for want of sustainable strategies and techniques.

Figure 25. Summer Solstice. Interior of the Jesuit Church of San Francesco Saverio (St. Francis Xavier) in Palermo, Sicily (Italy). Source: Cabeza-Laïnez.

In this article, we continue in proving that simulation is a feasible tool for enhancing our knowledge of human architectural heritage [36], as well as in the matters of understanding the

production and restoration of space, modulation of energy and eventually needs for supplementary artificial means (Figure 27).

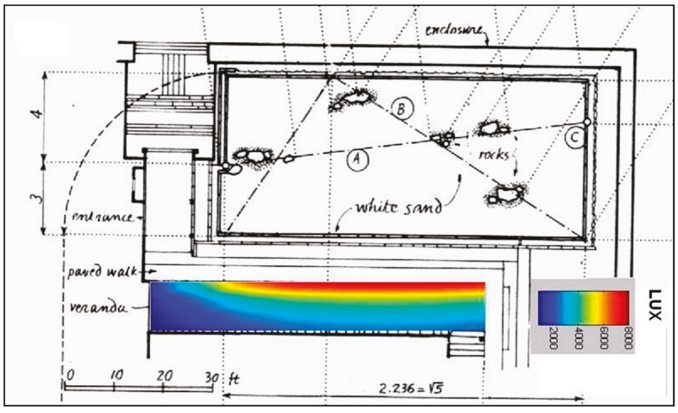

Figure 26. Summer Solstice. Simulation of reflected radiation by white sands, under the eaves of the Buddhist temple of Ryoanji in Kyoto (Japan). Values reach 10,000 lux as monitored by Joseph Cabeza-Laïnez.

Through geometrical parameters within which the subtle mathematics of configuration factors resides, we are finally able to recognize the importance of geometry related to lighting [37] and by extension to sustainability matters.

Not in vain, one of the architects hereby analysed—the sublime priest Camillo Guarino Guarini—wrote in his treatise "Euclides Adauctus et Methodicus":

> "Since the magic of insuperable wondrous mathematics shines brightly on marvellous and truly regal Architecture"
>
> (*Sed insuper Thaumaturga Mathematicorum miraculorum insigne vereque Regali Architectura coruscat*)

The famed quote praised the Savoyard King for his architectural wisdom but the author of the immortal Chapel of the Holy Shroud in Turin, inexplicably ruined by arson in 1998, dawned the Era of Baroque Reason.

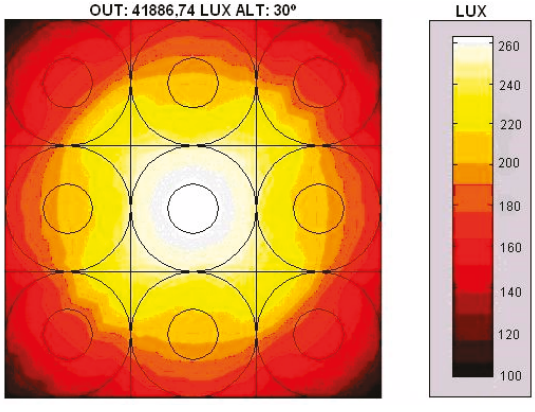

Figure 27. Simulation of an array of nine circular skylights in the Paris National Library. Clear sky with sun. Architect Henri Labrouste. Source: Cabeza-Laïnez.

Author Contributions: Each author contributed equally to the article.

Acknowledgments: Joseph Cabeza-Laïnez and Jose M. Almodovar-Melendo are grateful for the consistent help of the following young researchers: Lorenzo Muro Álvarez, Miguel Gutiérrez Villarrubia, César Puchol Barcina, Juan Martínez Bonilla and Gonzalo Pulido López. Inmaculada Rodriguez-Cunill would like to thank the artist and conserver Eva Guil Walls as well as professor and lighting artist Begoña Gutiérrez San Miguel. The assistance of professor and art historian Paula Revenga Dominguez is deeply recognised.

Conflicts of Interest: The authors declare no conflict of interest.

References

1. Ne'eman, E. Visual Aspects of Sunlight in Buildings. *Light. Res. Technol.* **1974**, *6*, 159–164. [CrossRef]
2. Giedion, S. *The Eternal Present. The Beginning of Architecture*; Oxford University Press: Oxford, UK, 1964.
3. Cabeza, J.M.; Takahito, S.; Almodovar, J.M.; Jiménez, J.R. Lighting Features in Japanese Traditional Architecture. In Proceedings of the 23rd International Conference on Passive and Low Energy Architecture, Geneva, Switzerland, 6–8 September 2006; pp. 192–198.
4. Cabeza, J.M. *Fundamentals of Luminous Radiative Transfer*; Netbiblo: Seville, Spain, 2010. (In Spanish)
5. Almodovar, J.M.; La Roche, P. Effects of window size in daylighting and energy performance in buildings. In Proceedings of the American Solar Energy Society Annual Conference, San Diego, CA, USA, 3–8 May 2008; pp. 4345–4351.
6. Cabeza, J.M. Solar radiation in buildings, simulation and transfer procedures. In *Solar Radiation*; InTech: Shanghai, China, 2012; pp. 291–314.
7. Baker, N.V.; Fanchiotti, A.; Steemers, K.N. *Daylighting in Architecture. A European Reference Book*; Commission of the European Communities; Directorate General XII; Routledge: London, UK, 1993.
8. Yamauchi, J. *Theory of Field of Illumination*; No. 339; Researches of the Electro-Technical Laboratory: Tokyo, Japan, 1932.
9. Moon, P.H. *The Scientific Basis of Illuminating Engineering*; Dover Publications: New York, NY, USA, 1962.
10. Moon, P.H.; Spencer, D.E. *The Photic Field*; The MIT Press: Cambridge, MA, USA, 1981.
11. Jammer, M. *Concepts of Space: The History of Theories of Space in Physics*; Dover Publications: New York, NY, USA, 1993.
12. Cabeza-Lainez, J.M. The Quest for Light in Indian architectural heritage. *J. Asian Archit. Build. Eng.* **2008**, *7*, 39–46. [CrossRef]
13. Almodóvar-Melendo, J.M.; Cabeza-Lainez, J.M. Nineteen thirties architecture for tropical countries: Le Corbusier's brise-soleil at the Ministry of Education in Rio de Janeiro. *J. Asian Archit. Build. Eng.* **2008**, *7*, 9–14.
14. Almodovar, J.M.; La Roche, P.; Jimenez, J.R.; Dominguez, I. Scientific design of skylights: the case of an office building in Gelves, Seville. In Proceedings of the 28th World Conference on Passive and Low Energy in Architecture, Lima, Peru, 7–9 November 2012.
15. Cabeza-Lainez, J.M.; Almodóvar-Melendo, J.M. The Japanese Experience of Environmental Architecture through the Works of Bruno Taut and Antonin Raymond. *J. Asian Archit. Build. Eng.* **2007**, *6*, 33–40. [CrossRef]
16. Cabeza-Lainez, J.M.; Almodóvar-Melendo, J.M. Architectural Simulation for Sustainability. In Proceedings of the World Sustainable Building Conference, Tokyo, Japan, 27–28 September 2005; pp. 1023–1031.
17. Cabeza-Lainez, J.M. Lighting Features in Indian-Style Traditional Architecture. In *Sun Wind and Architecture, Proceedings of the 24th International Conference on Passive and Low Energy Architecture, Singapore, 22–24 November 2007*; National University of Singapore: Singapore; pp. 446–4550.
18. Cabeza-Lainez, J.M. Radiative Performance of Louvres, Simulation and Examples in Asian Architecture. In Proceedings of the 6th International Conference on Indoor Air Quality, Ventilation and Energy Conservation in Buildings (IAQVEC), Sendai, Japan, 28–31 October 2007; pp. 445–452.
19. Cabeza-Lainez, J.M. Some Considerations on the Environmental Properties of Domes. In *Architecture and Urban Space, Proceedings of the 6th International Conference on Passive and Low Energy Architecture, Sevilla, Spain, 24–27 September 1991*; Springer: Heidelberg, Germany; pp. 541–547.

20. Cabeza-Lainez, J.M. The Library in the Faculty of Engineering a case of Holistic Simulation. In *Sustainable Communities and Architecture, Proceedings of the International Conference on Passive and Low Energy Architecture, Kushiro, Japan, 8–10 January 1997*; PLEA 1997 Japan Committee: Kushiro, Japan; pp. 75–80.
21. Cabeza-Lainez, J.M.; Almodovar-Melendo, J.M. Simulation of Baroque religious Buildings. In *Environmentally Friendly Cities, Proceedings of the International Conference on Passive and Low Energy Architecture, Lisboa, Portugal, 1–5 June 1998*; James & James Science Publishers Ltd.: London, UK; pp. 421–424.
22. Cabeza-Lainez, J.M. Scientific Design of Skylights. In *Sustaining the Future, Energy-Ecology-Architecture, Proceedings of PLEA International Conference, Brisbane, Australia, 22–24 September 1999*; PLEA International: Brisbane, Australia; pp. 541–546.
23. Cabeza-Lainez, J.M.; Almodovar-Melendo, J.M. The Quest for Daylight: Evolution of Domes in South American Baroque. In *Renewable Energy for a Sustainable Development, Proceedings of the Plea 18th Conference, Florianopolis, Brazil, 7–9 November 2001*; Universidade Federal de Santa Catarina: Florianópolis, Brazil; pp. 161–168.
24. Banda y Vargas, A. *La Iglesia Sevillana de San Luis de los Franceses*; Diputación Provincial de Sevilla: Sevilla, Spain, 1977. (In Spanish)
25. Rodriguez-Cunill, I. Painting through the eye of a camera. *Comunicación Revista Internacional de Comunicación Audiovisual, Publicidad y Estudios Culturales* **2003**, *4*, 51–65. (In Spanish)
26. Higbie, H. *Lighting Calculations*; John Wiley & Sons: New York, NY, USA, 1934.
27. Lambert, J.H. *Photometry, or, on the Measure and Gradations of Light, Colors and Shade*; DiLaura, D.L., Translator; Illuminating Engineering Society of North America: New York, NY, USA, 2001.
28. Kittler, R.; Kocifaj, M.; Stanislav, D. *Daylighting Science and Daylighting Technology*; Springer: Heidelberg, Germany, 2012.
29. Ashdown, I. *Radiosity: A Programmer's Perspective*; John Wiley & Sons: New York, NY, USA, 2004.
30. Fok, V.A. *Zur Berechnung von Beleuchtungsstärke (On the calculations of Lighting Power)*; Institute of Optics, St. Petersburg University: Saint Petersburg, Russia, 1924. (In German)
31. Bailey, G.A. *Art of the Jesuit Missions in Asia and Latin America, 1542–1773*; University of Toronto Press: Toronto, ON, Canada, 2001.
32. Pierpoint, W. A Simple Sky Model for Daylighting Calculations. In Proceedings of the International Daylighting Conference, Phoenix, AZ, USA, 16–18 February 1983.
33. Katunský, D.; Dolníková, E.; Doroudiani, S. Integrated Lighting Efficiency Analysis in Large Industrial Buildings to Enhance Indoor Environmental Quality. *Buildings* **2017**, *7*, 47. [CrossRef]
34. Molina, F.Q.; Yaguana, D.B. Indoor Environmental Quality of Urban Residential Buildings in Cuenca—Ecuador: Comfort Standard. *Buildings* **2018**, *8*, 90. [CrossRef]
35. Almodovar-Melendo, J.M.; Cabeza-Lainez, J.M. Environmental Features of Chinese Architectural Heritage: The Standardization of Form in the Pursuit of Equilibrium with Nature. *Sustainability* **2018**, *10*, 2443. [CrossRef]
36. Mohelníková, J.; Míček, D.; Floreková, S.; Selucká, A.; Dvořák, M. Analysis of Daylight Control in a Chateau Interior. *Buildings* **2018**, *8*, 68. [CrossRef]
37. Katunský, D.; Dolníková, E.; Dolník, B. Daytime Lighting Assessment in Textile Factories Using Connected Windows in Slovakia: A Case Study. *Sustainability* **2018**, *10*, 655. [CrossRef]

sustainability

MDPI

Article

The Problem of Lighting in Underground Domes, Vaults, and Tunnel-Like Structures of Antiquity; An Application to the Sustainability of Prominent Asian Heritage (India, Korea, China)

Francisco Salguero Andujar [1], Inmaculada Rodriguez-Cunill [2] and Jose M. Cabeza-Lainez [2,*]

[1] School of Engineering, University of Huelva, Ctra, Huelva-Palos, 21071 Palos, Spain; salguero@didp.uhu.es
[2] School of Architecture, Architecture, University of Sevilla, 41012 Sevilla, Spain; cunill@us.es
* Correspondence: crowley@us.es; Tel.: +34-95-490-6793

Received: 30 September 2019; Accepted: 20 October 2019; Published: 22 October 2019

Abstract: Lighting in heritage is complex because of the forms intervening in it. The historical evolution of cultures has not been analytical and therefore, the shapes involved differ greatly from the cuboids typically found in 21st century architecture. As a vector, light inevitably attaches to surface sources. In this research, we focused on 3D curved geometries. Following a different trail to radiative transfer by virtue of detailed knowledge of the spatiality of volumes, we present new expressions, previously undefined in the literature, that are derived from a combination of surfaces that we have found in many archaeological sites around Asia. In the discussion, we start from the particularities of spherical surfaces where a normal vector has to pass through the center. By means of easy calculations, we deducted innovative laws. These in turn, allowed us to formulate several new expressions for configuration factors based on the adroit use of spherical fragments. The method easily extends to organic shapes that are often contained in the sustainable architecture of the past. The method finishes with suitable algorithms to assess the reflections in such curved forms. Finally, we implemented the results in our creative software. In this way, we enhanced the sustainable paradigms for heritage structures in Asia that we present as a conclusion of the article.

Keywords: lighting of tunnels and domes; Asian architecture; lighting of heritage; curvilinear radiative transfer; new solutions for equations of geometric optics

1. Introduction

The fundamental question of light in heritage architecture remains unsettled due to a lack of scientific advances in the field. The main objective of our research in this article was to implement the adroit correlations and expressions that we found, in order to deal with the variegated phenomena of light as it distributes over complex architectural surfaces from the past. It is known that daylight stems from surface sources. However, many designers do not properly understand the radiative performance of such surfaces, especially when typical cuboid shapes are absent, which is the main reason behind our efforts.

Disregard of surface sources of a three-dimensional shape in radiative transfer analysis is altogether usual. This can be explained by the complexities of the integral equations involved and is partly due to the want of a sufficiently geometric approach to the problem, if scholars come from fields of expertise outside design or architecture. When dealing with complex radiant surfaces, assimilation to a cluster of point sources is the base for the application of the iterative method common to finite element approaches in software, and sometimes direct integration is unable to yield adequate expressions, so only insufficient results exist for fewer basic forms [1,2]. By virtue of this, an ample list of meaningful

geometries that are often present in heritage architecture has remained neglected and energy waste or inaccuracies are evident. In order to increase the sustainability of the whole process from the restoration of ancient vestiges to public exhibition, we considered it necessary to start from a different approach.

In the ensuing research, we begin by focusing on the curved surfaces and derived shapes. Following a similar approach to radiation exchanges through detailed reflection on the particular details of different volumes, we hereby offer innovative and simpler expressions obtained from geometric adjustments that we have found in many sites around Asia.

As an initial discussion, we depart from the well-known spherical trigonometry. By means of basic calculation, we devised a new set of promising laws. These, in turn, result in previously unknown configuration factors for several fragments that involve the sphere. Afterward, the method can be extended to other organic shapes often contained in the architecture of the past.

In the second part, we accomplish the research by adding the equations concerned with finding inter-reflections in the said curved elements.

At all times, we conveyed the findings to an innovative software that enhances luminous radiative transfer simulation for a significant quantity of products and designs, especially of the paradigmatic cases that we give in our conclusions.

2. Physical Outline of the Problem

The reciprocity principle appears in Lambert's treatise *Photometria* [3], written in Latin in 1761 and is explicit in Equation (1). It produces the ensuing differential Equation (2), which still constitutes the scientific fundament of form factor exchanges for all kind of surfaces.

$$d\varnothing_{1-2} = (E_{b1} - E_{b2})cos\theta_1 \times cos\theta_2 x \frac{dA_1 x dA_2}{\pi x r^2} \quad (1)$$

$$\varnothing_{1-2} = (E_{b1} - E_{b2}) \int_{A_1} \int_{A_2} cos\theta_1 \times cos\theta_2 \times \frac{dA_1 x dA_2}{\pi x r^2} \quad (2)$$

where E_{bi} is the radiative power exiting from surface 1 or 2; A_i is the extension of each surface; dA_i is the elementary area; r is the vector that measures distance; and θ_i is the angle between distance vector and the normal to the surface for each elementary area considered (Figure 1).

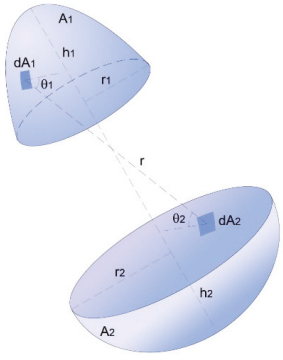

Figure 1. The reciprocity principle and equation for arbitrary surfaces A_1 and A_2.

The above equation indicates that radiative exchanges in any shape depend partly on the size, but also on its relative situation within the space under consideration (Figure 1). From the influential book of Lambert to the 21st century, engineers and scholars of either optics or radiation heat transfer have tried hard to find ways of solving the canonical Equation (2) for sundry elements [4]. This implies a

considerable effort as the said equation takes us on many occasion to a four-fold integration and the doubled primitive of simple functions implies many complex operations.

The variable, or internal part of the integral, is a dimensionless ratio called the form factor [1]. From the quantum electrodynamic point of view, the form factor represents the probability that the photons uniformly emitted from a certain surface can hit another to which it exposes in some manner [5]. Curvilinear forms may acquire distinct features that make a new system of calculation based on stable diffuse radiation, but without treating the integral directly, feasible [6].

3. Derivations from Spherical Caps

Beginning with elementary forms, it is possible to obtain a number of useful factors with perfect ease. It is only necessary to know the geometric properties of the intervening shapes. In a volume encircled by one surface, the sphere, let us consider diffuse irradiation to the inside of the form; in this case, the energy going to the interior of the volume has no way out and must be received on the same surface; if we call the spherical surface 1, the configuration factor to be found must be:

$$F_{11} = 1 \tag{3}$$

Considering the former for one-half of the sphere, the form factor could give $F_{11} = \frac{1}{2}$. In concordance with this familiar result, we decided to delve into the analysis of basic volumes composed of a limited number of surfaces. If we have two elements and one is flat (the base) and the other covers such a base in a sphere-like fashion, we would have a spherical cap.

Employing the previous finding to a spherical cap (called element 1), and the said disk of radius a (element 2); the radiative transfers in Figure 2 are deducted from the algebraic properties:

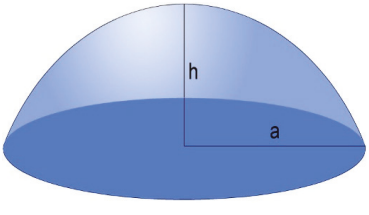

Figure 2. A spherical segment of uniform brightness featuring *h* as the height and radius *a*.

$A_1 x F_{12} = A_2 x F_{21}$. As $F_{21} = 1$, the expression produces $F_{12} = \frac{A_2}{A_1}$, and in this particular case:

$$F_{12} = \frac{a^2}{a^2 + h^2} \tag{4}$$

$$F_{11} = \frac{h^2}{a^2 + h^2} = \frac{h}{2 \times R} \tag{5}$$

Note that in planar surfaces F_{22} equals null.

A couple of basic principles are inferred from here. These are defined as the laws of Cabeza-Lainez.

The first principle says that:

For a volume composed of perfectly fitting elements presenting no internal obstruction and one of them being a disk, the view factor from the non-planar surface to the disk equates a fraction whose numerator is the area of the disk and the denominator is the area of the curved geometry.

The second principle of Cabeza-Lainez states that:

Under any spherical element, the so-called reflexive factor (or self-given energy) can be determined by the fraction of the area of the element divided by the total area of the spherical surface.

Bearing in mind that any segment of the sphere is the Nth fraction of the total surface (of radius R), and using Pythagoras's theorem,

$$(h^2 + a^2) = 2 \times R \text{x} h \tag{6}$$

Therefore,

$$N \times (h^2 + a^2) = 4 \times R^2 \; ; \; N = 2 \times \frac{R}{h} \; ; \; h = 2 \times \frac{R}{N} \tag{7}$$

This implies that

$$F_{11} = \frac{h}{2 \times R} = \frac{h^2 \text{x} N}{4 \times R^2} = \frac{1}{N} \tag{8}$$

The second principle informs us that the self-given energy for an Nth part of the sphere is a fraction of value 1/N. In this way, the previous supposition for one-half of the sphere is true; ensuing that divisions for one third or one quarter would give 1/3, 1/4, and so forth.

Such a principle will be fulfilled for many imaginable elements of the sphere that do not fall on typical categories as segments. Consequently, the properties expressed in Equations (5) and (8) are unique to the spherical surface and critical to settle the issue.

The former two principles can be extended to other adjustments that involve the sphere. Take for instance, a volume limited by two half-disks under any angle x, which varies between zero and π degrees (Figure 3):

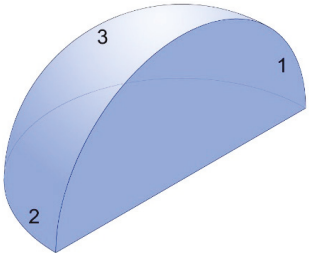

Figure 3. Depiction of elements in a spherical wedge, areas 1 and 2 show half-disks, and surface 3 is a part of the sphere.

Recalling the findings from above, the Nth fraction in the wedge gives $1/N = x/2\pi$ and so,

$$F_{33} = \frac{x}{2\pi} \tag{9}$$

Consequently,

$$F_{31} = F_{32} = \frac{1}{2} \times \left(1 - \frac{x}{2\pi}\right) \tag{10}$$

Incorporating the surfaces of the half-disks, $\pi R^2/2$

$$F_{13} = F_{23} = \frac{2x}{\pi} \times \left(1 - \frac{x}{2\pi}\right) \tag{11}$$

Continuing with the deduction at Equation (11), the pair of half-disks can cover any angle x ranging from 0 to π degrees (Figure 4). In this manner, the expression found below, and termed as the Cabeza-Lainez third law, is not described in any reference that we many know of [1]. Thus, we claim it to define the configuration factors that involve two semicircles with a common diameter, if x covers the magnitude of the angle comprised between them (Figure 5).

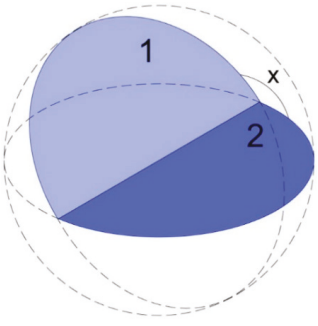

Figure 4. Two half-disks with equal radius R, sharing their diameters for any angle of X° degrees.

The above result simplified produces:

$$F_{12} = 1 - \frac{2\alpha}{\pi} + \left(\frac{\alpha}{\pi}\right)^2 \tag{12}$$

Transforming the equation into degrees,

$$F_{12} = 1 - \frac{x}{90} + \frac{x^2}{32400} \tag{13}$$

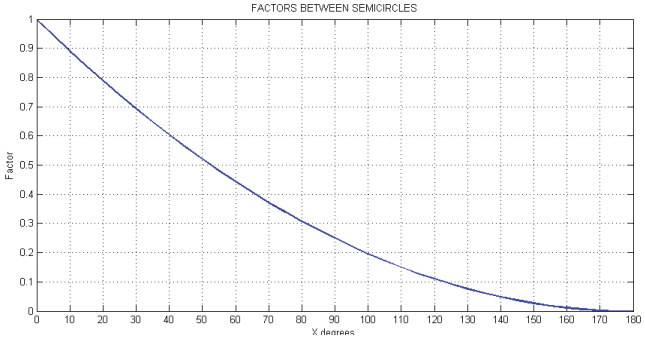

Figure 5. Luminous energy factors for two half-disks sharing the diameter and covering an angle of x^o sexagesimal degrees.

Cabeza-Lainez invented a fourth law based on the former (unpublished) and we can express it in the following way. For any couple of planar sections of a sphere (1–2) with a common edge and irrespective of the angle they form α, or if they pass through the center of the sphere or not, the form factor from surface 1 to surface 2 is:

$$F_{12} = \frac{A_1 + A_2 + A_3 \times (F_{33} - 1)}{2 \times A_1} = \frac{1}{2}\left(1 + \frac{A_2 - A_3}{A_1} + \frac{A_3^2}{A_s \times A_1}\right) \tag{14}$$

F_{33} is the factor of a sphere's fragment over itself, which is defined in the Cabeza-Lainez second law as the ratio between the area of the said fragment and the whole sphere (Equation (8)), in other words, $\frac{1}{2}$ for a hemisphere, $\frac{1}{4}$ for a quarter of sphere, and successively, it equals A_3/A_{sphere}.

A_i is the respective areas of surfaces 1 and 2 (segments of circle or ellipse), and 3 is the comprised fragment of the sphere (Figure 6).

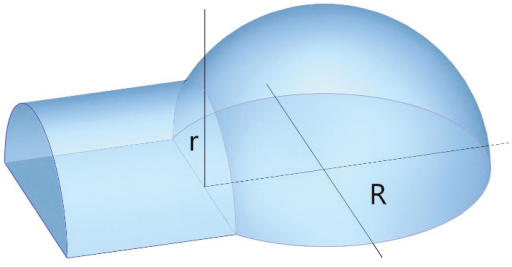

Figure 6. A spherical underground chamber susceptible to solve with our laws of radiation.

It is important to stress that Equations (12) to (14) have been demonstrated by numerical computation methods.

4. Further Developments

In Appendix A (Equations (A1) to (A12) and Figures A1–A3), a more complete collection of curved shapes to explain the different energy exchanges can be found. Following the discussion, we introduce an equation that correlates the radiative transfers of circular sectors with connected rectangles (Figure 7). This clearly applies to the geometry of the tunnel, a form that has been never been calculated previously due to is difficulty in integration [7].

For any vertical circular sector with a center situated in the middle of the edge x of a horizontal rectangle of dimensions x, y; by virtue of the Cabeza-Lainez seventh law, the form factor from the said rectangle to the sector of radius r will be (Figure 8):

$$\begin{gathered} t = r^2 + y^2 + x^2;\ m = \sqrt{x^2 \times \sin^2\theta_1 + y^2};\ n = \sqrt{x^2 \times \sin^2\theta_2 + y^2} \\ F_{21} = \frac{y}{2\pi} \times \left(\frac{cos\theta_1}{m} \times arctan \frac{r}{m + \frac{cos\theta_1 x}{m} \times (cos\theta_1 x - r)} - \frac{cos\theta_2}{n} \times arctan \frac{r}{n + \frac{cos\theta_2 x}{n} \times (cos\theta_2 x - r)} \right) \\ + \frac{y}{4\pi \times x} ln \left[\frac{(t - 2\ cos\theta_1 \times r \times x)}{(t - 2\ cos\theta_2 \times r \times x)} \right] \end{gathered} \tag{15}$$

The sector is comprised between the angles θ_2 and θ_1, being its radius r.

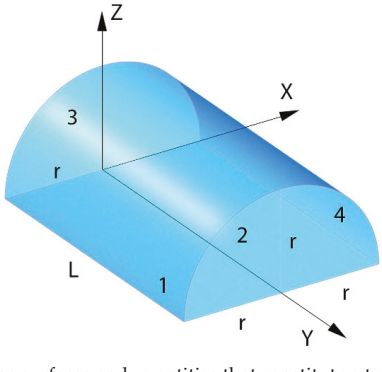

Figure 7. The surfaces and quantities that constitute a tunnel figure.

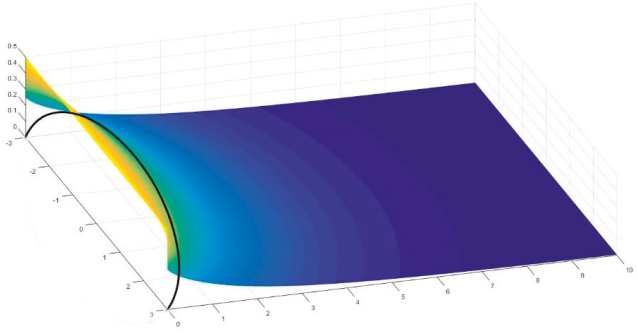

Figure 8. Energy distribution on the floor of a tunnel with a radius of 3 and a length of 10 (non-dimensional).

These important results lead to more possibilities of a simulation where different fragments of figures like conoids, spheres, cones, or circular sections are involved (Figure 8). All of these are very important to the appropriate study of lighting in heritage architecture, given that, as mentioned previously, the cuboid rarely appears in Asian or baroque temples [8].

Careful numerical integration methods give us the Cabeza-Lainez sixth law (Figure 9), which might be considered as a further generalization of the fourth law. We present them together in the graphs below (Figure 10).

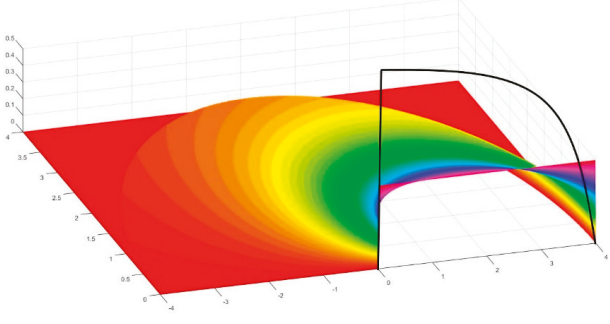

Figure 9. A quarter of a circle with a radius of 4 non-dimensional, and the energy spread over a semicircle with common edge.

The sixth law is described as:

$$F_{23} = 1 - 2 \times F_{21} - \frac{\alpha}{\pi} + \frac{1}{2}\left(\frac{\alpha}{\pi}\right)^2 \tag{16}$$

where α has the same angular meaning as before, but this time the law compares a quarter of the circles instead of semicircles.

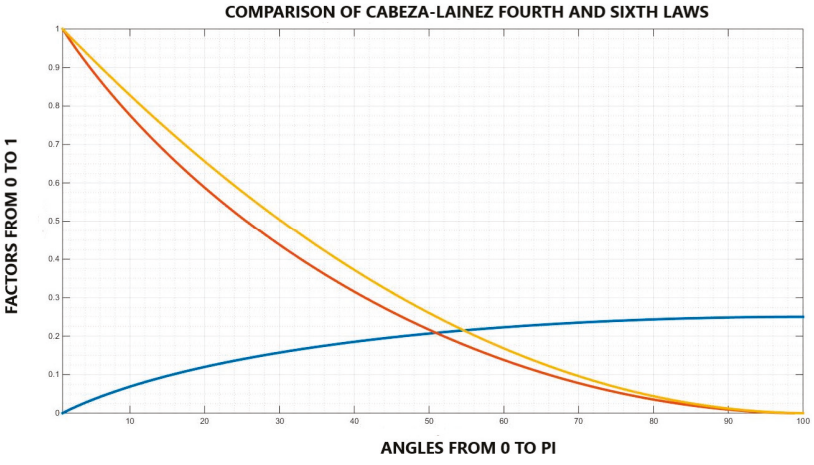

Figure 10. Fourth law (in orange) compared to the new sixth law (Equation (16), red), which directly connects to the seventh law (blue) f.

At this point of the discussion, we believe that a vast repertoire of unsuspected curved shapes in the literature has been covered in a robust way. Some other forms that have also been defined by the authors can be found in [9,10]. The forms solved can be applied with perfect ease to any kind of radiant energy, for example, artificial lighting, emitted heat, or daylight. In each case, we need to find the climatic data and boundary conditions that will appear in the particular problem considered. Appendix B (Equations (A13) and (A14)) gives some hints as to the above issue.

5. Inter-Reflections

One last point needs to be explained before presenting some relevant case studies, which is the question of inter-reflection. To this aim, we developed the following procedure.

The total balance of energy depends on the equation

$$E_{tot} = E_{dir} + E_{ref} \tag{17}$$

where E_{dir} is the fraction of direct energy and E_{ref} is the reflected fraction. If these quantities are summed, we obtain the global amount of radiation E_{tot}. Usually, several surfaces intervene in the process of reflection, and thus a set of expressions can be built. It is possible to introduce a pair of instrumental arrays that we will call F_d and F_r. For a volume enclosed by three surfaces (see Figure 11), such matrices would have the ensuing form:

$$F_d = \begin{pmatrix} F_{11} \times \rho_1 & F_{12} \times \rho_2 & F_{13} \times \rho_3 \\ F_{21} \times \rho_1 & F_{22} \times \rho_2 & F_{23} \times \rho_3 \\ F_{31} \times \rho_1 & F_{32} \times \rho_2 & F_{33} \times \rho_3 \end{pmatrix} \tag{18}$$

$$F_r = \begin{pmatrix} 1 & -F_{12} \times \rho_2 & -F_{13} \times \rho_3 \\ -F_{21} \times \rho_1 & 1 & -F_{23} \times \rho_3 \\ -F_{31} \times \rho_1 & -F_{32} \times \rho_2 & 1 \end{pmatrix} \tag{19}$$

with factors F_{ij} as previously found, yielding the energy transfer between the respective surfaces involved. Here, ρ_i represents the ratio of reflection (direct or otherwise) assigned to a particular element i [1].

Notice that in the matrix called F_d (Equation (18)) the diagonals are not null as the F_{ii} (with two ii) elements have definite values for curved surfaces, unlike the exchange in a cuboid.

If after careful integration by the procedures described previously, we are able to fix all the elements in Equations (18) and (19), we can establish new expressions (Equations (20)–(22)) in order to correlate the primary direct energy with the one extracted by reflections.

$$F_r \times E_{ref} = F_d \times E_{dir} \tag{20}$$

$$F_{rd} = F_r^{-1} \times F_d \tag{21}$$

$$E_{ref} = F_{rd} \times E_{dir} \tag{22}$$

As the amount of internally diffused energy is now a function of direct transfer, the problem is settled. A novel operation defined by Cabeza-Lainez is termed as the *product of form factors*, and being a sort of convolution operator it is still unrevealed how it applies in the calculation of these shapes.

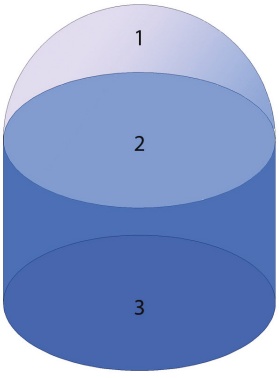

Figure 11. Volume composed only of curved figures, which is usual in heritage architecture.

6. Case Studies

6.1. Ajanta Caves and Underground Temples, India

For this article, we analyzed the Buddhist compound of Ajanta in the Wagora River, India, in detail. This consists of more than 30 artificial caves with either statues of the Buddha or frescoes of its past miraculous lives, also known as jataka [11,12]. The caves were excavated around the 5th century A.D. and could be clear precedents of the Silla Buddhist' temples of Korea (analyzed in Case Study 2).

In these famous underground temples, named Chaitya, daylight comes exclusively from an unglazed aperture, which resembles the semicircular mouth of a tunnel, although more prone to architectural expression. The reason behind these highly inspiring constructions is altogether sustainable (Figures 12 and 13).

When the Buddhist monks could not wander in pilgrimage preaching the doctrine of the dharma due to harsh monsoon weather, they instead decided to honor Shakyamuni by building stupas inside the cliff. In this manner, they protected themselves from discomfort, but still kept expounding the sutra, by virtue of prodigious images, to future believers.

The tunnel-like constructions were necessary to have some light and air during this hard but refined work, whilst the thermal inertia of the rock moderated the excessive oscillations in such a torrid region. Any waste material was accommodated in a natural fashion to the surroundings.

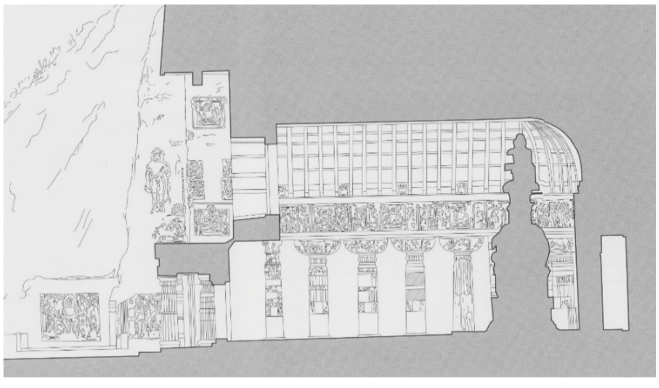

Figure 12. Section of Chaitya number 19.

Let us for instance describe the analysis performed in cave number 26 (Figure 14), which shows a western orientation that is ideal for ceremonies in early morning or evenings, depending on the season of the year.

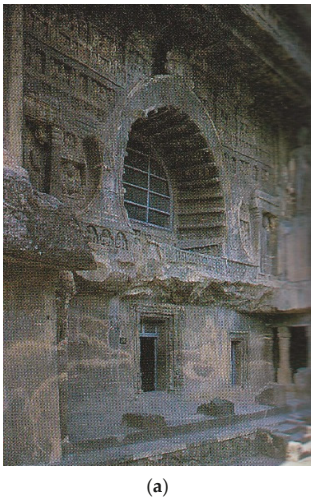

(**a**)

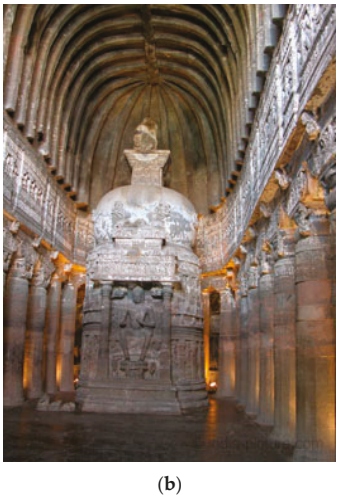

(**b**)

Figure 13. (**a**) View of the entrance to Chaitya number 26. (**b**) Interior stupa showing the sculpture of the Buddha.

By late summer, after the inevitable rainy season, the sky is cloudy (technically, overcast) and the illuminance levels may reach 10,000 lux. Assuming the radius of the opening to be 2 m and the span to the inner shrine is 14 m; we employed our tunnel shape simulation model to obtain, on the horizontal plane, values of only 6 lux. This means a very scant level of light (Figure 15).

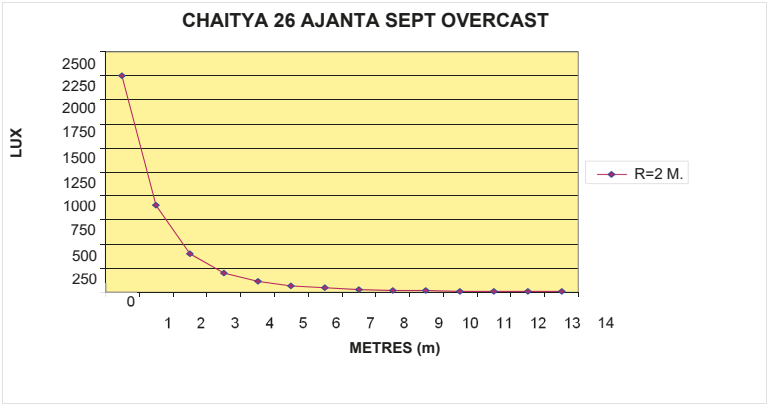

Figure 14. Graph of illuminance distribution in the chaitya. Source: Cabeza-Lainez.

Forewarned by this result, we suggested to the restoration team that inner reflections would be critical to perform any activities in the space, and that the materials employed should have enhanced extreme diffusion of light. Not much later, archaeological evidence corroborated this fact in remnants of stucco, gilt, or inlayed areas, and other kinds of reflective veneers.

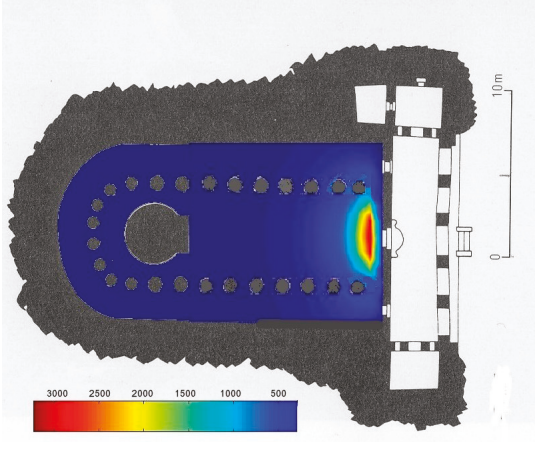

Figure 15. Plans of Chaitya 26 of Ajanta (India) with day-lighting values (3000–50 lux). Source: Cabeza-Lainez.

This was one of the first experiences with hypogeal precincts in Asia in which first-hand knowledge of sustainability through lighting was attained, but also in that it could help to raise meaningful restoration efforts.

6.2. The Seokguram Grotto, Gyeongju, Korea

Stimulated by our initial experience outside Europe, the Kyungil University invited us to research at another temple excavated in the mountain, which is in fact of paramount heritage for the Republic of Korea. It is also controversial from the point of view of political sustainability since it had been unearthed at the time of Japanese domain, and maintained for years in neglect and disrepair.

We had to carefully study the geometry and characteristics of the Seokguram Grotto (Figures 16–18), not only in connection with the sunlight, but also to determine the structural stability of the cupola enshrining the magnificent Buddha statue [13].

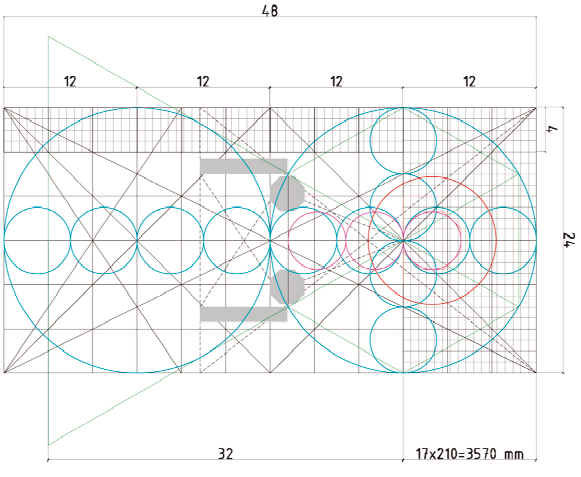

Figure 16. Geometric exactitude and proportions of the Seokguram artificial cave.

Figure 17. An interior view of the Buddha sculpture on a lotus pedestal. Source: Juhyung Lee.

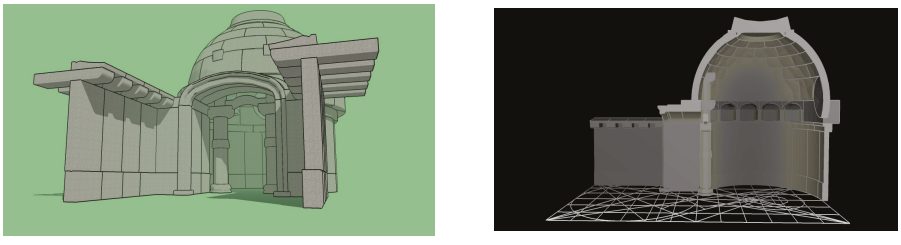

(**a**) (**b**)

Figure 18. Model of Seokguram underground temple. (**a**) View from the entrance of the model. (**b**) Interior with proportions and dome. Source: Salguero-Andujar.

We simulated the resistance and solidity of the new structure (Figure 19), which incorporated only fragments of the ancient one. The type of stone and the soil mechanics around the tumulus were also calculated [13].

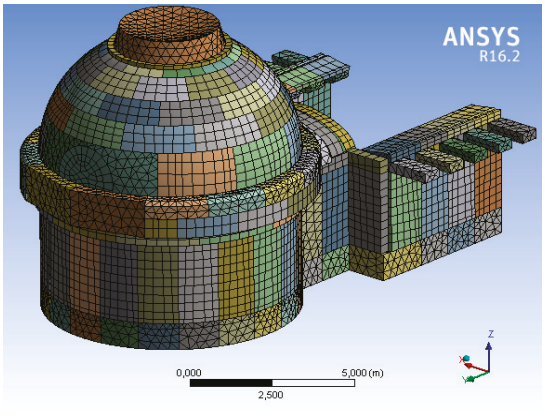

Figure 19. An example of the simulation model employed to find the stresses of the special type of granite stone employed for the dome. Source: Salguero-Andujar.

Finally, regarding the lighting conditions, we were asked to simulate the possibility of a circular opening with a diameter of 0.8 m in the low eastern area of the dome (Figure 20), which has been lost, according to evidence and other sources. Since this chamber is a spherical cap, the use of the equations presented in the previous chapters of the article was almost immediate and the results encouraging. However, we have to say that such a window would permit adumbrating the Statue of the Buddha, but common activities inside the temple would have to rely on reflections as in the case of Ajanta, or some sort of artificial lighting (Figure 21). We hope that in the near future and following our stint, some perforations of the dome could be implemented in accordance with a much more efficient electrical system.

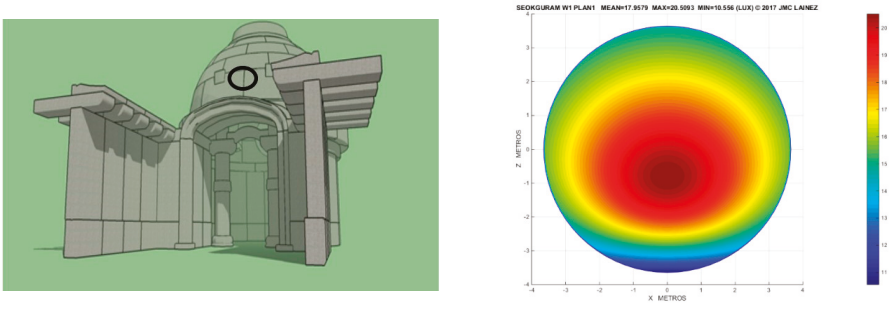

(**a**) (**b**)

Figure 20. Radiative model of Seokguram underground temple. (**a**) Tentative location of the archaeological opening (**b**) Distribution of daylight in the plan of the shrine, generated by the simulation software. Average values of 17.95 lux. Source: Cabeza-Lainez.

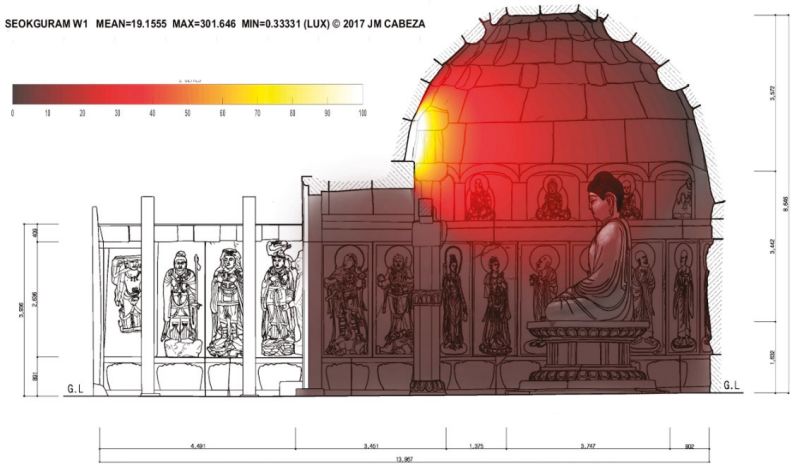

Figure 21. Sectional view of the grotto including lighting levels by a surmised circular opening. Source: Rodriguez-Cunill.

6.3. The Nantang Cathedral in Beijing, China

The third example discussed in this paper is no longer an extant catholic church in Beijing. It was built by Jesuit Missionaries at the beginning of the 17th century, but suffered several disasters until it was ruined by the second Opium War in the 19th century.

A new church was erected on the site, but it does not retain any of the excellent features that the former incorporated. The ancient church was a paradigm of Sinicization, as we will try to demonstrate (Figure 22).

The Jesuits had prepared detailed plans and a very unusual drawing perspective to facilitate the construction of the church.

Many curious features appear in the original drawings that the Portuguese Historic Archives maintain today. One of them is the triple ceremonial gate flanked by stone lions to protect the building from evil spirits.

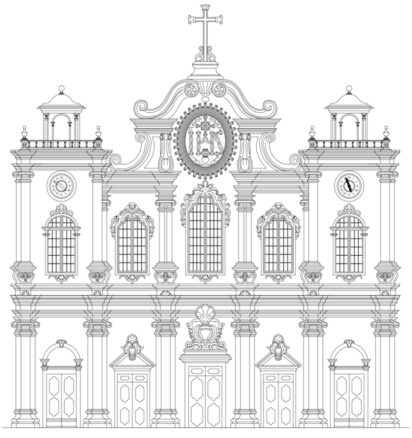

Figure 22. South façade of the Nantang Cathedral, reconstructed from the original plans preserved at the Arquivo Historico Ultramarino (Lisbon. Source: H. Ojeda and J. Cabeza-Lainez).

The plans present writings in Portuguese language, but detailed inscriptions in Chinese also appear. One such inscription shows the cardinal points or directions of Heaven, as mentioned in Daoist scriptures, specifically indicating that the main façade has to face due south for the same reason of harmonizing with the cosmos and to avert calamities [14].

Based on such magnificent drawings the authors have accurately reconstructed the floor plan and façade with the help of CAD systems.

The elevations reveal that the fundamental source of lighting was the main façade oriented to the south, which was in striking contrast with Catholic churches in Europe that usually face west, according to the authors' own surveys and measurements [8,15]. Here instead, slender framed windows are the sole elements of fenestration.

The overall style of the building did not resort to classic ornaments to resolve typical problems of expression, but rather seems to adopt baroque features as a starting point to create something new and capable of accommodating Chinese sensibility.

The Jesuits at the Qing Court had justly excelled in astronomical knowledge and subsequent control of time by manufacturing watches, astrolabes, and other mechanical tools of measurement for the Emperor. This fact is elegantly marked in the cathedral with the inclusion of two voluminous clocks at each side of the main façade, simultaneously displaying the time in Beijing and that of Rome.

The former indicates that they had guessed by exchanging letters in the occasion of eclipses, about the significant magnitude of the time lag between both places, although they were still unable to trace a meridian [15].

In this case, the simulation included the curved elements of the vaults that the European missionaries introduced as a novelty for interior spaces. The vault and the dome had not developed much in Eastern Asia for several reasons including the want of compressive materials and weather tending to heavy rains and winds [14].

In Figure 23, we present the trajectories of solar movement for the vicinity of the church and its probable exposure to sunlight.

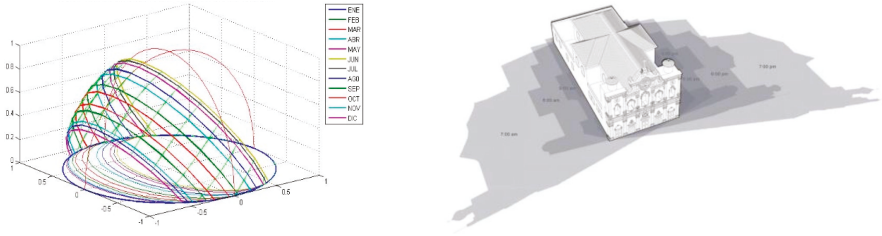

(**a**) (**b**)

Figure 23. Daylighting model of Nantang Cathedral. (**a**) Solar Chart for Beijing. (**b**) Solar exposure at different hours. Source: Cabeza-Lainez.

Figures 24 and 25 depict a more vectorial approach to the radiation phenomena of the interior for the situations of summer and winter.

As previously stated, the key here is the southern orientation of the main façade, which is very unusual in the West, but required from cosmological and cultural points of view. Such disposition may have contradicted the catholic liturgy on many occasions.

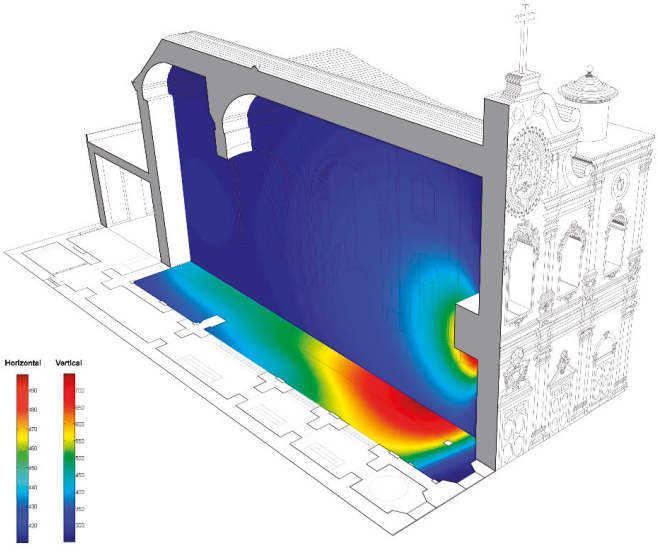

Figure 24. Radiative field inside the church in winter. Source Cabeza-Lainez.

The levels were revealed to be adequate for the performance of activities in the range of 400 lux. This is important because most Chinese temples and precincts were dark and gloomy and a new religion could easily prove its supremacy by revealing even the darkest corners of its faith by means of its architecture.

If harmony with thesun and environment is demonstrated by virtue of architecture, it is easier to spread any belief that is taught precisely at that architecture. The Jesuits were always conscious of such a fact in all of their churches [16].

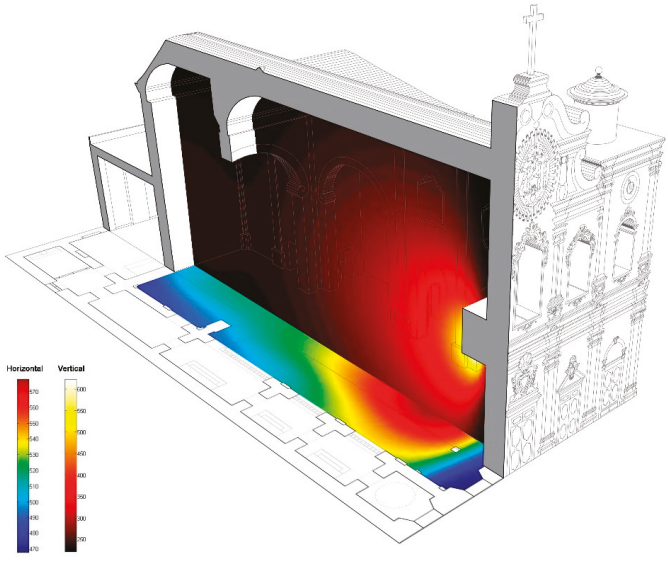

Figure 25. Summer distribution of radiation for the Nantang Cathedral. Source: Cabeza-Lainez.

Except for the façade, the exterior of the church remains simple in character. However, from another original etching, we know that the interior was lavishly decorated, the ceilings were vaulted with carved and painted wooden panels using naturalistic motifs. It is on the inner walls of the Cathedral that the spectacular frescoes of Giuseppe Castiglione once stood.

Master Castiglione, or Lang Shining in Chinese, was considered by many to be the last great Chinese painter who used another European effect to beckon the believers: focal perspective. As a curiosity, we reconstructed the following descriptions of the contemporaries of some of the paintings that once adorned the interiors conceived by Castiglione. We can only regret that they are lost . . . forever? (Figure 26).

(**a**)

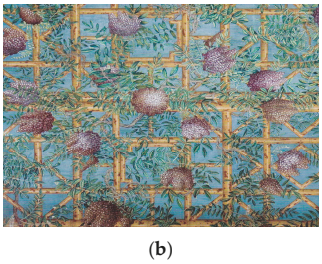

(**b**)

Figure 26. Frescoes by Giuseppe Castiglione. (**a**) Reconstruction of Nantang Cathedral. (**b**) Inside the JuanqinZhai (Pavillion at the Forbidden City) pergola of wisteria. Source: Rodriguez-Cunill.

7. Discussion

Through the previous paragraphs, we have readily made available an ample scope of possibilities for sustainable lighting in the heritage of East Asia. New principles proposed by the authors have been devised and incorporated to facilitate the simulation process of many curvilinear geometries. Such innovative formulations are difficult to obtain, but still, due to their mathematical exactitude, the radiative transfer procedures are significantly clarified and valuable computational time is reduced to

a mere fraction in comparison with previous analysis. The complex issue of inter-reflections in curved volumes has been completed with perfect ease and this is an important novelty.

Regarding the monuments presented as case studies, some of them have been rebuilt (Seokguram) and the Nantang Cathedral is no longer extant. Therefore, we cannot monitor them properly to check the hypothesis is validated. We have to trust in other studies that the authors conducted in European heritage. For example, the Guarini Church in Torino (Italy), the Jesuit novitiate of San Luis (Seville), or the research initiated at the Egyptian Hall of Thutmose III in Luxor. We feel that perhaps more detailed work should still be done on the less complex aspect of the issue: the artificial lighting of such precincts. However, this is resolved in most cases by national consultants with little or no intervention of foreign experts and techniques. We would like to stress that all the methods hereby presented are suitable for immediate application to every kind of fixture or luminaire, and is especially appropriate for Light Emitting Diodes (LED systems, which tend to become surface distributed sources of low intensity and energy consumption.

Our unceasing effort to bring light to the darkest depths appears to be similar to the myth exposed in the Platonic cave. Nonetheless, we still believe that lighting design and predictions are a valuable resort for the qualification of the space and of heritage in this fashion. We only strive to provide a foremost advance in the scientific knowledge of design sources for natural light and issue clear expedients of how the prediction of the dynamic (radiant) energy and climate response of very resilient architectural structures has produced real sustainability through the ages.

The findings hereby reveal, for instance, to what extreme cross-cultural relationships influenced the development of the so-called Baroque Reason, which extends from Mathematics and Geometry to Art and Design. Adopting the architectural point of view, the lessons that we are to learn relate with adequacy to the climate and harmonious sustainable coexistence between the environment and civilization. A superb weapon for the fight against climate change.

Not in vain, the Swiss architectural historian, Sigfried Giedion once stated: "it is light that induces the sensation of space. Space is annihilated by darkness. If light is eliminated, the emotional content of space disappears, becomes impossible to apprehend. In the dark there is no difference between the emotional evaluation of a chasm and of a highly modeled interior." [17], p. 495.

Decades have passed since this wise dictum was pronounced and yet architecture, in a word, does not seem fit to sustain life on our menaced planet.

A sad paradox, as it is clear that if we can neither separate history from climate nor climate from history, then, how are we to live?

The Chinese sage Zhuangzi suggested, "Be Infinite like space and the four directions—they are boundless and form no enclosures. Sustain all things in your love."

Author Contributions: I.R.-C. and J.M.C.-L. were helpful in conceptualizing the scope and issues. F.S.A. brought the instrumentation and the structural software as well as the momentum at low tide epochs. J.M.C.-L. developed the software for radiative simulation and created algorithms that sustained the whole process. I.R.-C. was instrumental in visualizing the cultural and artistic implications of our work.

Funding: This research received no external funding.

Acknowledgments: Francisco Salguero Andujar appreciates the kindness and help of Juhyung Lee and all the personnel at Seokguram. Inmaculada Rodriguez Cunill desires to honor the memory of Antonia Cunill Aragon by virtue of her contribution. Ioseph Cabeza-Lainez would like to dedicate this article to Jose Cuadrado Moreno for his continuous support and endurance. Ana, Rocio, and Humphrey Ojeda are well remembered.

Conflicts of Interest: The authors declare no conflict of interest.

Appendix A

In the discussion that we sustained at point 3 about the spherical cap; we demonstrated that the necessary form factor was (Equation (4)),

$$F_{12} = \frac{a^2}{a^2 + h^2}\,. \tag{A1}$$

If we may define a fraction β, composed of the squared heights and radiuses, expression A1 is reduced as

$$\beta = \frac{h^2}{a^2} \tag{A2}$$

$$F_{12} = \frac{1}{\beta^2 + 1} \tag{A3}$$

- Since the Cabeza-Lainez first law is more encompassing, it can be used for other curved elements outside of the sphere, like the conoid and the hyperboloid.
- Prolate Semispheroid (Figure A1)

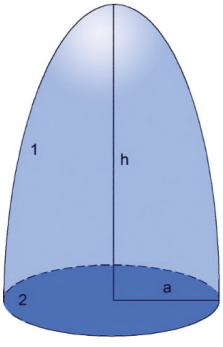

Figure A1. Prolate spheroid.

Element 1 is an oblong ellipsoid and element 2 is the circle that serves as a base to the curved figure, h > a.

Previously, we defined the dimensionless relation m:

$$m = \sqrt{1 - \frac{a^2}{h^2}} \tag{A4}$$

Employing the first law,

$$F_{12} = \frac{a \times m}{a \times m + h \times \arcsin(m)} \tag{A5}$$

$$F_{21} = 1 \tag{A6}$$

$$F_{11} = \frac{h \times \arcsin(m)}{a \times m + h \times \arcsin(m)} \tag{A7}$$

Making it as before in the spherical cap

$$\beta = \frac{h^2}{a^2};\ m = \sqrt{1 - \frac{1}{\beta^2}} \tag{A8}$$

$$F_{12} = \frac{\sqrt{1 - \frac{1}{\beta^2}}}{\sqrt{1 - \frac{1}{\beta^2}} + \beta \times \arcsin\left(\sqrt{1 - \frac{1}{\beta^2}}\right)} \tag{A9}$$

- Paraboloid of revolution (Figure A2).

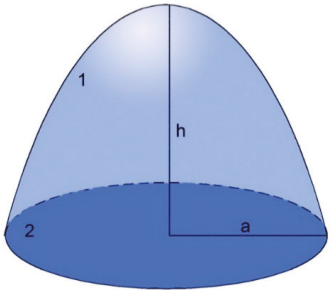

Figure A2. Paraboloid of revolution.

In this case, element 1 is the paraboloid and element 2 is the circle that serves as a base to the upper curved surface

$$F_{12} = \frac{6 \times a \times h^2}{\left[(a^2 + 4 \times h^2)^{3/2} - a^3\right]} \times F_{21} = 1 \tag{A10}$$

$$F_{11} = 1 - \frac{6 \times a \times h^2}{\left[(a^2 + 4 \times h^2)^{3/2} - a^3\right]} \tag{A11}$$

$$\beta = \frac{h}{a} \times F_{12} = \frac{6 \times \beta^2}{\left[(1 + 4 \times \beta^2)^{3/2} - 1\right]} \tag{A12}$$

In Figure A3, we plotted the evolution of factor F_{12} for some usual geometric bodies. The cone presents higher values of emitted energy while the sphere and the ellipsoid are less prone to diffuse radiation internally. Other forms such as the conoid or the hyperboloid could be included in the future.

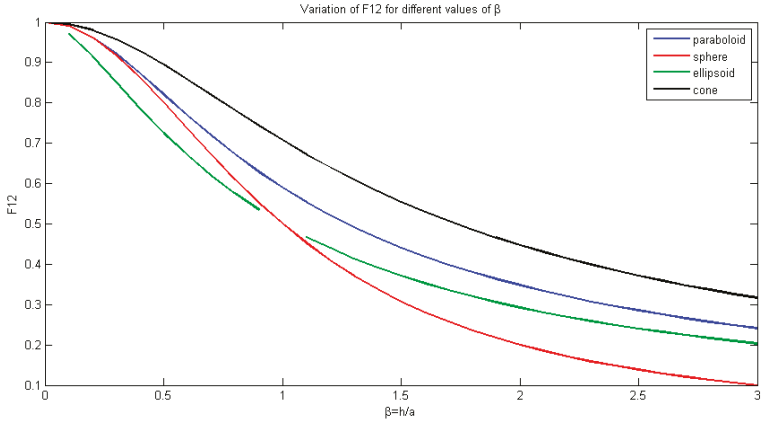

Figure A3. Comparison of four common curved geometries (non-dimensional).

Appendix B

Some useful formulas proposed in the absence of direct climatic data of irradiance.

To study the incidence of radiation on a vertical surface, we need to resort to formulas somewhat more complex. For the clear sky, vertical illuminance due to a half-hemisphere is, following Gillete and Pierpoint [18],

$$E_v = 4000 \times \theta^{1.3} + 12000 \times \sin^{0.3} \theta x \cos^{1.3} \theta \times \left[\frac{2 + \cos \varnothing}{3 - \cos \varnothing}\right], \tag{A13}$$

where ∅ is the azimuth, and θ is the solar altitude.

The algorithm allows the daylight intensities to be obtained for the vertical and horizontal surfaces as a function of the location's latitude. In the situation of an overcast sky, typically defined by the CIE standards, the former expression simplifies as:

$$E_v = 8500\ \mathrm{xsin}\theta, \tag{A14}$$

The authors have also proposed a computer simulation program (not detailed here) that automatically gives the data required, following a few input parameters like solar altitude, the number of sun-hours per month, and the cloudiness index, if available.

References

1. Cabeza-Lainez, J.M. *Fundamentals of Luminous Radiative Transfer*; Netbiblo: Seville, Spain, 2010. (In Spanish)
2. Moon, P.H.; Spencer, D.E. *The Photic Field*; The MIT Press: Cambridge, MA, USA, 1981.
3. Lambert, J.H. *Photometry, or, on the Measure and Gradations of Light, Colors and Shade*; DiLaura, D.L., Ed.; Illuminating Engineering Society of North America: New York, NY, USA, 2001.
4. Higbie, H. *Lighting Calculations*; JohnWiley & Sons: New York, NY, USA, 1934.
5. Feynman, R. *Quantum Electrodynamics: The Strange Theory of Light and Matter*; Penguin Books: London, UK, 1990.
6. Yamauchi, J. Theory of Field of Illumination. *Res. Electro Tech. Labor.* **1932**, *339*, 1–37.
7. Yamauchi, J. The Light Flux Distribution of a System of Interreflecting Surfaces. *Res. Electro Tech. Labor.* **1927**, *190*, 1–91.
8. Almodovar-Melendo, J.M.; Cabeza-Lainez, J.M.; Rodríguez-Cunill, I. Lighting Features in Historical Buildings: Scientific Analysis of the Church of Saint Louis of the Frenchmen in Seville. *Sustainability* **2018**, *10*, 3552. [CrossRef]
9. Howell, J.R. *A Catalog of Radiation Configuration Factors*; University of Texas: Austin, TX, USA, 1982; ISBN 978-0-07-030606-6. Online version (2019); Available online: http://www.thermalradiation.net/indexCat.html (accessed on 18 September 2019).
10. Modest, M.F. *Radiative Heat Transfer*, 3rd ed.; Academic Press Elsevier: San Francisco, CA, USA, 2013.
11. Jain, K.; Jain, M. *Thematic Space in Indian Architecture*; India Research Press: New Delhi, India, 2002.
12. Kamiya, T. *The Guide to the Architecture of the Indian Subcontinent*; Toto Shuppansha: Tokyo, Japan, 1996.
13. Salguero Andujar, F. Comparative, geometric and structural analysis of the Seokguram Temple at Gyeongju (Korea). In Proceedings of the International Conference on Advances on Heritage Preservation, Korea, Gyeongju, September 2017; pp. 3–1031.
14. Cabeza-Lainez, J.M.; Almodóvar-Melendo, J.M. Daylight, Shape, and Cross-Cultural Influences Through the Routes of Discoveries: The Case of Baroque Temples. *Space Cult.* **2018**, *21*, 340–357. [CrossRef]
15. Almodovar-Melendo, J.M.; Cabeza-Lainez, J.M. Environmental Features of Chinese Architectural Heritage: The Standardization of Form in the Pursuit of Equilibrium with Nature. *Sustainability* **2018**, *10*, 2443. [CrossRef]
16. Rodríguez-Cunill, I. Pintar a través del ojo de la cámara. *Rev. Int. Comun. Audiov. Public. Lit.* **2004**, *1*, 51–65.
17. Giedion, S. *The Eternal Present. The Beginnings of Architecture*; Bollingen Foundation: Princeton, NJ, USA, 1964; p. 495.
18. Pierpoint, W. A Simple Sky Model for Daylighting Calculations. In Proceedings of the International Daylighting Conference, Phoenix, AZ, USA, 16–18 February 1983.

sustainability

MDPI

Article

Let There Be Light! Investigating Vernacular Daylighting in Moroccan Heritage Hammams for Rehabilitation, Benchmarking and Energy Saving

Magda Sibley

Sheffield School of Architecture, The University of Sheffield, Arts Tower, Western bank, Sheffield S10 2TN, UK; m.sibley@sheffield.ac.uk or sibleym3@gmail.com; Tel.: +44-7930-988-8193

Received: 11 August 2018; Accepted: 28 October 2018; Published: 31 October 2018

Abstract: This paper provides the first study of vernacular daylighting provision in Moroccan heritage public bathhouses in order to rehabilitate it for experiential authenticity, energy saving and improved users' well-being. The analysis of a representative sample of 13 still working hammams reveals recurrent patterns of oculi numbers and configurations. These consist of one to three rows of eight circular roof openings (oculi) of 18 to 20 cm diameter, arranged along the roof vault of each bathing space. The ratio of total roof openings' area to internal floor area rarely exceeds 2%. Synchronised measurements of horizontal illuminance on the roof and inside the bathing spaces in a case study hammam were conducted in July and August 2016, after rehabilitating all roof oculi. Recorded levels indicated that maximum horizontal illuminance never exceeds 60 lx. The calculation and plotting of daylight factor based on real data reveal levels under 2% and a sudden decline in the hot room early afternoon due to steam accumulation. The paper provides the first benchmark of vernacular daylight rehabilitation in Moroccan heritage hammams and the illuminance it affords. It introduces an innovative combination of historical, architectural and building science methodologies that can be extended to other heritage building types.

Keywords: hammam; oculi; vernacular roof lighting; energy saving; well-being; daylighting rehabilitation; authenticity; horizontal illuminance

1. Introduction

The provision of daylight in heritage buildings is rarely considered adequate in terms of responding to contemporary standards issued by international institutions and which have been wrongly based on Daylight Factor (DF) or climate-based daylight modelling (CBDM) [1]. Therefore, daylighting levels afforded by the original daylighting strategy in heritage buildings are rarely maintained as an intrinsic heritage experiential value in the rehabilitation or re-use of these buildings. In the context of public bathhouses (hammams), daylight provision is frequently done from the roof space. A single oculus at the centre of a dome is a feature that is commonly found in the architecture of large Roman public bathhouses as illustrated in Pompeii's Roman baths [2].

The decline of the Roman and Byzantine public bath institution in the West was followed by the development and proliferation, during the early Islamic era, of small public baths, reminiscent of the Roman baths known as balnea. These baths feature three successive bathing rooms of increasing temperature, as well as the underfloor heating system known as hypocaust, both were maintained in the architecture of Islamic hammams. However, daylighting provision was replaced by a number of small oculi, pierced in the vaults and domes of the hammam roof, becoming a distinctive characteristic of hammam buildings. This architectural feature can be seen in two early Islamic baths: Hammam Qusayr Amra, an 8th Century structure [3] in the Jordanian desert (Figure 1) and in Hammam Aghmat, an 11th Century Almoravid structure [4] excavated in Aghmat, 30 kilometres South East of Marrakech

in Morocco [4,5]. The Aghmat hammam [6] displays rows of circular openings or oculi in the three vaults covering the cold, warm and hot rooms (Figure 2). Such a configuration will continue unchanged in the architecture of Moroccan and Andalusian hammams for many centuries onwards [7–9]. The small circular piercings of 18 to 25 cm in diameter, located in the vaults and domes of the hammam roof are capped with blown glass bells. These allow shafts of daylight and sunlight to penetrate into the bathing spaces, cutting through the thick steam and creating different atmospheres at different times of the day. They constitute one of the unique and authentic experiential qualities of hammam buildings as illustrated in the case of one Mamluk and one Ottoman hammam (Figure 3a,b). Known in Arabic as little moons "Qamariyyat" or little suns "Shamsiyyat", they make a clear connection between the bather and the changing sunlight conditions of the sky. They also allow low levels of daylight into the steamy bathing spaces, hence maintaining some level of visual privacy, bearing in mind the strict religious codes governing nudity and gazing at another bathers' body. The act of washing one's body is indeed not a task that requires high levels of daylight, however, the manipulation of daylight in hammam spaces is believed to be highly linked to cultural and spiritual norms. It is argued in this paper that the vernacular daylighting system in hammams constitutes an intrinsic part of the heritage value and authenticity of this building type that needs to be fully understood in order to be properly rehabilitated in existing heritage structures and carefully reintroduced in the architecture of contemporary hammams in Morocco and beyond.

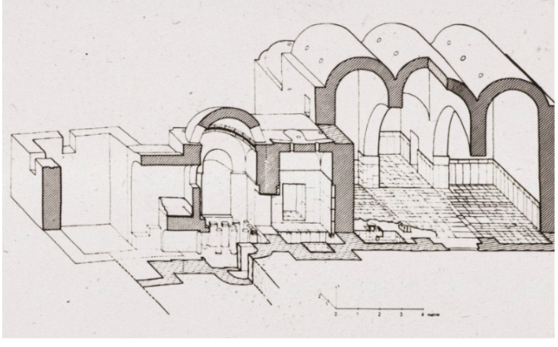

Figure 1. Qusayr Amra three vaulted bathing rooms with small oculi [2].

Figure 2. Hammam Ahgmat: 11th Century Almoravide era, Morocco [3].

(**a**) (**b**)

Figure 3. Hammam lightscape in the hot room of (**a**) Hammam al Hussayniya in Cairo (Mamluk era); (**b**) Hammam al Bacha in Acre (18th Century Ottoman era).

Existing studies on hammam daylighting systems are few and far apart. The most recent studies focus on Ottoman hammams that have lost their original function. This is the case of the study conducted by Al Maiyah et al. [10] which rightly argue the importance of understanding the daylighting system in vernacular buildings, as this is rarely considered as a key feature worth preserving as part of adaptive reuse strategies of heritage buildings. The study focuses on how to maintain the original daylighting conditions in the hot room of the Demirci hammam in Bursa, while allowing it to function as a museum or an art gallery; the hot room being the only surviving part of this Ottoman structure. The main concern is to establish how to reuse the existing vernacular daylighting system without exposing the exhibited artefacts to levels of light that are likely to be damaging. Measurements were made to validate a simulation modelling tool, Radiance, used with a digital model of the building produced using Integrated Environmental Solutions (IES) software. The aim was to develop an understanding of the behaviour of daylight in this Ottoman hammam hot room during a whole year and determine the most appropriate spaces for placing museum or art gallery exhibits. The study highlights that the average monthly illuminance level on the South wall of the hot room remains under 140 lx in the summer months in Bursa-Turkey (Latitude: 40°11′44″ N Longitude: 29°03′36″). Although this study rightly argues the need to avoid relying solely on lighting standards for the adaptive reuse of heritage buildings, and work with the existing lighting qualities of the spaces in a vernacular hammam, it does not provide an understanding of the nature of the hammam vernacular daylighting system in all the bathing spaces as it concentrates on analysing one main redundant space.

Another study focuses on investigating the vernacular daylight provision in seven still surviving Ottoman hammams in the city of Thessaloniki in Greece [11]. Measurements of daylight levels were, however, conducted in one case study building only, the Bey Hammam, a 15th Century twin structure used as a cultural centre was selected for recording daylight levels under different sky conditions in March 2008. The results of these measurements are presented graphically on the plan of the building with illumination levels plotted on a grey scale, ranging from 0 lx to 120 lx at a step of 10 lx [10]. Measurements were made using a lux meter at different points of the three bathing spaces and were carried out during a single day. This study indicates a clear correlation between the intensity of

daylight, the type of activities carried out in the spaces and the level of visual privacy they require. The central spaces under the domes received the most light (due to the large number of oculi found in the domes of Ottoman hammams). This is the case of the central marble table in the hot room (the main shared space in Ottoman baths), whereas the peripheral spaces used for individual washing have much lower levels of daylight, indicating a clear correlation between the intensity of daylight and the level of privacy required by the bathers.

It is clear that the al Maiyah [10] and Tsikadoulaki et al. [11] studies focused on a single case study of Ottoman hammams that have lost their original function: One in Bursa, (Turkey) the other one in Thessaloniki (Greece). In both studies, daylight measurements, limited in time and space, were made in redundant structures without the steam conditions typical of a working hammam. Furthermore, all case study buildings where daylight levels were measured focus on a single bathing space, usually the hot room. However, it is clear from these studies that daylight levels in Ottoman hammam bathing spaces are relatively low and are in most cases below 140 lx as one moves away from the central domed part of the hot room.

This low level of daylighting in hammam bathing spaces is also confirmed by an earlier study carried out by Mahdawi and Orehounig [12,13] in the context of an EU-funded research project (HAMMAM 2008). Mahdawi and Orehounig collected data on indoor environmental (thermal) conditions and outdoor microclimatic conditions in the immediate vicinity of one traditional hammam in each of Egypt, Turkey, Morocco, Syria, and Algeria over a period of one year. Horizontal illuminance was measured (at one metre from the floor) at a single point in the centre of the different bathing spaces of the five case-study hammams of Cairo, Ankara, Fez, Damascus and Constantine. These measurements are of indicative character only and not reliable as they were carried out at different seasons in each of the five hammams and under different sky conditions in different geographies. Furthermore, measurements were made in conditions where the vernacular daylighting system was either in a poor state of repair or completely redundant and did not exclude the contribution of electric lighting at the time of the measurements. However, the results of horizontal illuminance measurements clearly indicate consistently low levels of lighting (mostly below 100 lx) in the five case study buildings of different historic eras and geographical locations. These measurements present however a number of limitations as they do not link to outdoor sky conditions at the time of the measurements and are not directly comparable. Furthermore, they fail to convey a clear understanding of the hammam daylighting levels afforded by the vernacular oculi system. Despite their limitations, it is clear from these previous studies that daylight levels in the bathing spaces of hammam case-studies located in different geographies (north and south of the Mediterranean) are generally low, varying between 50 and 150 lx.

This literature review has revealed that there have been no studies so far that attempt to develop an understanding of daylight levels in all the bathing spaces of heritage hammams under working steam conditions. Measurements of daylight levels in working heritage hammams where the vernacular daylighting system is still in operation, or has been fully restored, are completely non-existent. The lack of such studies makes it difficult to specify the vernacular hammam natural lighting for hammam rehabilitation purposes and for the design of new built structures that aim to create an authentic daylighting hammam experience. This is needed in all of the Maghreb countries of North Africa where the hammam tradition is still alive. Morocco is where the largest number of working heritage hammams are found and where housing planning regulations dictates the inclusion of a hammam facility in every new residential neighbourhood [14]. It is estimated by the Moroccan federation of hammam managers, that Morocco has more than 12,000 operating hammams, however, it is very likely that the number is much higher as there have never been a systematic national census for hammams. These operate day and night and tend to rely on electric lighting during daylight hours because of their redundant vernacular daylighting system or their poorly designed daylight provision. No studies have been carried out so far to develop an understanding of the hammam vernacular daylighting strategy and the unique spatial experiential qualities it provides. This paper provides a timely and much

needed historical and architectural understanding of the hammam vernacular daylighting strategies that embed tacit cultural and social norms for visual privacy and spiritual connection to the sky. In order to do so, the following methodology was adopted.

2. Materials and Methods

A representative sample of heritage hammams from different historical periods was selected in the old city of Marrakech. A total of 13 still functioning heritage hammams out of a total of fifteen were surveyed and recorded for the first time by the author, allowing the production of their plans, sections and elevations, as well as their roof plans and a photographic record of their various spaces (see Table 1 and Figures 4–6). More recently built hammams were deliberately excluded as the focus of this study is on the original vernacular daylighting system in heritage structures. The examined sample of hammams represents 90% of the total number of heritage hammams, located in every residential neighbourhood, within the proximity of small or large mosques inside the UNESCO world heritage intra-muros urban fabric of the city of Marrakech.

Table 1. List of the surveyed hammams in the world heritage medina of Marrakech.

Map Reference	Hammam Name	Dynasty When Originally Built	Dynasty When Rebuilt
1	Bab Ailan	Merinid	Saadi-Alaouite
2	Dhahab	Saadi (16th Century)	Alaouite
3	Bab Doukala	Saadi (16th Century)	NA
4	Darb Arjaan	Saadi (16th Century)	Alaouite
5	Laksour	Saadi (16th Century)	Alaouite
6	Qannaria	Saadi (16th Century)	Alaouite
7	Al Souq	Saadi (16th Century)	Alaouite
8	Mouassine	Saadi (16th Century)	Alaouite
9	Al Ziani (Sensla)	Saadi (16th Century)	Alaouite
10	Azbezt	Almohade	Saadi/Alaouite
11	Sidi AbdelAziz	Saadi	Alaouite
12	Sidi Ayyoub	Saadi	Alaouite
13	**Ben Cherga**	**Saadi**	**Alaouite**
14	**Dabbachi**	**Alaouite**	**NA**
15	El Bacha	1930s	NA

Hammams 13 and 14, bolded in Table 1, have not been surveyed as they were transformed into spas.

In order to establish a clear understanding of the hammam vernacular daylighting system, the following methodological steps have been followed:

Step 1: Architectural analyses of heritage hammam roof plans with their oculi number, location and configuration

The plans and roof openings of the 13 hammams, documented during field work in Marrakech, are systematically analysed to establish whether there are recurrent patterns in the number, location and configuration of roof openings (oculi). The aim of such analyses is to identify any tacit rules that are applied for the configuration of the Moroccan hammam vernacular daylighting strategy.

Step 2: Analyses of ratios of total roof openings area over internal floor area in each the three bathing spaces of the 13 surveyed hammams

The calculation of the percentage of the total area of roof openings for each bathing space in relation to its internal floor area will reveal whether there are any recurrent ratios and whether there any variations between the cold, warm and hot rooms. This is achieved through the comparison of these ratios in the 13 investigated historic structures. This analysis also allows for the extraction of any underlying tacit rules that can inform both the rehabilitation of existing heritage structures and the design of future new hammams.

Step 3: Measurement of horizontal illuminance afforded by the vernacular daylighting system after its rehabilitation in a working heritage hammam

A working heritage hammam, presenting a vernacular lighting configuration of roof oculi over its bathing spaces, has been selected in order to restore the blown glass caps that originally covered the roof openings and carry out measurements of daylight levels afforded by the system in each of the three bathing spaces under working conditions. Water resistant HOBO pendant data loggers for temperature (range of −20 °C to 70 °C) and light (range of 0 to 320,000 lx) were chosen due to their discreet small size and their ease of installation in working hammam spaces with high levels of humidity [15].

They were installed at similar and comparable locations in each of the three retrofitted bathing spaces (of similar size, colour and texture and hence similar reflectance) and on the roofs to record outdoor horizontal illuminance under open sky conditions. The data loggers were placed on the south facing parallel walls of each of the three bathing spaces and at a height of two metres from the floor (away from the bathers), allowing for comparable points of measurements. All data loggers were synchronised to measure horizontal illuminance continuously every 20 min in July, August and September of 2016. This allowed for three measurements per hour for three months which is sufficient to establish the levels of horizontal illuminance falling at similar points in each of the three similar hammam bathing spaces during the summer season of 2016.

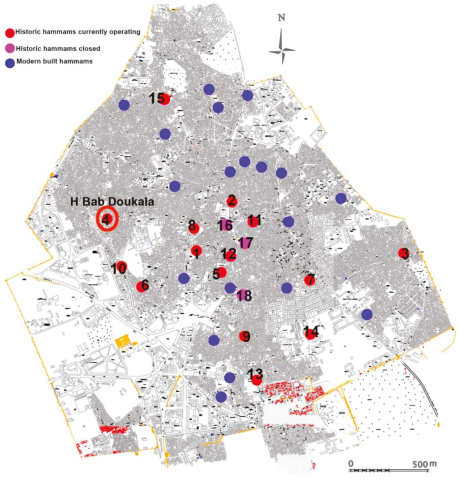

Figure 4. Location of the surveyed heritage hammams of Marrakech with numbers corresponding to the names of the hammams in Table 1.

3. Results

3.1. Analyses of Roof Oculi Configuration in the Representative Sample of 13 Heritage Hammams

During the field work survey, it became clear that all the visited hammams had their roof oculi poorly repaired or completely blocked and none of the original blown glass caps covering the oculi had survived in any of the hammams. Furthermore, the identification from the roof spaces of the original oculi, their number and position was not always possible. This was due to inadequate roof maintenance practices consisting of different layers of cement applied to the roof surfaces. This not only reduced the roof openings' diameter (and the light penetrating to bathing spaces) but completely covered some of the original openings (Figure 5) leading to the use of poor indoor electric lighting during daytime hours. The examination of the hammam ceiling from the inside of the bathing spaces was therefore necessary (although not always easy) to locate and count the blocked oculi.

The examination of the architecture of the 13 documented hammams reveals a consistent linear organisation of three successive rectangular parallel bathing spaces of increasing temperature and steam and are as follows:

- The cold room, called "al-Barrani" (The Roman Frigidarium)
- The warm room, called "al-Wasti" (The Roman Tepidarium)
- The hot room, called "al-Dakhli" (The Roman Calidarium)

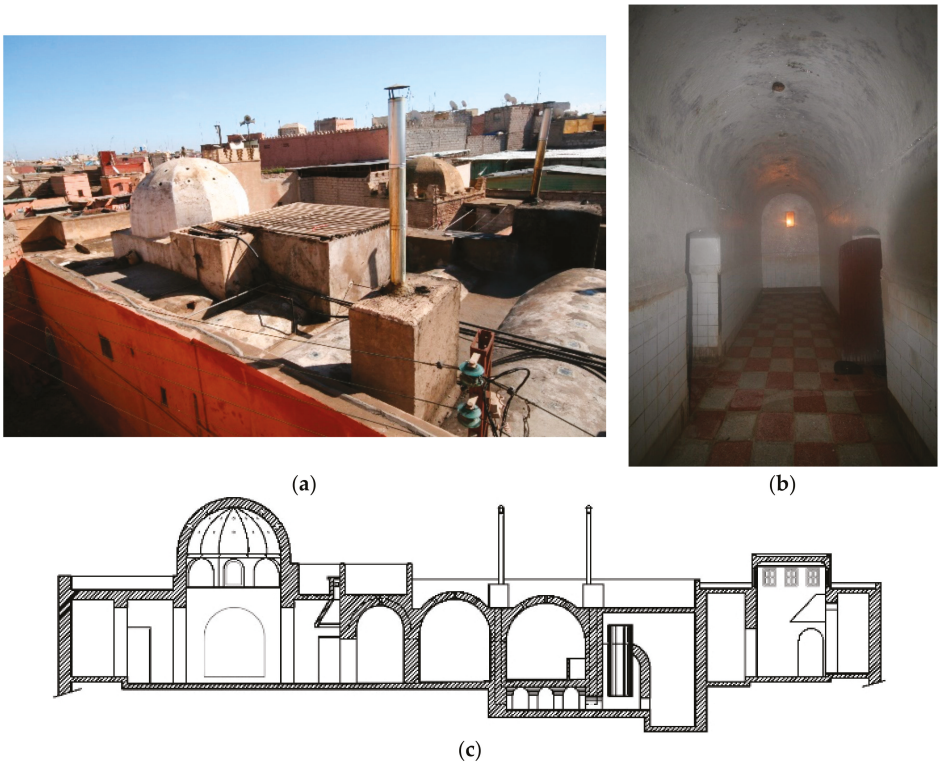

(**a**) (**b**) (**c**)

Figure 5. *Cont.*

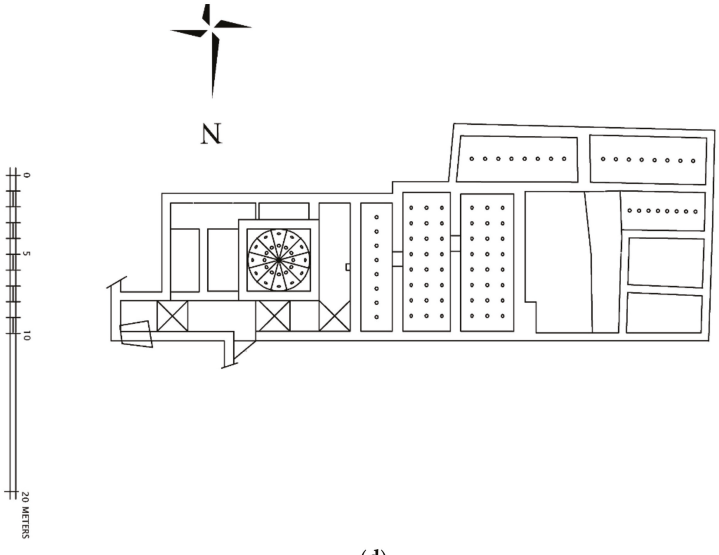

(**d**)

(**e**)

Figure 5. Hammam Sidi Ayyub (16thC) from left to right (**a**) view of the roof; (**b**) internal view of the blocked oculi in the cold room; (**c**) building section illustrating the proportions of the three bathing spaces; (**d**) roof plan with oculi location; (**e**) internal view of the blocked oculi in the warm room.

This organisation is found in the vast majority of the hammams (11 out of 13) as illustrated in the case of hammam Sidi Ayyub (Figure 5) and is reminiscent of the early Moroccan Islamic hammams excavated near the Roman settlement of Volubilis and the Alomravid settlement of Aghmat. In addition to the bathing spaces, all hammams comprise a changing room with an intermediate space with toilets connecting the changing room to the cold room. The configuration of three successive vaulted rectangular bathing rooms is reflected in the roof architecture of 11 out of the 13 heritage hammams surveyed as illustrated in Figure 6. The architecture of the cold and hot rooms, consisting of

long rectangular rooms of varying dimensions, remains constant in all the surveyed hammams. The three rooms are covered by barrel and/or crossed vaults pierced by a number of roof openings.

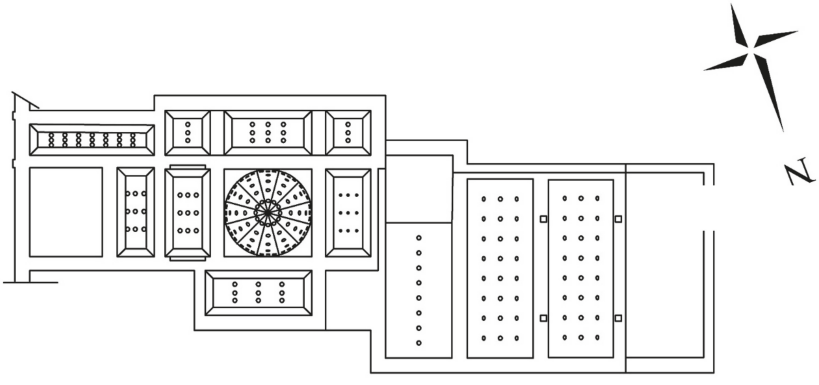

(**a**) Hammam al suq

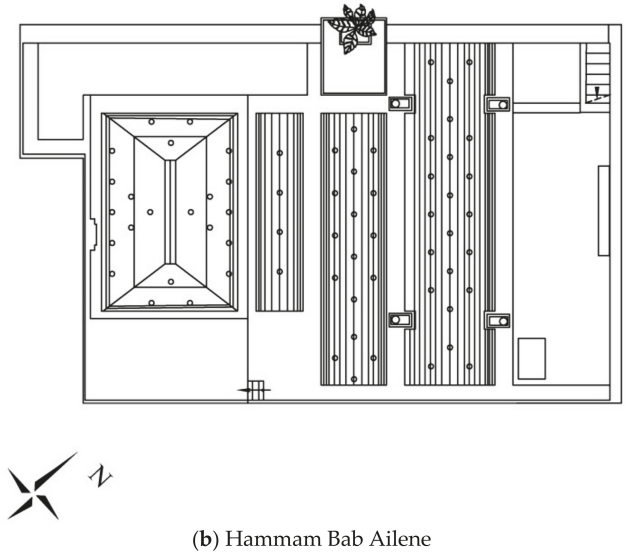

(**b**) Hammam Bab Ailene

Figure 6. *Cont*.

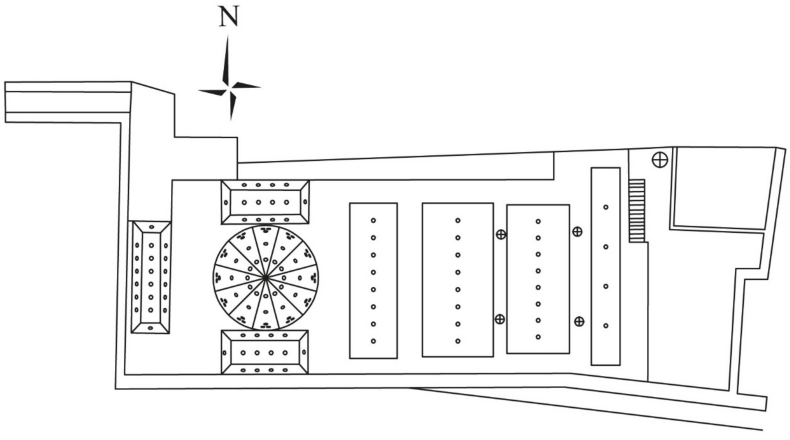

(**c**) Hammam Ziani

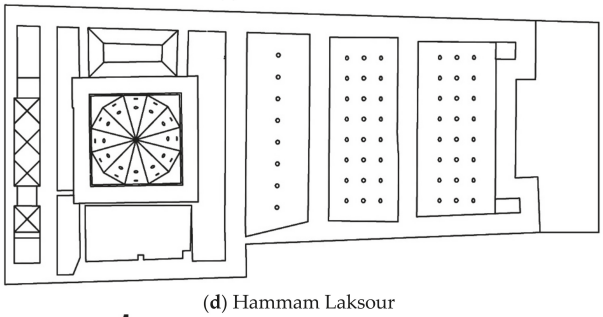

(**d**) Hammam Laksour

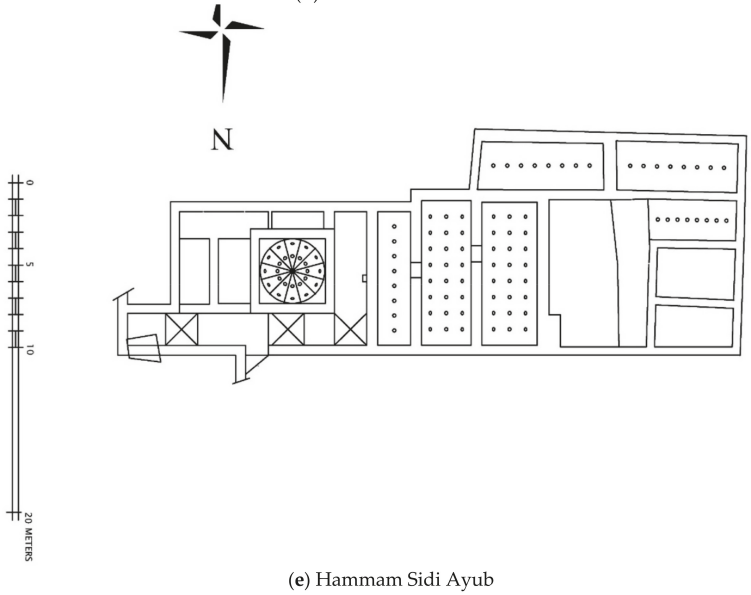

(**e**) Hammam Sidi Ayub

Figure 6. *Cont*.

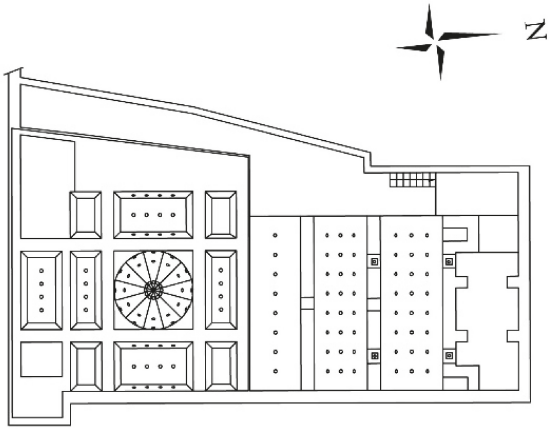

(**f**) Hammam Qannaria

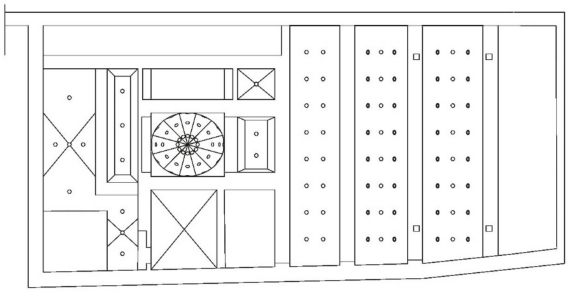

(**g**) Hammam Sidi Abdelaziz

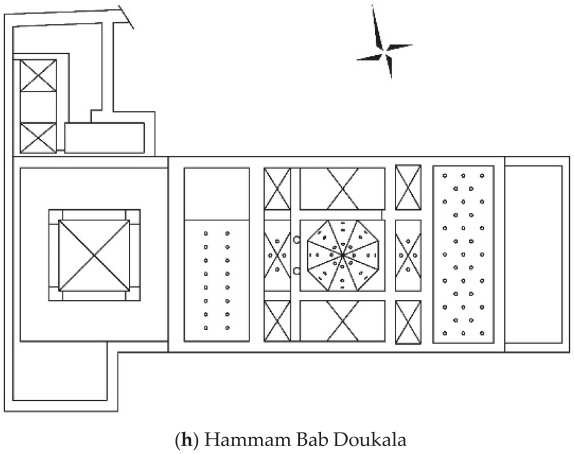

(**h**) Hammam Bab Doukala

Figure 6. *Cont*.

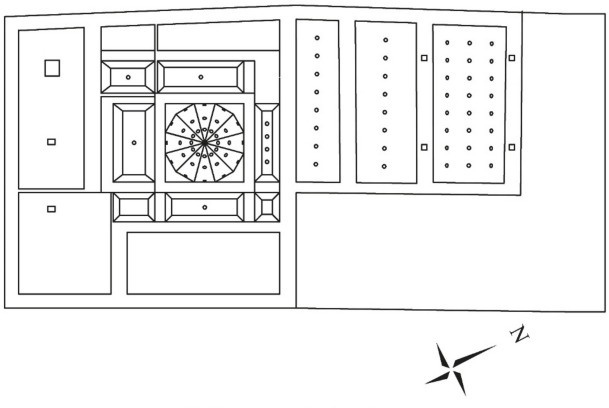

(**i**) Hammam Derb Arjane

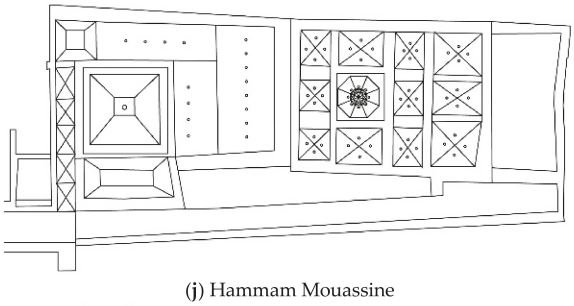

(**j**) Hammam Mouassine

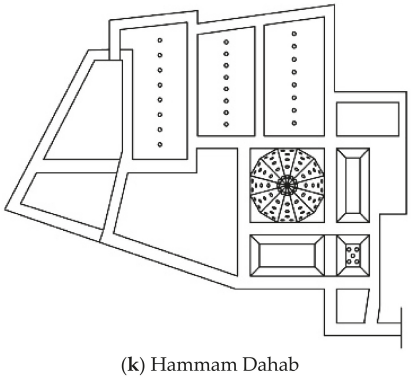

(**k**) Hammam Dahab

Figure 6. *Cont*.

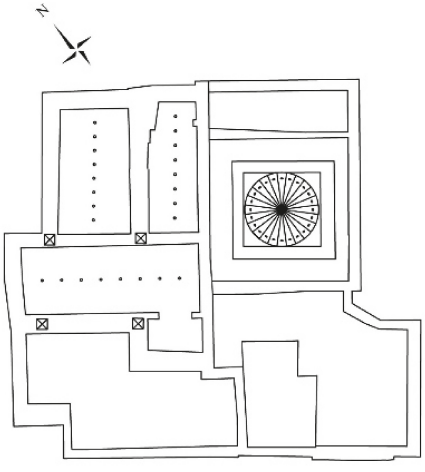

(**l**) Hammam Azbezt

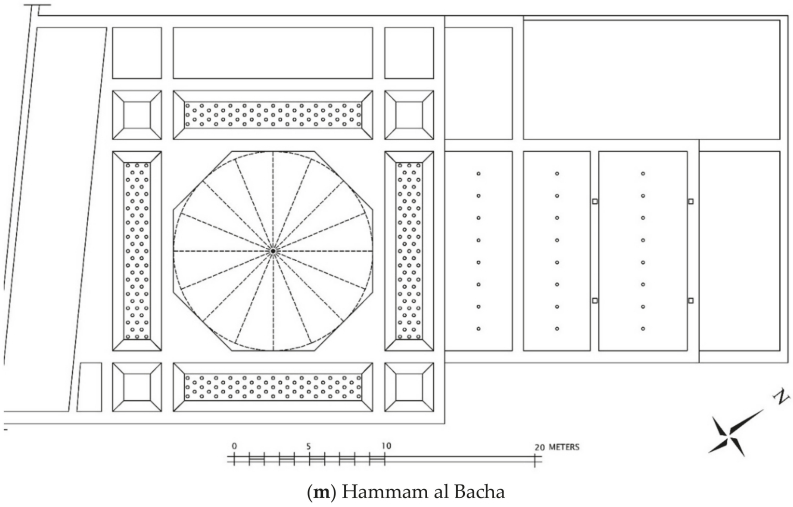

(**m**) Hammam al Bacha

Figure 6. Roof plans of the 13 surveyed hammams. (**a**) Hammam al suq (**b**) Hammam Bab Ailene (**c**) Hammam Ziani (**d**) Hammam Laksour (**e**) Hammam Sidi Ayub (**f**) Hammam Qannaria (**g**) Hammam Sidi Abdelaziz (**h**) Hammam Bab Doukala (**i**) Hammam Derb Arjane **(j)** Hammam Mouassine (**k**) Hammam Dahab (**l)** Hammam Azbezt (**m**) Hammam al Bacha.

The examination of the number and location of roof oculi eveals some recurrent patterns as follows:

- There is a recurrence in the number of eight oculi or multiples of eight, ranging from 8 to 24 oculi (of 18 cm diameter) in the roof vaults covering the bathing spaces (see Table 2).
- The configuration of oculi on the roofs of the cold, warm and hot bathing spaces tends to be in rows of eight along the length of the vaults. The number of rows can vary from one to a maximum of three rows, depending on the width of the bathing space. A single row seems to be a constant feature of the cold room and is not dependent on its floor area (Figure 6).
- Pierced masonry domes tend to be found in the majority of changing rooms' roofs as illustrated in 10 out of the 13 surveyed hammams (Figure 6). They are also found in the warm room of a few

larger hammams, as illustrated in the roof plans of hammams Mouassine and Doukala (Figures 7 and 8). The dome openings are based on the octagonal formation of the dome resulting from a 45-degree rotation of one square plan over another. This explains the number of dome openings as multiples of four.

- The number of oculi on a dome is generally much larger than that of a vault and can exceed 60 oculi.
- The warm room is the only bathing space where a central dome with a large number of oculi is sometimes found and is surrounded by cross vaulted spaces (Figures 7b and 8d).
- Three of the 13 surveyed hammams have a tiled roof wooden structure covering the central area of their changing room as illustrated in the case of hammams Doukala and Mouassine (Figures 7 and 8).

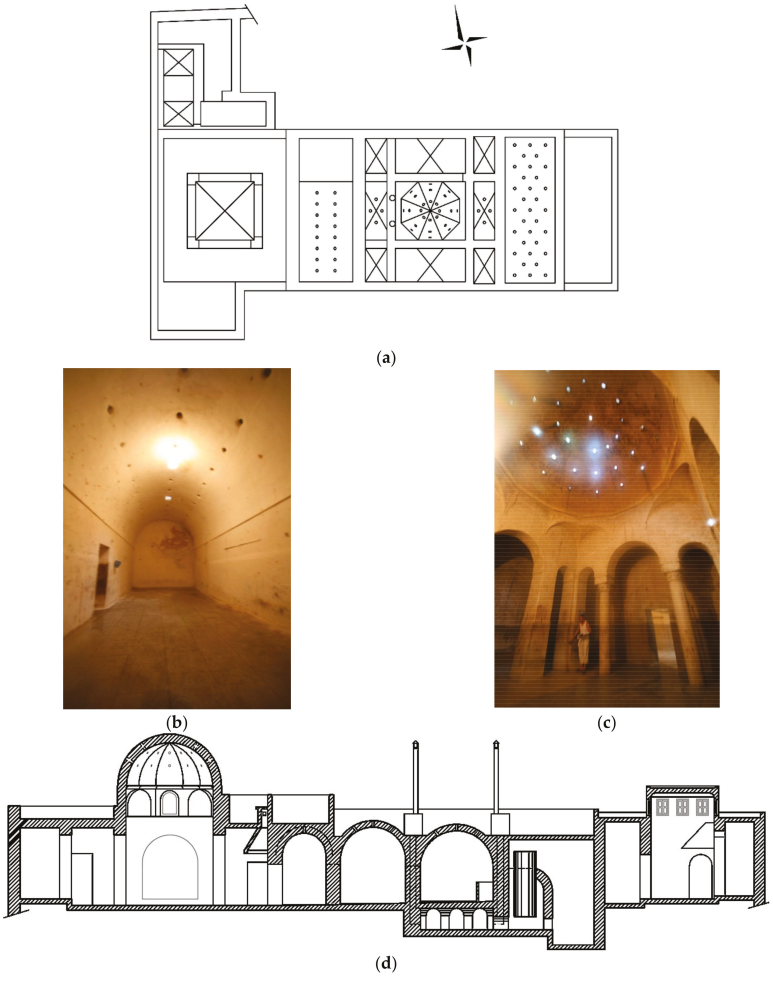

(**a**)

(**b**)

(**c**)

(**d**)

Figure 7. *Cont.*

(**e**)

Figure 7. Hammam Bab Doukala from top left clockwise: (**a**) Roof plan; (**b**) interior view of hot room pierced vault; (**c**) warm room central pierced dome; (**d**) building section; (**e**) warm room pierced cross vault.

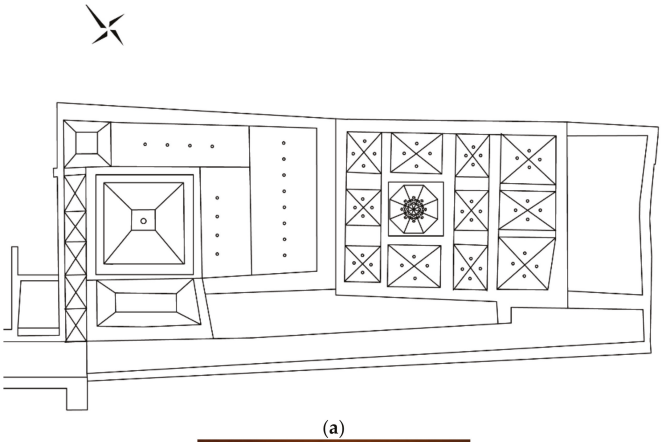

(**a**)

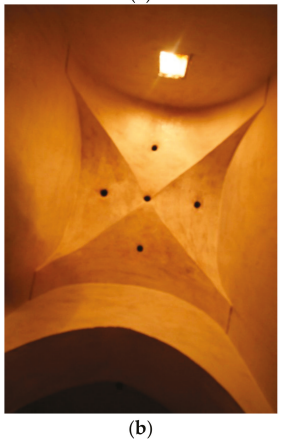

(**b**)

Figure 8. *Cont.*

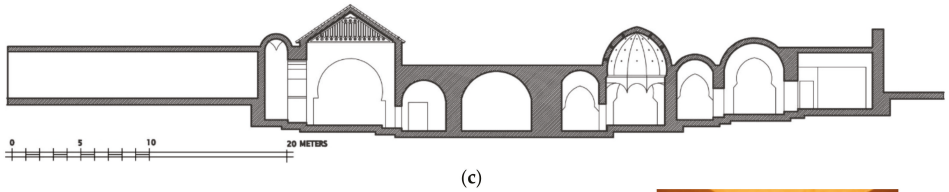

(**c**)

(**d**)

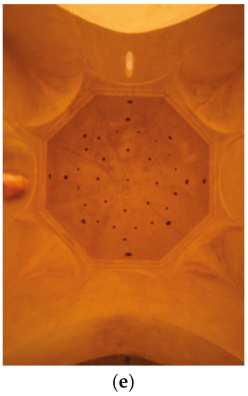

(**e**)

Figure 8. Hammam Mouassine: From top left clockwise: (**a**) Roof plan; (**b**) warm room cross vault; (**c**) section across all the hammam spaces; (**d**) external view of warm room's dome; (**e**) internal view of the warm room's dome.

The comparative analysis of the plans of the 13 hammams reveals that the warm room and the changing area are the main spaces where more architectural variations and elaborate oculi configurations are to be found. This is clearly illustrated in the hammams of Bab Doukala (Figure 7) and Mouassine (Figure 8). Both hammams display the same principle of space and roof configuration in their warm room where the space is based on a central square configuration with a central pierced dome and a series of pierced cross vaults surrounding the central domed square. More elaborate architecture in their changing room is also found as illustrated in Figures 7 and 8. A systematic examination of the location of these two hammams in their wider urban context reveals their proximity to a large complex of a Friday mosque, madrassa and public fountain. Being part of a cluster of important public facilities at the wider urban scale, these two hammams enjoy a larger catchment area of bathers. Since the changing room and the warm room are the spaces where bathers spend most of their time, this explains their larger scale and more elaborate architecture. Furthermore, the changing room acts as a hub for bathers' relaxation and social interaction and as a venue for pre-wedding hammam celebrations for future grooms and brides. The majority of the hammams are, however, smaller structures with modest size and architecture and are located in the proximity of small residential neighbourhood mosques. The roof configuration as well as the number and location of oculi is therefore dependent on the size of the hammam, which depends on its location in the city within the medieval urban fabric's hierarchical system of clusters of facilities. Hammam al Bacha, a very large hammam built in the 1950s, is an exception due to its relatively recent construction.

Table 2. Floor area, number of roof openings and ratios of total roof opening area in the three bathing spaces of the 13 surveyed hammams.

Hammam Name	HR Floor Area (m^2)	HR Oculi	HR Total Oculi Area/Floor Area (%)	WR Floor Area (m^2)	WR Oculi	WR Total Oculi Area/Floor Area (%)	CR Floor Area (m^2)	CR Oculi	CR Total Oculi Area/Floor Area (%)
Bab Ailan	44.24	24	1.38	26	16	1.57	13.68	8	1.49
Dhahab	22	8	0.92	17	8	1.20	20	8	1.02
Bab Doukala	43	32	1.89	69	34	1.25	32	16	1.27
Darb Arjaan	37	24	1.65	32	8	0.64	23	8	0.68
Laksour	39	24	1.57	34	24	1.80	30	8	0.68
Qannaria	40	24	1.53	32	24	1.91	29.5	8	0.69
Al Souq	33	24	1.85	30	12	1.02	30	8	0.68
Mouassine	46	15	0.83	103	62	1.53	48	8	0.42
Al Ziani (Sensla)	40	8	0.51	29.50	8	0.69	24	8	0.85
Azbezt	48	16	0.85	45	8	0.45	34	8	0.60
Sidi AbdelAziz	37	24	1.65	34	24	1.80	32.5	8	0.63
Sidi Ayyoub	29	24	2.10	26	24	2.35	16.2	8	1.26
El Bacha	60	24	1.02	40	24	1.53	40	3	1.49
Averages	39.86	20.84	1.37	39.80	21.23	1.36	28.68	8.23	0.90

3.2. Analyses of Total Area of Roof Openings Expressed as a Percentage of the Internal Floor Areas of Each of the Three Bathing Spaces in the 13 Surveyed Hammams

The internal floor area, the number of roof oculi, and the ratio (in percentage) of total area of roof openings in relation to internal space floor area have been calculated in each of the three bathing spaces of the 13 hammams as presented in Table 2.

The number of oculi in the roof of each of the bathing spaces is dependent on its floor area as illustrated in Figure 9a,b, where the graphs show (as expected) a clear correlation between the floor area of the space and the percentage of roof openings' total area in both the hot and warm rooms as illustrated in Figure 9a,b. The largest number of oculi is found in the warm room, when this has a central dome as is the case of hammam Mousassine (Table 2). However, the key finding here is that the cold room's total area of roof openings, consisting on one row of eight oculi, is not related in any way to its internal space floor area (Figure 9c).

As the cold room is the first space bathers cross on their way to the warm and hot rooms (where most of the bathing takes place), its low levels of daylight help bathers' sight to adjust to the low light levels in the steamy bathing spaces of the warm and hot rooms. This indicates an underlying principle of allowing bathers' sight to adjust to the lowest level of light in the cold room so that they get accustomed to the slightly higher light levels in the warm and hot rooms, where most of the bathing activities take place. The bathers' journey through different spaces of increasing or decreasing temperature and steam is matched with an increasing or decreasing amount of daylight. The darkest room is the cold room where the number of oculi is not dependent on its internal floor area. There seems to be some symmetry in the transitions between extremes conditions of hot and lighter, cold and darker. The warm room presenting conditions of transitions between the two extremes of cold and hot room.

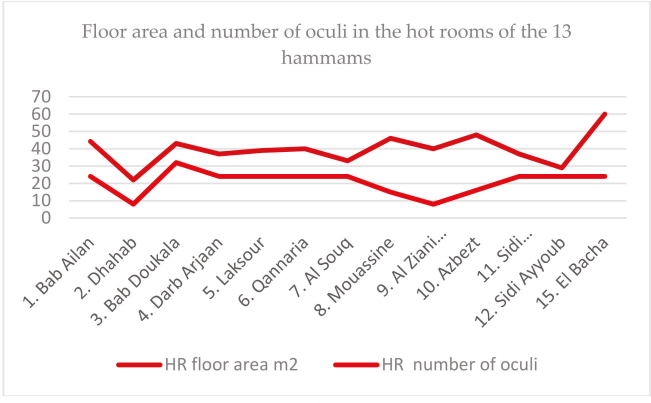

(**a**)

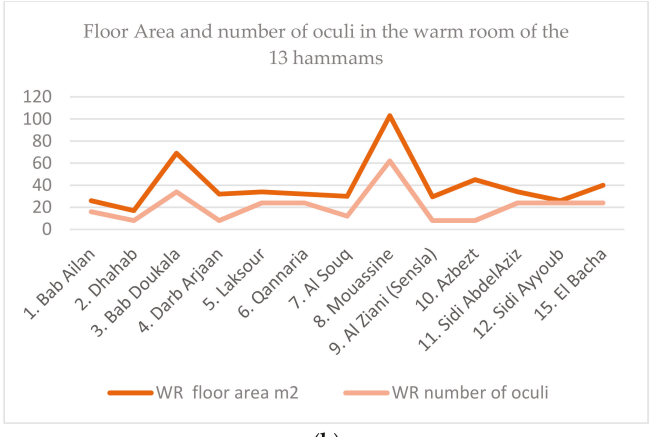

(**b**)

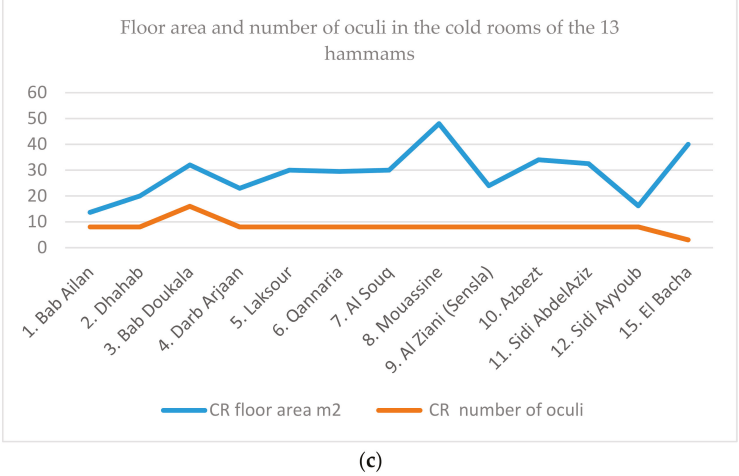

(**c**)

Figure 9. Relationship between floor area and number of roof oculi per type of bathing space: (**a**) The hot room; (**b**) the warm room; (**c**) the cold room. The horizontal axis is the hammam as they appear in Table 1.

It is clear from Table 2 and Figure 10 that the cold room has the smallest proportions of roof openings as compared to the hot and warm rooms in the vast majority of the surveyed hammams. It is also interesting to note that the maximum total area of oculi roof openings does not exceed 2% of the internal floor area of the bathing space above which they are located as illustrated in 12 of the 13 surveyed hammams (Figure 10).

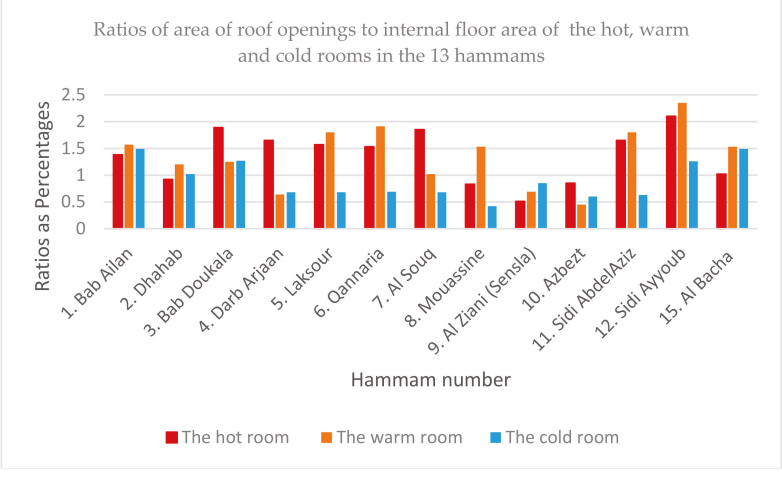

Figure 10. Comparison of ratios of roof opening total area in relation to floor area in the three bathing spaces of the 13 surveyed hammams.

3.3. Restoring the Vernacular Daylighting System and Quantifying Horizontal Illuminance Afforded by It in the Three Bathing Spaces of a Working Hammam

All surveyed heritage hammams have completely lost the original daylight qualities in their bathing spaces, as the vernacular blown glass caps (Figure 11) have all been replaced by poor alternatives, such as glass bricks or flat sheets of reinforced glass (Figure 12a), or have been completely blocked by layers of cement. Poor incandescent or fluorescent electric lighting that is neither appropriate nor safe for the steam conditions of these spaces was found to be used all day long in the surveyed hammams, increasing consumption of electricity. Furthermore, face-to-face interviews conducted with three female hammam workers in Marrakech indicated the occurrence of headaches and fatigue which they attributed to the lack of daylight and natural ventilation in the bathing spaces. A follow-on discussion with the head of the hammam managers association in Marrakech revealed that there was a lack of knowledge of the original blown glass caps which used to cover the roof oculi amongst most hammam managers. This situation is further exacerbated by the loss of glass blowing workshops in Moroccan cities, with the exception of the one and only glass blowing workshop opened by a French entrepreneur in Marrakech and employing the last two glass blowers in Morocco. Based on the form of vernacular glass bells, the transparent blown glass bells of 18 cm in diameter was used by the author as a prototype to produce locally 48 glass bells, using recycled glass (Figures 11 and 12).

Figure 11. Samples of blown glass bells produced in Syria in 2007 based on vernacular prototypes examined to restore hammam daylighting. The blue version is an openable oculus glass cap for natural ventilation.

Figure 12. The roof of Hammam Rjafalla: (**a**) Removing poor alternatives of oculi covers; (**b**) re-opening the oculi and placing the blown recycled glass caps; (**c**) solar panels over the warm room affecting indoor daylight measurements; (**d**) blocked oculi in the hot room; (**e**) vernacular daylight restored; (**f**) oculi natural light effect.

Access to a working heritage hammam in Marrakech to restore the blown glass caps over the oculi system was impossible. However, the opportunity to restore the vernacular daylighting system in a working heritage hammam presented itself in Rabat (the administrative capital of Morocco) in July 2016. Built in the 1950s, during the French protectorate, the Hammam Rjafalla is located in an informal, low-income housing neighbourhood, known as Hay Rjafalla, in the area of Yacoub al Mansour. The building presents a typical Moroccan vernacular hammam architecture, consisting of three successive rectangular parallel rooms with two rows of eight oculi in each of the three north/south facing vaulted roofs (Figure 12c).

The rehabilitation of the vernacular daylighting system took place in July 2016, under the initiative and supervision of the author, at a time when the hammam was temporarily closed for its annual maintenance work. The hammam manager has been in charge of the building for the last 36 years and is the only active female member of the National Federation of Moroccan hammam managers. She is also one of the key participants to the sustainable hammam initiative in Morocco which was presented at the COP22 in Marrakech in November 2016 [16]. The re-opening of the closed oculi and the installation of the blown glass bells was carefully conducted in order to avoid damaging the pottery

tubes located in the masonry of the vaults and which form the base for the glass cap (Figure 12c). Once the vernacular daylighting system was restored, HOBO data loggers were installed in the same position within each of the three parallel bathing rooms at a height of two metres from the floor and at the base of the vault. This allowed for the recording of horizontal illuminance at a similar point on the internal south facing wall under the steam conditions of a working hammam and without interfering with bathers' activities (Figure 13).

Figure 13. Installation of HOBO data loggers for measuring temperature and light: Temperature range: −20 °C to 70 °C, light measurement range: 0 to 320,000 lx (0 to 30,000 lumens/ft^2).

The data loggers were set to record light levels simultaneously in the three bathing spaces, under the working hammam heat and steam conditions and with the oculi openings being the only source of daylight. A fourth HOBO data logger was placed on the hammam roof (on top of the warm room) to measure the horizontal illuminance on the roof, simultaneously with the data loggers installed inside the building. Measurements were taken from 19 July to 30 September 2016 at 20 min intervals.

The plotting of weekly averages of horizontal illuminance (recorded every 20 min between 11:00 a.m. and 17:00 p.m.) over a period of almost two months and a half, clearly indicates that the averages of daylight levels do not exceed 25 lx and that the cold room tends to have slightly higher averages than the hot room despite their same configuration and orientation (Figure 14). However, when examining daily plotting of recorded illuminance in the three spaces, the results show that horizontal illuminance (lx) recorded in the hot and cold rooms varies between 10 and 60 lx with the hot room recoding slightly higher levels than the cold room (Figure 15 and Table 3).

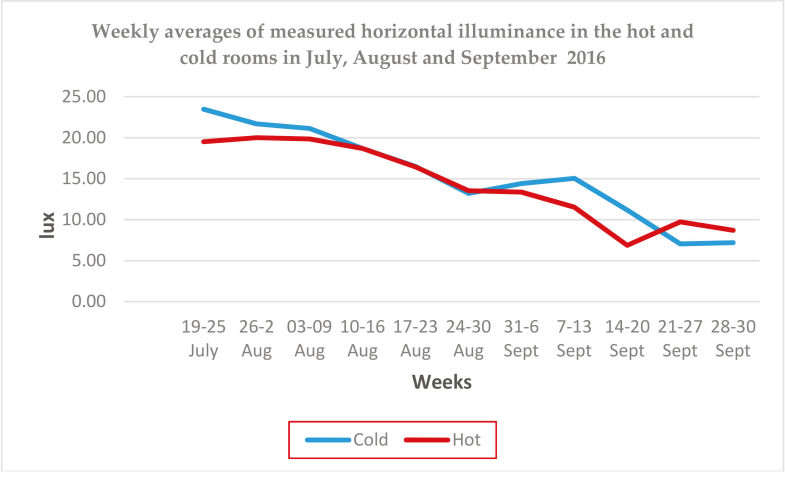

Figure 14. Weekly averages of horizontal illuminance (lx) recorded in the hot and cold rooms (19 July to 30 September 2016).

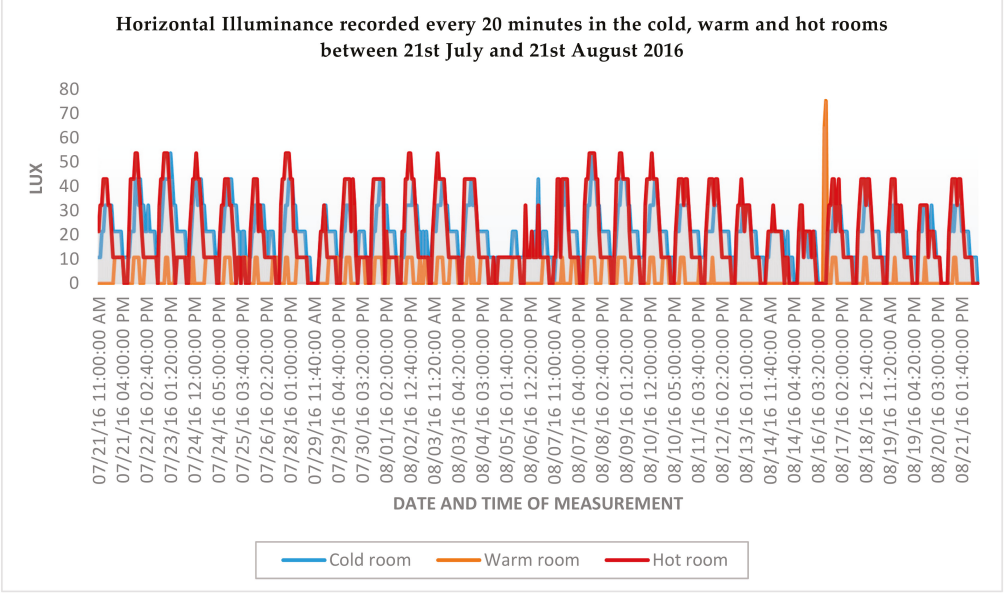

Figure 15. Horizontal illuminance values recorded in the three bathing spaces during the summer of 2016 on a daily basis between 11:00 a.m. and 05:00 p.m.

Table 3. Weekly averages of horizontal illuminance recorded in the cold room, the hot room and the room.

		Weekly Averages			Weekly Maximum			Weekly Minimum		
Wk	**Days**	**Roof**	**Cold Room**	**Hot Room**	**Roof**	**Cold Room**	**Hot Room**	**Roof**	**Cold Room**	**Hot Room**
0	19–25 July	159.3	23.48	19.52	204.49	29.46	23.82	128.35	12.48	13.60
1	26 July–2 August	177.9	21.69	20.01	190.56	25.50	25.51	170.84	14.73	9.07
2	3–9 August	173.8	21.13	19.85	194.34	26.63	27.21	132.26	11.92	8.53
3	10–16 August	136.0	18.69	18.69	177.51	22.66	24.38	32.03	11.33	11.90
4	17–23 August	128.0	16.51	16.44	148.80	22.10	22.11	66.86	3.98	1.14
5	24–30 August	118.3	13.20	13.54	146.91	16.99	18.26	76.875	9.64	8.51
6	31 August–6 September	125.5	14.41	13.36	148.36	19.26	19.28	86.583	6.82	5.10
7	7–13 September	130.3	15.04	11.52	138.50	15.85	13.03	113.70	12.46	10.77
8	14–20 September	112.1	11.18	6.87	144.59	15.86	10.34	21.355	3.96	0.00
9	21–27 September	103.4	7.05	9.73	131.68	10.77	19.27	50.035	0.57	5.67
10	28–30 September	112.6	7.20	8.70	112.97	7.39	13.04	111.23	6.82	3.98

The plotting of horizontal illuminance levels over a period of two months and a half clearly indicate that it is in the hot room where the highest levels of horizontal illuminance were recorded (Figure 15). However, these levels remain well below 100 lx and do not exceed 60 lx (Figure 14). The levels recorded for the warm room remain the lowest as they have been jeopardised by the installation of two large solar panels, casting shadows over the oculi (Figure 12c) and resulting in levels being at 10 lx or below despite the sunny and clear sky conditions during the summer months. However, this indicates that the vernacular daylighting provision works best in conditions where the roof vaults have a good sky exposure and are not shaded by roof installations or adjacent buildings.

There is a rapid decline in weekly illuminance averages in September leading to much lower levels inside the bathing spaces (Figure 14).

The plotting of the 21 July 2016 measurements in the cold, warm and hot room, as well as on the roof, reveals a more detailed pattern of illuminance variation in the three bathing spaces and the roof sky conditions (Figure 16). These plots, together with Table 3, illustrate a clear correlation between the sky conditions and the daylight levels afforded by the vernacular system.

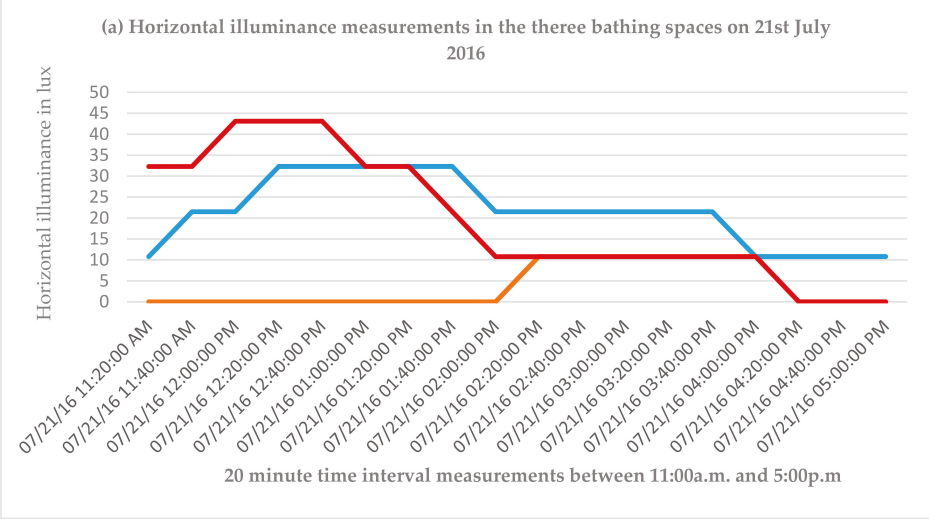

Figure 16. *Cont.*

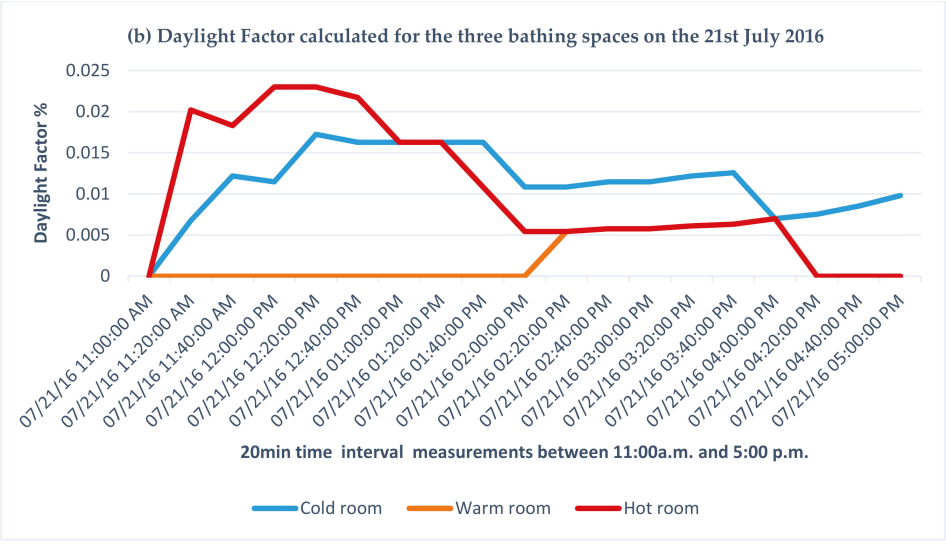

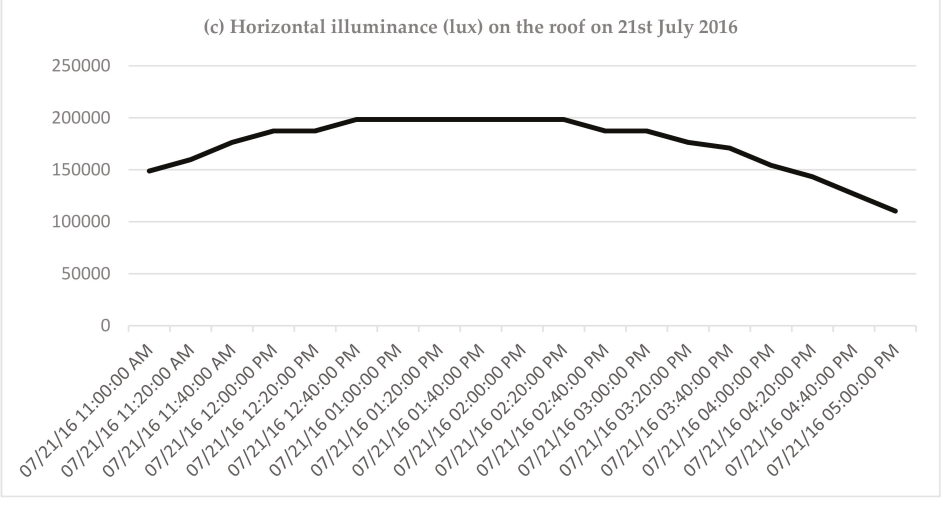

Figure 16. Horizontal illuminance in the three bathing rooms and on the roof and the calculated daylight factor on the 21 July 2016 between 11:00 and 17:00.

The drop in light levels is much more sudden in the hot room than in the cold room and this could be explained by the high level of steam (98% humidity) reached in the space by early afternoon, when the use of the hot room by bathers is at its highest. The daylight factor calculation for the same day, based on real data, reveals that there is a sudden reduction in the DF in the hot room early afternoon (Figure 16b) below that of the cold room as the humidity and steam in the hot room reach saturation levels.

The comparison of recorded illuminance on the roof and the three bathing spaces on the 21 July 2016 (between 11:00 and 17:00) clearly illustrates that the sky conditions are directly reflected into indoor daylight levels in the hammam bathing spaces (Figure 16). This indicates that the vernacular

daylighting system in hammam buildings allows for users' strong connection to outdoor sky conditions and to the movement of the sun in the sky which is known to be important for users' well-being.

4. Discussion

Heritage public bathhouses (hammams) of North African Maghreb cities continue to provide an affordable hygiene and well-being facility for their residents. This is particularly the case in Morocco which has the largest number of heritage hammams. It is estimated that there are at least 12,000 hammams operating in Morocco. However, this number is likely to be much higher as new hammams are being built in every single new residential neighbourhood and no recent statistics are available to date. As hammams operate day and night, their electricity bill for lighting the building constitutes 25% of their energy consumption, the remaining 75% are for water and building heating [17]. The reintroduction of daylight into the bathing spaces is therefore estimated to reduce energy consumption by at least 12.5% (half the time is at night) and create healthier environments for both bathers and hammam workers.

The repair of the vernacular lighting system in heritage hammams of all historic urban centres in Morocco and in other North African cities can have a cumulative effect on reducing CO_2 emissions and increase users' well-being as well as revive the glass blowing crafts using recycled glass for the production of oculi glass caps. Furthermore, its adoption and adaptation to contemporary hammam projects can achieve higher levels of horizontal illuminance by increasing the number of roof oculi in the design of new structures in order to meet contemporary expectations of visual comfort from the users while maintaining architectural and cultural authenticity. Bathers, however, lack experience of the original luminous environment and their expectation of higher levels of illuminance has been reported through discussions with the manager of hammam Rjafalla. Although, bathers and staff were happy to see more daylight in the bathing spaces after the rehabilitation of the vernacular system, and commented positively about it, they still expected additional electric lighting to be used, particularly at the end of the summer months. The cultural and religious norms relating to nudity and visual privacy still apply to some extent in the use of the bathing spaces, although they are not always adhered to.

Despite the limitations of previous studies on hammam daylighting in other geographies, it is clear from the results of this study that the horizontal levels recorded in the present case study fall far below those measured in Ottoman hammams where the number of oculi in the roof is much higher than those found in Moroccan hammams.

Moroccan hammams fall under the umbrella of the Ministry of Habous and Religious Affairs (who own the majority of the heritage structures) and the Ministry of Culture and Traditional Crafts. Serious attempts have been made to reduce wood consumption in hammam furnaces to reduce CO_2 emissions, particularly after the COP 22 event held in Marrakech in 2016. However, the reduction of electricity consumption through the reintroduction of daylighting has not been considered. It has also been omitted by a study conducted by the Ministry of Culture and Moroccan Crafts aimed at establishing benchmarks of what constitutes an authentic Moroccan hammam [18]. Furthermore, the integration of bespoke off-grid LED solar powered lighting within the vernacular daylighting system for night illumination, as developed by the author in 2015, can lead to a highly sustainable hybrid innovative solution [17].

5. Conclusions

This paper has provided the first systematic study of the vernacular daylighting provision in Moroccan heritage public bathhouses (hammams). It combines historical and architectural analyses of a representative sample of 13 working heritage structures to reveal tacit rules underlying the number, location and configuration of roof oculi. These are then restored in a working hammam to establish the first benchmark for levels of horizontal illuminance afforded by the vernacular system in the bathing spaces under real working conditions. The results reveal a recurrent pattern of oculi number and

configuration consisting of one to three rows of eight circular openings (of 18 to 20 cm in diameter) arranged along the roof vaults covering the bathing spaces.

The total area of roof openings for each bathing space was found to rarely exceed two percent of its internal floor area. Measurements of horizontal illuminance on the roof of sky conditions, as well as that of inside the bathing spaces, were carried out continuously and simultaneously in July, August and September of 2016 at 20 min intervals and at comparable locations. This has resulted in real time values, allowing for the calculation of daylight factor under real changing sky conditions. The results of horizontal illuminance measurements indicate that maximum levels are reached between 12:00 and 14:00 when the sun is high in the sky, but never exceeded 60 lx. The impact of the saturated air humidity on the daylight factor is evident in the hot room where the highest levels of DF are registered but suddenly decrease below that of the cold room as the air humidity levels reach almost 100%. Levels of horizontal illuminance are generally much lower than those recorded in previous studies in Ottoman baths and remain well below 60 lx as compared to 100 or 150 lx recorded in Ottoman hammams. Low levels of daylight are therefore a genuine experiential quality of Moroccan hammams afforded by small oculi in the vaults and domes of the bathing spaces.

This paper has provided a new understanding of the experienced luminous environment afforded by the vernacular daylighting system in Moroccan hammams and established the first benchmark for its rehabilitation in heritage structures and its future integration in new Moroccan hammams. Further studies are needed to investigate bather's sensorial experiences of heritage hammams daylighting ambiences to understand elements of comfort that are outside the norms of numerical quantification of light. As argued by Tregenza and Marjaldevic [19] in their review of half a century of research on daylighting, there are still important questions which fifty years of study have not fully answered: What are the criteria of good daylighting? What should be the central aim of the designer? What regulations or standards are required? "Describing lighting only in terms of illuminance is equivalent to describing music in terms of sound pressure level" [20]. As Bille and Sørensen [20] argue, light works as a significant constituent of experience. In their introduction to *an anthropology of luminosity*, they coin the term *lightscape* and highlight that "*by introducing an anthropology of luminosity; an examination of how light is used socially to illuminate places, people and things, and hence affect the experiences and materiality of these, in culturally specific ways.*" From a phenomenological point of view, Merleau-Ponty [21] argues that "*we do not so much see light as we see in it*."

Further research is needed to carry out wider measurements of illuminance as experienced and perceived by building users, combining real time measurements with recordings of users' space use and reactions during a whole bathing session in a working rehabilitated heritage hammam.

This paper opens up new avenues for further research based on the innovative combination of historical, architectural, building science research and environmental psychology methodologies to reveal tacit rules underlying the luminous environment of heritage buildings, as well as their perceived experimental qualities, in order to provide benchmarks for the rehabilitation of original luminous environment and their reinterpretation in contemporary designs.

Funding: The architectural survey part of the research on the public baths in Marrakech was funded by the Arts and Humanities Research Council (AHRC) as part of the UK grant number [AH/D503019/1].

Acknowledgments: The author would like to thank Khadija Kadiri, the manager of Hammam Rjafalla, for providing me with the opportunity to retrofit the vernacular daylighting system in her hammam, install data loggers and carry out measurements and interviews during the summer months of 2016. Sincere thanks to Mr Hadj Youssef, president of the hammam managers association of Marrakech and to all the hammam managers of Marrakech for allowing me to complete the roof surveys.

Conflicts of Interest: The author declare no conflicts of interest.

References

1. Mardaljevic, J.; Brembilla, E.; Drosou, N. Real-world validation of climate-based daylight metrics: Mission impossible? In Proceedings of the CIBSE Technical Symposium, Heriot-Watt University, Edinburgh, UK, 14–15 April 2016.
2. Morales-Segura, M. The skylight in the Roman Baths: The construction. In Proceedings of the Third International Congress on Construction History, Cottbus, Germany, 20–24 May 2009.
3. Almagro, M.; Caballero, L.; Zozaya, J.; Almagro, A. *Qusayr Amra: Residencia ybaños omeyas en el desierto de Jordania*, 2nd ed.; Fundación El Legado Andalusí: Granada, Spain, 2002; pp. 70–71.
4. Naji, S. Archéologie coloniale au Maroc, 1920–1956: Civiliser l'archaïque. *Les nouvelles de l'archéologie* **2011**, *126*, 23–28. [CrossRef]
5. El Habashi, A.; Moujoud, T.; Zizouni, A. The Conservation and Reconstruction of the Islamic Bath at Volubilis, Morocco. In *The Journal of Fasti Online: Archaeological Conservation Series*; The International Centre for the Study of the Preservation and Restoration of Cultural Property: Rome, Italy, 2016; pp. 1–11. ISSN 2412-5229.
6. Moujoud, T.; Al Jattari, M.; Zizouni, A. Site Conservation in Morocco: The Emergence of a Practice at Aghmat. *Conserv. Manag. Arch. Sites* **2010**, *12*, 237–253. [CrossRef]
7. Sibley, M. The Historic Hammams of Damascus and Fez. In *Lessons from Vernacular Architecture*; Yannas, S., Weber, W., Eds.; Routledge: Abingdon, UK, 2013.
8. Sibley, M.; Jackson, I. The Architecture of Islamic public baths of North Africa and the Middle East: An analysis of their internal spatial configurations. *Archit. Res. Q.* **2012**, *16*, 155–170. [CrossRef]
9. Raftani, K.; Radoine, H. The Architecture of the hammams of Fez, Morocco. *ArchNet-IJAR* **2008**, *2*, 56–68.
10. Al Maiyah, S.; Elkadi, H.; Aygen, Z. Modelling Daylight for Preserving Identity: Simulation of daylight levels for successful intervention in historic buildings. In Proceedings of the 29th Conference, Sustainable Architecture for a Renewable Future, Munich, Germany, 10–12 September 2013.
11. Tsikaloudaki, K.; Cocen, O.N.; Tasopoulou, K.; Milonas, I. Daylighting in Historic Bathhouses: The Case of Ottoman hammams. *METU JFA* **2013**. [CrossRef]
12. Mahdawi, A.; Orehounig, K. An inquiry into the thermal, acoustical, and visual aspects of indoor environment. *ArchNet-IJAR* **2008**, *2*, 136–149.
13. Orehounig, K.; Mahdavi, A. Energy performance of traditional bath buildings. *Energy Build.* **2011**, *43*, 2442–2448. [CrossRef]
14. Destino, T.; Sibley-Behloul, M. The Hammam Living Traditions. In *Hammam Rehabilitation Reader*; Dumreicher, H., Levine, R.S., Sibley Behloul, M., Eds.; Sonderzhal Verlag: Vienna, Austria, 2012; pp. 49–67.
15. HOBO Pendant®Temperature/Light Data Logger 8K-UA-002-08. Available online: https://www.hobodataloggers.com.au/hobo-pendant-temperaturelight-data-logger-8k-ua-002-08 (accessed on 30 October 2018).
16. Hammams Durables. Available online: http://www.initiativesclimat.org/Les-nomines/Hammams-durables. (accessed on 30 October 2018).
17. Sibley, M.; Sibley, M.J.N. Hybrid Green Technologies for Retrofitting Heritage Buildings in North African Medinas: Combining Vernacular and High-tech Solutions for an Innovative Solar Powered Lighting System for Hammam Buildings. *Energy Procedia* **2013**, *42*, 718–725. [CrossRef]
18. Ministère de L'Artisanat, de l'Economie Sociale et Solidaire-Royame du Maroc. Reglement d'Usage Relatif a la Marque Collective de Certification "Hammam Marocain Niveau 1". Unpublished work; 2016.
19. Tregenza, P.; Mardaljevic, J. Daylighting buildings: Standards and the needs of the designer. *Light. Res. Technol.* **2018**, *50*, 63–79. [CrossRef]
20. Bille, M.; Flohr Sørensen, T. An Anthropology of Luminosity: The Agency of Light. *J. Mater. Cult.* **2007**, *12*, 263–284. [CrossRef]
21. Merleau-Ponty, M. Eye and Mind. In *The Primacy of Perception and Other Essays on Phenomenological Psychology, the Philosophy of Art, History and Politics*; Edie, J.M., Ed.; North-Western University Press: Evanston, IL, USA, 1964; pp. 159–190.

MDPI
St. Alban-Anlage 66
4052 Basel
Switzerland
Tel. +41 61 683 77 34
Fax +41 61 302 89 18
www.mdpi.com

Sustainability Editorial Office
E-mail: Sustainability@mdpi.com
www.mdpi.com/books

MDPI
St. Alban-Anlage 66
4052 Basel
Switzerland

Tel: +41 61 683 77 34
Fax: +41 61 302 89 18

www.mdpi.com

ISBN 978-3-03928-345-3